# Open Research Online

## Role of microRNAs in leukocyte adhesion to human brain microvascular endothelium

## Thesis

For guidance on citations see FAQs.

## oro.open.ac.uk

# Role of microRNAs in leukocyte adhesion to human brain microvascular endothelium

**Miss Camilla Cerutti B.Sc M.Sc**

A thesis submission to
The Open University for the degree of Doctor of Philosophy

**The Open University**

Faculty of Science

Department of Life, Health and Chemical Sciences

The Open University

Walton Hall

Milton Keynes

United Kingdom

August 2013

# THESIS CONTAINS

# VIDEO

# CD

# DVD

# TAPE CASSETTE

## Declaration

The work in this thesis is entirely my own and is the result of my own academic and experimental enquiry. Contributions to the work by colleagues are fully acknowledged in the manuscript.

I further assert that this thesis does not exceed 300.000 words, including headers and references.

# Acknowledgements

# Publication list

## Poster presentations at scientific conferences

*MiR-126 and miR-126\* play a role in flow-based leukocyte adhesion on cytokine activated human brain microvascular endothelium in vitro.*
11th International Congress of Neuroimmunology (ISNI). November 4 to 8, 2012 Boston (MA) USA

*MiR-126 and miR-126\* play a role in flow-based leukocyte adhesion on cytokine-activated human brain microvascular endothelium in vitro.* MicroRNAs Europe&singlemolecules biology Europe 2012 meeting. 1-2 November 2012 University of Cambridge, Cambridge, UK

*An in vitro human blood-brain barrier model to study the role of microRNAs in leukocyte adhesion to endothelium in inflammation.*
RNA control mechanisms in development and stress. 22 November 2011 Charles Darwin House, London, UK

*An in vitro human blood-brain barrier model to study the role of microRNAs in leukocyte adhesion to endothelium in inflammation.*
14th symposium on signal transduction in the blood brain barriers. 07-09 September 2011, Celal Aga Konagi Hotel, Istanbul

*An in vitro human blood-brain barrier model to study the role of microRNAs in leukocyte adhesion to endothelium in inflammation.*
9th International Conference on Cerebral Vascular Biology. 21-25 June, 2011 Pieterskerk, Leiden, the Netherlands.

## Oral presentations at scientific conferences

*MiR-126 and miR-126\*: two new players in flow-based leukocyte adhesion on cytokine-activated human brain microvascular endothelium in vitro.*
Joint Franco-Belgian-British multinational meeting on blood-brain interfaces. 15-17 May 2013. Universite d`Artois, Arras, France

*Role of microRNAs in leukocyte adhesion to human brain microvascular endothelium*
Postgraduate annual meeting of Life Sciences. 18th of May 2012
The Open University, Walton Hall, Milton Keynes MK7 6AA, UK

*MiR-126 and miR-126\* play a role in flow-based leukocyte adhesion on cytokine-activated human brain microvascular endothelium in vitro.*
2nd UK & Ireland Early Career Blood-Brain Barrier Symposium 23rd of November 2012 University of Liverpool, Foresight centre, Liverpool, UK

*Role of microRNAs in leukocyte adhesion to human brain microvascular endothelium.*
1st UK & Ireland Early Career Blood-Brain Barrier Symposium 25th of October 2011
The Open University, Walton Hall, Milton Keynes MK7 6AA, UK

*The blood-brain barrier in inflammation: Role of microRNAs in leukocyte adhesion to human microvascular endothelium*
Postgraduate annual meeting of Life Sciences. 12th of May 2011
The Open University, Walton Hall, Milton Keynes MK7 6AA, UK

*An in vitro human blood-brain barrier model to study the role of microRNAs in leukocyte adhesion to inflamed endothelium.*
Postgraduate annual meeting of Life Sciences. 13th of May 2010
The Open University, Walton Hall, Milton Keynes MK7 6AA, UK Awarded as second best presentation.

**Research articles**

Camilla Cerutti, Basil Sharrack, David K.Male and Ignacio A. Romero
*MiR-126 and miR-126\* play a role in flow-based leukocyte adhesion on cytokine-activated human brain microvascular endothelium in vitro.* In preparation for *Journal of Immunology*

Camilla Cerutti, Patricia Soblechero-Martin, Basil Sharrack, David K.Male and Ignacio A. Romero
*MiR-155 a new old-player of leukocyte adhesion on cytokine-activated human brain microvascular endothelium.* In preparation for a Letter in *Journal of Neuroscience*

Camilla Cerutti, Basil Sharrack, David K. Male and Ignacio A. Romero
*A new in vitro model to study leukocyte trafficking to human endothelial cells under flow.* In preparation for *Fluids and Barriers of the CNS* Blood-brain barrier

# Abstract

MicroRNAs (miRs) are small non-coding regulatory RNAs that act through repression of protein translation and/or mRNA degradation at the post-transcriptional level. MiRs are critical players in the pathogenesis of many diseases, including neuroinflammatory disorders such as multiple sclerosis (MS). MS is characterized by leukocyte adhesion and infiltration subsequently leading to demyelination of nerve fibres. Leukocyte adhesion on brain endothelial cells (BEC) - the main cellular constituent of the blood-brain barrier (BBB) - is a complex multi-step process where activated BEC overexpress chemokines such as CCL2 and endothelial adhesion molecules (CAM) such as selectins, VCAM1 and ICAM1. Several therapies for MS target the common known mechanisms of leukocyte adhesion.

Here, we studied whether specific endothelial miRs act as regulators of leukocyte adhesion to cultured human BEC *in vitro*, and hence whether they could be a potential therapeutic tool to prevent adhesion to endothelium. First, we characterised leukocyte adhesion using the monocytic (THP1) and T cell (Jurkat) lines under static conditions, interacting with the immortalized hCMEC/D3 endothelial cell line as an *in vitro* model of the human BBB. Increased adhesion of both leukocytic cell lines to BEC was observed following treatment with TNFα and IFNγ compared to unstimulated cells. Increased expression of both ICAM1 and VCAM1 by hCMEC/D3 cells was also observed following cytokine treatment. Cytokine-induced maximal VCAM1 and ICAM1 expression coincided with the observed maximal leukocyte adhesion to BEC at 24 h. Next, we established a novel flow-based leukocyte adhesion assay coupled with time lapse image acquisition, to mimic more closely the *in vivo* conditions. We successfully cultured and transfected hCMEC/D3 cells in six-channel chambers, connected to a flow system, to study leukocyte-endothelium interactions and firm adhesion. Second, we performed an initial screening of five cytokine-regulated BEC miRs. Of these five, miR-126 and miR-155 appeared to have the most significant effects on leukocyte adhesion to hCMEC/D3cells. We further investigated the roles of miR-126, miR-126* (the complement of miR-126), and miR-155 in leukocyte adhesion to BEC. MiR-126 and -126* were down-regulated in cytokine stimulated BEC. Low levels of miR-126 increased adhesion of both cell lines, while low levels of miR-126* increased THP-1, but reduced Jurkat adhesion. Elevated miR-126 and miR-126* levels significantly prevented Jurkat and THP-1 cell adhesion to BEC both in unstimulated and cytokine-treated conditions. Furthermore, elevated miR-126 partially prevented cytokine-induced VCAM1 and CCL2 expression on BEC and an increased level of miR-126* partially prevented cytokine-induced E-selectin expression. In cytokine stimulated-BEC miR-155 was up-regulated, and decreasing the level of miR-155 reduced both T cell and monocyte adhesion to endothelium and VCAM1 expression both in basal and in cytokine-stimulated conditions. The opposite effect on leukocyte adhesion was observed when miR-155 expression was increased in unstimulated hCMEC/D3 cells, but not in cytokine-stimulated endothelium. These data suggest that miR-155, miR-126 and miR-126* modulate leukocyte adhesion on human brain microvascular endothelium. To our knowledge, this study is the first to report a role for miR-155 and miR-126* in the interactions between human brain endothelium and immune cells and the first to confirm the regulation of VCAM1 and CCL2 by miR-126 in brain endothelium.

# Table of Contents

# List of figures

# List of tables

# Abbreviations

**ADAM9** a disintegrin and metalloprotease domain 9
**AG 0, 1, 4** Acute grade AG 0, 1, 4
**AGO** Argonaute
**AJ** *Adherens* junctions
**AL** Active lesion
**ALCAM** Activated leukocyte cell adhesion molecule
**AP-1** Activator protein-1
**APC** Antigen presenting cells
**AQP4** Aquaporin 4
**AT1R** Angiotensin II type 1 receptor
**ATP** Adenosine triphosphate
**BBB** Blood-brain barrier
**BCRP** Breast cancer resistance protein
**BCSFB** Blood-cerebrospinal fluids barrier
**BEC** Brain endothelial cells
**bEND5** Mouse brain endothelioma cell
**bFGF** Basic fibroblast growth factor
**BSA** Albumin from bovine serum
**CADM1** Cell adhesion molecule 1
**CAL** Chronic active lesion
**CAM** Cell adhesion molecule/s
**CCL** Chemokine (C-C motif) ligand with a number
**CCR** C-C chemokine receptor type with a number
**CEACAM** Carcinoembryonic antigen-related cell adhesion molecule
**CHL1** Cell adhesion molecule 8with homology to L1CAM
**CL** Chronic lesion
**CMFDA** Chloromethylfluorescein diacetate
**CNS** Central nervous system
**CNT2** concentrative nucleoside cotransporter-2
**cP** centipoise
**CRP** Complement regoulatory protein
**CSF** Cerebrospinal fluid
**CX3C** Chemokine fractalkine
**CX3CR1** CX3C chemokine receptor type 1
**CXCL** C-X-C motif chemokine with a number
**CXCR** C-X-C chemokine receptor with a number
**Cy3™** Cyanine 3
**DAPI** 4',6-diamidin-2-fenilindolo
**DGCR8** DGCR8 microprocessor complex subunit
**DMSO** Dimethyl sulfoxide
**EAE** Experimental autoimmune encephalomyelitis
**EBM®-2** Endothelial Basal Medium-2
**EC** Endothelial cells
**EDTA** Ethylenediaminetetraacetic acid
**EGF** Epithelial growth factor

*Egfl7* Epithelial growth factor-like domain 7

**ELAM-1** Endothelial-leukocyte adhesion molecule 1

**ELISA** Enzyme-Linked ImmunoSorbent Assay

**Em** Emission

**ERK** Extracellular signal-regulated kinase

**Est-1** Ever Shorter Telomeres 1

**Ex** Excitation

**FACS** Fluorescence-activated cell sorting

**FADD** Fas-associated protein with death domain

**FAM™** Phosphoramidite

**FBS** Fetal bovine serum

**FOV** Field of view

**GAG** Glicosaminoglycans

**GLUT-1** Glucose transporter-1

**GPCR** G-protein-coupled receptor/s

**h** hours

**HBMEC** Human brain microvessel endothelial cells

**HBSS** Hank's Balanced Salt Solution

**HCEC** Human cerebral endothelial cells

**hCMEC/D3** Human cerebral microvascular endothelial cell line D3

**HEC** High endothelial cells

**HEPACAM** Hepatocyte cell adhesion molecule

**HL-60** Human promyelocytic cell line – 60

**HLA** Human leukocyte antigen

**HLA-DR2b** HLA class II histocompatibility antigen, DRB2 beta chain

**HRPE** Human retinal pigment epithelial cells

**Hsa** *Homo sapiens*

**hTERT** Human telomerase reverse transcriptase

**HUVEC** Human umbelical vein endothelial cells

**ICAM1-5** Intracellular cell adhesion molecule 1-5

**IFN** Interferon

**IFNGR** Interferon-γ receptor

**Ig** Immunoglobulin

**IGF** Insulin-like growth factor

**IgG** Immunoglobulin G

**IKK** I kappa B kinase

**IL** Interleukin

**IRAK1** Interleukin-1 receptor-associated kinase 1

**IRF** IFN regulatory factor

**ISF** Interstitial fluid

**JAK-STAT** Janus kinase- signal transducer and activator of transcription

**JAM** Junctional adhesion molecules

**JNK** c-Jun N-terminal kinase

**LAT1** L-type amino acid transporter 1

**LECAM2** Leukocyte-endothelial cell adhesion molecule 2

**LFA** Lymphocyte function-associated molecule

**LFB** Luxor fast blue

**LNA** Locked nucleic acid
**LPA** Lysophosphatidic acid
**LPS** Lipopolysaccharide
**MADCAM1** Mucosal vascular addressin cell adhesion molecule 1
**MAPK** Mitogen-activated protein kinases
**MCP-1** Monocyte Chemotactic Protein 1 (CCL2)
**MCP-3** Monocyte Chemotactic Protein 3 (CCL7)
**MEK** MAP kinase kinase
**MHC** Major histocompatibility complex
**miR/s** microRNA/s
**mm** millimeters
**MMP** Matrix metalloproteinase
**mRES** miR recognition elements
**MRI** Magnetic resonance imaging
**mRNA** Messenger RNA
**MRP** Multidrug resistance-associated protein
**MS** Multiple sclerosis
**N.d.** Not determined
**N/A** No information available
**NAWM** Normal appearing white matter
**NK** Natural killer
**NK-κB** Nuclear factor kappa-light-chain-enhancer of activated B cells
**nt** Nucleotides
**NVU** Neurovascular unit
**OCNT2** Na-dependent organic cation transporter
**OD** Optical density
**ORFs** Open reading frames
**PAEC** Primary porcine aortic endothelial cells
**PBL** Peripheral blood lymphocytes
**PBMC** Peripheral blood mononuclear cells
**PBS** Phosphate buffered saline
**PCR** Polimerase chain reaction
**PECAM-1** Platelet EC adhesion molecule-1
**pgp-1** p-glycoprotein
**PKC** Protein kinase C
**pMBMEC** primary mouse brain microvascular endothelial cells
**PNS** Peripheral nervous system
**PPMS** Primary progressive form of MS
**PRMS** Progressive relapsing form of MS
**PSGL-1** P-selectin glycoprotein ligand-1
**RhoA** Ras homolog gene family, member A
**RISC** RNA-Induced Silencing Complex
**RPMI** Roswell Park Memorial Institute
**RRMS** Relapsing remitting form of MS
**RT** room temperature
**RT$^2$-qPCR** Real time reverse-transcription quantitative PCR
**s** Seconds

**SCAMP1** Secretory carrier-associated membrane protein 1
**SEM** Standard error of mean
**SI** International system
**SMAD2** Mothers against decapentaplegic 2
**SOCS1** Suppressor of cytokine signalling 1
**SPMS** Secondary progressive form of MS
**Spred1** Sprouty-related, EVH1 domain-containing protein 1
**STAT1** Signal transducer and activator of transcription 1
**SV40** Simian vacuolating virus 40
**TARBP** TAR RNA-binding protein 1
**TEER** Transendothelial electric resistance
**TGFβ** Transforming growth factor-β
**THBMEC** Transfected human brain microvascular endothelial cells
**TJ** Tight junctions
**TM** Thrombomodulin
**TNF** Tumor necrosis factor
**TNF-R1** Tumor necrosis factor receptor 1
**TNF-R2** Tumor necrosis factor receptor 2
**tPA** tissue plasminogen activator
**TRAF6** TNF Receptor associated factor 6
**U** Unit
**UTR** Untranslated region
**VCAM1** Vascular cell adhesion molecule 1
**VE-Cadherin** Vascular endothelial-cadherin
**VEGF** Vascular endothelial growth factor
**VLA-4** Very late antigen-4
**XBP1** X-box binding protein 1
**ZO** *Zonula occludens*

# Chapter 1: Introduction

## 1.1 The blood-brain barrier in health

In the late 19th century, Paul Ehrlich observed that, following injection of water-soluble vital aniline dyes in the peripheral circulation, all organs were stained except the brain and spinal cord [Ehrlich 1885 cited in (Bechmann, Galea et al. 2007)]. Edwin Goldmann observed, some years later, that following injection of aniline dyes in the cerebrospinal fluid (CSF), the central nervous system (CNS) was stained but not peripheral tissues [Goldmann 1913 cited in (Bechmann, Galea et al. 2007)]. These observations suggested that the CNS is a unique anatomical compartment separated from the rest of the body. In 1900 Lewandoski demonstrated that different compounds when injected directly in the brain were highly neurotoxic, while injected intravenously they were not [Lewandowski cited in (Bechmann, Galea et al. 2007)]; this observation led Lewandoski to conclude that the capillary wall can apparently block the access of certain molecules.

The concept of a blood-brain barrier (BBB) was thus established but, it was not until the 1960s, when electron microscopy techniques allowed the identification of the anatomical site of the barrier, that it was discovered that the CNS is tightly sealed from other organs at the level of the endothelial cells (EC) within the CNS vasculature (Reese and Karnovsky 1967; Bodenheimer and Brightman 1968). More recently, the BBB has also been termed the neurovascular unit (NVU) as it has been shown that the barrier properties of the cerebral vasculature is the result of elaborated interactions between many cell types.

The BBB is one of a number of blood-CNS interfaces, which also includes the blood-CSF barrier (BCSFB), the blood-retinal barrier, the blood-nerve barrier and the blood-labyrinth barrier, all of which are important for the physiological function of the CNS (Neuwelt, Bauer et al. 2011). The BBB is one of the three principal barrier sites between blood and brain (Abbott, Patabendige et al. 2010), which constitutes the largest interface for blood-brain exchange with a surface area between 12 and 18 m$^2$ for the average human adult brain [Nag S. and Begley DJ cited in (Abbott, Patabendige et al. 2010)]. A second interface is the above mentioned BCSFB, and the third one is the arachnoid epithelium (Abbott, Ronnback et al. 2006).

### 1.1.1 Localization of the blood-brain barrier

The CNS, formed by the spinal cord and the brain (Fig. 1.1 left), is highly vascularised. All together, it has been estimated that the total perfused cerebral vascular length in the adult human is approximately 600-700 km (Zlokovic 2005). Constant blood supply is critical and fundamental to maintain constant oxygen levels in the brain and the spinal cord. The brain receives blood from the internal carotid arteries and the vertebral arteries which join the circle of Willis, at the base of the brain. These arteries divide into pial arteries, after penetrating into the CNS by the intracerebral arteries, and finally branching into the human brain microvasculature. Arteries branches and narrow into arterioles, then further into capillaries (5-10 μm) inside the CNS parenchyma (Fig. 1.1 right). After the CNS has been perfused, capillaries become post-capillaries venules, venules and veins, with a gradual increase in diameter vessel. The cellular composition of the BBB varies from arteriole, to capillary and to venule (Bechmann, Galea et al. 2007) (Table 1.1). Leukocyte adhesion and

infiltration mainly occurs at the level of post-capillary venules (reviewed in (Engelhardt

and Coisne 2011).
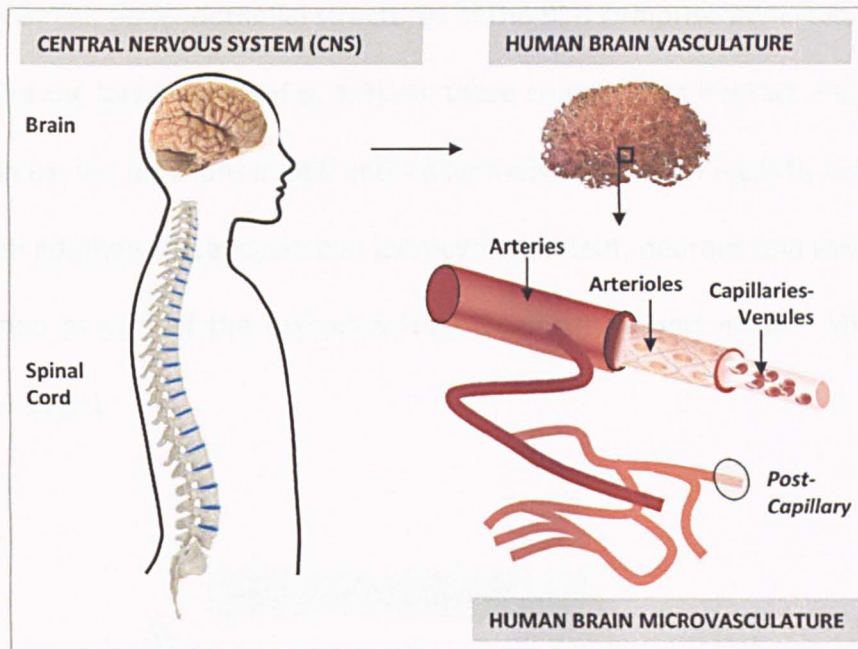


**Fig. 1.1: Central nervous system (CNS) (left) and human brain vasculature and microvasculature (right).** Pictures of brain, spinal cord and human brain vasculature adapted from three sources:
http://riaus.org.au/articles/boffins-use-brain-power-to-fire-gun-15-december-2010/,
http://www.scienzachiropratica.com/visita/,
http://cochin.inserm.fr/departments/3i/group-p.o.-couraud.

| Cell and features | Arteriole | Capillary | Venule |
|---|---|---|---|
| Mean diameter | 30 μm | 8 μm | 20 μm |
| Mean wall thickness | 6 μm | 0.5 μm | 1 μm |
| Smooth muscle cells | + | - | + |
| Pericytes | + | + | + |
| Endothelial tight junctions | N.d. | Belts of TJ | Non specialized |
| Permeability for BBB markers | N.d. | No | Yes |
| Intimate contact between astrocytic end-feet and the vascular wall/perivascular space | No/Yes | Yes/No | No/Yes |
| Perivascular macrophages | + | + | + |

**Table 1.1: Features of the cellular components of the CNS microvasculature.** Abbreviations: + (present), - (absent), **N.d.** (not determined). Table from (Bechmann, Galea et al. 2007) pictures from www.as.miami.edu/chemistry/2086/.../new-chap21_class_part1.htm.

### 1.1.2 The structure of the neurovascular unit

The BBB is formed by the brain endothelial cells (BEC) that line the cerebral microvessels. The periendothelial structures of the BBB comprise pericytes, astrocytes, neurons and the basal lamina (Fig. 1.2). All these components interact and contribute to maintain barrier functions in BEC and, collectively, have been recently referred to as the NVU. In addition to pericytes and astrocytic end-feet, neurons and microglia have been defined as part of the extended NVU (Neuwelt, Abbott et al. 2008; Neuwelt, Bauer et al. 2011).
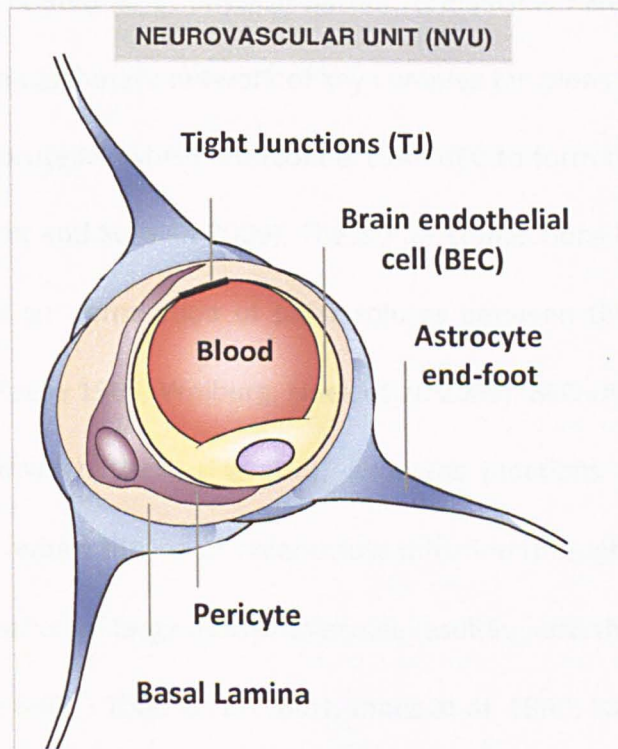


**Fig. 1.2: Cellular structure of the neurovascular unit.** Cross-section of the NVU shows that the microvasculature vessel is formed by a single brain endothelial cell BEC (yellow, nucleus in lilac) closed by tight junctions (black). The EC formed-vessel is surrounded by the basal lamina (pink) which includes pericytes (purple). The astrocyte end-feet (blue) completely surround the basal lamina to maintain the structure of the BBB completing the so-called NVU. Illustration based on (Abbott, Ronnback et al. 2006)

*Brain endothelial cells*

The BEC are the cells of the BBB that represent the interface between the blood (luminal membrane surface) and the brain (abluminal membrane surface). BEC are considered the main anatomical site of the BBB for their unique characteristics which distinguish them from all other EC. Morphologically, the cytoplasm of BEC has a uniform thickness with very few pinocytotic vesicles. It lacks fenestrations (Abbott, Ronnback et al. 2006) and has a high number of mitochondria compared with non-CNS EC.

Structurally, BEC express a unique feature essential for their biological barrier function, mainly related to a 'physical barrier' (Persidsky, Ramirez et al. 2006). This feature involves an elaborate network of key complex junctions (Fig. 1.3) composed by transmembrane proteins, which interconnect the BEC to form the brain microvascular vessels (Engelhardt and Sorokin 2009). These interconnections between the EC tightly regulate paracellular permeation of polar solutes between the blood and the brain (Brightman and Reese 1969; Wolburg, Noell et al. 2009). BEC express two types of cell-cell junctions between them (Fig. 1.3), *adherens* junctions (AJ) and unique tight junctions (TJ). TJ reduce the ion or polar solute diffusion through the paracellular space and block penetration of large macromolecules resulting into the high *in vivo* electrical resistance of the BBB, >1000 $\Omega \cdot cm^2$ (Butt, Jones et al. 1990; Santaguida, Janigro et al. 2006). TJ are formed by occludin, claudins and junctional adhesion molecules (JAM) (Abbott 2000; Wolburg and Lippoldt 2002; Wolburg, Noell et al. 2009; Alsam, Kim et al. 2003). Occludin and claudins are four transmembrane molecules with two symmetrical loops.
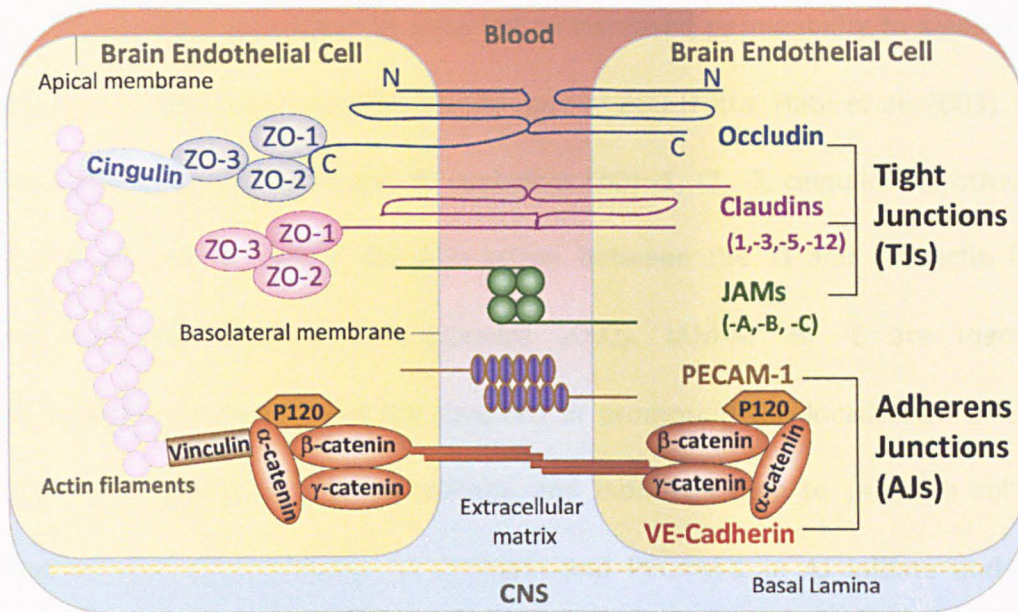
**Fig. 1.3: Simplified and partially incomplete scheme showing the molecular composition and structure of brain endothelial junctions.** Luminal side (blood, red), BECs (yellow) and apical side (CNS, blue) of the BBB. Representation of tight junctions (TJ) and *adherens* junction (AJ) structures at the interface between EC plasma membranes. Transmembrane proteins of the TJ include occludin, claudins (for example, claudin-3, -5, -12) and JAM (for example, JAM-A, -B and -C). AJ are composed by PECAM-1 (platelet EC adhesion molecule-1) and vascular endothelial (VE)-cadherin. Schematic representation based on illustrations in (Abbott 2000; Gonzalez-Mariscal, Betanzos et al. 2003; Stamatovic, Keep et al. 2008; Engelhardt and Sorokin 2009; Abbott 2010).

Occludin was the first integral TJ transmembrane protein described (Furuse, Hirase et al. 1993). The first extracellular loop is mostly involved in intercellular adhesion, while the second one is responsible for transendothelial electrical resistance (TEER) regulating the TJ (Nusrat, Brown et al. 2005). Claudins are the principal barrier-forming proteins, and they belong to the claudin family formed by more than twenty different isoforms (1-20) with unique patterns of expression in different tissues. BEC possess claudins-1,-3, -5 and -12 (Stamatovic, Keep et al. 2008; Verma, Kumar et al. 2010). Claudin-5 is a major adhesion molecule in TJ specifically and highly expressed by BEC with a key role in BBB permeability (Nitta, Hata et al. 2003). It has been shown that

loss of claudin-5 expression in mice led to increased permeability to small molecules through an otherwise morphologically normal BBB (Nitta, Hata et al. 2003). Occludin and claudins are linked to *zonula occludens* (ZO) -1, -2, -3, cingulin and other protein complexes, which control the interaction between the TJ and the actin filaments (cytoskeleton) (Wolburg and Lippoldt 2002). JAM-A, -B, -C are members of immunoglobulin family and are involved in promoting the localization of ZO-1 and occludin at points of cell-cell contact, and indirectly help to establish cell polarity (Bazzoni and Dejana 2004). VE-cadherin and PECAM-1 in AJ initiate and maintain endothelial cell-cell contact holding the BEC together to give structural support. In addition they are essential for TJ formation during development and it has been reported that their disruption leads to the BBB breakdown (Wolburg and Lippoldt 2002). AJ are linked to actin filaments by a complex of proteins – $\alpha$- and $\beta$-catenins, vinculin and $\alpha$-actinin (reviewed in (Ebnet 2008)).

In order to provide the CNS with necessary nutrients and remove waste products, the BEC also constitute a 'transport barrier' that regulates the transport of micronutrients and macronutrients in and out of the CNS parenchyma (for a review see (Begley 2003; Abbott, Ronnback et al. 2006). Moreover BEC regulate a key physiologic event such as leukocyte trafficking in immunologically-mediated diseases (Persidsky, Ramirez et al. 2006).

The blood-stream surface of BEC has a 0.4 µm thick layer of irregularly shaped membrane-bound glycocalyx, which contains glycosaminoglycans (GAG) including heparan sulphate, chondroitin sulphate and hyaluronan (Reitsma S 2007). It has been demonstrated that the principal role of the glycocalyx is to maintain plasma and vessel wall homeostasis, acting as 'barrier of the barrier' to transvascular exchanges of fluid

and macromolecules (Weinbaum, Tarbell et al. 2007). Moreover, the glycocalyx being negatively charged, it contributes to maintain the antiadhesive nature of the EC surface, preventing leukocyte adhesion (Constantinescu, Vink et al. 2003).

### *Pericytes*

Pericytes were described in the late 1800s by Rouget, a French scientist, and were initially called the Rouget cells (reference cited in (Dore-Duffy and Cleary 2011)). In the early 1900s, Rouget's finding was confirmed by Doré and due to their anatomical location, abluminal to the BEC and luminal to the parenchyma, the Rouget cell was renamed as pericyte (Dore-Duffy and Cleary 2011). Although pericytes were discovered almost 150 years ago, their biology was investigated only recently. Pericytes are flat and undifferentiated connective tissue cells which are uniquely located at the abluminal surface of EC of different tissues, more abundantly in the CNS. At the NVU, pericytes are located within the capillary basal lamina (Fig. 1.2) surrounding the BEC (Engelhardt and Sorokin 2009). The association of pericytes with blood vessels suggested that they may regulate BEC proliferation, survival, migration, differentiation and vascular branching (Lai, Kuo et al. 2005). It has been reported that pericytes (i) regulate the permeability of the BBB (Armulik, Genove et al. 2010), thereby modulating BBB-specific gene expression patterns in EC, and, inducing polarization of astrocytic end-feet surrounding blood vessels. However, pericytes are also located in non-CNS tissues, suggesting that astrocytes may be an important helper for pericytes; (ii) regulate BBB maturation during development, including the formation of TJ and vesicle trafficking in BEC (Daneman, Zhou et al. 2010); (iii) control neurovascular function, integrity and phenotype, thereby maintaining the

microcirculation at the capillary level and modulating blood flow thanks to the expression of contractile proteins and serum proteins uptake and/or distribution (Peppiatt, Howarth et al. 2006; Bell, Winkler et al. 2010). Moreover, pericytes are thought to constitute a second barrier of defence due to their ability to phagocytose (Dore-Duffy 2008), to play a critical role in both angiogenesis and vasculogenesis (Kamouchi, Ago et al. 2011), and to help maintain high TEER (Garberg, Ball et al. 2005). All these studies indicate that pericytes are essential for the maintenance of all the key functions and structure of NVU, suggesting that pericyte loss results in neurovascular dysfunction leading to neurodegenerative diseases.

### *Basal lamina*

BEC are connected to astrocytic end-feet by a thin and continuous layer of basal lamina that also surrounds pericytes (Fig. 1.2). The basal lamina is extracellular matrix composed of more than 27 proteins including collagen type IV, elastin, fibrillin, laminin, fibronectin, fibrinogen and tenascin, which together contribute to maintain a negatively charged interface (Scherrmann 2002). The basal lamina also contains cell adhesion molecules (CAM) and integrins at the endothelial abluminal surface (Persidsky, Ramirez et al. 2006; Engelhardt and Sorokin 2009), and neural cell adhesion molecules L1 (Chun, Scott et al. 2011). BEC, astrocytes and pericytes all probably contribute to form the basal lamina. *In vitro*, pericytes secreting laminins induced BEC to secrete basal lamina components (Brachvogel, Pausch et al. 2007). Matrix metalloproteinases (MMP), in particular MMP9, affect the integrity of the BBB related to basal lamina degradation (Rosenberg 2002; Rosell, Cuadrado et al. 2008). Disruption

of the basal lamina can lead to BBB breakdown due to alterations in BEC cytoskeleton and TJ protein expression (Stolp and Dziegielewska 2009).

### *Astrocytes*

Astrocytes are characteristic star-shaped glial cells that envelop 99% of the BBB endothelium with their astrocytic perivascular end-feet (Hawkins and Davis 2005, Will and Doris 2008). Astrocytes have a number of important physiological functions that help maintain the function of the NVU (Dong and Benveniste 2001). One of their main functions is to induce and modulate the development of the specific BEC phenotype (Davson and Oldendorf 1967) and contribute to the structural and functional integrity of the BBB (Dong and Benveniste 2001). Astrocytes are essential for proper neuronal function, and the low distance (10 µm) of the neuronal body from the vessels indicates that the astrocyte and BEC interactions are essential for a functional NVU.

In cell culture studies, it was observed that astrocytes can up regulate many BBB features leading to tighter cell-cell junctions and to the expression and polarized localization of transporters and of specialized enzyme systems, but the factors responsible for inducing these features are not yet fully established (Abbott, Ronnback et al. 2006). For example, the astrocytic perivascular end-feet appear to regulate water transport as evidenced by the polarized expression of aquaporin-4 (AQP4) on the astrocytic terminals (Satoh, Tabunoki et al. 2007). Indeed, recent studies have extensively shown that astrocytes are able to secrete a range of agents that induce the barrier phenotype *in vitro*, suggesting that the cross-talk between BEC and astrocytes is crucial for maintaining the BBB phenotype.

*Neurons*

Due to their activity and to the dynamic nature of their metabolic needs, neurons require a tight regulation of the microcirculation and tissue supply of metabolites. There is a close relationship between neurons and astrocytes that modulate microvessel blood flow by constriction and dilatation and that regulate the entry of nutrients and oxygen to the CNS when necessary (Lee and Benveniste 1999).

## 1.2 Functions of the blood-brain barrier

The BBB is a highly specialized and sophisticated barrier that changes its features in accordance with the needs of the CNS (Willis and Davis 2008). The BBB has several roles, the predominant one being the regulation of the brain microenvironment through several functions, all focused on the homeostasis of the brain (Abbott, Ronnback et al. 2006).

### 1.2.1 Physical barrier

The main function of the BBB is to regulate the passage of substances from the blood to the brain (and vice-versa) maintaining the homeostasis of the neural microenvironment that is crucial for neuronal activity and function (Abbott, Ronnback et al. 2006). The presence of TJ limits paracellular diffusion of hydrophilic molecules (water-soluble agents) across the BBB (Engelhardt 2008). Small lipid-soluble agents such as barbiturates and ethanol can diffuse freely through the phospholipid membrane (Abbott, Ronnback et al. 2006). The BBB is a strictly regulated gate between CNS and peripheral nervous system (PNS), restricting entry not only of blood-

borne cells thereby constituting a barrier for leukocyte trafficking, but also of neurotoxins and macromolecules (Abbott, Patabendige et al. 2010).

### 1.2.2 Transport barrier

The function of the BBB goes beyond a simple compartmentalization between the blood and the interstitial fluid (ISF) of the brain. The BBB regulates the ability of some solutes to cross from one compartment to the other (Neuwelt, Abbott et al. 2008). Indeed, the BBB supplies the brain with essential nutrients (influx) and mediates the efflux of many waste products (Abbott, Ronnback et al. 2006) by the actions of several fundamental brain endothelium transport proteins (carriers). Blood-to-brain influx transporters (passive carriers or secondary active transporters) include, for example, glucose transporter-1 (GLUT-1), L-type amino acid transporter 1 (LAT1), concentrative nucleoside cotransporter 2 (CNT2) and Na-dependent organic cation transporter (OCTN2) which supply glucose, amino acids, nucleosides and other substances to the brain (Abbott, Ronnback et al. 2006; Ohtsuki and Terasaki 2007). Drug efflux pumps, the most important element of the barrier to limit movement of drugs and toxins, are the adenosine triphosphate (ATP)-binding cassette transporters, so-called ABC-transporters, a large super family of 48 members in humans, including p-glycoprotein (pgp), breast cancer resistance protein (BCRP) and the multidrug resistance-associated protein (MRP) (Begley 2004). Brain-to-blood efflux transporters prevent accumulation of metabolites and neurotoxic compounds in the brain (for a review see (Ohtsuki and Terasaki 2007)). In addition, the BBB regulates ionic traffic, with specific ion transporters and channels, that provide an optimal composition for neuronal and synaptic signalling (Abbott, Patabendige et al. 2010).

### 1.2.3 Enzymatic and Metabolic barrier

The BBB expresses asymmetrically localized enzymes (Abbott, Ronnback et al. 2006; Biegel 2005) such as peptidase and nucleotidase at the abluminal membrane to metabolize peptides and ATP, whereas at the luminal membrane, it presents enzymes such as γ-glutamyl transpeptidase, alkaline phosphatase (Pardridge 2005), cytochrome P450 that can inactivate neuroactive and toxic compounds and aromatic acid decarboxylase to metabolize drugs and nutrients (Abbott, Ronnback et al. 2006; Persidsky, Ramirez et al. 2006). Also substances that act as neurotransmitters such as monoamines or dopamine are taken up by brain capillaries and transformed and released as inactive products from BEC (Betz 1986).

### 1.2.4 Immune barrier

The BBB is more than a metabolic and transport barrier, it possesses a very important neuroimmune function. It secretes substances such as cytokines, chemokines, prostaglandins and nitric oxide (Persidsky, Ramirez et al. 2006) which can be secreted either in the blood or in the CNS compartments. Indeed, the BBB is unique in that, it can receive stimulation from one compartment and at the same time respond by secretion of immunomodulators into another one. Furthermore, the constant cross-talk between neurons, astrocytes, pericytes and BEC influences BBB function in the context of immune regulation, and the ability of this unit to communicate with circulating leukocytes forms a major basis for neuroimmune interactions (Quan and Banks 2007; Neuwelt, Abbott et al. 2008).

## 1.3 Cell trafficking and blood flow at the blood-brain barrier

### 1.3.1 Immunosurveillance

Under physiological conditions, immune cells exert their immunological function mainly through direct contact with antigens. In order to do this, lymphocytes have to navigate through blood vessels and across the EC to the target organs; this process is called homing or immunosurveillance. In the past, because of the presence of the BBB, the CNS was described as an immune privileged site where there was complete absence of immunosurveillance, but later studies demonstrated physiological trafficking of leukocytes (T and B cells, monocytes and others) across the BBB to screen the CNS parenchyma for antigens and re-enter the blood stream (Hickey 1991). Leukocyte traffic into the CNS is very low, tightly controlled and occurs solely at the post-capillary venules level (Engelhardt 2006). However, studies of leukocyte entry into the non-inflamed CNS produced contrasting results, possibly due to different experimental approaches (Engelhardt and Ransohoff 2005).

Blood-borne lymphocytes can reach the CNS through several routes via: 1) the choroid plexus, 2) the subarachnoid space, and 3) the EC of brain vessels and circumventricular organs (Ousman and Kubes 2012), but immune cells have to overcome one of the CNS barriers at some point (Engelhardt and Ransohoff 2005; Loeffler, Dietz et al. 2011). Leukocyte trafficking for extravasation across the BBB is a multi-step process (Butcher 1991; Springer 1994), where leukocytes, recruited from the blood, are (1) captured by the endothelium with immediate arrest as there appears not to be any rolling (Vajkoczy, Laschinger et al. 2001), (2) and then activated

for (3) adhesion and (4) transmigration. This process and the molecules involved will be described in Section 1.4.4 in the context of inflammation.

## 1.3.2 Central nervous system blood flow and leukocyte recruitment

The blood is a suspension of red blood cells, white blood cells (leukocytes), and platelets in plasma. Blood plasma is an incompressible Newtonian fluid with dynamic viscosity about 1.2 cP (centipoise) = 0.012 gram per centimetre-second (= 0.0012 Pascal second, SI for dynamic viscosity), but during inflammation, blood cells are highly concentrated at specific sites and influence the blood rheological properties. Leukocytes are spherical, 6-8 μm in diameter, not greatly deformable and constitute only 1% of the total volume of blood. Leukocytes were not usually used to study hemodynamic flow, reproduced in glass microvessels *in vitro*, but recent studies reported that leukocytes are critical for the resistance to flow due to their interaction with BEC (Sugihara-Seki 2001; Sugihara-Seki and Schmid-Schonbein 2003).

In microvessels with a diameter smaller that 25 μm, every leukocyte that adhered to the endothelial surface, increased significantly the flow resistance (Sugihara-Seki and Schmid-Schonbein 2003; Fu, Adamson et al. 2005). In addition, the geometry and topology of the vasculature influence the blood flow, depending on how the individual vessels connect to each other, and how the circulating cells are distributed (Hirsch, Reichold et al. 2012). Decreases in vessel lumen (Fig. 1.4) have been shown to lead to fewer blood-borne cells passing through the vessel and decreased blood viscosity (Papaioannou and Stefanadis 2005). Moreover, due to the high physical plasticity of brain capillaries, the geometry of the vessel appears to adapt to abnormal physiological and metabolic conditions as a result of increases or

decreases in blood flow when needed. Within the microvessels, exchange of cells and

molecules takes place contributing to pressure changes (Ito, Kanno et al. 2003).

The blood velocity of the rat microvasculature has been measured with different

techniques, and appears to vary between 0.34 to 3.15 mm/s (Hudetz, Feher et al.

1996), 0.7 to 4.6 mm/s (Ma, Koo et al. 1974) and 0.5 to 1.5 mm/s in rat cerebral

capillaries (Ivanov, Kalinina et al. 1981). In humans, blood velocity is similar, from 0.52

to 3.26 mm/s, measured at the conjunctival pre-capillary level (Koutsiaris, Tachmitzi et

al. 2010).
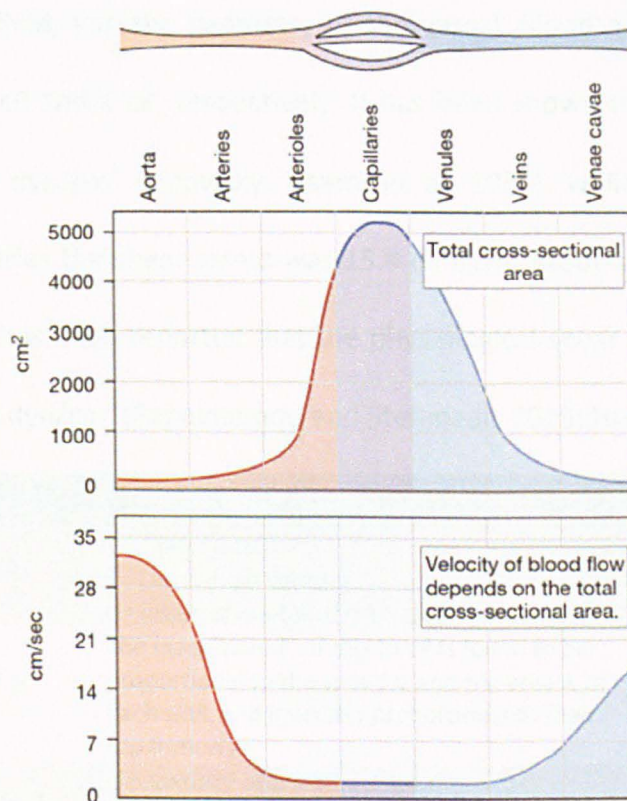


**Fig. 1.4: Blood flow along the vascular tree. Cartoon.** Relative cross-sectional area of different vessels of the vascular bed, capillaries in the middle. **Top graph.** Total cross-sectional area in cm$^2$ in different vessel types. **Bottom graph.** Blood flow velocity in cm/s in different vessel types. Capillaries possess the highest cross-sectional area, since they have the lowest blood flow velocity. From
http://faculty.pasadena.edu/dkwon/chapter%2015/chapter%2015_files/textmostly/slide16.html

### 1.3.3 Shear stress in blood vessels

The hemodynamic conditions inside blood vessels promote superficial stresses near the vessel walls: the circumferential stress (due to the pulse pressure variation inside the vessels), and the shear stress due to the blood flow against the vessel walls. It has been found that in the microvasculature the flow is laminar, which is characterized by flow in parallel layers due to unvaried pressure (Hirsch, Reichold et al. 2012). Shear stress will be further described as follow. Shear stress ($\tau$) (Table 1.2) depends on shear rate ($\gamma$) and dynamic viscosity ($\mu$), which are related to the properties of the fluid, and the geometry of the vessel. Blood and water`s dynamic viscosities are 1.2 cP and 1 cP, respectively. It has been shown that in cat capillaries shear stress is 40 dyn/cm$^2$ (Lipowsky, Usami et al. 1980), while in normal human conjunctival capillaries the shear stress was 15.4 dyn/cm$^2$ (Koutsiaris, Tachmitzi et al. 2007). However it has been reported that the physiological shear stress in small veins is on average 0.5-6 dyn/cm$^2$ (Papaioannou and Stefanadis 2005; Hudetz 1996).

| Parameter | Equation | Definitions | Unit |
|---|---|---|---|
| Shear rate ($\gamma$) | $\gamma = \dfrac{8v}{d}$ | $\gamma$ = Shear rate<br>$v$= Linear fluid velocity<br>$d$= Inside diameter of the vessel | [1/s] |
| Dynamic viscosity ($\mu$) (mu) | $F = \mu A \dfrac{u}{y}$ | The magnitude $F$ of this force is found to be proportional to the speed $u$ and the area $A$ of each wall, and inversely proportional to their separation $y$. | cP(centipoise)<br>1cP= 1mPa s<br>=[0.01dyn.s/cm$^2$]<br>= $\eta$ (eta) |
| Flow rate ($\Phi$) | $\Phi = v \cdot A$ | $V$ = Velocity of the blood flowing<br>$A$ = Cross sectional vector of the vessel | $\Phi$ [ml/min] |
| Shear stress ($\tau$) | $\tau = \mu \cdot \gamma$ | Newtonian fluids flowing upon a planar surface<br>$\tau$ = Shear stress<br>$\gamma$ = Shear rate<br>$\mu$ = Dynamic viscosity | [dyn/cm$^2$] |

Table 1.2: **Parameters to determine shear stress for vessel blood flow.** Assuming that the vessel is inelastic, cylindrical and straight, and, the blood is a Newtonian fluid and flow is laminar, the Haagen-Poiseuille equation indicates that the shear stress is directly proportional to blood shear rate and inversely proportional to vessel diameter From (Sirs 1991; Sutera and 1993).

### 1.3.4 Shear stress on endothelial cells

Shear stress on the endothelium activate various downstream pathways that result in alteration of EC functions (for a review see (Ando and Yamamoto 2013)). Different levels of shear stress at different times act on the so-called shear stress sensors in EC (Fig. 1.5), such as CAM, cell-cell matrix adhesion molecules, G-protein coupled receptors and the glycocalyx. For example, variations in flow may change the glycocalyx conformation on EC, when randomly coiled heparan sulphate proteoglycans become unfolded. This conformational change results in exposure of binding sites for $Na^+$, facilitating its transport by concentration gradient as well as transport of other ions, growth factors and amino acids.
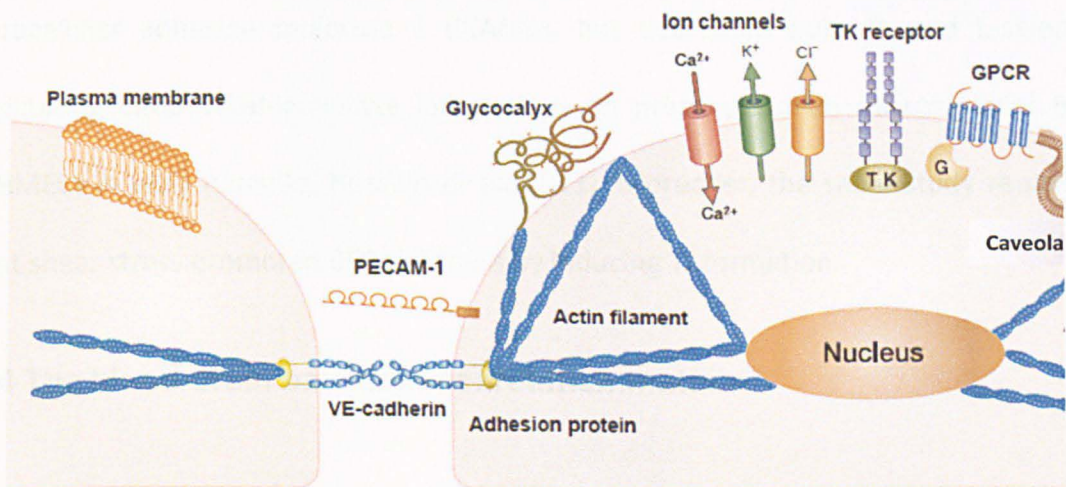


**Fig. 1.5: Shear stress sensors. Ion channels.** Ion channels including $K^+$ channels, $Cl^-$ channels, and $Ca^{2+}$ channels have been shown to be shear-stress-responsive. **GPCRs** have been shown to be activated by shear stress. **Caveola.** Caveolae membrane microdomains containing a variety of receptors, ion channels, and signalling molecules, and their component protein, caveolin-1, have been demonstrated to be involved in shear stress sensing and response mechanisms. **Adhesion proteins.** Cell-cell and cell-matrix attachment are subjected to tension under shear stress, resulting in the activation of downstream signal transduction pathways. PECAM-1 and AJ (VE-cadherin). **Cytoskeleton** is responsible for cell shape regulation and its components such as actin filaments and microtubules may directly sense mechanical forces that deform cells. **Glycocalyx.** Random-coiled glycocalyx unfolds into a filament structure under flow. **Plasma membrane.** Shear-stress-induced changes in the physical properties of the plasma membrane lead to activation of various membrane-associated molecules and microdomains. Adapted from (Ando and Yamamoto 2013).

Shear stress can also affect the passage of blood through narrow capillaries and leukocyte adhesion and their interactions with EC in post-capillary venules (Lawrence, Kansas et al. 1997; Lipowsky and Lescanic 2013). It has been shown that shear stress down-regulated vascular adhesion molecule 1 (VCAM1) expression on the cell surface of EC in mouse venules (Ohtsuka, Ando et al. 1993) and at the messenger RNA (mRNA) level in a time-dependent manner (1 to 24 h) *in vitro* (Ohtsuka, Ando et al. 1993; Korenaga, Ando et al. 1997). Furthermore, a decrease in the number of endothelium-adhered lymphocytes cultured from mouse lymph nodes was observed (Ando, Tsuboi et al. 1994). Contrastingly, Cucullo reported that long exposure (days) to shear stress increased transcription of relevant adhesion molecules such as VCAM1 and intracellular adhesion molecule 1 (ICAM1), but decreased both P- and E-selectin facilitating endothelial-leukocyte interactions on primary human microvascular BEC (HBMEC) *in vitro* (Cucullo, Hossain et al. 2011). Moreover, the same study reported that shear stress promoted BEC tightness by inducing TJ formation.

## 1.4 The blood-brain barrier in neuroinflammation

Alterations in BBB function have been observed in many CNS pathologies (Table 1.3). In neuroinflammation, the modifications at the level of BBB are related to two main events: BBB breakdown and BBB activation. The first one implies an increase of endothelial permeability and alteration of junctional components (and also possibly of transporters). BBB activation is related to the capacity of BEC, astrocytes and pericytes to express and secrete immune factors able that influence the recruitment of leukocytes from the blood to the brain (Alvarez, Cayrol et al. 2011). These alterations

in BBB function are usually identified through histological analysis in brain samples or by using imaging techniques such as magnetic resonance imaging (MRI). To understand these two pathogenic events, it is fundamental to first describe some key elements involved in BBB inflammation in the next paragraphs.

## Pathological states involving BBB breakdown or disorder

### Stroke
• Astrocytes secrete transforming growth factor-β (TGFβ), which down-regulates brain capillary endothelial expression of fibrinolytic enzyme tissue plasminogen activator (tPA) and anticoagulant thrombomodulin (TM).

• Proteolysis of the vascular basement membrane/matrix.

• Induction of AQP4 mRNA and protein at the sites of BBB disruption.

• Decrease in BBB permeability after treatment with arginine vasopressin V1 receptor antagonist in a stroke model.

### Trauma
• Bradykinin, a mediator of inflammation, is produced and stimulates production and release of interleukin-6 (IL-6) from astrocytes, which leads to opening of the BBB.

### Infectious or inflammatory processes
Examples include bacterial infections, meningitis, encephalitis and sepsis.

• The bacterial protein lipopolysaccharide affects the permeability of BBB tight junctions. This is mediated by the production of free radicals, interleukin (IL)-6 and IL-1β.

• Interferon-β prevents BBB disruption.

### Multiple sclerosis
• Breakdown of the BBB.

• Down-regulation of laminin in the basement membrane.

• Selective loss of claudin 1/3 in experimental autoimmune encephalomyelitis.

### HIV
• BBB tight junction disruption.

### Alzheimer's disease
• Increased glucose transport, up-regulation of glucose transporter GLUT1, altered agrin levels, up-regulation of AQP4 expression.

• Accumulation of amyloid-β, a key neuropathological feature of Alzheimer's disease, by decreased levels of P-glycoprotein transporter expression.

• Altered cellular relations at the BBB, and changes in the basal lamina and amyloid-β clearance.

### Parkinson's disease
• Dysfunction of the BBB by reduced efficacy of P-glycoprotein.

### Epilepsy
• Transient BBB opening in epileptogenic foci, and up-regulated expression of pgp-1 and other drug efflux transporters in astrocytes and endothelium

### Brain tumours
• Breakdown of the BBB.

• Down-regulation of tight junction protein claudin 1/3; redistribution of astrocyte AQP4 and Kir4.1 (inwardly rectifying K⁺ channel).

### Pain
• Inflammatory pain alters BBB TJ protein expression and BBB permeability.

**Table 1.3: Diseases of the CNS involving blood-brain barrier breakdown.** From (Abbott, Ronnback et al. 2006).

### 1.4.1 Blood-brain barrier activation

Inflammation in the CNS is characterized by the development of activated, adhesive and inflamed BEC which mediate the adhesion and migration of activated leukocytes (Hickey 1991). During this process, there is production of proinflammatory cytokines/chemokines (Olson and Ley 2002) and increased expression of endothelial CAM which lead to the recruitment of immune cells from the blood (Bartholomaus, Kawakami et al. 2009).

### 1.4.2 Role of proinflammatory mediators (cytokines and chemokines) in neuroinflammation

Cytokines are soluble polypeptides, generally associated with inflammation, immune activation and cell differentiation or death (Allan and Rothwell 2001). Cytokines found in early stages of neuroinflammation include IL, interferons (IFN), tumor necrosis factors (TNF), chemokines and growth factors (Allan and Rothwell 2001). The most studied cytokines in CNS inflammation that contribute to early brain injury are TNFα, INFγ, IL-1 and IL-6 (de Vries, Blom-Roosemalen et al. 1996) (Feghali and Wright 1997).

*Cytokines*

Human TNFα or cachectin is a trimer of 17 kDa involved in acute inflammation (Vilcek and Lee 1991). TNFα expression is induced in inflammation and in autoimmune

diseases and its increase precedes that of most other cytokines in CNS disorders (Allan and Rothwell 2001). TNFα has been considered as a possible master inflammatory regulator (Kraft, McPherson et al. 2009); It is produced by activated macrophages/monocytes, fibroblasts, mast cells, some T and natural killer (NK) cells (Vilcek and Lee 1991), and by BEC (Verma, Nakaoke et al. 2006).

TNFα acts through its two receptors TNF-R1 and TNF-R2 (Vandenabeele, Declercq et al. 1995; Pober 2009), that are differentially controlled and expressed in human EC (Bradley, Thiru et al. 1995) and in the BEC line, human cerebral microvascular endothelial cell line D3 (hCMEC/D3) (Lopez-Ramirez, Fischer et al. 2012). Moreover, TNFα has been demonstrated to be relocated from the apical surface (bloodstream) to the cytoplasmic side by TNF-R1 and -R2 (Pan and Kastin 2007) and mouse BEC can respond to activation from one side of the neuroimmune axis by releasing cytokines into the other (Verma, Nakaoke et al. 2006). TNF-R1 and -R2 activation by TNFα (Fig. 1.6) has been shown to lead to the downstream activation of nuclear factor kappa-light-chain of activated B cells (NF-κB), JNK and p38MAPK signalling pathways which trigger diverse biological responses (see (Montgomery and Bowers 2012) for a review).

In particular, TNFα has been shown to induce overexpression of multiple CAM by BEC (Butcher 1991; Kallmann, Hummel et al. 2000; Wosik, Biernacki et al. 2007), and to promote leukocyte adhesion and migration to the CNS (see (Pober 2002) for a review). In addition, increases in leukocyte adhesion to TNFα–stimulated mouse aortic and human BEC (SV-HCEC) *in vitro* have been previously reported (Butcher 1991; Chandrasekharan, Siemionow et al. 2007; Dasgupta, Yanagisawa et al. 2007). Other

actions of TNFα on the BBB include an increase in permeability altering the expression and localization of endothelial TJ proteins (Lopez-Ramirez, Fischer et al. 2012).
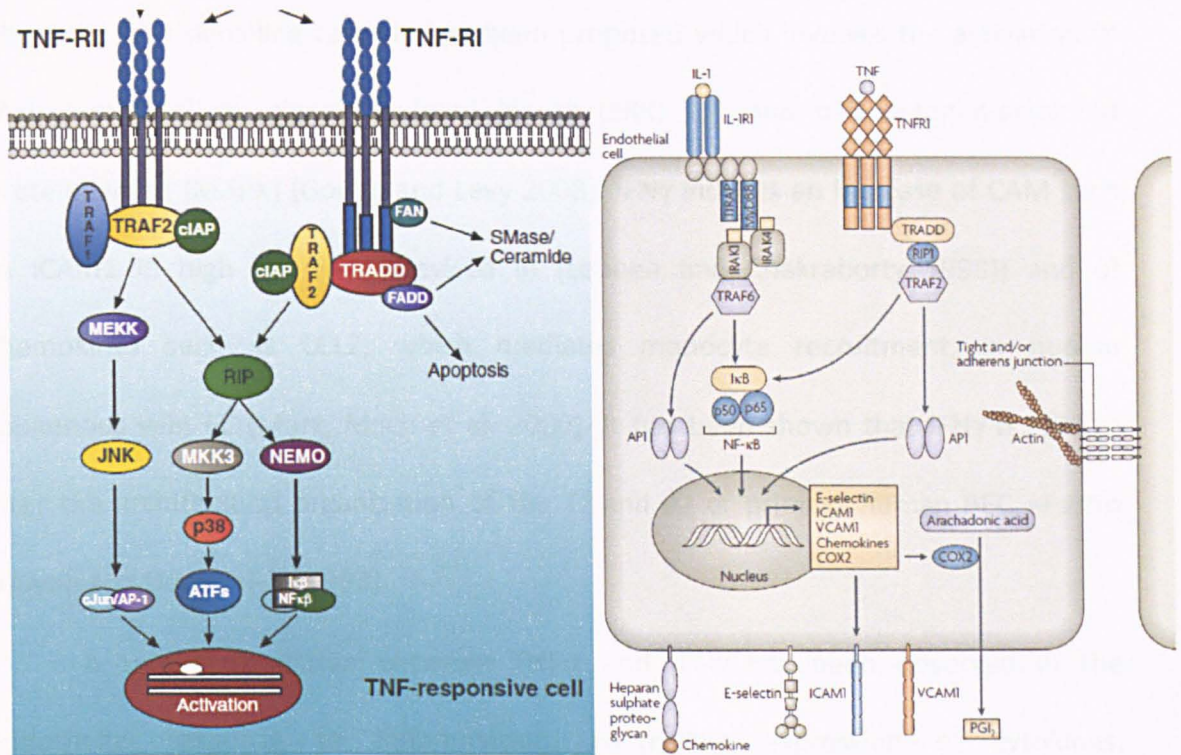


**Fig. 1.6: TNFα signalling pathways through TNF-R1 and -R2. Left.** Canonical pathway of TNFα signalling through TNF-R1 and -R2. **Right.** Human TNFα signalling through TNF-R1 which is partly shared by the IL-1 signalling pathway. Adapted from (Montgomery and Bowers 2012) and (Pober and Sessa 2007).

Human IFNγ or immune interferon is a homodimer of 20 kDa and belongs to the type II group of interferons (Boehm, Klamp et al. 1997). IFN-γ is a pleiotropic cytokine whose expression has been associated with a number of inflammatory and autoimmune diseases (Schoenborn, Wilson et al. 2007) and it has been reported to be produced by activated T cells and NK cells (Boehm, Klamp et al. 1997). The functional IFNγ receptor (IFNGR) is constitutively expressed by human brain endothelium (Lopez-Ramirez, Fischer et al. 2012), and its activation by homodimeric IFNγ initiates the Janus kinase- signal transducer and activator of transcription (JAK-STAT) pathway (Fig. 1.7),

which is a common pathway for numerous cytokines, activating transcription factors including IFN regulatory factor-1 (IRF-1) and NF-κB (Gough, Levy et al. 2008). An alternate IFNγ signalling cascade has been proposed which involves the activation of MEK1/ extracellular signal-regulated kinase (ERK) 1/2 and p38 mitogen-activated protein kinase (MAPK) (Gough and Levy 2008). IFNγ induces an increase of CAM such as ICAM1 in high EC (HEC) (revised in (Ledeen and Chakraborty 1998)) and of chemokines such as CCL2, which mediates monocyte recruitment, in human saphenous vein EC (Marx, Mach et al. 2000). It has been shown that IFNγ is able to alter the architectural organization of the TJ and AJ of primary human BEC *in vitro* (Huynh and Dorovini-Zis 1993).

A synergistic action between TNFα and IFNγ has been observed in the endothelial response to inflammation, controlling expression of cytokines, chemokines, chemokine receptors and cell surface molecules (Cassatella, Gasperini et al. 1997; Ohmori, Schreiber et al. 1997; Piali, Weber et al. 1998; Hillyer, Mordelet et al. 2003; Matsumiya, Ota et al. 2010). In a microarray analysis revealing genes modulated by TNFα and IFNγ in primary microvascular and macrovascular human EC, it appeared that expression of cytokines, chemokines and CAM was most altered in cytokine-activated endothelium (Sana, Janatpour et al. 2005). The main mechanism to explain the synergistic effect of TNFα and IFNγ on these genes, focused on signal transducers and activators of transcription 1 (STAT1), activated by IFNγ, and NF-κB activated by TNFα (Lombardi, Cantini et al. 2009). As previously described, these two signalling molecules, when translocated to the nucleus from the cytoplasm, induce transcriptional activation of several genes encoding cytokines and CAM.
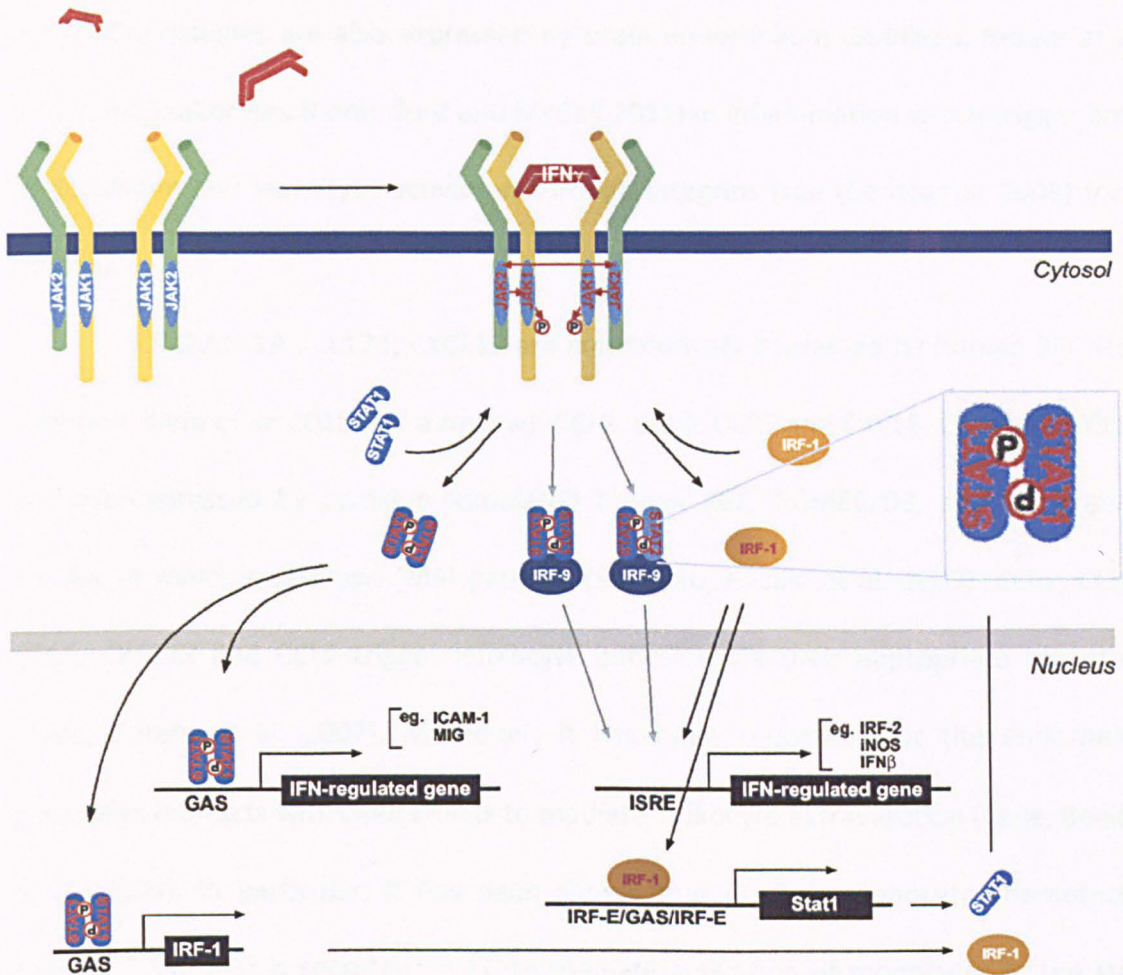
**Fig. 1.7: Human IFNγ signalling pathway through IFNGR.** Adapted from (Schroder, Hertzog et al. 2004).

*Chemokines*

Chemokines are a superfamily of chemoattractant cytokines of 8-10 KDa that includes CC, CXC, and CX3 subfamilies of ligands and their GPCRs. Chemokines are complex and critical extracellular mediators of inflammation and immune system development, which direct important events such as leukocyte chemotaxis, adhesion to endothelium and migration (Baggiolini 1998; Sallusto and Baggiolini 2008). Chemokines and their receptors are expressed and secreted by microglia/macrophages, astrocytes and neurons in the CNS (Mennicken, Maki et al.

1999). Chemokines are also expressed by brain endothelium (Subileau, Rezaie et al. 2009) and leukocytes (Comerford and McColl 2011) in inflammation which trigger both endothelium and leukocyte activation through integrins (see (Constantin 2008) for a review).

CCL2,CCL19 , CCL21, CXCL12 are constitutively expressed by human BEC (see (Holman, Klein et al. 2011) for a review); CCL2, CCL3, CCL5 and CXCL8, CXCL10, CXCL12 are overexpressed by cytokine-stimulated human BEC, hCMEC/D3, and in cerebral vessels of multiple sclerosis (MS) patients (Subileau, Rezaie et al. 2009). CCL2, CCL3, CCL5, CXCL12 and CCL7 trigger leukocyte adhesion via their appropriate receptors (Tsou, Peters et al. 2007). Moreover, it has been reported that the endothelial glycocalyx interacts with chemokines to mediate leukocyte extravasation (Celie, Beelen et al. 2009). In particular, it has been shown that CCL2 or monocyte chemotactic protein 1 (MCP-1) is secreted by EC to mediate activation of monocytes in the step between the selectin-mediated rolling and VCAM1-mediated firm adhesion. In addition, human BEC express chemokine receptors such as CXCR1 to -5 and CCR1 to -6 which are expressed on hCMEC/D3 cell membranes (Weksler, Subileau et al. 2005) although their function in neuroinflammation is less well known. Recent studies have also suggested CXCR3 or fractalkine receptor, as one of the principal inflammatory receptors involved in T cell trafficking (Constantin 2008).

### 1.4.3  Molecules involved in leukocyte-endothelial cell adhesion in neuroinflammation

*Selectin family*

Selectins belong to the C-type lectin (N-terminal calcium-dependent) family of sialoglycoproteins. There are three types of selectins: L-selectin, expressed by peripheral blood leukocytes, E-selectin expressed by endothelium, and P-selectin, previously called endothelial-leukocyte adhesion molecule 1 (ELAM-1), expressed by platelets and EC. Selectins are adhesion molecules involved in the cell-cell adhesion between endothelium and leukocytes (Graber, Gopal et al. 1990) (Fig. 1.8 and 1.10). P- and E-selectin play an important role in leukocyte rolling (Ulfman, Kuijper et al. 1999) (Abbassi, Kishimoto et al. 1993), and the initial adhesion of monocytes (Carlos, Kovach et al. 1991; Lim, Snapp et al. 1998), T lymphocytes (Alon, Rossiter et al. 1994) and neutrophils (Zarbock, Ley et al. 2011).

There are contrasting results about basal E- and P-selectin expression on EC. It has been reported that P- and E- selectin are exclusively expressed by EC under shear stress (Kubes and Ward 2000). However, in a static culture model, E- and P-selectin were found to be expressed by HUVEC (Charles, Karen et al. 1997) and endothelium from different vascular beds (Hillyer, Mordelet et al. 2003) under resting conditions. Under inflammatory conditions, both selectins appear to be up-regulated on cytokine-stimulated endothelium. Indeed, E- and P-selectin expression is regulated by mediators such as TNFα, IFNγ and IL-1 (Charles, Karen et al. 1997; Gough, Levy et al. 2008).

*Immunoglobulin superfamily of cell adhesion molecules*

Endothelial CAM are adhesion molecules (Fig. 1.8) belonging to the immunoglobulin super family, which is characterised by repeated immunoglobulin domain-like loop structures (Ig-loops) and a single transmembrane domain (see review (Frijns and Kappelle 2002). VCAM1 or CD106 is a molecule of 110 kDa with 6 or 7 Ig-like domains. VCAM1 is constitutively expressed by EC, leukocytes, epithelial cells and fibroblasts (Osborn, Hession et al. 1989). ICAM1 or CD54 is a protein of 80-114 kDa formed by a single chain with 5 Ig-like domains, a single trasmembrane region and a short cytoplasmic domain, while intracellular cell adhesion molecule 2 (ICAM2) or CD102 is a protein of 55-65 kDa with 2 Ig-like domains.
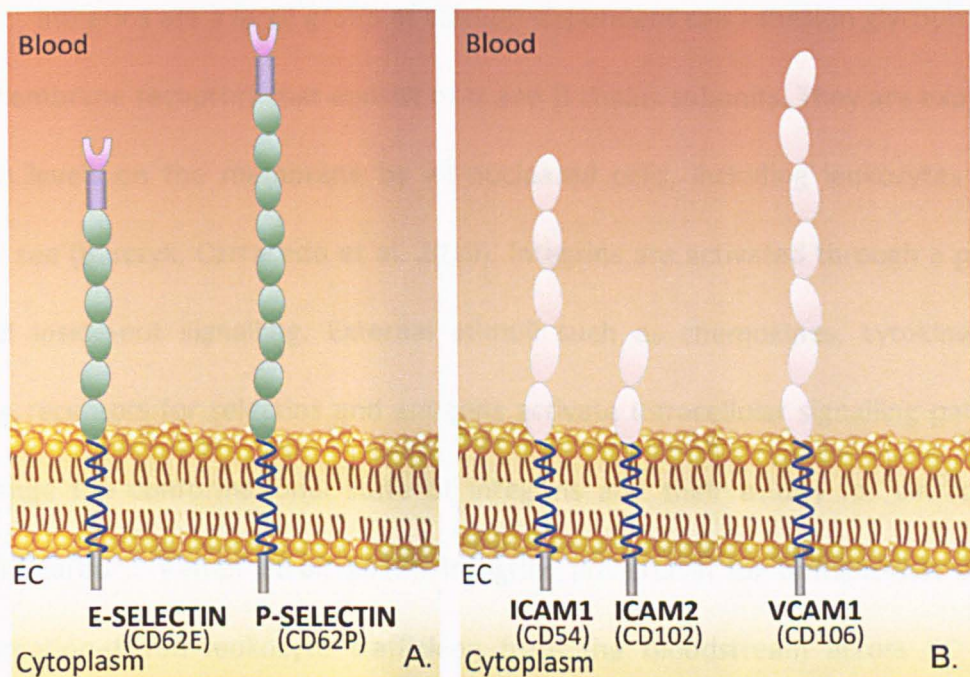


Fig. 1.8: Some membrane-associated endothelial molecules involved in neuroinflammation. A. Selectin structure. Each selectin is composed by a short cytoplasmic C-terminal domain (grey), a transmembrane domain (blue), complement regulatory protein (CRP) like domains (green), epithelial growth factor (EGF) like domain (purple) and an N-terminal C-type lectin domain (NH$_2$-lectin) (pink) B.CAM structure. Each CAM is composed by a short cytoplasmic C-terminal domain (grey), a transmembrane domain (blue) and a variable number of Ig-loops (pink). Schematic representation based on illustrations in (Springer 1994; Vestweber 1999).

Pro-inflammatory cytokines such as IL-1, TNF-α and IFN-γ increase VCAM1 and ICAM1 expression on primary cultures of human BEC between 4 and 24 h (Cayrol et al. 2008). This effect has been extensively shown *in vitro* and *in vivo* on human EC including the BEC line, hCMEC/D3 (Weksler, Subileau et al. 2005). Furthermore, it has been shown that in HUVEC, ICAM2 is down-regulated by TNFα and IL-1 (McLaughlin, Hayes et al. 1998). Endothelial CAM mediate binding of activated leukocytes to the inflamed endothelium through activation of integrins as it will be described in the next subsection.

### *Integrin family*

Integrins are a large group of calcium-dependent cell adhesion glycoproteins/ transmembrane receptors that consist of α and β chains subunits. They are expressed at high levels on the membrane by all nucleated cells, including leukocytes (for a review see (Barczyk, Carracedo et al. 2010). Integrins are activated through a process termed inside-out signalling. External stimuli such as chemokines, cytokines, cell surface receptors for selectins and antigens activate intracellular signalling pathways to change the conformational state of integrins and their avidity for extracellular ligands (Zarbock, Kempf et al. 2012). Integrins are crucial for homeostasis and for inflammation-driven leukocyte trafficking from the bloodstream across EC (for a review see (Rose, Alon et al. 2007)). Indeed, expression of these proteins by immune cells is responsible for all steps that characterise leukocyte trafficking to BEC during inflammation (Table 1.4).

**Table 1.4: Leucocyte-endothelial cells adhesion molecules involved in leukocyte trafficking in inflammation.** From (Frijns and Kappelle 2002).

## Leucocyte-Endothelial Adhesion Molecules

| Adhesion Molecule | Action | Cells of Origin | Expression | Counterreceptor | Target Cells |
|---|---|---|---|---|---|
| **Selectins** | | | | | |
| E-selectin, CD62E | Rolling | Activated EC | Induced by cytokines | SLe$^x$ on PSGL-1, L-selectin, $\beta$2 integrins | Neutrophils, monocytes, lymphocytes |
| P-selectin, CD62P | Rolling | Stored in granules of platelets and EC | Surface expression induced by thrombin, histamine | SLe$^x$ and Le$^x$ on PSGL-1, L-selectin | Neutrophils, monocytes |
| L-selectin, CD62L | Rolling | All leukocytes | Constitutive | SLe$^x$, P- and E-selectin | Activated EC, platelets, eosinophils |
| **Immunoglobulin gene superfamily** | | | | | |
| ICAM-1, CD54 | Firm adhesion and transmigration | EC, leukocytes, fibroblasts, epithelial cells | Constitutive (low), upregulated by cytokines | LFA-1, Mac-1 | All leukocytes |
| ICAM-2, CD102 | Firm adhesion | EC, platelets | Constitutive | LFA-1 | All leukocytes |
| VCAM-1, CD106 | Firm adhesion and transmigration | EC | Constitutive (low), upregulated by cytokines | VLA-4 | Monocytes, lymphocytes |
| PECAM-1, CD31 | Leukocyte transmigration and adhesion | EC, platelets, leukocytes | Constitutive | PECAM-1 | EC, platelets, leukocytes |
| **$\beta$2 (CD18) integrins** | | | | | |
| CD18/11a (LFA-1) | Firm adhesion and transmigration | All leukocytes | Constitutive, function on leukocyte activation | ICAM-1 and ICAM-2 | EC |
| CD18/11b (Mac-1) | Firm adhesion and transmigration | Neutrophils, monocytes, NK cells | Constitutive, surface expression increased after activation | ICAM-1 | EC |
| CD18/11c | Minor role in leukocyte adhesion | Neutrophils, monocytes, NK cells | Constitutive, surface expression increased after activation | Complement fragments | |
| **$\beta$1 (CD29) integrins** | | | | | |
| VLA-4, CD49d/CD29 | Firm adhesion and transmigration | Lymphocytes, monocytes | | VCAM-1 | Monocytes, macrophages, EC, epithelial cells |

EC indicates endothelial cells; SLe$^x$, sialyl Lewis X (fucosylated tetrasaccharide); Le$^x$, Lewis X (trisaccharide); PSGL-1, P-selectin glycoprotein ligand-1; Mac-1, macrophage antigen-1; and NK, natural killer.

### 1.4.4 Leukocyte trafficking at the blood-brain barrier in neuroinflammation

In inflammation, there is an increased blood supply (to provide, for example, antibodies and complement molecules) to the inflamed area and an increase in the leakiness of local microvessels, that result in an increase in infiltrated leukocytes from the blood to the inflamed organ and/or tissue. In the brain, under inflammatory conditions, there is a high increase of leukocyte adhesion and migration across the BBB at post-capillary level (Owens, Bechmann et al. 2008). In neuroinflammation, leukocyte trafficking across the BBB is a multi-step process (Fig. 1.9) characterized by: 1) endothelial activation and leukocyte tethering and rolling on activated endothelium, 2) activation of leukocytes which involves the inside-out signalling by chemokine stimulation of GPCR leading to affinity and avidity changes in integrins due to clustering. 3) leukocyte firm adhesion mediated by a specialized set of CAM expressed by BEC and integrins expressed by leukocytes, 4) firm arrest, polarization and crawling, and finally 5) transmigration across the BBB (Nourshargh, Hordijk et al. 2010 ; Luster, Alon et al. 2005; Ley, Laudanna et al. 2007). Once in the CNS parenchyma, leukocytes (T and B cells, monocytes and other immune cells), exert their immunological function mainly through direct contact with antigens or antigen presenting cells (APCs) (Aloisi, Ria et al. 1998; Aloisi, Ria et al. 1999), and by triggering key inflammatory events such as increasing the expression of CAM, cytokines and chemokines to recruit additional immune cells to the CNS.

The steps involved in leukocyte trafficking across the BBB will be further described in the following subsections.
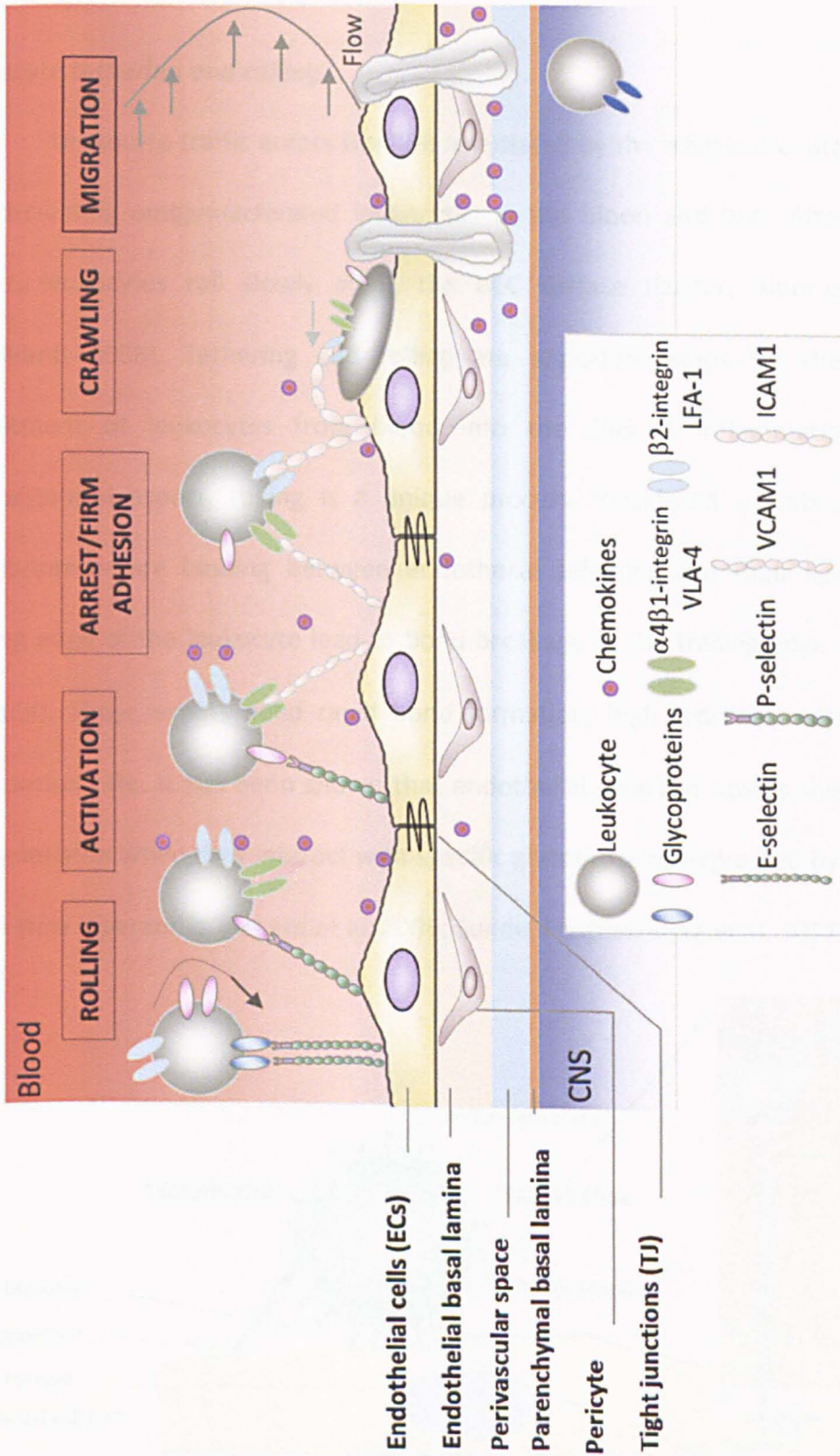
**Fig. 1.9: Leukocyte trafficking cascade across the blood-brain barrier in inflammation.** Schematic representation based on illustrations in (Nourshargh, Hordijk et al. 2010 ; Carlos and Harlan 1994; Engelhardt 2008).

### *Leukocyte tethering and rolling*

Leukocyte traffic across the BBB is initiated by the transient contact between the circulating antigen-activated leukocytes in the blood and BEC. After the initial tether, leukocytes roll slowly along the BEC surface (Luster, Alon et al. 2005; Engelhardt 2008). Tethering and rolling are important steps for the successful recruitment of leukocytes from blood into the CNS in inflammation. From a biomechanical aspect, rolling is a unique process considered a state of dynamic equilibrium where binding between endothelial selectins and their ligands at the leading edge of the leukocyte lead to bond breakage at the trailing edge as shown in Fig. 1.10. These events need rapid bond formation, high tensile strength and fast dissociation rate. It has been shown that endothelial selectins posses these essential characteristics when they interact with specific glycoproteins expressed by leukocytes, under flow (Sperandio, Pickard et al. 2006; Sundd, Pospieszalska et al. 2011).
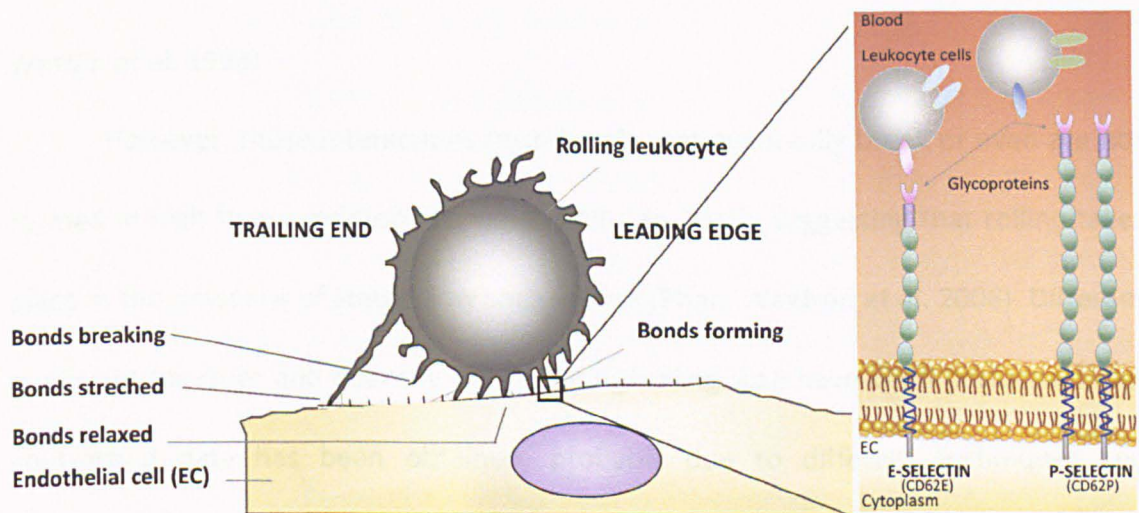


**Fig. 1.10: Leukocyte rolling on endothelium.** Bonds between endothelial selectins and glycoproteins, expressed by leukocytes, in a relaxed, stretched and breaking state which characterise rolling. **Enlargement.** E- and P-selectin expressed on endothelial membranes mediating leukocyte selectin ligands (P-selectin glycoprotein ligand-1) binding during rolling. Adapted from (Sperandio, Pickard et al. 2006).

Rolling and tethering were widely studied using intravital microscopy on mouse CNS microvessels *in vivo,* while studies on human leukocyte rolling on EC have been performed using *in vitro* (Luu, Rainger et al. 2003) or *in silico* (Hammer and Apte 1992; Beste and Hammer 2008). Cell tethering and rolling has been shown to be mediated by both P- and E-selectin, and either one, if adequately expressed on EC, is sufficient for this process (Kubes and Ward 2000). Selectins expressed by BEC bind P-selectin glycoprotein ligand-1 (PSGL-1) expressed by circulating CD4+ and CD8+ T cells (Westmuckett, Thacker et al. 2011), slowing down the leukocytes circulating in the blood in mouse brain microvessel *in vivo* (Battistini, Piccio et al. 2003), and on human HEC *in vitro* (Luscinskas, Ding et al. 1995) and in HBEC (Bahbouhi 2009). It has been demonstrated that to support this binding both selectins and their ligands need to be associated and anchored onto the cytoskeleton (Setiadi, Sedgewick et al. 1998; Snapp, Heitzig et al. 2002). In addition, it has been shown that leukocytes induce clustering of E-selectin and its association with cytoskeletal proteins in HUVEC *in vitro* (Yoshida, Westlin et al. 1996).

However, these interactions form bonds that eventually break or even are not formed in high flow conditions (Efremov and Cao 2011), suggesting that rolling takes place in the presence of stable, low shear stress (Phan, Waldron et al. 2006). Different studies to measure and quantify the tethering/rolling step have been performed, but contrasting data has been obtained, probably due to different techniques and approaches used (Luu, Rainger et al. 2003; Westmuckett, Thacker et al. 2011; Lee, Kim et al. 2012; Su, Lei et al. 2012).

*Leukocyte activation*

Leukocytes rolling with reduced speed are able to sense chemokines present on the BEC surface or released in the blood. Chemokines bind to serpentine 7-transmembrane GPCR on the leukocyte surface, delivering a G-protein mediated signal, thereby activating `inside-out` signalling to increase integrin affinity. In acute inflammation, chemokines such as CCL2, CCL5, CCL19, CCL21, CXCL-4, 9, -10, -11 and-12 are expressed/released into the blood stream to activate leukocyte integrins such as αL-β2 integrin (LFA-1) (Butcher 1991; Engelhardt 2008; McCarty 2009; Kuckleburg, Yates et al. 2011) .

*Cell-cell adhesion (leukocytes-BEC)*

The firm adhesion between activated leukocytes and inflamed BEC is mediated by tightly regulated binding of integrins to the Ig superfamily CAM expressed on the BEC surface (Fig. 1.11). To have a good firm adhesion, high affinity of the integrins for the active conformation of their endothelial ligands on EC is needed. The most critical integrins involved in leukocyte firm adhesion are α4β1 integrin or very late antigen-4(VLA-4) (Chan, Hyduk et al. 2001; Chigaev, Zwartz et al. 2003) as well as αLβ2-integrin lymphocyte function-associated molecule-1 (LFA-1) which binds ICAM1 and ICAM2, and is important especially for adhesion of monocytes/macrophages and THP-1 cells (Kim, Carman et al. 2003; Engelhardt and Ransohoff 2012).

It has been shown that either VLA-4 or LFA-1 are required for peripheral blood mononuclear cells (PBMC) firm adhesion under flow to TNF-α stimulated HUVEC (Cinamon, Shinder et al. 2001) and to transfected human microvascular BEC (THBMEC) (Man, Tucky et al. 2009). In addition, blocking VLA-4 and LFA-1, reduce adhesion of

peripheral blood lymphocyte to TNFα-stimulated HUVEC by 85% (Cinamon, Shinder et al. 2001). LFA-1 binds to ICAM1 (Rothlein, Dustin et al. 1986) and ICAM2 on brain endothelium, whereas VLA-4 binds VCAM1 (Lobb, Antognetti et al. 1995) as shown in the Fig. 1.11. In addition to CAM and integrins, other inflammatory mediators such as chemokines are involved in leukocyte firm adhesion to endothelium. Chemokine CCL2 has been shown to mediate lymphocyte adhesion to human brain-derived microvascular endothelium (Maus, Henning et al. 2002) through LFA-1 (Jiang, Zhu et al. 1994).

As indicated above, firm adhesion occurs in postcapillary venules *in vivo* (reviewed in (Engelhardt and Coisne 2011). Most studies *in vitro* on leukocyte adhesion to brain endothelium have been performed using static assays omitting physiological flow. More recently interesting results about leukocyte adhesion in inflammation were obtained using flow based assays, in which it was shown that VCAM1 and ICAM1, but not ICAM2, mediate shear-resistant firm PBMC adhesion to mouse brain endothelium (Steiner, Coisne et al. 2010), and polymorphonuclear leukocyte adhesion to cytokine-stimulated HBMEC (Wong, Prameya et al. 2007).
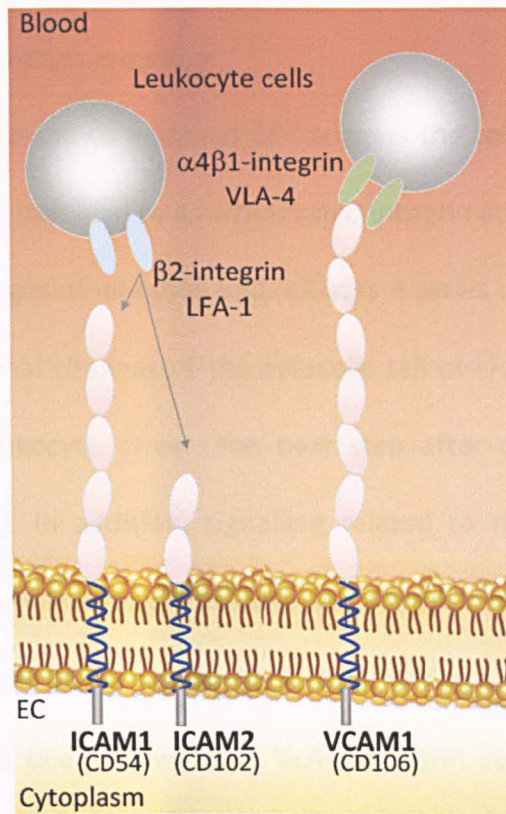
**Fig. 1.11: Leukocyte adhesion.** Leukocyte integrins α4β1 (VLA-4) and αLβ2-integrin (LFA-1) bind VCAM1 and ICAM1 and ICAM2 expressed on endothelial cell (EC) membrane, respectively. Schematic representation based on illustrations in (Springer 1994; Carlos and Harlan 1994).

### *Leukocyte arrest-polarization-crawling*

Leukocyte adhesion to inflamed BEC triggers the release of chemokines and other chemoattractants that lead to a further rapid integrin activation. This event leads to conformational changes of integrins and initiates a series of signalling pathways. In particular, conformational changes of the cytosolic tail of LFA-1 upon ICAM1 binding may play a role in leukocyte arrest, the next step after rolling-adhesion (Shamri, Grabovsky et al. 2005). In addition, signalling related to the `outside-in` signalling seems to be important maintaining firm leukocyte adhesion under flow, acting via LFA-1 (Giagulli, Ottoboni et al. 2006; Smith, Deem et al. 2006) and VLA-1 integrin (Hyduk, Oh et al. 2004). It has been shown that VLA-1 integrin can engage laterally CD44 improving the leukocyte's ability to arrest on endothelium under flow (Nandi, Estess et al. 2004). Using *in vitro* time lapse imaging, it has recently been reported that leukocytes arrest and polarize on cytokine-stimulated primary mouse BEC and start to crawl on the surface of EC, preferentially against the direction of flow as shown in Fig. 1.12 (Steiner, Coisne et al. 2010).
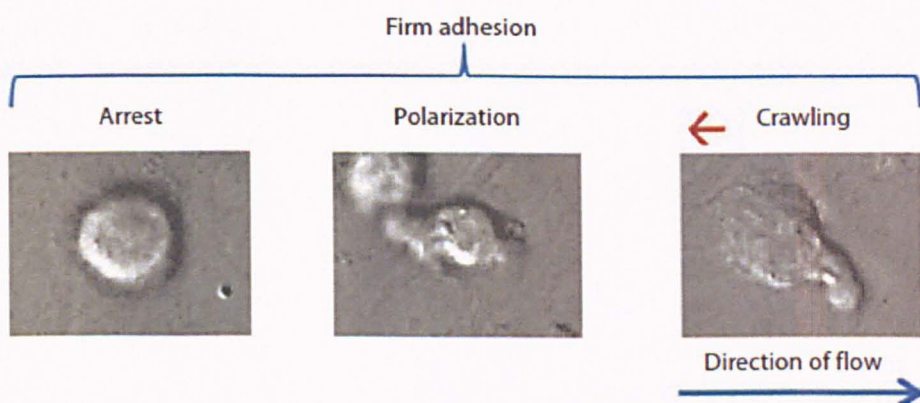


**Fig. 1.12: Leukocyte firmly adhered: arrest-polarization-crawling.** Adhered leukocytes firmly arrest on EC (left), and then polarize (middle) and start to crawl for long distances before transmigration. From (Lyck and Engelhardt 2012).

*Leukocyte migration*

Following leukocyte arrest, leukocytes can extravasate from the BEC surface to the CNS, by either paracellular or transcellular migration (Wittchen 2009). In the paracellular route, the leukocyte diapedesis occurs across the TJ, thereby reducing barrier properties of BEC. The transcellular route leaves the TJ intact (for a review see (Muller 2011), and leukocytes are engulfed by BEC and released at the abluminal side (Stolp and Dziegielewska 2009). Leukocyte transmigration requires a rapid reorganization of the cytoskeleton of leukocytes to migrate from the apical side to the abluminal side of endothelium (for a review see (Nourshargh, Hordijk et al. 2010)). Regardless the route of migration, adherent leukocytes expressing chemokine receptors extend pseudopods to bind the abluminal chemokines which guide the migration process. ICAM1 and PECAM-1 play an important role in the leukocyte infiltration in the brain, mediating the step after firm adhesion between leukocytes and activated EC (Alvarez, Cayrol et al. 2011 ; Banks and Erickson 2010 ; Persidsky, Ramirez et al. 2006; Engelhardt 2008; Stolp and Dziegielewska 2009).

## 1.5 Multiple Sclerosis

MS is associated with alterations in BBB function, as reported in Table 1.5. MS affects approximately one million people in the world and is one of the most common chronic and disabling autoimmune disorders of the CNS. MS is primarily characterized by progressive neurodegeneration caused by demyelination (loss of the myelin sheath) of nerve fibres. This neurological condition was first identified by Robert Carswell in 1838 who described it as *'a remarkable lesion of the spinal cord accompanied with atrophy'* (Carswell 1838).

MS mainly starts in young adulthood, and almost 70% of patients with clinical symptoms are between the ages of 20 and 60 years old. This disease affects women more than men with a ratio of 2:1 (Maria Malfitano, Matarese et al. 2005). The worldwide distribution and incidence of MS is highly variable (Noseworthy, Lucchinetti et al. 2000). The incidence of MS is higher in northern and central Europe, North America, Canada and Australia than in the rest of the world and it is considered that both genetic and geographical factors, yet to be unravelled, influence its prevalence (Weiner 2009; Compston and Coles 2008).

In the early 1970s it was observed that there is an association between MS and the major histocompatibility complex (MHC), the major genetic factor in MS. Genetic studies identified MHC gene variants that are associated with MS, and that the alleles linked to disease severity were DRB5*0101 and DRB1*1501 allele encoding MHC class II cell surface receptor (HL-DR)2b and alleles of the human leukocyte antigen (HLA) class II region which are the highest risk-conferring genes for this major autoimmune

disease (Dyment, Ebers et al. 2004). The role of environmental factors is much less well

defined (Compston and Coles 2008). Epidemiological observations indicate that viruses

might contribute to the development of MS. Among the studied viruses, Epstein-Barr

virus, a ubiquitous virus, is a major candidate for triggering MS even if the mechanisms

responsible for this association are far from understood (Kakalacheva, Münz et al.

2011). Four main clinical forms of MS have been described as shown in Table 1.5

(Rejdak, Jackson et al. ; Lassmann, Brück et al. 2007; Malfitano, Proto et al. 2008; Bradl

and Lassmann 2009).

| Forms of MS | |
| --- | --- |
| Relapsing-remitting form of MS (RRMS) | More than 80% of the patients develop the RRMS which is characterised by recurring periods of disease in which clinical symptoms worsen (once a year), but from which the majority of the patients make a full or a partial recovery.<br>RRMS appears to be driven, mostly, by the inflammatory process which causes focal demyelinating lesions mainly in the white matter of the brain and spinal cord. Over time the number of relapses decrease, and 10% of RRMS patients have benign MS, where relapses are rare and, normally, does not result in disability. |
| Secondary-progressive form of MS (SPMS) | It is a progressive neurological deterioration phase that occurs following RRMS and is developed by 70% of MS patients. |
| Primary-progressive form of MS (PPMS) | The remaining 20% of MS patients develop a primary progressive (PPMS) form characterised by a steady neurological decline, without relapses. |
| Progressive-relapsing form of MS (PRMS) | A small percentage of MS patients develop a rare fourth form, progressive relapsing MS (PRMS), considered a variant of PPMS where there is a gradual neurological decline from the onset of disease but with relapses. |

Table 1.5: Forms of multiple sclerosis (MS).

The most common symptoms observed in MS patients are generally the

result of a progressive loss of muscle control, sensation, vision, speech and/or

intellectual ability, but its clinical manifestations are manifold.

In the context of pathology, MS is characterized by four main features: inflammation, demyelination, axonal loss and gliosis. The earliest pathogenic event in MS is the inflammation caused by infiltrating lymphocytes, monocytes and antibody-producing plasma cells from blood into the CNS, specifically in the periventricular region of white matter in the brain and the spinal cord, to form a perivascular cuff. The perivascular cuff is the area surrounding an inflamed vessel, containing inflammatory leukocytes, and delimited by endothelium on one side and basement membrane on the other side (Steinman 2009).

It was observed that CD4+ T cell and CD8+ T cell migration into the CNS causes secretion of cytokines, chemokines and other molecules, damaging oligodendrocytes. At the same time, T cell infiltration activates microglia and astrocytes in the CNS (Lassmann, Bruck et al. 2001). Infiltrating plasma cells produce myelin-specific antibodies that result in further demyelination (Steinman 2009). The subsequent axonal injury and axonal loss are caused by the chronic activation of microglia, in the absence of lymphocytic inflammation, due to a failed remyelination of the axons, which involve a redistribution of the ion channels on demyelinated axons (Coman, Aigrot et al. 2006). In experimental autoimmune encephalomyelitis (EAE), an animal model of MS, axonal injury can also occur before myelin loss (Tsunoda, Tanaka et al. 2007), which means that demyelination could be independent or secondary to axonal degeneration (Huizinga, Linington et al. 2008). Gliosis is caused by proliferation of astrocytes in the injured areas in response to chronic tissue injury, leading to scars.

### 1.5.1 Chemokines in multiple sclerosis

A high number of chemokines are involved in MS (for a review see (Hamann, Zipp et al. 2008)) to convert low affinity interactions mediated by integrins between leukocytes and activated BEC into high affinity interactions that promote leukocyte migration across the BBB (Murphy, Long et al. 2000).

CXCL12 is increased by brain blood vessels and in astrocytes both in active and inactive MS lesions (Alexander, Zivadinov et al. 2011). In both MS and in EAE, it has been shown that CXCL12 shifts from the abluminal side of brain endothelium to the blood-stream surface where it is recognized and bound by activated CXCR4 on leukocytes, with consequent infiltration and formation of the perivascular cuff (McCandless, Zhang et al. 2008). It was suggested that CXCL12 relocation promotes leukocyte infiltration, increasing their capture at the BBB level (reviewed in (Holman, Klein et al. 2011) and induced monocyte transmigration across THBMEC *in vitro* under flow (Man, Tucky et al. 2012). In addition, it had been reported that CXCL12 and CXCR4 are important in the recruitment of CD8+ T cells by BEC *in vitro* (Liu 2009). However, it appears that CXCL12 is more important in angiogenesis than in inflammation.

CCR1 and 2 chemokine receptors, as CXCR4, are involved in T cell and monocyte infiltration to the CNS, targeting CCL7 and CCL2. CCL2 is expressed in MS lesions and it is increased by proinflammatory cytokines in hCMEC/D3 cells *in vitro* (Subileau, Rezaie et al. 2009). CCR2, expressed by immune cells, binds CCL2 and it is down-regulated by CCL2 itself once leukocytes infiltrate into the brain across the BBB (Mahad, Callahan et al. 2006). CX3CR1 receptor is increased in late active and inactive

demyelination, In addition, its deletion in EAE mice results in increased mortality (Hulshof, van Haastert et al. 2003).

### 1.5.2 IFNγ and TNFα: proinflammatory cytokines in multiple sclerosis

In RRMS patients there are high levels of proinflammatory cytokines IFNγ and TNFα in plasma during relapses, which dramatically increase during long periods of active disease and decreased rates of remission (Minagar and Alexander 2003). Indeed, elevated plasma TNFα has been correlated with disease progression (Sharief and Hentges 1991), it has been detected in acute and chronic MS lesions (Selmaj 1991; Canella 1995), and TNFα has also been detected in lesions in post-mortem MS brains. Indeed, TNFα is produced by astrocytes and microglia in acute and chronic active MS brain lesions (Navikas and Link 1996) to trigger T cell responses, lymphocyte infiltration and many other events in MS pathogenesis (reviewed in (Constantinescu and Gran 2010)). Therefore, anti-TNFα antibodies ameliorate disease in EAE mice (Selmaj, Raine et al. 1991), it has been hypothesized that TNFα may have a dual action in MS pathogenesis: it carries out a proinflammatory function being involved in inflammation, demyelination, neuronal apoptosis and astrocytic toxicity, and at the same time, a neuroprotective function supporting tissue regeneration (Weihong and Kastin 2008).

IFNγ was found expressed on circulating lymphocytes in MS patients (Navikas and Link 1996) and on infiltrated lymphocytes in MS lesions (Lock, Hermans et al. 2002), in CSF of MS patients (Nicoletti, Patti et al. 1996) and in the CNS of EAE mice (Renno, Krakowski et al. 1995).

Together, IFNγ and TNFα, have been shown to have a synergistic effect on endothelium by activating transcription factors, such as NK-κB, which induce the expression of CAM (VCAM1 and ICAM1) and E-selectin (Pober and Sessa 2007).

### 1.5.3 Leukocyte trafficking across the blood-brain barrier in multiple sclerosis

During MS relapses, there is a massive adhesion and migration of activated lymphocytes and monocytes across the BEC (Hickey 1991). Cytokines, chemokines and CAM cooperate in the control of leukocyte adhesion and migration across the BBB and determine the cellular composition of the inflammatory infiltrate in MS (Schall and Bacon 1994; Hohlfeld 1999). In brain endothelium, it is widely accepted that both EAE and MS endothelium highly express VCAM1, ICAM1 and P- and E-selectin (Lee and Benveniste 1999; Carrithers, Visintin et al. 2000; Piccio, Rossi et al. 2002; De Vries 1997, Engelhardt 2008).

In MS inflammatory infiltrates, T lymphocytes, monocytes, macrophages and B cells are present (Lucchinetti, Brück et al. 2000; Bradl and Lassmann 2009), and both ICAM1 and VCAM1 overexpressed on endothelium (Alvarez, Cayrol et al. 2011). CD4+ and CD8+ T cells migrate into the CNS, following the multi-step process described in Section 1.4.4 which includes rolling via P-selectin-PSGL-1 and firm adhesion via VCAM1-VLA-4 integrin interactions (Piccio, Vermi et al. 2005). It was found that CD4+ and CD8+ T cells from RRMS patients expressed an increased level of PSGL-1 (Battistini, Piccio et al. 2003). In addition, it has been shown that CD4+ and CD8+ T cells expressing LFA-1 (R.A.Sobel 1990) and VLA-4 (Engelhardt 2006), first roll on brain endothelium prior to becoming firmly adhered (Kerfoot and Kubes 2002). It has been

shown that VLA-1 and LFA-1 expression on lymphocytes and monocytes in both blood

and CFS of PPMS and SPMS patients were highly increased when compared with non-

MS immune cells (Ukkonen, Wu et al. 2007).

### 1.5.4 Multiple sclerosis therapies related to leukocyte infiltration

Current treatment of MS is based on anti-inflammatory, immunosuppressive,

and immunomodulatory drugs, but normally this kind of therapy is only partially

effective. Clinical studies on Natalizumab, a humanized monoclonal antibody against

the cellular adhesion molecule VLA-4, were completed with good results (Sidorenko,

KOLYAK et al. 2009), but with some important side effects. Natalizumab has been

designed to bind the integrin VLA-4 expressed on leukocyte surface, to prevent

leukocyte binding to VCAM1 and extravasation. The big limitation of this treatment is

that is not selective: Natalizumab does not act only at the BBB level, but on many other

sites in the body, preventing immune cell entry into inflamed, infected and/or injured

organs not affected by MS. Recently, a combination therapy targeting leukocyte

adhesion using monoclonal antibodies for VCAM1 and ICAM1 have been successfully

used during a clinical trial, but disappointingly still with systemic side effects

(Compston and Coles 2008).

# 1.6 MicroRNAs

### 1.6.1 Definition of microRNAs

MicroRNAs (miRs) are a class of 20-25 nucleotide-long highly conserved, single-strand, non-coding RNA molecules, that modulate gene expression (Carthew and Sontheimer 2009). In 1993 the first miR was identified in the nematode *Caenorhabditis elegans*, lin-4 (Lee, Feinbaum et al. 1993; Wightman, Ha et al. 1993). The Lin-4 gene, or small and non-protein-coding transcript, regulates lin-14 through the 3'UTR region of its messenger RNA (mRNA) at the post-transcriptional level. A second miR, let-7, was discovered in 2000 in *Caenorhabditis elegans* (Pasquinelli, Reinhart et al. 2000; Reinhart, Slack et al. 2000). These two findings triggered a revolution in the investigation of miRs and the field has grown massively and quickly, becoming soon clear that miR expression was critical for a myriad of biological processes such as differentiation, cell cycle, development, apoptosis and disease in various organisms and in humans (Friedman and Jones 2009). Current estimates suggest that the human genome contains over one thousand distinct miRs (Bartel 2009).

Mirs are named using the 'miR' prefix and a unique identifying number (e.g., miR-1, miR-2,...miR-126 etc) (Ambros and Bartel 2003).

### 1.6.2 MicroRNAs on the genome

In humans, 1% of the genes have been found to encode for miRs, which are often highly conserved across species (Bartel 2009), and all miR genes have been mapped in all chromosomes, except in the Y-chromosome (Ul Hussain 2012). Based on their location, human miR genes have been identified either as intergenic, intronic or

exonic (Rodriguez, Griffiths-Jones et al. 2004), and may be located in non-coding regions or in coding regions (Fig. 1.13) (see for reviews (Olena and Patton 2010; Ul Hussain 2012)).
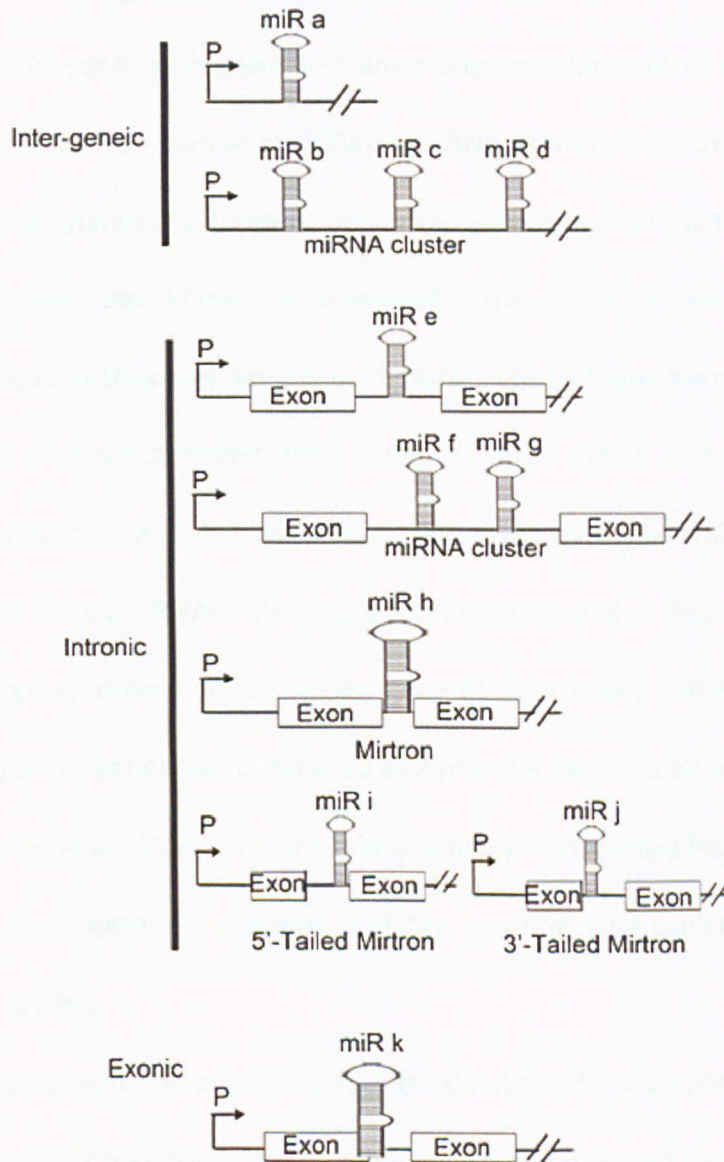


**Fig. 1.13: Genomic organisation of miRs**. An **intergenic miR** is under the control of its own promoter, either as a single gene (miR **a**) or as a cluster (miR **b–d**). An **intronic miR** is present in the intronic region of a functional transcriptional unit and is under the control of a protein-coding promoter as a single intronic miR (miR **e**) or a cluster of intronic miRs (miR **f**, miR **g**) or as a mirtron (miR **h**) in which the whole intron of a protein-coding gene acts as the exact sequence of the pre-miR and hence a microprocessing step is not required in this case. Mirtrons having a sequence extension at the 5′ end are called 5′-tailed mirtrons (miR **i**), whereas mirtrons having a sequence extension at the 3′ end are called 3′-tailed mirtrons (miR **j**). **Exonic** miRs (miR **k**). Legend: bent arrow, P promoter, hairpin miRs, rectangular boxes [Exon] protein-coding exons). Taken from (Ul Hussain 2012).

### 1.6.3 MicroRNA biogenesis

The canonical pathway of miR biogenesis to generate mature miRs is a complex process as shown in Fig. 1.14. In the nucleus, miR genes are transcribed by RNA polymerase II (RNA pol II) with a similar transcription mechanisms of genes coding for protein-coding mRNA (Lee, Kim et al. 2004). The RNA primary transcript of a miR gene is capped, polyadenylated and contains one or more hairpin-like structures of about 80 bases called pri-miR (also known as pri-miRNA). The structural features of pri-miR hairpins are unique as they contain a long imperfect stem of approximately 30 bp with flanking 5` and 3`-single-stranded ends (Zeng, Yi et al. 2005). The pri-miR flanking regions are recognized and cut by a microprocessor complex which includes the nuclear enzyme Drosha (RNAse III type endonuclease) and a RNA-binding protein DGCR8 (DiGeorge syndrome critical region gene 8) (Morlando, Ballarino et al. 2008). The hairpin sequence generated is denoted as a pre-miR, which is about 70 nucleotides (nt) long (Han, Lee et al. 2006). The pre-miR is actively transported from the nucleus to the cytoplasm by exportin-5 proteins and the guanine triphosphatase Ran (Lund, Guttinger et al. 2004).

In the cytoplasm, the pre-miR is recognized at the 3`-end generated by Drosha, and cleaved by DICER RNAase III type endonuclease complex and by TAR RNA-binding protein (TARBP) near the terminal loop into a 20 nt mature miR/miR* duplex (without loop) (Bernstein, Caudy et al. 2001). One strand, the most abundant, called the leading or guide strand (mature miR) of about 20-25 nt is transferred and incorporated into the RNA-Induced Silencing Complex (RISC), while the passenger strand (miR*), the less abundant, is thought to be degraded and removed (Inui, Martello et al. 2010; Bi, Liu et

al. 2009). It has been shown that in some miRs the data are not sufficient to determine which sequence is the predominant one, so the names are like miR-number-5p (from the 5' arm) and miR-number-3p (from the 3' arm). If two or more miRs have closely related mature sequences, letter suffixes are used (e.g. miR-146a, miR-146b).

Recent findings are in contrast with the view of the canonical pathway for miR biogenesis, as reported below. RISC is an RNA polymerase-RNA dependent endonuclease which contains Argonaute (AGO) family and other accessory proteins. The proteins of the AGO family contain three conserved domains PAZ, MID and PIWI, which are known to interact with 3`- and 5`-ends of miRs (Kawamata and Tomari 2010). AGO proteins 1-4 (AGO1-4) mediate the miR-mRNA translational repression. AGO2 has a RNaseH-like PIWI domain which cleaves the mRNA of the miR target internally (Peters and Meister 2007). Recent studies show that miRs can be processed without Dicer, but instead require AGO2 (Dueck and Meister 2010).

Very recent findings underline how the miR star (miR*) species are not all degraded, but they can act as mature miRs too, albeit less abundant. Yang et al. have calculated, based on mirbase database, that of over $2 \times 10^6$ mature strands reads in human, 78.500 are star strands (Yang, Phillips et al. 2011) Furthermore, it has been found that more than 3% of star miR strands are associated with Ago complexes in humans (Yang, Phillips et al. 2011) and in *Drosophila Melanogaster* (Okamura, Phillips et al. 2008; Czech, Zhou et al. 2009; Ghildiyal, Xu et al. 2010), providing evidence that miR* species also contribute substantially to the endogenous miR population in eukaryotic cells. In addition, it has been shown that miR* species are stringently conserved over vertebrate (human, mouse, dog, chicken) evolution (Yang Phillips 2011).

Experimentally, expression levels of both species miR and miR* can be measured using different techniques *in vivo* and *in vitro*. One of the most used techniques is the microarray analysis of miR gene expression followed by validation by real time reverse-transcription PCR (RT²-qPCR).
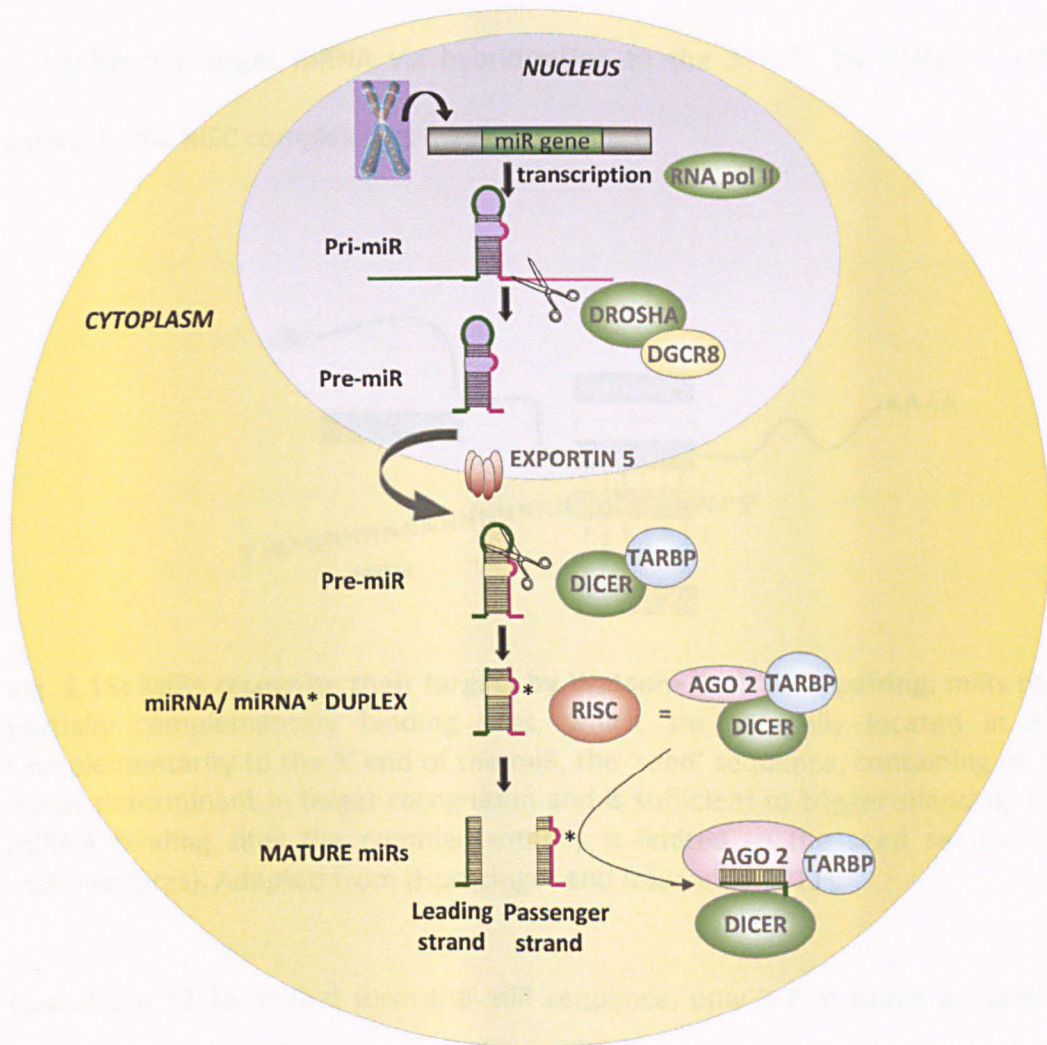


**Fig. 1.14: Biogenesis of miRs.** miR biogenesis takes place in the nucleus (violet) and in the cytoplasm (yellow) of the cell. A miR gene is transcribed to generated Pri-miR, which is further processed as described in the text to originate mature miRs, which include miR (leading) and miR* (passenger) species. Mature miRs in the cytoplasm are incorporated into the RISC complex by AGO2 to carry out their functions. Schematic representation based on illustration in (Inui, Martello et al. 2010).

## 1.6.4 Function of microRNAs: target mRNA

MiRs regulate gene expression mostly, but not always, by repression of their target genes at the post-transcriptional level (Pillai, Bhattacharyya et al. 2007; Vasudevan, Tong et al. 2007). In mammals, miRs are predicted to control more than 60% of all protein coding genes (Friedman, Farh et al. 2009). In particular, mature miRs recognize the target mRNA via hybridization to the 3' UTR by Watson–Crick base pairing in the RISC complex (Fig. 1.15).
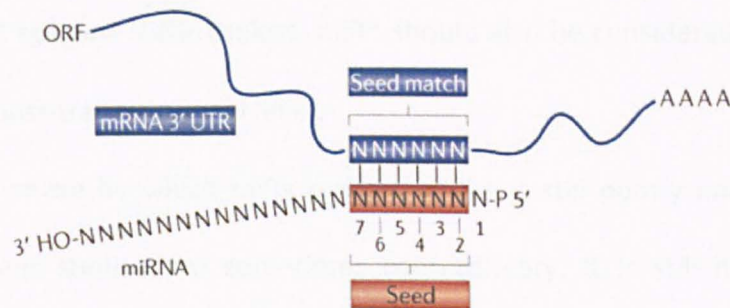


**Fig. 1.15: MiRs recognize their targets by Watson–Crick base pairing.** miRs recognize partially complementary binding sites, which are generally located in 3' UTRs. Complementarity to the 5' end of the miR, the 'seed' sequence, containing nt 2–7, is a major determinant in target recognition and is sufficient to trigger silencing. For most miRNA binding sites the complementarity is limited to the seed sequence (seed-matched sites). Adapted from (Huntzinger and Izaurralde 2011).

Out of the 22-25 nt that form the miR sequence, only 2-7 nt called a `seed` region, form a perfect match with the 3'UTR of the target mRNA (Bartel 2009). MiRs can (i) repress translation of mRNA into protein, blocking it at the initial stage or at the post-initiation stage when there is an missmatch base pairing between mRNA and miR (Bartel 2004), or (ii) degrade the mRNA target by deadenylation if there is a perfect match (Fig. 1.16) (Filipowicz, Bhattacharyya et al. 2008).

miR* species exhibit great conservation in their seed regions and directly repress the 3` UTR region of their target mRNA (Okamura, Phillips et al. 2008; Yang, Phillips et al. 2011). It has been reported that miR-19* in Hela cells directly represses five targets via its seed site (Yang Phillips 2011) and that miR-30c-2* directly represses XBP1 in human fibroblasts (Byrd A.E. 2012). Furthermore, it has been shown that miR-155* directly targets IRAKM in human plasmacytoid dendritic cells (Zhou, Huang et al. 2010) and IFN regulatory factor 3 (IRF3) in human astrocytes (Tarassishin, Loudig et al. 2011). Therefore miR* species regulatory activity has been compared with that of miR species. However, the regulatory effect of miRs*, being less abundant, is modest compared to miR species. Nevertheless, miR* should also be considered as important regulator at the post-transcriptional level.

The mechanism by which miRs repress mRNA is still poorly understood, and results of different studies are sometimes contradictory. It is still highly debated whether the identified mechanisms of miR repression depend on the specific features the mRNA targets and their abundance. In addition, mRNA turnover is highly related to the mRNA decay rate, which is highly variable in mammalian cells and can range from minutes to days (Ross 1995). It has been shown that the more an mRNA is unstable the less it is targetable by miRs (Larsson, Sander et al. 2010). Figure 1.16 summarises the possible mechanisms of translational repression and degradation of mRNA targets mediated by miRs.
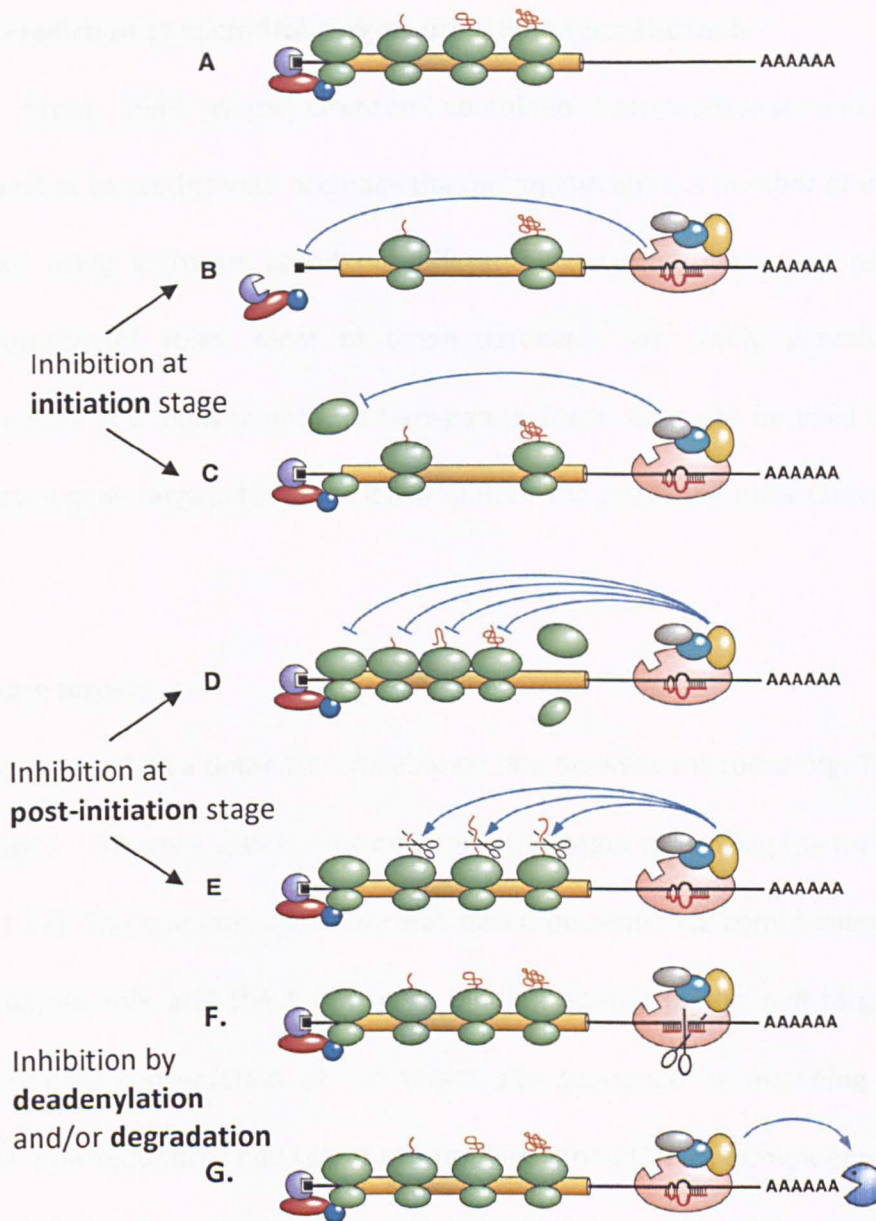
**Fig. 1.16: Mechanisms of mRNA target translational repression and degradation by miRs. A.** mRNA undergoing translation in the absence of a bound miR. **B.** Inhibition of translation initiation by competition between RISC and eIF4E for cap binding. **C.** Inhibition of translation initiation at a step after cap recognition, such as by impeding the association of the small and large ribosomal subunits. **D.** Inhibition of translation elongation coupled to premature termination. **E.** Cotranslational degradation of nascent polypeptides. **F.** mRNA undergoing endonucleolytic cleavage by Ago2, as guided by a fully complementary miR. **G.** mRNA undergoing poly(A) removal by the Ccr4/Not deadenylase (Pac-Man), as directed by a partially complementary miR.

**Legend**: Black square, m7G 5`cap; amber cylinder, protein-coding region; and AAAAAA, poly(A) tail. Ribosomes are coloured green, nascent polypeptides are brown, and the eIF4E subunit of the cap-binding complex is violet, RISC is depicted as a ribonucleoprotein complex comprising a miR (red), Ago (pink), and other protein subunits. Adapted from (Wu and Belasco 2008).

### 1.6.5 Prediction of microRNA targets using bioinformatic tools

From 1997 when Grimson combined computational and experimental approaches to predict with accuracy the miR:mRNA pairs, a number of databases were created using software based on different algorithms, numerical parameters and position-specific roles. Most of these databases are freely available on-line for researchers in a `convenient and transparent form`, that can be used to find out the predicted gene targets for a particular miR, or the predicted miRs targeting one single gene.

### *miRBase targets*

miRBase targets is a database available on-line on www.microrna.org. The mammalian and fish 3' UTR were scanned for miR potential target sites using the miRanda software (Fig. 1.17). The scanning algorithm was based on sequence complementarity between the mature miR and the target site, binding energy of the miR-target duplex, and evolutionary conservation of the target site sequence by matching with currently known miR sequences and target position in aligned UTR of homologous genes. A total of 2,273 target genes have been identified in mammals with one conserved target (90% conservation) and 660 target genes with 100% conservation. The algorithm and cut-off parameters were chosen to provide a flexible mechanism for position-specific constraints and to capture what is currently known about experimentally verified miR target sites: (1) non uniform distribution of the number of sequence-complementary target sites for different miRs; (2) 5'–3' asymmetry; and (3) influence of G:U wobbles on binding. In choosing these parameters, they drew on experience from careful

analysis of target predictions in Drosophila as well as proposed human targets of virus-

encoded miRs (Griffiths-Jones, Grocock et al. 2006; Griffiths-Jones, Saini et al. 2008).
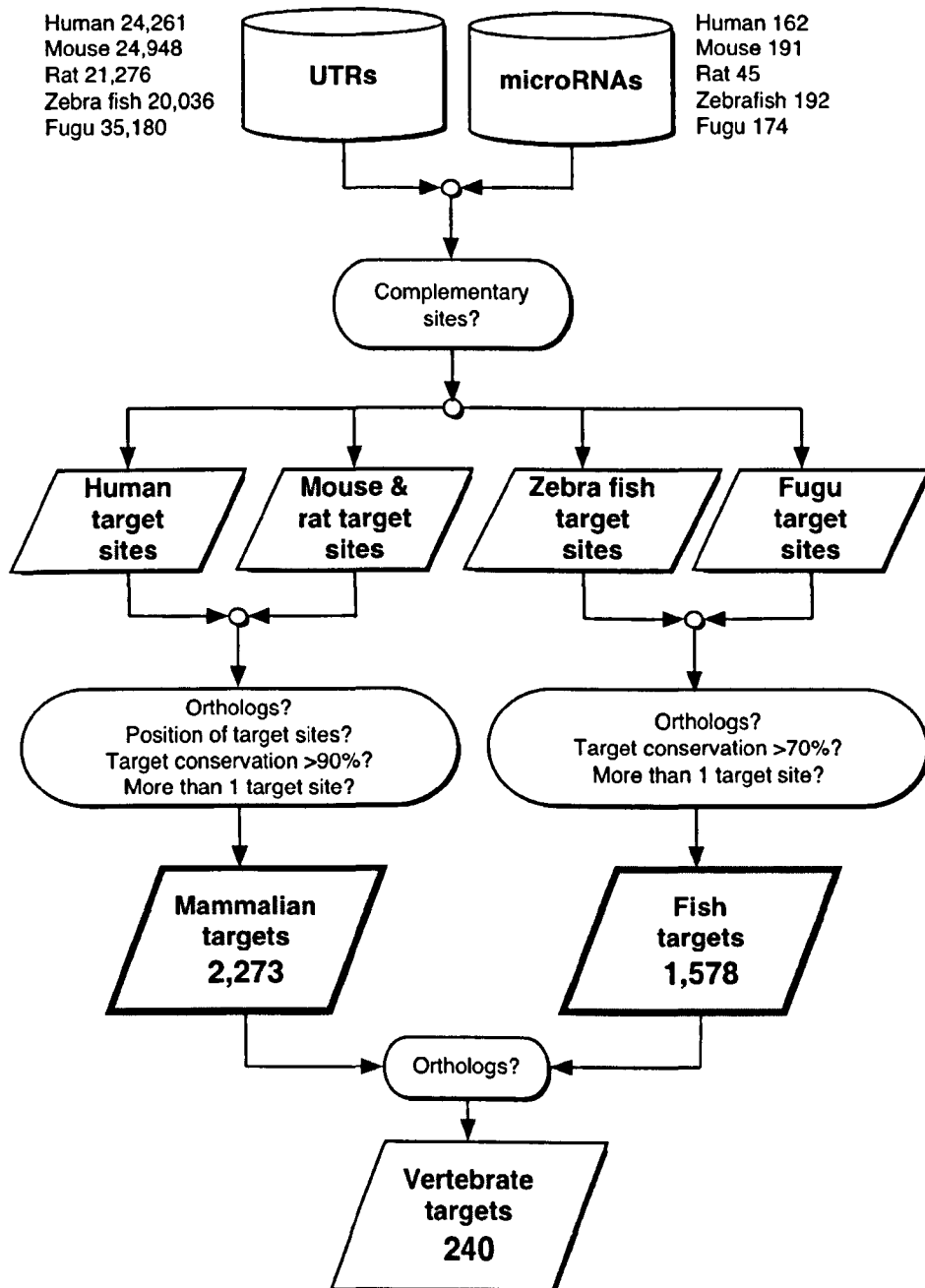


**Fig. 1.17: Scheme of how miRBase predicts targets for miRs.** From (Griffiths-Jones, Grocock et al. 2006; Griffiths-Jones, Saini et al. 2008).

***MicroCosm targets***

MicroCosm targets database is available online on http://www.ebi.ac.uk/enright-srv/microcosm/htdocs/targets/v5/ developed by the Enright Lab at the EMBL-EBI. They used the miRanda algorithm to identify potential binding sites for a given miR in genomic sequences (Fig. 1.18). The algorithm uses a weighted scoring system and rewards complementarity at the 5' end of the miR. Currently they demand strict complementarity at this so-called seed region in accordance with recent publications, that is, all alignments where more than one base in this region is not complementary to a target site are discarded. Target sites selected in this fashion are passed through the Vienna RNA folding routines in order to estimate their thermodynamic stability (Enright, John et al. 2003; Griffiths-Jones, Grocock et al. 2006; Griffiths-Jones, Saini et al. 2008).

***Targetscan Human: prediction of microRNA targets***

Targetscan Human was developed by David Bartel's group and is available on-line on http://www.targetscan.org. TargetScan predicts biological targets of miRs by searching for the presence of conserved 8 mer (an exact match to positions 2-8 of the mature miRNA (the seed + position 8) followed by an 'A') and 7 mer (7mer-m8: an exact match to positions 2-8 of the mature miR (the seed + position 8)) sites that match the seed region of each miR (Lewis, Green et al. 2003). As an option, non conserved sites are also predicted. Also identified are sites with mismatches in the seed region that are compensated by conserved 3' pairing (Friedman, Farh et al. 2009). In mammals, predictions are ranked based on the predicted efficacy of targeting as calculated using the context + scores of the sites. As an option, predictions are also

ranked by their probability of conserved targeting (Friedman, Farh et al. 2009). TargetScanHuman considers matches to annotate human UTRs and their orthologs, as defined by UCSC whole-genome alignments. Conserved targeting has also been detected within open reading frames (ORFs).
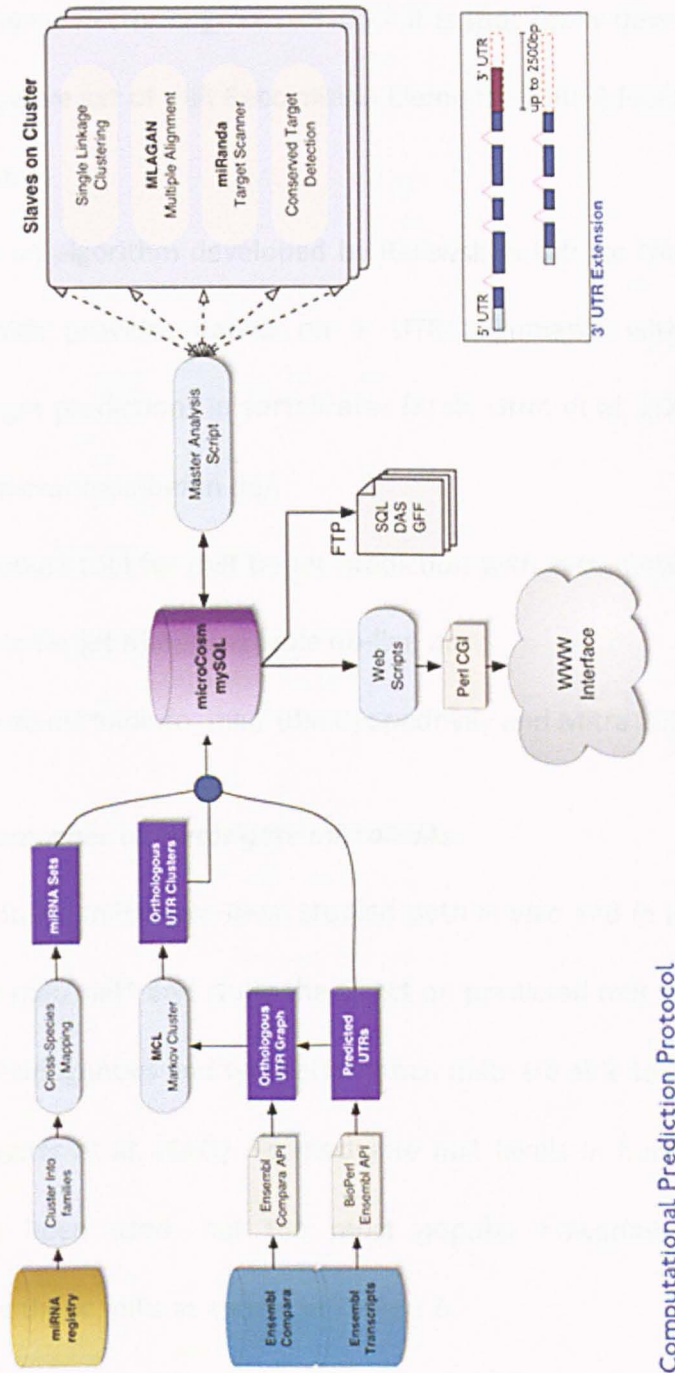


**Fig. 1.18: Scheme of how Targetscan Human predicts targets for miRs.**

*Other databases*

Others databases available on-line are DIANA-microT-CDS (coding DNA sequence), PicTar and Target Miner.

DIANA-microT-CDS database is based on the 5th version of the microT algorithm and is on-line on http://www.microrna.gr/microT-CDS. It is specifically developed to assess a positive and a negative set of miR Recognition Elements (MREs) located in both the 3' UTR and CDS regions.

PicTar is an algorithm developed by Rajewsky's Lab for the identification of miRs targets, which provides details on 3' UTR alignments with predicted sites regarding miR target predictions in vertebrates (Krek, Grun et al. 2005). It is available on-line on http://pictar.mdc-berlin.de/.

Another robust tool for miR target prediction with systematic identification of predicted targets is Target Miner available on-line on http://www.isical.ac.in/~bioinfo_miu/ (Bandyopadhyay and Mitra 2009).

*Experimental approaches to investigate microRNAs*

Experimentally, miRs have been studied both *in vivo* and *in vitro*. Most *in vitro* studies modulate miR/miR* and study the effect on predicted miR targets. It has been shown that both endogenous and synthetic human miRs are able to inhibit the cognate target (Zeng, Wagner et al. 2002). To modulate miR levels in human cells, different techniques have been used, but the most popular nowadays is the transient transfection of synthetic miRs as shown in Table 1.6.

| miR mimic (Pre) | miR inhibitor (Anti) | Supplier | Synthetic miRs (nM) | Transfection Reagent | Transfected cell line | Ref |
|---|---|---|---|---|---|---|
| - | 126 and 125 | Ambion | - | Lipofectamine 2000 | Human endothelial progenitor | (Chen, Huang et al. 2009; Meng, Cao et al. 2012) |
| 126 | - | Ambion | 30 | Siport NeoFX | Human homozygote bronchial epithelial | (Oglesby, Bray et al. 2010) |
| 126 | - | Ambion | 100 | Lipofectamine 2000 | Human gastric cancer | (Feng, Chen et al. 2010) |
| 93 | 93 | Ambion | 30 | Lipofectamine 2000 | Renal microvascular endothelial | (Long, Wang et al. 2010) |
| 146a | 146a | Applied Biosystem | 30 and 100 | Siport NeoFX | HUVEC | (Vasa-Nicotera, Chen et al. 2011) |
| 19a | 19a | Ambion | 40 | Lipofectamine 2000 | HUVEC | (Qin, Wang et al. 2010) |
| - | 34a | Dharmacon | 100 | Dharmafect 1 | Endothelial progenitor | (Zhao, Li et al. 2010) |
| 210 | 210 | Exiqon | 40 | SI RNA transfection reagent Santa Cruz | HUVEC | (Fasanaro, D'Alessandra et al. 2008) |
| - | 126 | Dharmacon | 100 | Dharmafect 1 | HUVEC | (Kuhnert, Mancuso et al. 2008) |
| - | 126 | Exiqon | 100 | Siport NeoFX | Lung carcinoma | (Crawford, Brawner et al. 2008) |
| 126 | | | 3,15,30 | Siport NeoFX or Amine reagent | HUVEC | (Harris, Yamakuchi et al. 2008) |
| 146a | 146a | Ambion | 40 | Lipofectamine 2000 | THP-1 | (Nahid, Pauley et al. 2009) |
| 146a | | Applied Biosystem | 10-20 pM | Lipofectamine plus | Synovial fibroblast | (Li, Gibson et al. 2011) |
| 146b | | | 50 | Lipofectamine 2000 | Human glioma | (Xia, Qi et al. 2009) |
| 155 | 155 | Genepharma | 10,20,80 and 200 | Lipofectamine 2000 | HEK293A | (Song, Liu et al. 2012) |
| 155 | 155 | Ambion | 3,30,100 | Lipofectamine 2000 | Human cardiomyocyte | (Liu, van Mil et al. 2012) |

**Table 1.6: List of transient transfections aimed at modulating miR levels in human cells adopted in previously published studies**

Moreover, predicted targets need to be experimentally validated using different strategies such as reporter assays using luciferase with the 3'UTR of the putative target mRNA. TarBase 6.0 lists all experimentally validated miR targets (http://www.microrna.gr/tarbase). It is the largest available manually curated target database, indexing more than 65,000 miR-gene interactions. The database includes targets derived from specific, as well as high throughput experiments, such as microarrays and proteomics (Vergoulis, Vlachos et al. 2012).

## 1.7 MicroRNAs in autoimmune and neuroinflammatory disorders

Recent studies have shown that miRs are integral elements in the post-transcriptional control of gene expression during the immune response (Baltimore, Boldin et al. 2008). MiRs are also involved in the regulation of the immune system (Sassen, Miska et al. 2008) and are particularly important in B and T cell homeostasis and immunological function (Li, Chau et al. 2007; Xiao, Calado et al. 2007; Xiao and Rajewsky 2009), suggesting that miRs may be also involved in the development of inflammatory and/or autoimmune diseases (Ceribelli, Satoh et al. 2012), in particular in neuroinflammation and in vascular inflammation (Pauley and Chan 2008; Urbich, Kuehbacher et al. 2008; Bi, Liu et al. 2009; Carissimi, Fulci et al. 2009). Several studies have shown miR dysregulation in neuroinflammatory and autoimmune diseases such as MS (Otaegui, Baranzini et al. 2009; Lindberg, Hoffmann et al. 2010; Junker, Hohlfeld et al. 2011).

A study of miR expression in active and inactive MS lesions revealed the most up-and down-regulated miRs as shown in Table 1.7 (Junker, Krumbholz et al. 2009). Studies of miR expression by miR microarray of total RNA extract from whole blood samples of RRMS patients have shown that there are 165 genes with changes in their expression, where miR-145 appears to be a suitable single marker for disease status. As for the other miRs, 43 miRs are in common with other human diseases (Human microRNA Disease Database) and 122 are probably exclusively associated with MS (Keller, Leidinger et al. 2009). Other studies have been performed on miR expression in

PBMC, whole blood, lymphocytes and regulatory T cells of MS patients, but the role of

endothelial miRs in

| miRs up-regulated in lesions | Percent surrogate housekeeping gene in lesions | Fold regulation in lesions compared to normal brain white matter | miRs down-regulated in lesions | Percent surrogate housekeeping gene in lesions | Fold regulation in lesions compared to normal brain white matter |
|---|---|---|---|---|---|
| miR profiles in active multiple sclerosis lesions | | | | | |
| miR-650 | 5.7 | 15.1** | miR-656 | 0.2 | 0.15** |
| miR-155 | 37.1 | 11.9** | miR-184 | 0.9 | 0.21** |
| miR-326 | 1.5 | 8.9** | miR-139 | 1.1 | 0.36** |
| miR-142-3p | 68.5 | 7.7** | miR-23b | 16.9 | 0.37** |
| miR-146a | 73.7 | 6.4** | miR-328 | 34.1 | 0.46** |
| miR-146b | 50.4 | 5.1** | miR-487b | 4.7 | 0.46** |
| miR-34a | 9.3 | 4.9** | miR-181c | 2.1 | 0.48** |
| miR-21 | 82.7 | 3.9** | miR-340 | 7.2 | 0.50** |
| miR-23a | 1.4 | 3.9** | | | |
| miR-199a | 1.2 | 3.3** | | | |
| miR-27a | 88.3 | 3.1** | | | |
| miR-142-5p | 8.3 | 3.0** | | | |
| miR-193a | 10.5 | 2.9** | | | |
| miR-15a | 12.3 | 2.8** | | | |
| miR-200c | 2.3 | 2.8** | | | |
| miR-130a | 9.8 | 2.6** | | | |
| miR-223 | 167.9 | 2.4** | | | |
| miR-22 | 25.1 | 2.4** | | | |
| miR-320 | 49.2 | 2.2** | | | |
| miR-214 | 2.5 | 2.1** | | | |
| miR profiles in inactive multiple sclerosis lesions | | | | | |
| miR-629 | 1.4 | 10.1** | miR-219 | 0.9 | 0.02** |
| miR-148a | 16.1 | 9.8** | miR-338 | 1.1 | 0.04** |
| miR-23a | 2.9 | 8.8** | miR-642 | 0.3 | 0.06** |
| miR-28 | 15.4 | 6.9** | miR-181b | 55.0 | 0.13** |
| miR-195 | 214.9 | 5.0** | miR-18a | 0.7 | 0.14** |
| miR-497 | 11.2 | 4.8** | miR-340 | 3.9 | 0.15** |
| miR-214 | 4.5 | 4.3** | miR-190 | 0.5 | 0.16** |
| miR-130a | 16.0 | 4.2** | miR-213 | 1.4 | 0.22** |
| miR-135a | 37.8 | 3.7** | miR-330 | 3.5 | 0.24** |
| miR-204 | 127.0 | 3.2** | miR-181d | 22.0 | 0.32** |
| miR-200c | 2.7 | 3.1** | miR-151 | 20.7 | 0.37** |
| miR-660 | 32.5 | 3.1** | miR-23b | 15.4 | 0.37** |
| miR-152 | 54.4 | 3.1** | miR-140 | 52.6 | 0.50** |
| miR-30a-5p | 424.8 | 3.0** | | | |
| miR-30a-3p | 73.7 | 3.0** | | | |
| miR-365 | 37.0 | 2.9** | | | |
| miR-532 | 16.2 | 2.9** | | | |
| miR-126 | 288.0 | 2.4** | | | |
| let7c | 136.2 | 2.4** | | | |
| miR-20b | 7.0 | 2.4** | | | |
| miR-30d | 67.0 | 2.3** | | | |
| miR-9 | 239.8 | 2.2** | | | |

**Table 1.7: MiR profiles in active and inactive multiple sclerosis lesions.** Taken from (Junker, Krumbholz et al. 2009)

MS was investigated only in one recent study, where they suggested miR-125a-5p as

key regulator of BBB tightness and immune cell migration in neuroinflammation and in

MS (Reijerkerk, Lopez-Ramirez et al. 2013). However, the role of miRs in MS and neuroinflammation is only starting to emerge and requires further investigation. This study has concentrated on identifying the roles of one miR (miR-155) and a miR:miR* pair (miR-126:miR-126*) in BBB dysfunction and these miRs will be further described in the context of neuroinflammation in the introduction to their respective Chapters.

### 1.7.1 MiR-126 and miR-126*

MiR-126 (referred to as miR-126-3p) and its complement miR-126*(referred to as miR-126-5p) are highly conserved and in mammals are encoded by intron 7 (Fig. 1.19) of the EGF-like domain 7 (*Egfl7*) gene in chromosome 9 (loc. 9q34.3). The egfl7 gene consists of 10 exons, 10 non-coding introns and 1 miR locus, the intron 7. In this intronic region, there is the pre-miRNA structure from which both miR-126 and miR-126* are originated (Kuhnert, Mancuso et al. 2008; Meister and Schmidt 2010). EGFL7 is specifically produced by endothelium and is implicated in EC migration and blood vessel formation, both under physiological and pathological angiogenesis (Musiyenko, Bitko et al. 2008).

MiR-126 has been shown to be specific to endothelium and it is the most highly enriched miR in EC (van Solingen 2009). In further studies, it has been shown to govern vascular integrity and angiogenesis both *in vivo* and *in vitro* (Fish, Santoro et al. 2008; Wang, Aurora et al. 2008; Zou, Li et al. 2011; Sessa, Seano et al. 2012). Indeed, miR-126 null mice developed vascular abnormalities which led to partial embryonic lethality due to vascular rupture (Wang, Aurora et al. 2008). Moreover, these mice showed cerebral edema and vascular leakage, loss of capacity to build an integrated retinal and corneal vascular network (Kuhnert, Mancuso et al. 2008). Mir-126 *in vitro*

regulates EC migration, organization of the cytoskeleton and capillary network stability in EC *in vitro* (reviewed in (Wu, Yang et al. 2009)). In vascular inflammation, increased expression of miR-126 has been shown to result in a decrease of VCAM1 expression and diminished leukocyte adhesion to TNFα stimulated-HUVEC (Harris, Yamakuchi et al. 2008). Furthermore, miR-126 was found down-regulated in HUVEC by TNF-α (Suarez, Wang et al. 2010).

Very little is known about the biological function/s of miR-126*. It has been shown that miR-126* is involved in cell proliferation, migration and invasion in different type of cancer (Meister and Schmidt 2010; Felli, Felicetti et al. 2013; Zhang, Yang et al. 2013) and that it inhibits erythropoiesis (Huang, Gschweng et al. 2011). MiR-126 and -126* are also involved in many other different biological events, targeting non vascular and non inflammatory genes as shown in Table 1.8, indicating that these two miRs are not only key regulators of vascular inflammation but also EC biology. However, further investigation on miR-126 and -126* is needed to unravel the role of these two intronic miRs in EC, in particular in brain endothelium, regulation of leukocyte trafficking.
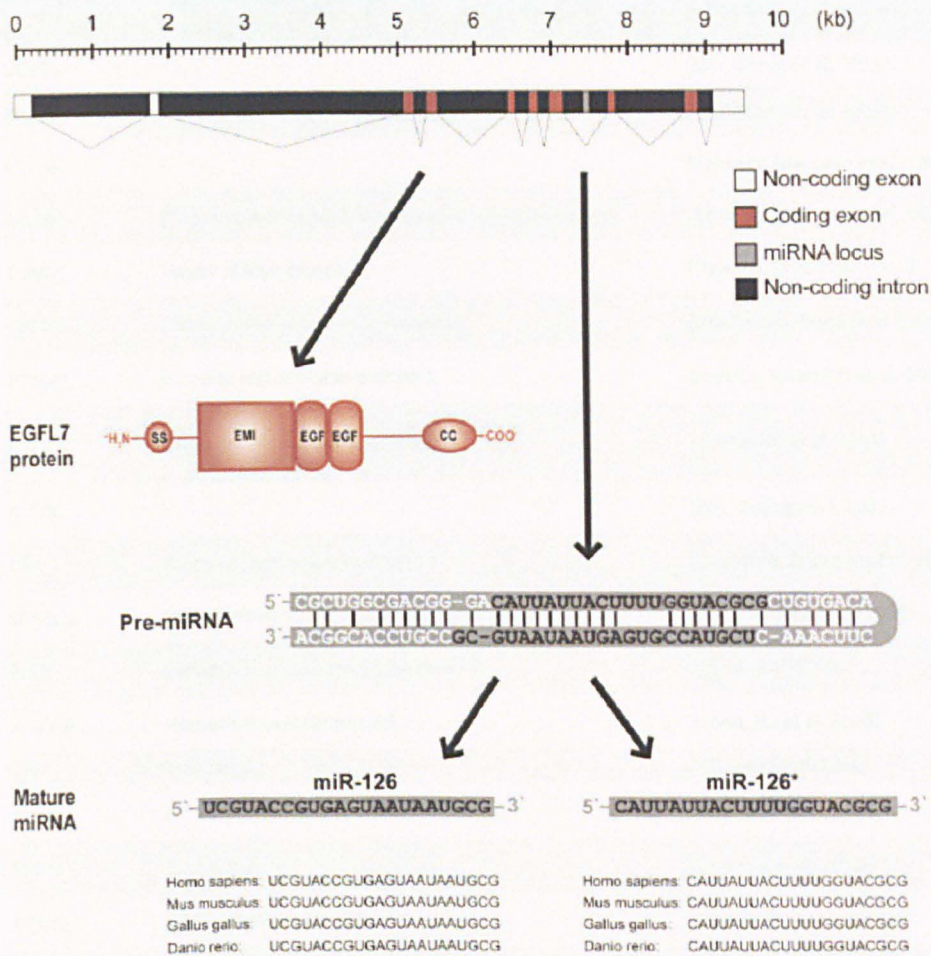
**Fig. 1.19: Mir-126 and -126\* originate from the same pre-miR structure, located in the intron 7 of the *egfl7* gene. Top.** Structural organization and products of the *egfl7* *gene*. **Middle**. Pre-miR structure located in intron 7, and mature mir-126 and -126\* sequences. **Bottom**. Conserved mir-126 and -126\* sequences in different species. Taken from (Meister and Schmidt 2010).

| miR | VALIDATED TARGET listed in TARBASE gene name | description | Reference |
|---|---|---|---|
| 126 | VEGFA | - | (Zhu, Zhang et al. 2011) |
| 126 | EGFL7 | EGF-like domain-containing protein 7 Precursor | (Zhu, Zhang et al. 2011) |
| 126 | P85beta | - | (Kuhnert, Mancuso et al. 2008) |
| 126 | PIK3R2 | Phosphatidylinositol 3-kinase regulatory subunit beta | (Kuhnert, Mancuso et al. 2008) |
| 126 | TOM1 | Target of Myb protein 1 | (Oglesby, Bray et al. 2010) |
| 126 | SLC45A3 | Solute carrier family 45 member 3 | (Musiyenko, Bitko et al. 2008) |
| 126 | VCAM1 | Vascular cell adhesion protein 1 | (Harris, Yamakuchi et al. 2008) |
| 126 | RGS3 | Regulator of G-protein signaling 3 | (Zhang, Du et al. 2008) |
| 126 | V-CRK | - | (Zhu, Zhang et al. 2011) |
| 126 | CRK | Proto-oncogene C-crk (p38) | (Crawford, Brawner et al. 2008) |
| 126 | SPRED1 | Sprouty-related, EVH1 domain-containing protein 1 | (Fish, Santoro et al. 2008) |
| 126 | PLK2 | Serine/threonine-protein kinase PLK2 | (Li, Lu et al. 2008) |
| 126 | HOXA9 | Homeobox protein Hox-A9 | (Shen, Hu et al. 2008) |
| 126 | TWF1 | Twinfilin-1 | (Li, Song et al. 2010) |
| 126 | IRS-1 | - | (Lee, Choi et al. 2011) |
| 126 | TWF2 | Twinfilin-2 | (Li, Song et al. 2010) |
| 126 | CCNE2 | G1/S-specific cyclin-E2 | (Zhang, Du et al. 2008) |
| 126 | IRS1 | Insulin receptor substrate 1 | (Zhang, Du et al. 2008) |
| 126 | SOX2 | Transcription factor SOX-2 | (Otsubo, Akiyama et al. 2011) |
| 126 | E2F2 | Transcription factor E2F1 | (Diaz, Silva et al. 2008) |
| 126* | prostein | Solute carrier family 45 member 3 | (Musiyenko, Bitko et al. 2008) |
| 126* | SLC45A3 | - | (Musiyenko, Bitko et al. 2008) |
| 126* | NM_033102 | - | (Musiyenko, Bitko et al. 2008) |

**Table 1.8: miR-126 and -126\* experimentally validated targets.** Since miR-126 and -126\* have different sequences, they have different gene targets. Mir-126 and -126\* targets are components of different cellular pathways involved in several physiological and pathological conditions.

**1.7.2 MiR-155**

MiR-155 is highly expressed in HUVEC (Zhu, Zhang et al. 2011) and originates from an exon of a non-coding sequence of the *bic* gene located in chromosome 21q21. The gene encoding miR-155 *bic* was classified as an oncogene, implicated in promotion of a tumor phenotype (Xu, Fewell et al. 2010). MiR-155 is highly conserved in different species, and it is one of the most studied miRs. It has been shown to be a multifunctional miR involved in numerous biological processes such as inflammation, cancer, immunity and hematopoiesis (for a review see (Faraoni, Antonetti et al. 2009)). In particular, it has been reported that proinflammatory cytokines such as TNF-$\alpha$ and IFN-$\gamma$ increase miR-155 expression levels in human retinal pigment epithelial (HRPE) cells (Kutty, Nagineni et al. 2010). It has also been shown that TNF-$\alpha$ alone was sufficient to up-regulate miR-155 in HUVEC (Suarez, Wang et al. 2010). In addition, miR-155 and its passenger strand, miR-155*, were found to be up-regulated in MS active lesions (Table 1.7) (Junker, Krumbholz et al. 2009). Furthermore, mir-155 promotes the production of proinflammatory cytokines in human CD14+ cells such as TNF-$\alpha$ and IL-1$\beta$ (Kurowska-Stolarska, Alivernini et al. 2011).

Concerning its biological function on endothelium, miR-155 appears to regulate the inflammatory response of HUVEC in response to angiotensin II, a vasoactive peptide, by down-regulating VCAM1 and CCL2 and decreasing Jurkat T cell adhesion (Zhu, Zhang et al. 2011). MiR-155 targets angiotensin II type 1 receptor (AT1R) and decreases ERK1/2 phosphorylation in fibroblasts, suppressing angiotensin efficacy (Zheng, Xu et al. 2010). AT1R activation by angiotensin II triggers endothelial dysfunction, structural remodelling and vascular inflammation (Kim and Iwao 2000).

Furthermore, a silent polymorphism +1166 A/C of the 3'UTR of the human AT1R gene was reported to play a role in vascular inflammation and cardiovascular complications. In addition, miR-155 targets Est-1 in HUVEC (Zhu, Zhang et al. 2011), a critical transcription factor involved in vascular angiogenesis (Sato 2001), inflammation and remodelling (Zhan, Brown et al. 2005). Est-1 is induced in response to stimuli such as TNFα and angiotensin II in EC, to act on genes involved in vascular inflammation such as VCAM1 and CCL2 (Sato 2001; Zhan, Brown et al. 2005). Taken together, the results of these studies have identified miR-155 as one of the miRs that contributes to specific endothelial inflammation and disease (Urbich, Kuehbacher et al. 2008).

In the CNS, miR-155 has been shown to be involved in neuroinflammation as a pro-inflammatory miR that contributes to activate macrophage and microglia, by targeting anti-inflammatory molecules (such as FADD, SOCS-1, IKK, SMAD-2) (Ponomarev, Veremeyko et al. 2013), and astrocytes by targeting a negative regulator of cytokine signalling (Tarassishin, Loudig et al. 2011).

## 1.8 *In vitro* models of the blood-brain barrier

### 1.8.1 Human brain endothelial cell lines

To study the BBB under physiological and/or pathological conditions, *in vivo* models and/or *in vitro* models using primary brain endothelium based on rat, mouse, sheep, cattle, pig, and human, have been widely used (Fig 1.20). However, these models are complex, expensive and, in the case of human, the samples are very difficult to obtain. For these reasons, from the 90s, BEC lines started to be created as a tool to overcome these complexities. Most of the immortalized cell lines used in BBB models were isolated from murine (Marelli-Berg, Peek et al. 2000) and rat (Tunkel, Rosser et al. 1991) tissues (Fig. 1.20).

The first immortalized human BBB cell line was developed in 1997 from capillaries and microvessels derived from small samples of human temporal lobe excised surgically from a patient treated for idiopathic epilepsy, transfected with simian vacuolating virus 40 SV40 large T antigen to develop an immortalized human cerebral endothelial cell (HCEC) line (Muruganandam, Herx et al. 1997). However, this cell line did not satisfy the major requirements that an ideal *in vitro* BBB model should meet, listed in Table 1.9 (Naik and Cucullo 2012). In effect, HCEC did not express selectins or adhesion molecules or TJ, but expressed BBB specific enzymes, and showed a partial endothelial phenotype (Weibel Palade bodies, Von Willebrand factor secretion and plasminogen activators) and lower (or equal) leakiness and higher TEER when compared to non-CNS primary microvascular EC (Bouïs, Hospers et al. 2001).

## Static BBB models
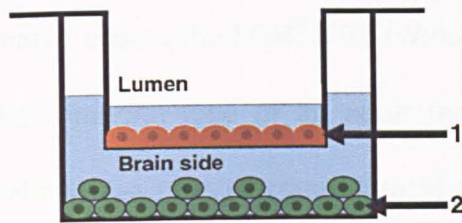


**1  Brain endothelial cells**

- Primary endothelial cells:

bovine (Cecchelli et al., 1999)

porcine (Meyer et al., 1990)

rat (Perrière et al., 2007)

mouse (Coisne et al., 2005)

human (Persidsky et al., 1997; Biernacki et al., 2005)

**2  Co-culture or not with**

- Glial cells / Astrocytes (Cecchelli et al., 1999)
- Pericytes (Zozulya et al., 2008)
- Astrocytes and Pericytes (Nakagawa et al., 2007)
- Neurons (Stanness et al., 1999)

- Endothelial cell lines:

bovine : SV-BEC (Durieu-Trautmann et al., 1991)

porcine : PBMEC (Teifel M & Friedl, 1996)

rat : RBE4 (Roux et al., 1994)

mouse : bEnd5 (Laschinger & Engelhardt B, 2000)

human : hCMEC/D3 (Weksler et al., 2005)

**Fig. 1.20: Static blood-brain barrier models of the blood-brain barrier and neurovascular unit *in vitro* that have also been used for leukocyte trafficking studies. 1.** Primary BEC or EC lines, grown in the upper compartment of Boyden chambers or filter transwells. **2.** In order to model the NVU, various other cell types (glial cells, pericytes or neurons) can be co-cultured in the lower compartment. Taken from (Weiss, Miller et al. 2009).

| Functional Features of an Ideal *In Vitro* BBB Model |
|---|
| Enable the expression of TJ between adjacent EC. |
| Negligible paracellular diffusion between EC. |
| Selective and asymmetric permeability to physiologically crucial ions (Na$^+$, K$^+$, Cl$^-$). |
| Functional expression of efflux systems and selective transport mechanisms (e.g., P-gp, MRPs, hexose, aminoacid, monocarboxylic acid, and other relevant transporters). |
| Expression of drug-metabolizing enzymes (P450s, MAO, etc.). |
| Exposure to laminar shear stress (apical membrane), glia (basal membrane), and other permissive factors that promotes growth inhibition and differentiation of endothelial cells. |
| Responsiveness to permeation modulators (e.g., hyperosmolar mannitol) as well as other stimuli (endogenous and exogenous) that can affect BBB integrity and function. |
| Ability to reproduce the effect of a wide range of physiological and pathological stimuli (hypertension, flow arrest, inflammation, etc.) that affect the BBB *in vivo*. |
| User friendly, scalable, and cost effective. |

**Table 1.9: Functional and structural requirements for an ideal *in vitro* blood-brain barrier model to mimic the *in vivo* blood-brain barrier.** Taken from (Naik and Cucullo 2012).

In 2005 a new immortalized cell line of brain endothelial cells was isolated and characterised, the hCMEC/D3 (Weksler, Subileau et al. 2005). BEC were isolated from the temporal lobe of an adult female with epilepsy, and transduced with hTERT (telomerase reverse transcriptase) and SV40 large T antigen. This cell line has been widely used in the last eight years (for a review of all studies made using this cells line see (Weksler, Romero et al. 2013). In 2008, THBMEC were immortalized and characterised and compared with HUVEC (Man, Ubogu et al. 2008). THBMEC strongly and continuously expressed ZO-1 and occludin, and exhibited higher TEER than HUVEC. In addition, Man et al. showed that the new model was more restrictive to monocyte and T cell migration than HUVEC and migration was promoted by CCL3 and CCL5 (Man, Ubogu et al. 2008).

To study the role of endothelial miRs in leukocyte adhesion *in vitro* we used the immortalized hCMEC/D3 cell line (Weksler, Subileau et al. 2005). hCMEC/D3 cells are the most characterised out of the three existing immortalized cell lines. Weksler et al. have shown that hCMEC/D3 cells expressed BBB-specific ABC transporters, tight junctions, adhesion molecules such as ICAM1, ICAM2, VCAM1, chemokines and chemokines receptors (Weksler, Subileau et al. 2005). However, hCMEC/D3 cells have a lower TEER compared to THBMEC. To study leukocyte adhesion to brain endothelium, this parameter seems not crucial as other more important parameters such as adhesion molecules and selectins. Recently, THBMEC were used to investigate leukocyte migration mediated by CXCL12 although no data on the adhesion molecules involved in migration was reported (Man, Tucky et al. 2012).

**1.8.2 *In vitro* flow-based systems to study leukocyte trafficking with live cell imaging**

Leukocyte trafficking has been extensively studied *in vitro* using static transwell culture models (Fig. 1.20), however, the lack of shear stress has been an experimental limitation because *in vivo* this event is subjet to continuous shear stress due to the blood flow. Since the mid-80s biomedical engineers have developed flow chambers capable of maintaining defined and stable laminar flow (Luscinskas, Lim et al. 2001). The first approach to flow-based assays was based on the observation of interactions between immune cells and a ligand (selectin or CAM) incorporated (Diacovo, Roth et al. 1996) or coated (Brunk and Hammer 1997) on a parallel plate flow chamber (Figs. 1.21 A and C) or incorporated into a flow-based system as described in Fig. 1.21 B. These methods were used to further investigate the early steps of leukocyte trafficking, rolling and adhesion, *in vitro*, which beforehand could only be observed *in vivo* by intravital microscopy (reviewed in (Sperandio, Pickard et al. 2006).

The *in vitro* flow-based assays have been further developed by using EC, particularly HUVEC, instead of single molecules (Abbassi, Kishimoto et al. 1993; Bahra, Rainger et al. 1998; Cinamon and Alon 2003; Sheikh, Rahman et al. 2005). These newer models use either the flow assay system described in Fig. 1.21 or the adapted system depicted in Fig. 1.22, which involve growing cells on either flattened glass capillaries (microslides), porous filters (Chakravorty, McGettrick et al. 2006) or transwells (McGettrick, Buckley et al. 2010) instead of glass slide supports. These systems may be used with different cells types, which can be cultured, stimulated, used for rolling-adhesion-migration assays and harvested for further studies. However, attachment of the growth support to the flow system is difficult and a high number of cells are required to obtain proper monolayers.
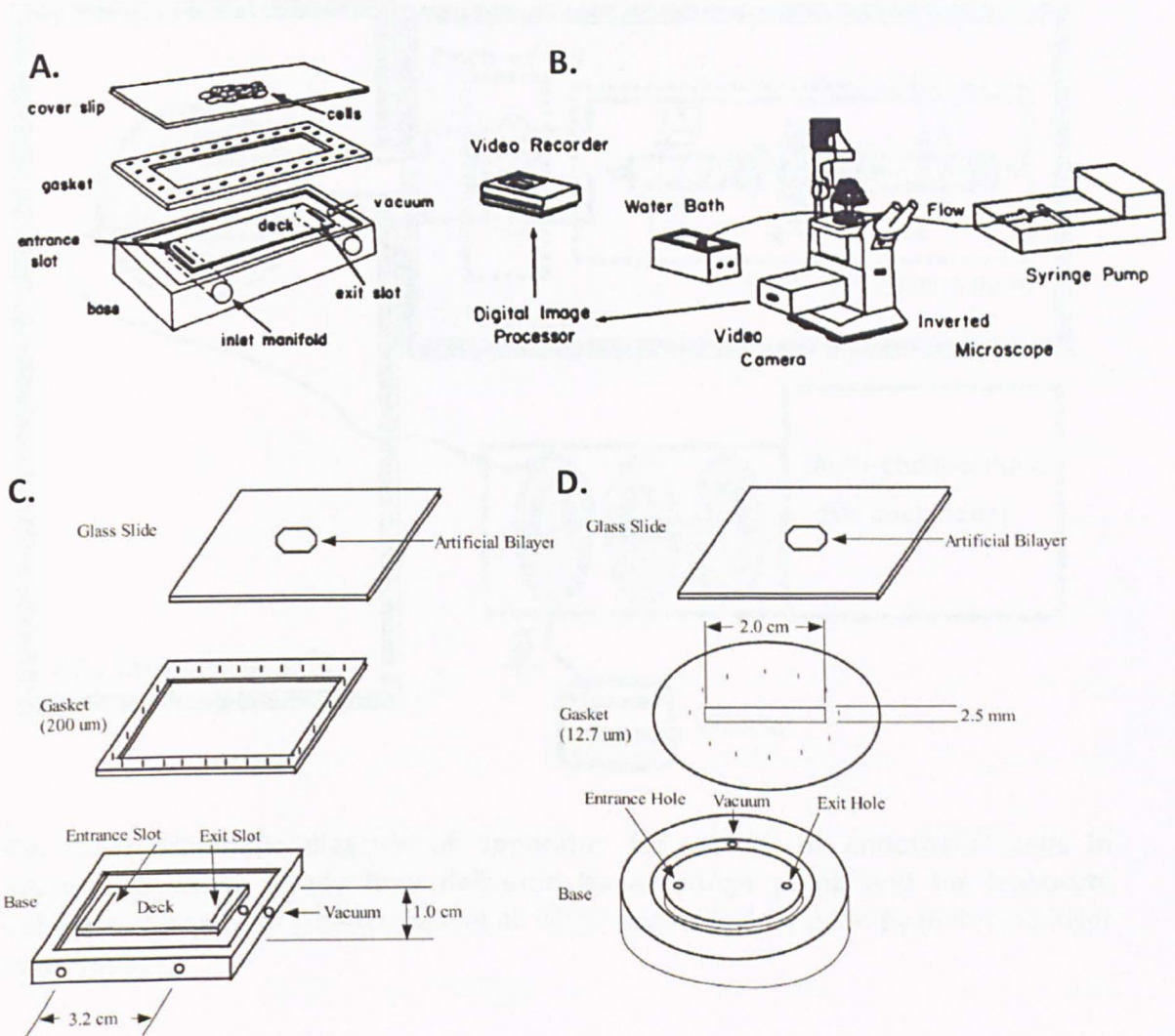
**Fig. 1.21: Schematic diagrams showing the parallel plate flow chamber widely used for leukocyte adhesion to endothelial cells. A.** The parallel plate flow chamber first described by Lawrence et al. (Lawrence, McIntire et al. 1987) **B.** The first flow-based assay system to investigate leukocyte trafficking set up by Lawrence et al. **C.** The parallel plate flow chamber as described by Lawrence et al. depicted by (Brown and Larson 2001) to study leukocyte rolling and adhesion to EC. **D.** The parallel plate available from Glycotech. Taken from (Lawrence, McIntire et al. 1987) for the top and (Brown and Larson 2001) for the bottom panels.
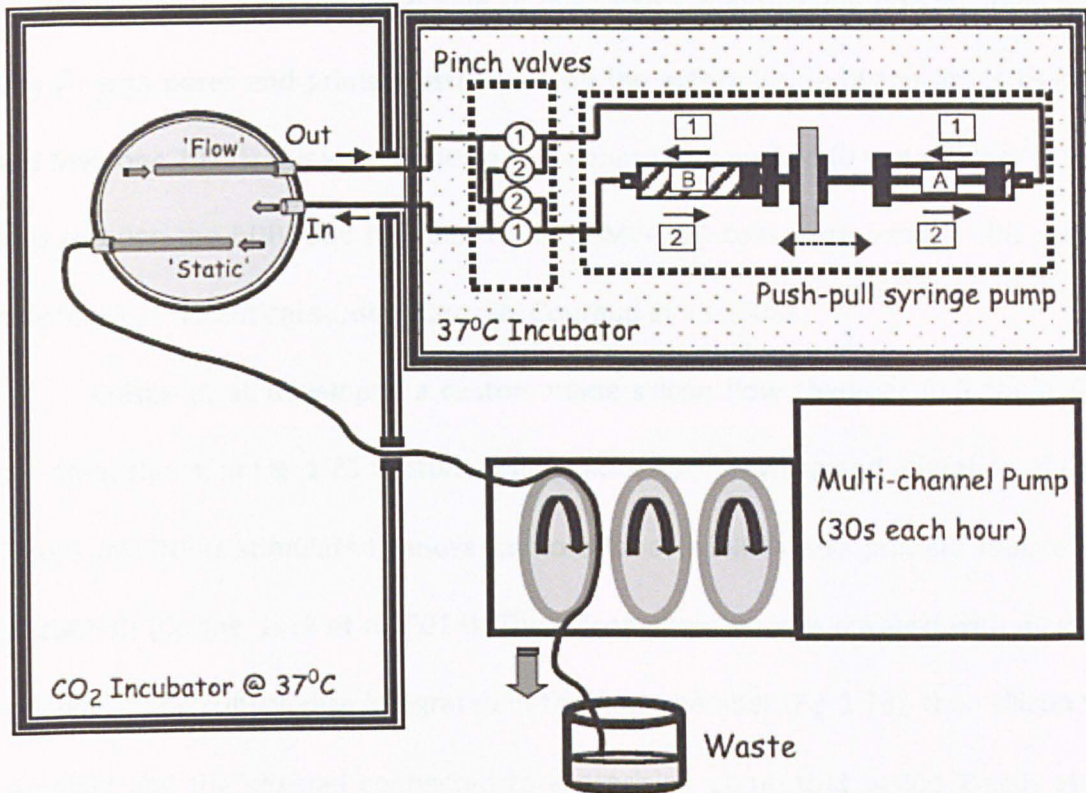
**Fig. 1.22: Schematic diagram of apparatus for culture of endothelial cells in microslides under steady flow delivered by a syringe pump and for leukocyte adhesion.** Taken from (Sheikh, Gale et al. 2004) originally developed by (Bahra, Rainger et al. 1998).

While tubing and temperature are important parameters that may influence leukocyte adhesion to EC in these models (Sheikh, Gale et al. 2004), shear stress is a critical factor that influences activation of endothelial cells. It has been shown that in these models, different shear stress rates (range: 0 to 15 dyn/cm$^2$) can be applied with steady or pulsatile flow. However, these models are technically difficult and not sterile.

Recently, a new generation of flow-based systems has been produced to study leukocyte adhesion to BEC. Cucullo et al. used a dynamic *in vitro* BBB model (Cucullo, Hossain et al. 2013), using hCMEC/D3 cells (Cucullo, Couraud et al. 2008) or with primary human microvascular BEC (primary, ScienCell) (Cucullo, Marchi et al. 2011). THP-1 extravasation was studied using a commercially available primary cell line of

human BEC seeded on the inner side of hDIV-BBB polypropylene hollow fibers (0.33 mm Ø) with pores and primary astrocytes on the external side of the fibres (Hassain and Mazzone 2011). This was connected to a pump that pushed (0 to 4 dyn/cm$^2$) THP-1 cells through the hDIV-BBB module, while hCMEC/D3 cells were used in this system only for pharmaceutical studies (Cucullo, Couraud et al. 2008).

Coisne et al. developed a custom-made silicon flow chamber (0.6 cm Ø, 0.28 cm$^2$ area) shown in Fig. 1.23 to study rolling, adhesion, crawling and migration of CD4+ T cells on TNF-α stimulated mouse immortalized (bEND5) and primary mouse BEC (pMBMEC) (Coisne, Lyck et al. 2013). The silicon chamber was covered with glass, EC monolayers on culture dish integrated in the flow chamber (Fig 1.23), then silicon was removed and the channel connected to a precision pump that pulled T cells at 1.5 dyn/cm$^2$. Man et al. modified a chemotaxis chamber (Neuro Probe AA12) made of acrylic top, middle, and bottom plates, with a silicone top and bottom silicon gaskets (Man, Tucky et al. 2012) to investigate transmigration of CD4, 8, 14 and 19+ cells across TNF-α and IFN-γ stimulated THBMEC line under flow (0.2 dyn/cm$^2$). These two innovative *in vitro* BBB model systems enabled flexible analysis of leukocyte trafficking across the BBB under physiological shear forces (flow) using immortalized models of the BBB. However, these systems are difficult to reproduce due to the high specialist material engineering knowledge and technology required.
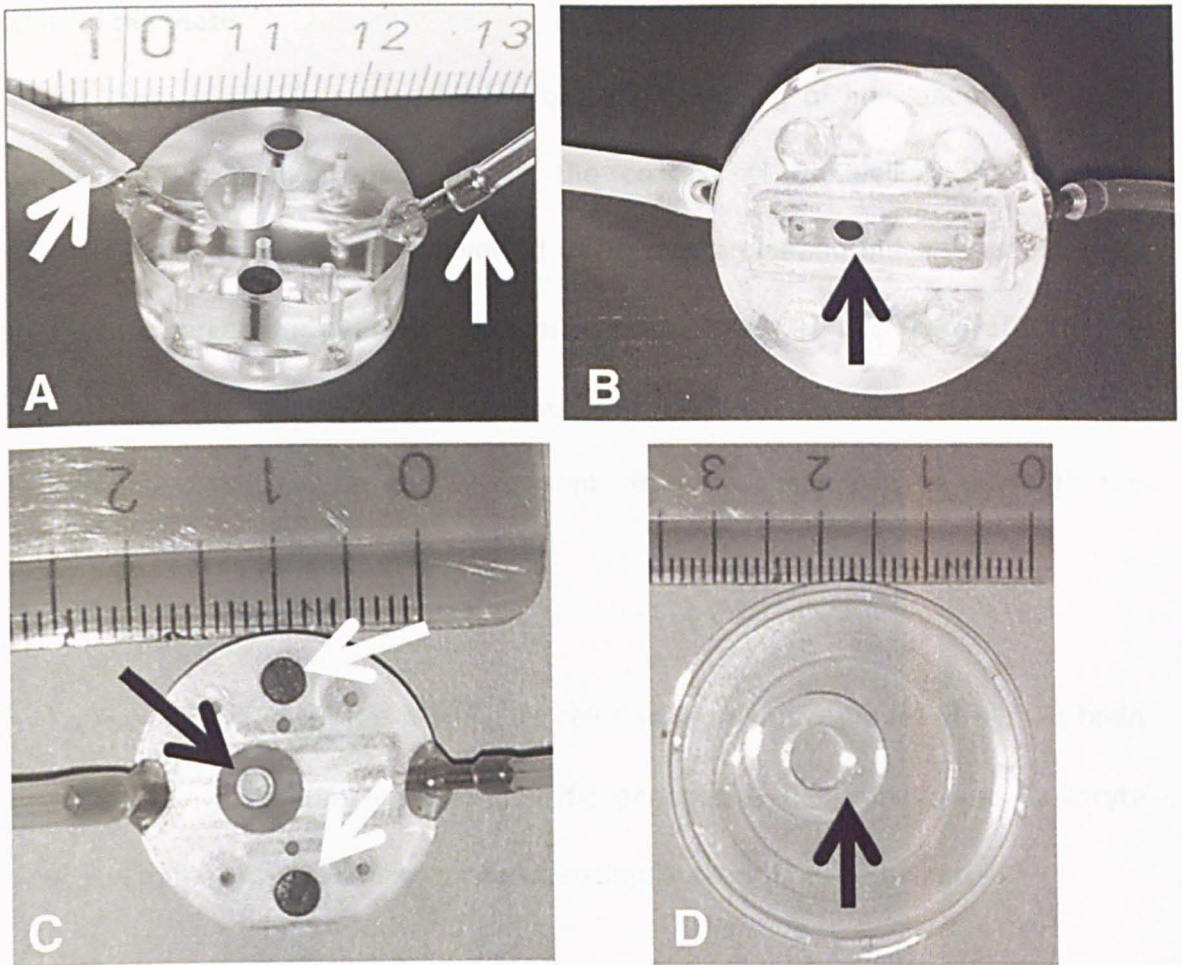
**Fig. 1.23: An *in vitro* blood-brain barrier model system with a flow chamber for studying leukocyte rolling, adhesion, crawling and migration**. A. The flow chamber is shown from the side, **B.** from the base **C.** and from the top. White arrows in panel **A.** show the inlet and outlet tubes. Black arrows in panels **B.** and **C.** show the field of view. A rectangle within the thin silicon mat visible in panel B surrounds the inflow and the outflow and restricts medium flow to a small chamber 2 mm wide and 0.25 mm high. White arrows in panel **C.** show the magnets embedded into the flow chamber to fix the chamber to fix the chamber via a metal ring opposed on the base of the culture dish. The cloning ring shown with a diameter of 0.6 cm in image **D.** restricts the surface area of brain endothelial cells 0.28 cm2. Scale is in cm. Taken from (Coisne, Lyck et al. 2013).

**Aims of the thesis**

There is a real need to further our understanding of how endothelial miRs modulate BBB function not only in the context of unravelling the complex pathophysiological mechanisms involved in neuroinflammation but also as potential therapeutic targets for neuroinflammatory disorders such as MS. The overall aim of this study is to investigate the role of endothelial miRs on leukocyte adhesion to BEC in neuroinflammation. To do so, the current study has been carried out with the following specific objectives in mind:

1. To establish whether the hCMEC/D3 cell line, an *in vitro* model of human brain endothelium, is suitable to study specific endothelial miRs and static leukocyte adhesion to the pro-inflammatory cytokine-stimulated brain endothelium.

2. To establish a new flow based assay to study leukocyte adhesion mimicking the blood flow in microvasculature using the hCMEC/D3 cell line as model of human brain endothelium.

3. To identify specific pro-inflammatory cytokine-up/down-regulated endothelial miRs with a role in alterations in leukocyte adhesion to brain endothelium, and, identify specific inflammatory gene targets.

# Chapter 2: Materials and methods

## 2.1 Materials

A list of chemicals and solutions used for this project is shown in Table 2.1.

**Table 2.1: List of chemicals or solutions used in this project**. List includes supplier and catalogue number.

| Chemical or solution | Supplier | Catalogue # |
|---|---|---|
| Alexa Fluor® 488 Goat Anti-Mouse IgG secondary antibody | Applied Biosystems, Warrington, UK | A-11001 |
| BSA albumin from bovine serum | Sigma-Aldrich, Dorset, UK | A9085 |
| Cell tracker™ green CMFDA (5-chloromethylfluorescein diacetate) | Invitrogen LTD, Paisley, UK | C2925 |
| Citric acid | Bdh analar, Sussex, UK | 10081 |
| Collagen type I from calf skin | Sigma-Aldrich, Dorset, UK | C9791 |
| DAPI-fluoromount-G™ 4',6-diamidino-2-phenylindole | Southernbiotech, Birmingham, USA | 0100-20 |
| DMSO Dimethyl sulfoxide | Sigma-Aldrich, Dorset, UK | D2438 |
| EGM®-2 MV supplements | Lonza, Basel, Switzerland | CC-4147 |
| Endothelial Basal Medium-2 EBM®-2 complete media | Lonza, Basel, Switzerland | CC-3156 |
| FBS Foetal bovine serum | Sigma-Aldrich, Dorset, UK | F7524 |
| Ficoll-Paque PLUS | GE Healthcare, Chalfont St Giles, UK | N.A. |
| Goat serum | Sigma-Aldrich, Dorset, UK | G9023 |
| Glutaraldehyde | Agar, Essex, UK | R1311 |
| HBSS Hank's Balanced Salt Solution with sodium bicarbonate, calcium and magnesium free, no phenol red | Sigma-Aldrich, Dorset, UK | H8264 |
| HBSS Hank's Balanced Salt Solution with sodium bicarbonate, calcium and magnesium, no phenol red | Sigma-Aldrich, Dorset, UK | H6648 |
| Hydrogen peroxide solution | Sigma-Aldrich, Dorset, UK | H1009 |
| Lipofectamine™ 2000 | Invitrogen, Paisley, UK | 11668-027 |
| N,N,N',N'-Tetramethylbenzidine | Sigma-Aldrich, Dorset, UK | T2885 |
| Nuclease free water | Ambion\|RNA Life Tecnologies™, Paisley, UK | AM9932 |
| Optimem® I reduced serum medium | Gibco® Invitrogen, Paisley, UK | 31985 |
| *p*-formaldehyde | Sigma-Aldrich, Dorset, UK | P6148 |
| PBS Phosphate-buffered saline | Sigma-Aldrich, Dorset, UK | P4417 |

| | | |
|---|---|---|
| Polyclonal goat anti-mouse IgG biotinylated | Dako A/S Denmark | E0433 |
| Recombinant human IFNγ | R&D systems, Abingdon, UK | 285-IF |
| Recombinant human TNFα | R&D systems, Abingdon, UK | 210-TA |
| RPMI 1640 w/glutamax | Gibco® INVITROGEN, Paisley, UK | 61870010 |
| Siport™ Polyamine Transfection Agent | Applied Biosystems, Warrington, UK | AM4503 |
| Sodium acetate | Sigma-Aldrich, Dorset, UK | 89718 |
| Streptavidin-biotinylated horseradish peroxidase complex | GE Healthcare, Chalfont St Giles, UK | RPN1051 |
| Streptomycin/Penicillin (15140-10000µg/ml+10000units/ml | Gibco® INVITROGEN, Paisley, UK | 15140 |
| Sulfuric acid | Sigma-Aldrich, Dorset, UK | 339741 |
| Trizma® Hydrocloride  Tris HCl | Sigma-Aldrich, Dorset, UK | T5941 |
| TRIzol® reagent | Ambion \| RNA Life Tecnologies™, Paisley, UK | 15596-018 |
| Trypsin-EDTA solution | Sigma-Aldrich, Dorset, UK | T4049 |
| Tween-20 Polyoxyethylenesorbitan monolaurate | Sigma-Aldrich, Dorset, UK | P7949 |

## 2.2 Cell culture

### 2.2.1 hCMEC/D3 cell line

The immortalized human brain endothelial cell line hCMEC/D3 used in this study had been previously derived from a primary cell culture at passage 0 through co-expression of hTERT and the SV40 large T antigen via a highly efficient DNA-flap lentiviral vector system (Weksler, Subileau et al. 2005). hCMEC/D3 cells were grown in Endothelial Basal Medium-2 (EBM-2) and supplements (0.025% v/v VEGF, IGF and EGF, 0.1% v/v bFGF, gentamycin and ascorbic acid, 0.04% v/v hydrocortisone, and 2.5% v/v foetal bovine serum (FBS)), hereafter referred to a EBM-2 complete media, and changed every two days unless specified. Prior to seeding cells, tissue culture surfaces were coated with 1/20 (v/v) collagen type I from calf skin (0.1% solution in 0.1 M acetic acid) in Hanks` Balanced Salt Solution (HBSS) for 1 h at RT. For all experiments, hCMEC/D3 cells (passage 25-35) were grown on collagen-coated plates/slides (Table 2.2) in a 95% air and 5% $CO_2$ incubator at 37 °C until confluent ($\sim$1x10$^5$ cells/cm$^2$) and treated with recombinant human (*E. coli*-derived) TNF$\alpha$ and IFN$\gamma$ cytokines at the times and concentrations indicated for each experiment.

| ASSAY | Plate/chamber | Company | Collagen |
|---|---|---|---|
| Static Leukocyte Adhesion | 96 well plate, white, μ clear | Greiner Bio One (Stonehouse, UK) | 50μl/well |
| Flow based Leukocyte Adhesion | μSlide VI – flat with 6 parallel channels | Ibidi® (Martinsried, Germany) | 30μl/channel |
| ELISA | 96 well plate, μ clear | Greiner Bio One (Stonehouse, UK) | 50μl/well |
| Sample for RNA extraction | 12 well plate, μ clear | Greiner Bio One (Stonehouse, UK) | 500 μl/well |

**Table 2.2: Types of tissue culture plates and slides and collagen solution volumes used to seed hCMEC/D3 cells.**

## 2.2.2 hCMEC/D3 cell culturing on slides

Collagen-coated Ibidi® μSlide VI–flat (Ibidi® GmbH, Martinstreid, Germany) with six parallel channels were seeded with $6 \times 10^5$ hCMEC/D3 cells/channel in 30 μl of EBM-2 complete media. Cells were left to grow in complete EBM-2 media until the required confluence for the experiment and treated at the times and concentrations indicated for each experiment. Prior to the adhesion assay, hCMEC/D3 cells were washed three times with HBSS and rested in complete EBM-2 media.

## 2.2.3 Jurkat and THP1 cell lines

The T lymphocyte cell line Jurkat from acute T cell leukaemia and the monocytic cell line THP1 from acute monocytic leukaemia were a kind gift from Dr V Male (Cambridge University). Jurkat and THP1 cells were grown in suspension in RPMI 1640 W/GLUTAMAX I culture medium (containing 10% FBS and 100 μg/ml + 100 units/ml Streptomycin/Penicillin) in a 95% air and 5% $CO_2$ incubator at 37 °C.

## 2.2.4 Peripheral blood mononuclear cells

PBMC were isolated from MS patients recruited by Dr. Giulio Podda and Dr. Bruno Gran during their routine consultations in the Neurology department at Nottingham Hospital. Blood samples were collected, transported, handled and used for the experiments following the approved protocols by the local research ethical committee at both Nottingham and the OU, the approved human tissue transfer agreement and the signed informed consents obtained from all blood donors. PBMC were isolated from fresh heparinised blood of three MS patients (Table 2.3) by density centrifugation using Ficoll-Paque PLUS by Dr. Laura Edward and frozen in liquid

nitrogen in 10% DMSO until use. Just before the adhesion assay, PBMC were thawed,

counted and suspended at $2x10^6$ cells/ml in EBM-2 complete media.

| MS patient PBMC sample | MS patient disease stage | Sex | Age | Treatment |
|---|---|---|---|---|
| MS1 | RRMS | Male | 48 | Interferon-beta |
| MS2 | SPMS | Female | 64 | no treatment |
| MS3 | PPMS | Male | 59 | no treatment |

**Table 2.3: Clinical characteristics of peripheral blood donors with multiple sclerosis.** Relapsing remitting MS (RRMS), secondary progressive MS (SPMS), primary progressive (PPMS).

## 2.3 Flow cytometry analysis

For quantification of transfection efficiency, hCMEC/D3 cells were trypsinized with 0.25 % (w/v) Trypsin-EDTA solution and centrifuged ($800 \times g$, 5 min, 4 °C) and suspended in HBSS at 4 °C. For each transfected sample, $1\times10^4$ cells were analyzed on a FacScan analyser (Becton Dickinson, Franklin Lakes, NJ, USA), with detector voltage set so that >90% of isotype-control cells registered <10 fluorescence units. The wavelengths used for Cy3-labelled scrambled miR were Excitation wavelength ($\lambda_{ex}$) max 550 nm and Emission wavelength ($\lambda_{em}$) max 570 nm, while for FAM-labelled scrambled miR, $\lambda_{ex}$ max 495 nm and $\lambda_{em}$ max 516 nm. Data were analyzed using Cell Quest (Pro BD Biosciences) software. The results were expressed as median fluorescence in arbitrary units.

For characterization of subpopulations in isolated PBMC, cells were thawed in warm RPMI and counted. PBMC were resuspended at $0.5\times10^6$ cells/ml in phosphate buffered saline (PBS) and placed in FACS tubes ($1\times10^6$ cells/2ml/tube), then spun down for 10 min at 254 x $g$. The cell pellet was resuspended in 50 µl of PBS ($1\times10^6$/100µl) and incubated with fluorescently labelled primary antibody for 30 min at 4 °C at the concentrations indicated in Table 2.4. Followed by two washes in PBA (1/200 (v/v) 20% sodium azide + 1/60 (v/v) 30% bovine serum albumin (BSA) in PBS), PBMC were resuspended in 400 µl in a solution of 0.5% methanol in PBS and stored at 4 °C until analysis using flow cytometry with Becton Dickinson FacsCanto II (BD, Oxford, UK). Data were analyzed using FACSDiva software (BD, Oxford, UK). Results are expressed as percentage of positive cells.

| Antibody | Fluorophore | Company | Clone | Excitation/Emission | Isotype | Volume | Final concentration |
|---|---|---|---|---|---|---|---|
| MONOCLONAL Anti-human CD4 | Brilliant Violet™ 421 | BD, Oxford, UK | RPA-T4 | Ex max 407 nm Em max 421 nm | Ms IgG1, κ | 2.5 µl | 25 µl/ml |
| MONOCLONAL Anti-human CD8 | PE-CF 594 | BD, Oxford, UK | RPA-T8 | Ex max 564 nm Em max 612 nm | Ms IgG1, κ | 2.5 µl | 50 µl/ml |
| MONOCLONAL Anti-human CD14 | PE | BD, Oxford, UK | MSE2 | Ex max 496 nm Em max 578 nm | Ms IgG2a, κ | 10 µl | 12.5 µl/ml |
| MONOCLONAL Anti-humanCD56 | FITC | BD, Oxford, UK | NCAM16.2 | Ex max 494 nm Em max 519 nm | MsIgG2b, κ | 10 µl | 6 µl/ml |

## 2.4 MicroRNA transfection

hCMEC/D3 cells were grown to 30-40% confluence in complete EBM-2 media, then media was replaced with EBM-2 complete media without antibiotics. At ~70% confluence hCMEC/D3 cells were transfected with either miR precursors (pre-miRs) or antagonists (anti-miRs). For hsa-pre-miR transfections, the Siport™ Polyamine Transfection Agent was used, while, for hsa-anti-miR transfections a lipid-based Transfection reagent, the Lipofectamine® 2000 was used.

For both transfection reagents, the supplier's protocols were followed. Pre- and -anti-miR oligonucleotides were transfected in hCMEC/D3 cells using the transfection protocols depicted in Fig. 2.1 and the concentrations indicated, together with their nomenclature, in Table 2.5.
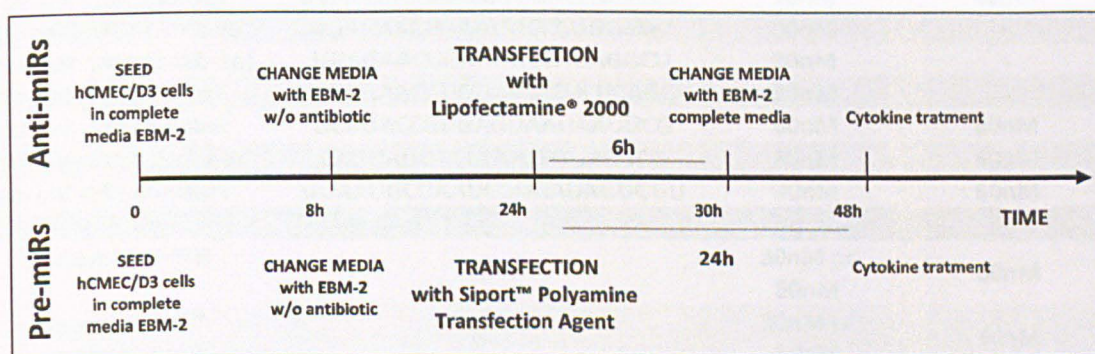


**Fig. 2.1: hCMEC/D3 cells seeding and transfection timeline.**

Briefly, Siport™ Polyamine Transfection Agent or Lipofectamine® 2000 was mixed with Opti-mem®I reduced-serum media to form the transfection complex. Negative control or pre- or anti-miR oligonucleotides were dissolved at the indicated concentrations in RNA-ase free water and mixed with Opti-mem®I reduced-serum media. The oligonucleotides were gently added to the transfection reagent complex, mixed and finally dispensed onto ~70% confluent hCMEC/D3 cells in EBM-2 complete

media without antibiotics. Anti-miR™ miRNA Inhibitor and Pre-miR™ miR precursor

negative controls were undisclosed random sequence RNA oligonucleotides that have

been extensively tested in human cell lines and tissues and validated to produce no

identifiable effects on known miR function by the manufacturers (Life Technologies,

Warrington, UK). Cy3™ and FAM™ dye-labelled anti- and pre-miR negative controls

were used for monitoring transfection efficiency in all experiments. Anti- or Pre-miR

Negative controls are labelled at their 5' end and have the same oligonucleotide

sequence as unlabeled Negative Controls (Life Technologies, Warrington, UK) used as

scrambled Anti- or Pre-miRs.

| MiR | Mature Sequence | Concentration Pre-miR | Concentration Anti-miR |
|---|---|---|---|
| hsa-miR-126 (126-3p) | UCGUACCGUGAGUAAUAAUGCG | 60nM | 60nM |
| hsa-miR-126* (126-5p) | CAUUAUUACUUUUGGUACGCG | - | 60nM |
| hsa-miR-155 (155-5p) | UUAAUGCUAAUCGUGAUAGGGGU | 30nM | 60nM |
| hsa-miR-146a (146a-5p) | UGAGAACUGAAUUCCAUGGGUU | 30nM | - |
| hsa-miR-146b (146b-5p) | UGAGAACUGAAUUCCAUAGGCU | 30nM | - |
| hsa-miR-30c (30c-5p) | UGUAAACAUCCUACACUCUCAGC | 30nM | - |
| hsa-miR-126 chamber | UCGUACCGUGAGUAAUAAUGCG | 60nM | 60nM |
| hsa-miR-126* chamber | CAUUAUUACUUUUGGUACGCG | 60nM | 60nM |
| hsa-miR-155 chamber | UUAAUGCUAAUCGUGAUAGGGGU | 30nM | 60nM |
| **Negative Controls** | | | |
| Scrambled-miR | N.A. | 30nM or 60nM | 60nM |
| Cy3™or FAM™ scrambled-miR | N.A. | 30nM or 60nM | 60nM |

**Table 2.5: List of the miRs transfected into hCMEC/D3 cells, their mature sequences and concentrations used**. MiR names or ids from MiRBase listed are the miR names used for the entire manuscript, while mature miR sequence names from MiRBase are listed in (). Anti-miR-155 and its scrambled anti-miR negative control were from Thermo Scientific (Dharmacon), Waltham, USA. All other miR-modulating oligonucleotides were from Ambion, Paisley, UK. Negative control was used at the same concentration as the corresponding miR-modulating oligonucleotide. Note that the sequence of the miR-modulating oligonucleotides (pre- and anti-miRs) or their negative controls are not disclosed by the manufacturing company. N.A. = sequence not available.

As experimental negative control and to establish the baseline fluorescence intensity, hCMEC/D3 cells were transfected with Siport™ Polyamine Transfection Agent or Lipofectamine® 2000 mixes without oligonucleotides.

The fluorescent label enabled direct observation of the cellular uptake, distribution, and localization of control oligonucleotides. Fluorescently labelled controls or the transfection reagent mix alone were added to hCMEC/D3 cells seeded in parallel to the experiment. To determine transfection efficiency, cells were then washed three times following the transfection procedure and visualized using a fluorescent inverted OLYMPUS IX70 microscope. Representative phase-contrast and fluorescent images (Cy3™ ~ $\lambda_{em}$ 554/ $\lambda_{ex}$ 568 nm and FAM™ ~ $\lambda_{em}$ 650/ $\lambda_{ex}$ 670 nm) were taken with a QICAM Fast (QImaging) camera and processed using Image Pro Plus software (Media Cybernetics Bethesda, USA) (Fig. 2.2).

Thereafter, hCMEC/D3 cells were collected by trypsinization and the median of cell fluorescence and the percentage of fluorescent cells were quantified by flow cytometry (FACS) as described in Section 2.3. First, negative control, cells with transfection mix only, were assessed to establish the baseline fluorescence intensity by adjusting the peak to the left of the histogram's X-axis (the control and standard peak). Then the samples, cells transfected with fluorescent oligonucleotides were quantified (Fig. 2.3).

The results were calculated by subtracting negative control background consisting of the average (median) fluorescence of hCMEC/D3 cells transfected with reagent mix only from the average (median) fluorescence of hCMEC/D3 cells transfected with Cy3™ or and FAM™ dye-labelled Anti- or Pre-miR drawing a marker

(M1) with <1% of the negative control peak inside the marker's left edge as shown in

the top panel of Fig. 2.3.
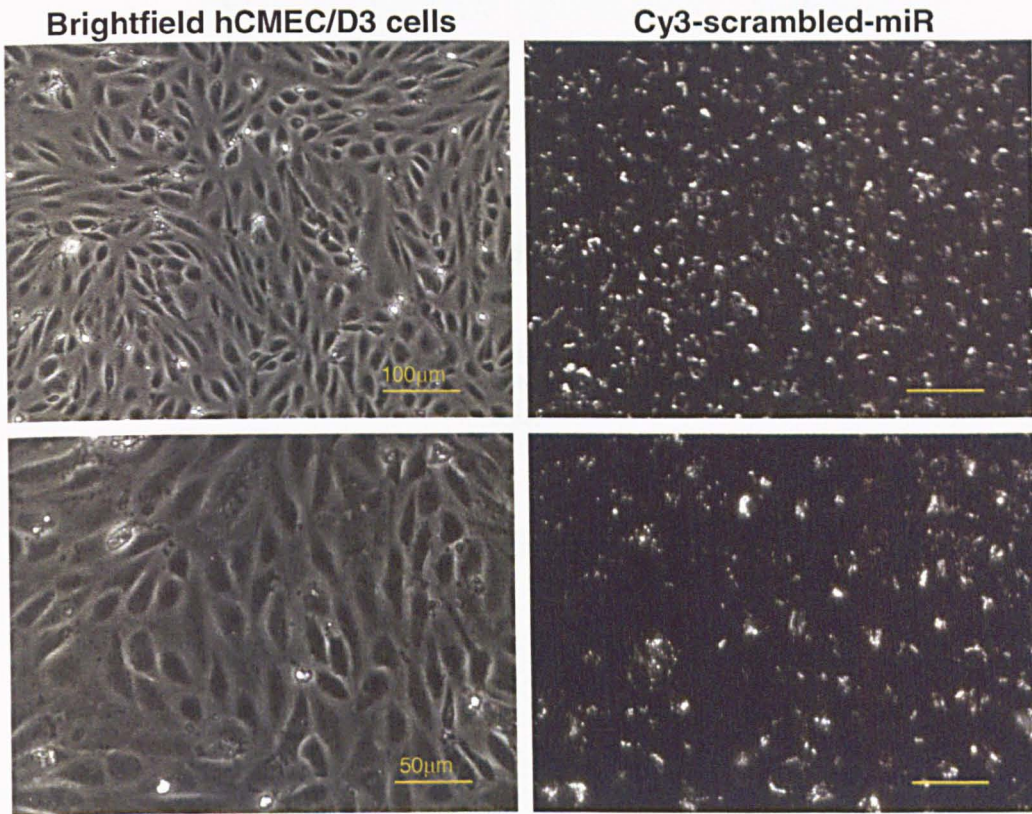


**Fig. 2.2: Representative image of oligonucleotide transfection efficiency in hCMEC/D3 cells determined by fluorescence microscopy.** hCMEC/D3 cells were transfected with Cy3-anti-miR using Lipofectamine™ 2000 following protocols depicted in Fig. 2.1 and the concentrations indicated in Table 2.5. After 24 h, transfected hCMEC/D3 cells monolayers were washed three times, then, Cy3-anti-miR expression was assessed using a fluorescence microscope. Representave phase-contrast (left) and fluorescent (right) pictures were taken at x20 (top) ad x40 (bottom).
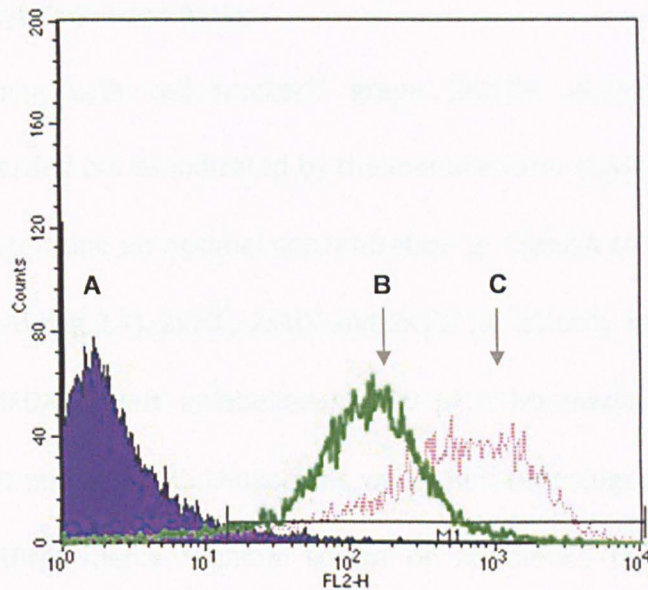
| A | Marker | Left, Right | Events | % Gated | % Total | Mean | Geo Mean | CV | Median |
|---|--------|-------------|--------|---------|---------|------|----------|-----|--------|
| | All | 1, 9910 | 10000 | 100.00 | 100.00 | 3.13 | 2.13 | 194.93 | 1.81 |
| | M1 | 11, 9910 | 355 | 3.55 | 3.55 | 24.55 | 20.32 | 90.76 | 17.94 |

| A | Marker | Left, Right | Events | % Gated | % Tota | Mean | Geo Mean | CV | Median |
|---|--------|-------------|--------|---------|--------|------|----------|-----|--------|
| | All | 1, 9910 | 10000 | 100.00 | 100.00 | 3.17 | 2.17 | 174.94 | 1.84 |
| | M1 | 14, 9910 | 260 | 2.60 | 2.60 | 27.73 | 24.09 | 73.21 | 20.72 |

| B | Marker | Left, Right | Events | % Gated | % Tota | Mean | Geo Mean | CV | Median |
|---|--------|-------------|--------|---------|--------|------|----------|-----|--------|
| | All | 1, 9910 | 10000 | 100.00 | 100.00 | 166.83 | 115.06 | 103.02 | 124.09 |
| | M1 | 14, 9910 | 9692 | 96.92 | 96.92 | 171.89 | 126.13 | 100.17 | 128.64 |

| C | Marker | Left, Right | Events | % Gated | % Tota | Mean | Geo Mean | CV | Median |
|---|--------|-------------|--------|---------|--------|------|----------|-----|--------|
| | All | 1, 9910 | 10000 | 100.00 | 100.00 | 835.69 | 484.07 | 97.35 | 577.72 |
| | M1 | 14, 9910 | 9865 | 98.65 | 98.65 | 847.01 | 512.93 | 96.02 | 588.21 |

**Fig. 2.3: Representative histogram showing transfection efficiency of anti-miR in hCMEC/D3 cells quantified by FACS. TOP**. Representative histogram showing the fluorescence intensity in hCMEC/D3 cells (x axes-FL2-H) versus the number of hCMEC/D3 cells (y axes- counts) and, the drawn M1 marker. **BELOW**. Data relative to the curves/peaks in the histogram of **All** cells (events 10 X 10$^4$) or above negative control values **M1,** quantified by FACS. **Left grey box** highlights the percentage of gated fluorescent positive cells (All and M1) and the **right grey box** highlights the average (median) cell fluorescence (All and M1) as (**A**) hCMEC/D3 cells transfected with reagent mixes only, Siport™ or Lipofectamine® 2000 (control), (only showed one histogram in the top figure) (**B**) hCMEC/D3 cells transfected with Cy3™ dye-labelled Anti-miR Negative using Siport™ Polyamine Transfection Agent (**C**) hCMEC/D3 cells transfected with Cy3™ dye-labelled Anti-miR Negative using Lipofectamine® 2000.

## 2.5 Static leukocyte adhesion assay

Cell loading with cell tracker™ green CMFDA (5-chloromethylfluorescein diacetate) was carried out as indicated by the manufacturer (Invitrogen, Paisley, UK). A pilot study to determine an optimal concentration of CMFDA to label leukocytes was initially performed (Fig.2.4). $2x10^3$, $2x10^4$ and $2x10^5$ Jurkat cells were labelled with 0.5, 1 or 5 mM CMFDA or left unlabelled in 100 μl RPMI media without serum and antibiotics for 30 min at 37 °C. Leukocytes were then centrifuged at (190 x $g$) and re-suspended in RPMI media without serum or antibiotics for 30 min at 37° C. Fluorescently labelled leukocytes were then centrifuged at 190 x $g$, counted again and re-suspended at $2x10^6$/ml cells in complete EBM-2 media. 100 μl cell suspension was dispensed onto a well in a 96 multi-well plate and fluorescence was measured using a FLUOstar Optima fluorescence plate reader (BMG LABTECH) at $\lambda_{ex}$ and $\lambda_{em}$ of 485nm and 520nm, respectively. Fig. 2.4 shows that incubation of $2x10^5$ cells with 5 mM CMFDA led to maximal total fluorescence intensity by labelled cells and these conditions were then selected for further adhesion experiments.
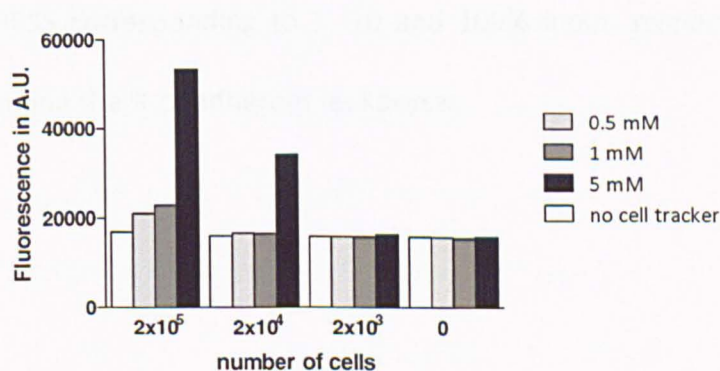


**Fig. 2.4: Standard curves of fluorescently labelled leukocytes with different concentrations of CMFDA.** The experiment was carried out once with two replicates.

Fluorescently labelled leukocytes in EBM-2 complete media ($2x10^5$ leukocytes cells/well) were added onto cytokine-treated hCMEC/D3 cells for 1 h at 37 °C. After washing three times with 200 µl HBSS, the fluorescence of leukocytes remaining adherent to the hCMEC/D3 monolayer was measured using a FLUOstar Optima fluorescence plate reader (BMG LABTECH) as above. This assay was adapted from static assays used previously (Solito, Romero et al. 2000; Hisano, Namba et al. 2005). The software Optima version 2.00R3 (BMG LABTECH, Tampa, USA) was used to acquire and analyse the data. The percentage of adherent leukocytes was calculated using the following formula:

$$\frac{\text{Fluorescence signal in experimental well - fluorescence signal blank well}}{\text{Fluorescence signal in input well - fluorescence signal input blank well}} \times 100$$

Where the experimental wells were hCMEC/D3 cells plus adhered leukocytes in EBM-2 media and the blank wells were hCMEC/D3 cells in EBM-2 media only. The input wells were $2x10^5$ leukocytes and the input blank wells were HBSS. A standard curve using the fluorescence intensities of labelled leukocyte suspensions with $2x10^3$, $2x10^4$ and $2x10^5$ cells in HBSS corresponding to 1, 10 and 100% input, respectively, was then plotted to determine the % of adherent leukocytes.

## 2.6 Flow-based leukocyte adhesion assay: live cell adhesion imaging under flow conditions

The flow-based adhesion assay was developed by adapting previously published assays (Sheikh, Rahman et al. 2005; Man, Tucky et al. 2009; Steiner, Coisne et al. 2011). For the flow based leukocyte adhesion assays, an Ibidi® μ-Slide VI$^{0.4}$ (six parallel channels 0.4 mm height, see Fig. 2.5 top and lower panel) containing confluent hCMEC/D3 cell monolayers was connected to two syringe pumps (Harvard Apparatus, Kent, UK), as depicted in Fig 2.5 (top panel), and placed onto the stage of a time lapse inverted OLYMPUS IX70 microscope within a 37 °C incubator. The flow rate (θ) applied to produce the required shear stress τ (dyn/cm$^2$) was calculated by Ibidi® for the μ-slideVI 0.4 according to the equation τ [dyn/cm$^2$] = η [(dyn*s)/cm$^2$]·176.1 Φ ml/min], where the relationship between shear stress (τ ) and flow rate (Φ) is based on the dynamic viscosity (η) of water at 22°C, η=0.01 dyn·s/cm$^2$ and other parameters specific to the geometry of the system.Leukocytes (2x10$^6$ cells/ml) were allowed to flow through the channel at low shear stress (0.5 dyn/cm$^2$ = 0.28 ml/min) for 5 min, then EBM-2 complete media was pulled trough the channel at a physiological shear stress (1.5 dyn/cm$^2$ = 0.85 ml/min) for 30 s or 1 min (Cinamon, Shinder et al. 2001; Steiner, Coisne et al. 2011). Dynamic T cell (Jurkat), monocyte (THP1) or PBMC interactions with hCMEC/D3 observed using a X10 objective, were recorded by Q-IMAGING *QICAM FAST* 1394 mono 12-bit camera connected to the Image Pro Plus software (Media Cybernetics Inc. Bethesda, USA). Time lapse videos were created by merging frames taken every 1 second (Image Pro Plus software, Media Cybernetics Bethesda, USA and Image J, Java-based image processing program developed at the National Institutes of Health). An example is shown in the attached CD-ROM (Appendix 1).

T cells (Jurkat), monocytes (THP1) or PBMC that remained stationary on human brain endothelium in the field of view (FOV: 640 x 480 μm Area = 0.307 mm$^2$) throughout the accumulation time (0.5 dyn/cm$^2$) and immediately after increasing the flow to 1.5 dyn/cm$^2$ were considered as cells that were firmly adhered. Leukocytes that adhered for at least 1 second to endothelial cells and thereafter detached were classified as transiently adhered. Leukocyte-endothelium interaction distance measurements were calculated from the point of initial contact between leukocytes and EC to the point of firm adhesion. Both transient adhesion and leukocyte-endothelium long interaction were quantified during the leukocyte accumulation phase and were manually tracked using Image Pro Plus software (Media Cybernetics Inc. Bethesda, USA), while firmly adhered leukocytes were manually counted at the end of the experimental time within five random FOVs along the centreline of the flow channel using Image Pro Plus software (Media Cybernetics Inc. Bethesda, USA).

**Fig. 2.5 (left): Flow based leukocyte assay**: (top) Schematic representation of the live cell adhesion imaging assay under flow conditions (middle) List of elements used in the assembly of the flow-based system for live cell adhesion (bottom) dimensions of the Ibidí® μ-slideVI used for the experiments and (*) illustration of how Ibidí® μ-slideVI was connected to the flow system.
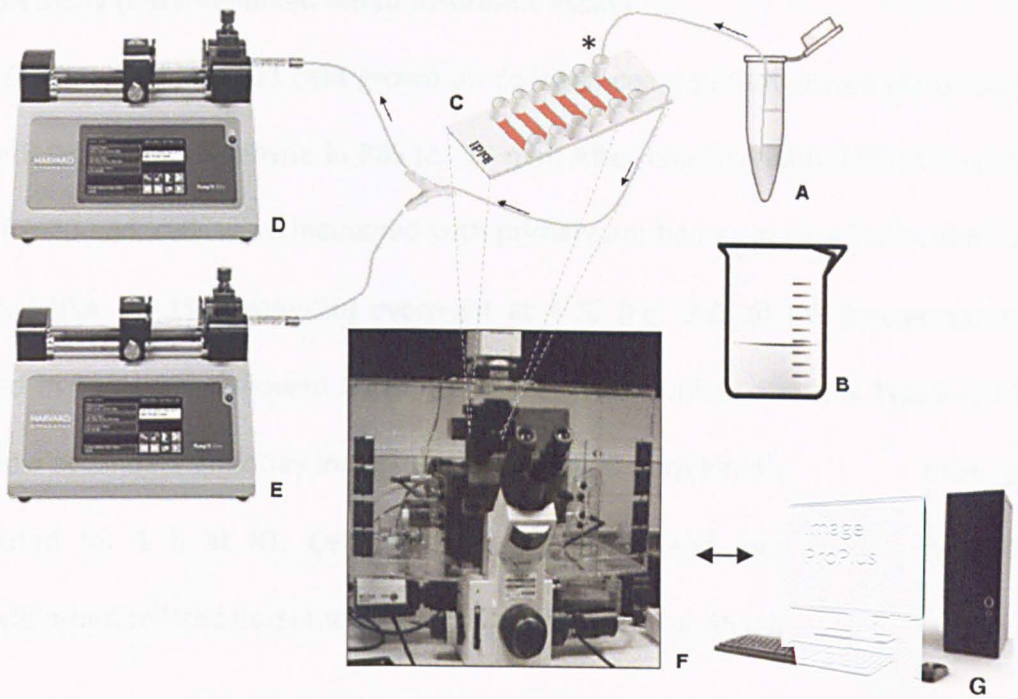
| COMPONENT | MANUFACTURER |
|---|---|
| A Fluorescently labelled leukocytes | N.A. |
| B EBM-2 complete media | Lonza |
| C Ibidí® µ-slideVI 0.4LUer, ibiTreat, sterile with hCMEC/D3 cells monolayer(red) | Ibidí |
| D Pumps PHD ULTRA pulling at 0.5 dyn/cm2 | Harvard Apparatus |
| Syringe 5ml | Hamilton |
| E Pumps PHD ULTRA pulling at 1.5 dyn/cm2 | Harvard Apparatus |
| Syringe 25ml | Hamilton |
| F Time lapse microscope | OLYMPUS IX70 |
| G Software Image Pro Plus for acquisition | Media Cybernetics |
| **CONNECTOR** | |
| Tygon 3350 Sanitary Silicone Tubing | Saint Gobain |
| Y connectors with 400 Series Barbs 3/32" Natural Polypropylene | Value Plastic, Inc. |
| Female Luer Lug Style to classic series barb 1/16" Natural Polypropylene | Value Plastic, Inc. |
| µ-slideVI 0.4 Luer flow kit, ibiTreat, T/Ctreated, sterile | Ibidí |

**Dimensions** Ibidí® µ-slideVI 0.4LUer, ibiTreat, sterile

| | |
|---|---|
| Number of channels | 6 |
| Channel volume | 30 µl |
| Channel length | 17 mm |
| Channel width | 3.8 mm |
| Channel height | 0.4 mm |
| Adapters | female Luer |
| Volume per reservoir | 60 µl |
| Growth area | 0.6 cm² per channel |
| Coating area using 30 µl | 1.2 cm² per channel |
| Bottom matches coverslip | No. 1.5 |

**Connection** Ibidí® µ-slideVI to the flow system



95
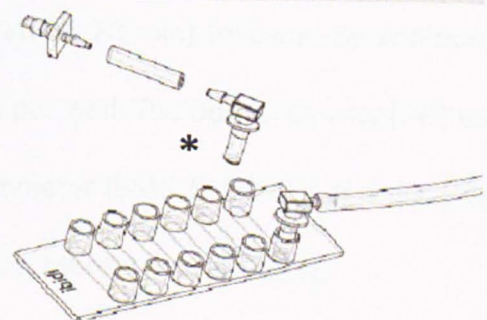
## 2.7 ELISA assay (Enzyme-linked Immunosorbent Assay)

Confluent hCMEC/D3 cells grown on collagen-coated 96-multiwell plates were fixed with 0.1% glutaraldehyde in PBS for 10 min. After blocking with 0.05 M Tris/HCl pH 7.5 for 20 min, cells were incubated with primary antibodies in Elisa buffer (PBS 1X + 5mg/ml BSA + 0.1% Tween-20) overnight at 4 °C (Fig. 2.6) at the concentrations indicated in Table 2.6, followed by three washes (wash buffer = 0.05% Tween-20 in PBS) and a secondary antibody incubation with 1/1000 polyclonal goat anti-mouse IgG biotinylated for 1 h at RT. Cells were then washed and incubated with 1/700 streptavidin-biotinylated horseradish peroxidase complex for 45 min at RT.

| Antibody | Company | Clone | Isotype | Concentration |
|---|---|---|---|---|
| MONOCLONAL Anti-human VCAM1 (CD106) | R&D SYSTEMS (Abingdon, UK) | BBIG-V1 (4B2) | Mouse IgG$_1$ | 2µg/ml |
| MONOCLONAL Anti-human ICAM1 (CD54) | R&D SYSTEMS (Abingdon, UK) | BBIG-I1 (11C81) | Mouse IgG$_1$ | 2µg/ml |
| MONOCLONAL Anti-human ICAM2 (CD102) | AbD SEROTEC (Oxford, UK) | B-T1 | Mouse IgG$_1$ | 3µg/ml |
| MONOCLONAL Anti-human E-SELECTIN (CD 62E) | AbD SEROTEC (Oxford, UK) | TEA 2/1 | Mouse IgG2b | 3µg/ml |
| MONOCLONAL Anti-human P-SELECTIN (CD 62P) | AbD SEROTEC (Oxford, UK) | Psel.KO.2.12 | Mouse IgG$_1$ | 3µg/ml |

**Table 2.6: List of monoclonal antibodies and the concentrations used for Elisa**

Chromogen solution (0.1M sodium acetate/citric acid buffer + 100 µg/ml N,N,N',N'-Tetramethylbenzidine in DMSO + 30% (v/v) hydrogen peroxide solution) was added to each well as a developer substrate (5-20 min) followed by addition of 1:4 (v:v) of stop solution (10% v/v sulfuric acid) per well. The optical density (OD) was then measured using a FLUOstar Optima spectrometer (BMG LABTECH) at a wavelength of 450 nm. This assay was adapted from (Hillyer, Mordelet et al. 2003).

Absorbance in the blank wells (without primary antibody) was deducted from each of the corresponding samples. ICAM2 was selected as a cell adhesion molecule whose levels are not increased by cytokine treatment (McLaughlin, Hayes et al. 1998) and hence served as a negative control for VCAM1 and ICAM1 primary antibodies in stimulated conditions whereas VCAM1 was used as a positive control for E- and P-selectin primary antibodies.
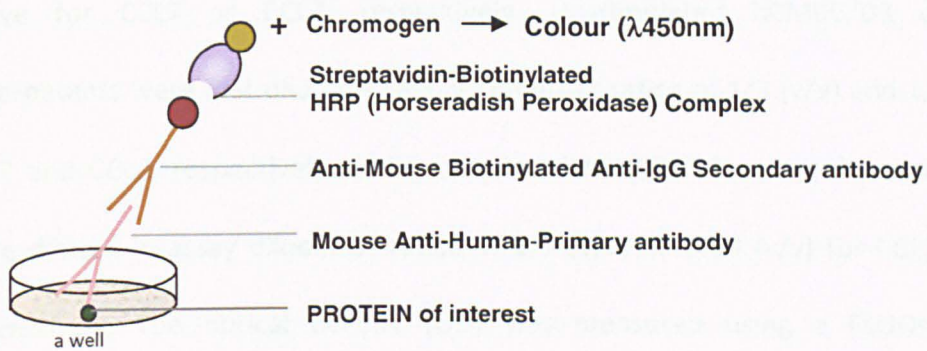


**Fig. 2.6: Schematic representation of the Elisa assay.**

## 2.8 Capture or sandwich ELISA assay

Culture supernatants of confluent hCMEC/D3 cells grown on collagen-coated 96-multiwell plates were collected and frozen at -20 °C. For chemokine quantitative determination, the human MCP-3 or CCL7 and the human MCP-1 or CCL2 Quantikine® ELISA kits (R&D systems, Abingdon, UK) were used following the supplier's protocols (Fig. 2.7). The detection limits ranged from 15.6 pg/ml for CCL7 to 31.2 pg/ml for CCL2 whereas signal saturation was observed at concentrations of 1000 or 2000 pg/ml and above for CCL7 or CCL2, respectively. Unstimulated hCMEC/D3 cell culture supernatants were first diluted in assay diluent at ratios of 1/3 (v/v) and 1/10 (v/v) for CCL7 and CCL2, respectively, while stimulated hCMEC/D3 cells culture supernatants were diluted in assay diluent at ratios of 1/3 (v/v) or 1/50 (v/v) for CCL7 and CCL2, respectively. The optical density (OD) was measured using a FLUOstar Optima spectrometer (BMG LABTECH) at a wavelength ($\lambda$) of 450 nm. Absorbance in the blank wells (assay diluent only) was deducted from the absorbance of each sample and the standards. The concentration of chemokines was determined by interpolation from the standard curve.



Colour
+Chromogen (hydrogen peroxide + tetramethylbenzidine)

Anti-human CCL2 or CCL7 Polyclonal antibody conjugated to horseradish peroxidase

Protein of interest (in supernatant)

Monoclonal antibody specific for human CCL2 or CCL7 (Capture antibody)

a well
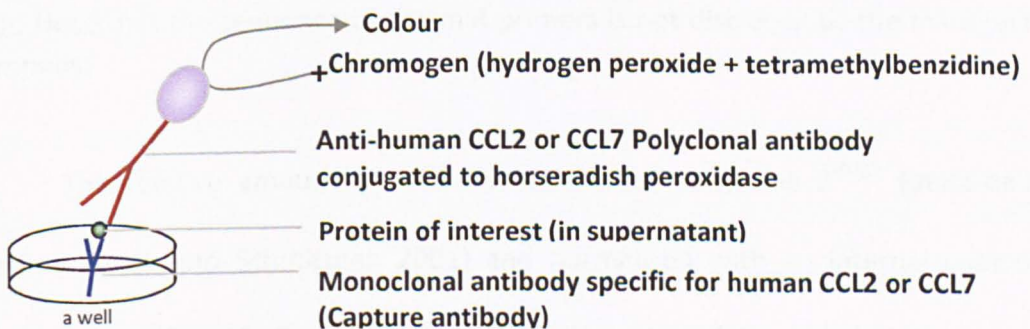
**Fig. 2.7: Schematic representation of the capture or sandwich Elisa assay.**

## 2.9 Reverse transcription-Real time-qPCR

For assessment of miR levels in cultured cells, total RNA was isolated from confluent cells either treated with TNFα and IFNγ at the indicated concentrations (0.1-1 ng/ml) or left untreated, using TRIzol® Reagent following the manufacturer's protocol. cDNA was generated from total RNA using a TaqMan High Capacity cDNA Reverse Transcription kit (Applied Biosystem, Life Technologies, Warrington, UK) with specific primers for miRs as shown in Table 2.7. RT$^2$-qPCR was performed using the TaqMan MicroRNA assay (Applied Biosystem Life Technologies, Warrington, UK) with specific primers according to the manufacturer's protocol.

Cellular hsa-miR levels were detected using DNA Engine Opticon2 Real-Time System (MJ Research, St. Bruno, Canada) thermal cycler and Opticon Monitor software (MJ Research, St. Bruno, Canada) for data analysis.

| MicroRNA | Catalog # | Company |
|---|---|---|
| Hsa-mir-126 | 002228-4427975 | Applied Biosystems (Foster City, USA) |
| Hsa-mir-126* | 000451-4427975 | Applied Biosystems (Foster City, USA) |
| Hsa-mir-155 | 002623-4427975 | Applied Biosystems (Foster City, USA) |
| Control | Catalog # | Company |
| U6 snRNA | 001973-4427975 | Applied Biosystems (Foster City, USA) |

Table 2.7: List of specific miR primers used for reverse transcription and real time PCR. Note that the sequence of the miR-primers is not disclosed by the manufacturing company.

The relative amount of miR was calculated using the $2^{-\Delta\Delta Ct}$ (delta-delta Ct) method (Livak and Schmittgen 2001) and normalized with an internal control, the small nuclear RNA U6. Threshold cycle (Ct) values were determined by the number of cycles required for the fluorescent signal to cross the threshold (background fluorescence), which in our experiments was between 5 and 10 times the standard

deviation of the background fluorescence. The difference in Ct between the target (miRs) and the internal control (the small nuclear RNA U6) was calculated according to the following formula:

$$\Delta Ct = [(Ct\ target) - (Ct\ internal\ control)]$$

The differences between $\Delta Ct$ of treatment (cytokines) and the vehicle (media) was calculated according to the following formula:

$$\Delta\Delta Ct = [\Delta Ct\ treatment] - [\Delta Ct\ vehicle]$$

From this formula, a positive result indicated a decrease in the expression of miR studied in hCMEC/D3 cells, whereas a negative result would indicate an increased expression of miR. The relative levels of miR ($\Delta\Delta Ct$) were transformed into absolute values calculated according to the following formula:

$$miR\ relative\ expression\ levels = 2^{-\Delta\Delta Ct}$$

Results of hsa-miR relative levels in treated and/or transfected hCMEC/D3 cells were expressed as fold increase over hsa-miR levels in unstimulated and control transfected hCMEC/D3 cells.

## 2.10 Immmunocytochemistry

### 2.10.1 Detection of VCAM1 expression in hCMEC/D3 cells grown on flow chambers

hCMEC/D3 cell monolayes in Ibidí chambers were washed twice with pre-warmed HBSS and fixed for 10 min at RT with 4% *p*-formaldehyde in PBS pH 7.4, and, washed three times with PBS. hCMEC/D3 cells were incubated with blocking solution, 5% (v/v) goat serum in PBS for 2 h and then 1/20 (v/v) anti-human VCAM1 primary antibody (Section 2.7, Table 2.6) in PBS + 5mg/ml BSA (Sigma) + 0.1% (v/v) Tween-20 (Sigma Ultra) was added at 4 °C in a wet chamber overnight. After washing nine times with PBS, hCMEC/D3 cells were incubated with 1/200 (v/v) Alexa Fluor® 488 Goat Anti-Mouse IgG secondary antibody for 1.5 h. Cells were washed six times with PBS and mounted using mounting media with DAPI. Pictures were acquired with a Zeiss microscope using axiophot prism filter set ($\lambda_{ex}$-$\lambda_{em}$: blue 450-490 nm, green 395-440 nm) with X40 objective. The signal was quantified using the software, Image J (Java-based image processing program developed at the National Institutes of Health).

### 2.10.2 Identification of subpopulations CD4+, CD8+, CD14+ and CD56+ adhered cells to hCMEC/D3 monolayers

Following leukocyte adhesion assays as described in Section 2.6, hCMEC/D3 cell monolayers in Ibidí chambers were washed twice with pre-warmed HBSS and incubated with a cocktail of fluorescently labelled primary antibodies (anti-human CD4, CD8, CD14 and CD56) (Section 2.3, Table 2.4) for 15 min at RT in the dark. After three washes slides were mounted using mounting media with DAPI. Pictures were acquired with a Leica DMIRBE confocal microscope (Leica Microsystems, Milton Keynes, UK)

using Leica LAS imaging software. Pictures were the projection of twenty-five 1 μm

sections in the Z plane.

## 2.11 Bioinformatic analysis

Predicted mRNA targets for hsa-miR-126 and 126* were identified using eight

well known miRNA target prediction programs/databases (27th of April 2012 latest

access date):

Targetscan v5.0 (http://www.targetscan.org/),

Miranda (http://www.microrna.org/microrna/home.do),

Pictar (http://pictar.mdc-berlin.de/),

Microcosm (http://www.ebi.ac.uk/enright-srv/microcosm/cgibin/targets/v5/search.pl),

Tarbase (http://diana.cslab.ece.ntua.gr/tarbase/),

DianaLab Microt (http://diana.cslab.ece.ntua.gr/microT/),

Diana Lab (http://diana.cslab.ece.ntua.gr/mirgen/),

Target Miner (http://www.isical.ac.in/~bioinfo_miu/),

MirDB (http://mirdb.org/miRDB/).

All hsa-miR-126 and -126* targets were listed in Tables (4.2 and 5.5) and

elaborated as described in Chapters 4 and 5.

## 2.12 Statistical analysis

All data are presented as mean ± standard error of the mean and are the result of a number of independent experiments (n) with replicates specified in each legend. Paired $t$ tests were used for multiple comparisons in cell culture experiments. Statistically significant differences are presented as probability levels of $P < 0.05$ (*), $P < 0.01$ (**), $P < 0.001$ (***). Calculations were performed using the statistical software GraphPad Prism 5 (GraphPad Software, La Jolla, USA).

## Chapter 3: Characterization of a human *in vitro* model of the blood-brain barrier to study leukocyte adhesion in inflammation

### 3.1 Introduction

The pathogenesis of neuroinflammatory diseases such as MS is characterized by increased leukocyte trafficking across the cells forming the BBB. Leukocyte extravasation into the CNS is a multistep cascade involving first tethering or capture, slow rolling and firm adhesion. These early critical steps are mediated by endothelial CAM and selectins and their cognate ligands on leukocytes both in immuno-surveillance and inflammation. Pro-inflammatory cytokines TNFα and IFNγ are locally secreted by endothelium, other CNS-resident cells and/or activated infiltrating leukocytes (Schroder, Hertzog et al. 2004) and have been shown to be abundant in MS active demyelinating lesions (Sospedra and Martin 2005). They modulate specific EC surface molecules (Stolpen, Guinan et al. 1986; Stins, Gilles et al. 1997) which enhance leukocyte rolling and firm adhesion (Thornhill, Wellicome et al. 1991). However, the exact mechanisms of leukocyte trafficking, and in particular the early events leading to firm adhesion into the brain still remain to be fully elucidated.

Few *in vitro* models of the human BBB have been established to study leukocyte adhesion (Stins, Gilles et al. 1997; Zakrzewicz, Grafe et al. 1997; Kallmann, Hummel et al. 2000; Man, Tucky et al. 2009). Experimentally, most of the studies about leukocyte trafficking *in vitro* have been performed using static models involving human primary peripheral EC (i.e. HUVEC) or non-human primary CNS EC (i.e. rat, mouse or bovine)(Engelhardt and Ransohoff 2005; Ley, Laudanna et al. 2007). However, human brain primary cells are difficult to obtain, then immortalized non-human and human

BEC lines, described in Section 1.8, have been used as a model of BBB (Weiss, Miller et al. 2009). In particular the human brain endothelial cell line, hCMEC/D3 has been defined as a suitable model for experimental studies on the BBB (Poller, Gutmann et al. 2008).

In addition, because *in vivo* leukocyte recruitment and adhesion occur in a dynamic system dominated by the shear flow of the circulating blood on the endothelium, an *in vitro* model of the human BBB should incorporate a flow component in order to mimic the *in vivo* environment more closely. The first *in vitro* studies on leukocyte-endothelium interactions under flow conditions were published in the 90s (Shen, Luscinskas et al. 1992; Luscinskas, Kansas et al. 1994) although with limitations due to the complexity of the cellular composition of the NVU, blood composition and hemodynamic shear forces. Recently, effective parallel plate-based flow systems have been developed (Cucullo, Marchi et al. 2011; Michell, Andrews et al. 2011; Srigunapalan, Lam et al. 2011; Walsh, Murphy et al. 2011; Man, Tucky et al. 2012) and commercialized (www.cellixltd.com) (Benoit, Conant et al. 2010), but a system that mimics features of the complex milieu of the inflamed human BBB during leukocyte adhesion (suitable to study endothelial microRNAs), has not previously been developed.

Here, an immortalized human brain microvascular EC line, hCMEC/D3, as described previously in Section 1.8, was used as an *in vitro* human model of the BBB. The suitability of the hCMEC/D3 cell line to study leukocyte trafficking *in vitro* was first determined by investigating the expression of CAM and selectins. To study leukocyte adhesion, we used a well-established static assay (Greenwood, Wang et al. 1995; Solito, Romero et al. 2000; Grunewald and Ridley 2010; Michell, Andrews et al. 2011)

as well as a flow-based assay adapted from a recently developed system using a mouse BBB model (Steiner, Coisne et al. 2011) and others described in Section 1.8. The suitability of this novel flow-based leukocyte adhesion assay was assessed. Finally, the adhesion of a monocytic and a T cell line to hCMEC/D3 cells was investigated under basal and inflammatory conditions using the static and flow-based adhesion models.

## 3.2 Aims

The aim of the work described in this chapter was to set up and characterize a human *in vitro* model of leukocyte adhesion to the BBB both under static and flow-based conditions.

# 3.3 Results

## 3.3.1 Basal expression of CAM and selectins in hCMEC/D3 cells

Leukocyte rolling and adhesion are mediated mainly by selectins and CAM expressed by endothelium (Graber, Gopal et al. 1990; Carlos, Kovach et al. 1991; Lawrence and Springer 1991; Kallmann, Hummel et al. 2000). Previous studies have shown that the expression of VCAM1, ICAM1 (Weksler, Subileau et al. 2005) and P-selectin (Bahbouhi, Berthelot et al. 2009) by hCMEC/D3 cells increased following stimulation with TNFα. E-selectin expression has been shown to increase in TNFα-stimulated human BEC (Wong and Dorovini-Zis 1996). E-selectin is thought to mediate rolling of eosinophils (Ulfman, Kuijper et al. 1999), so we also included this selectin in our study on hCMEC/D3 cells. Therefore, the basal expression of VCAM1, ICAM1, ICAM2, and, P- and E-selectin by hCMEC/D3 cells was first investigated using ELISA (Fig. 3.1). The basal expression of these molecules was investigated using specific monoclonal antibodies against VCAM1, ICAM1, ICAM2, P- and E-selectin. Higher concentrations of colorimetric reaction product were detected in samples (presence of primary antibody) than in the negative control (absence primary of antibody) (Fig. 3.1), suggesting that these CAM were expressed by hCMEC/D3 cell under basal conditions. However, the signal intensities for different CAM and selectins were different from what the literature reported (Zhang, Chopp et al. 1998; Love and Barber 2001), reflecting the differences in either the affinity of the monoclonal antibodies for their specific epitopes or the actual CAM expression levels on hCMEC/D3 cells under basal conditions.
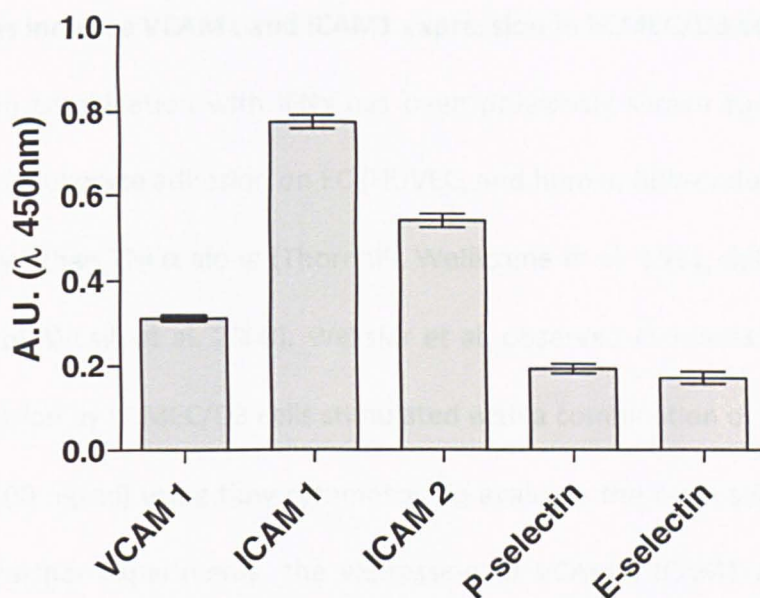
**Fig. 3.1: Basal expression of cell adhesion molecules and selectins in hCMEC/D3 cells.** Anti-human-VCAM1, -ICAM1, -ICAM2, P- and E- selectin antibodies were used to determine basal expression of VCAM1, ICAM1, ICAM2, P- and E-selectin by hCMEC/D3 cells using ELISA (see Section 2.7, Table 2.6)). Negative control (absence of primary antibody) signal intensity was subtracted from all samples. Experiments were carried out three times with six replicates. Data are mean ±SEM.

### 3.3.2 Cytokines increase VCAM1 and ICAM1 expression in hCMEC/D3 cells

TNFα in combination with IFNγ has been previously shown to increase CAM expression and leukocyte adhesion on EC (HUVEC, and human BBB-endothelial cells) to a greater extent than TNFα alone (Thornhill, Wellicome et al. 1991; Calabresi, Prat et al. 2001; Cayrol, Wosik et al. 2008). Weksler et al. observed increases of ICAM1 and VCAM1 expression by hCMEC/D3 cells stimulated with a combination of TNFα and IFNγ (100 U/ml + 100 ng/ml) using flow cytometry. To evaluate the most suitable cytokine stimulus for further experiments, the expression of VCAM1, ICAM1 and ICAM2 on hCMEC/D3 cells stimulated with proinflammatory cytokines TNFα, and IFNγ, alone or in combination, was first quantified. TNFα alone (0.1 ng/ml) increased ICAM1 (Fig. 3.2 A) and VCAM1 (Fig. 3.2 B) expression on hCMEC/D3 cells at 24 h by 1.5 respectively, and 2-fold, compared with basal levels. A similar, but larger, effect of TNFα on both VCAM1 and ICAM1 expression was observed at a higher dose (10 ng/ml). When hCMEC/D3 cells were stimulated with TNFα in combination with IFNγ (0.1 ng/ml) the increase in VCAM1 expression by hCMEC/D3 cells was significantly higher than that induced by TNFα alone (Fig. 3.2 B). However, no differences where observed when higher concentration of both cytokines were used. ICAM1 expression was not further increased by IFNγ in combination with TNFα.

In addition, IFNγ alone did not induce any changes in ICAM1 or VCAM1 expression levels at the concentrations tested (Figs. 3.2 A and B). No differences in ICAM2 expression were observed when hCMEC/D3 cells were stimulated either with TNFα alone or in combination with IFNγ for 24 h at all tested doses (0.1 and 10 ng/ml) compared to basal levels (Fig 3.2 C).
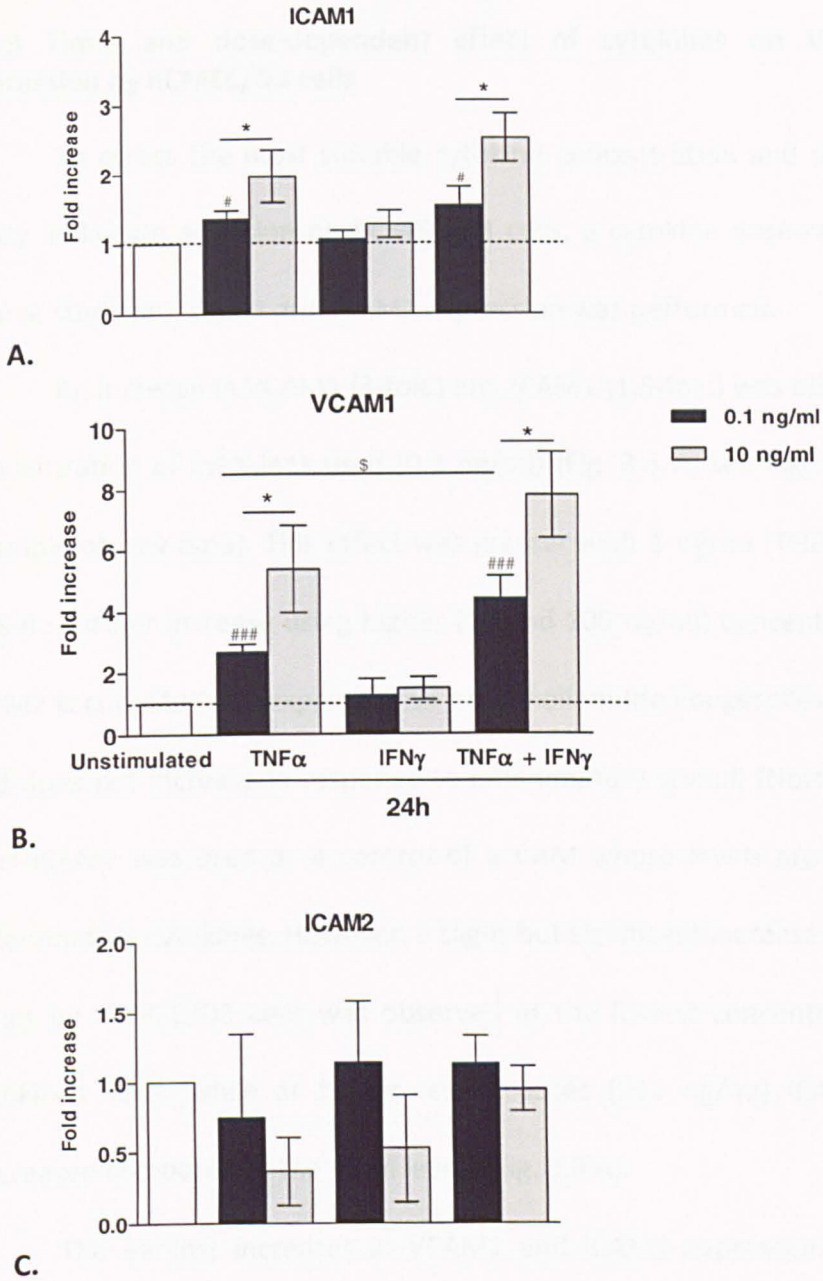
**Fig. 3.2: IFNγ potentiates TNFα-induced VCAM1 expression on hCMEC/D3 cells.** Confluent hCMEC/D3 cell monolayers were treated with TNFα or IFNγ alone or TNFα and IFNγ in combination at 0.1 and at 10 ng/ml for 24 h. **A.** Anti-human ICAM1 or **B.** Anti-human VCAM1 or **C.** Anti-human ICAM2 monoclonal antibodies were used to detect ICAM1 or VCAM1 expression levels by ELISA (see Section 2.7 for the antibodies and method details). Experiments were carried out three times with three replicates. Data are mean ±SEM. (#P<0.05, ###P<0.001, *P<0.05, $P<0.05, # significantly different compared with unstimulated cells; *significantly different compared to 0.1ng/ml; $ significantly different compared to TNFα alone).

### 3.3.3 Time- and dose-dependent effect of cytokines on VCAM1 and ICAM1 expression by hCMEC/D3 cells

To assess the most suitable cytokine concentration and time of treatment to study leukocyte adhesion on hCMEC/D3 cells, a cytokine dose-response and a time-course study on VCAM1 and ICAM1 expression was performed.

An increase in VCAM1 (3-fold) and ICAM1 (1.5-fold) was observed at the lowest concentration of cytokines used (0.1 ng/ml) (Fig. 3.3 A, see Fig. 1 Appendix 4 for an example of raw data). This effect was greater with 1 ng/ml (TNF$\alpha$ + IFN$\gamma$), but there was no further increase using higher (10 and 100 ng/ml) concentrations of cytokines. ICAM2 is constitutively expressed on endothelium (de Fougerolles, Stacker et al. 1991) and does not increase in response to inflammatory stimuli (Nortamo, Li et al. 1991), thus ICAM2 was used as a control of a CAM whose levels are not altered by pro-inflammatory cytokines. However, a slight but significant increase of ICAM2 expression levels by hCMEC/D3 cells was observed at the lowest concentration (0.1 ng/ml) of cytokines used, while at higher tested doses ($\geq$10 ng/ml) ICAM2 expression was decreased compared to the basal levels (Fig. 3.3 A).

The earliest increases in VCAM1 and ICAM1 expression by hCMEC/D3 cells were observed at 1 and 6 h, respectively (Fig. 3.3 B). VCAM1 and ICAM1 maximal expression, of 6- and 2-fold over the basal level, was at 24 h after stimulation and was maintained until 48 h after treatment. As previously observed (McLaughlin and Haise 1998; Huang, Mason et al. 2005), we found that cytokines decreased ICAM2 expression after 6 and 24 h following treatment on stimulated hCMEC/D3 cells (Fig. 3.3 B). Taken together, our results show that maximal expression of VCAM1 and ICAM1

was observed at 6-24 h following treatment with TNFα + IFNγ in combination at 1 or 10 ng/ml indistinctly.



A.



B.
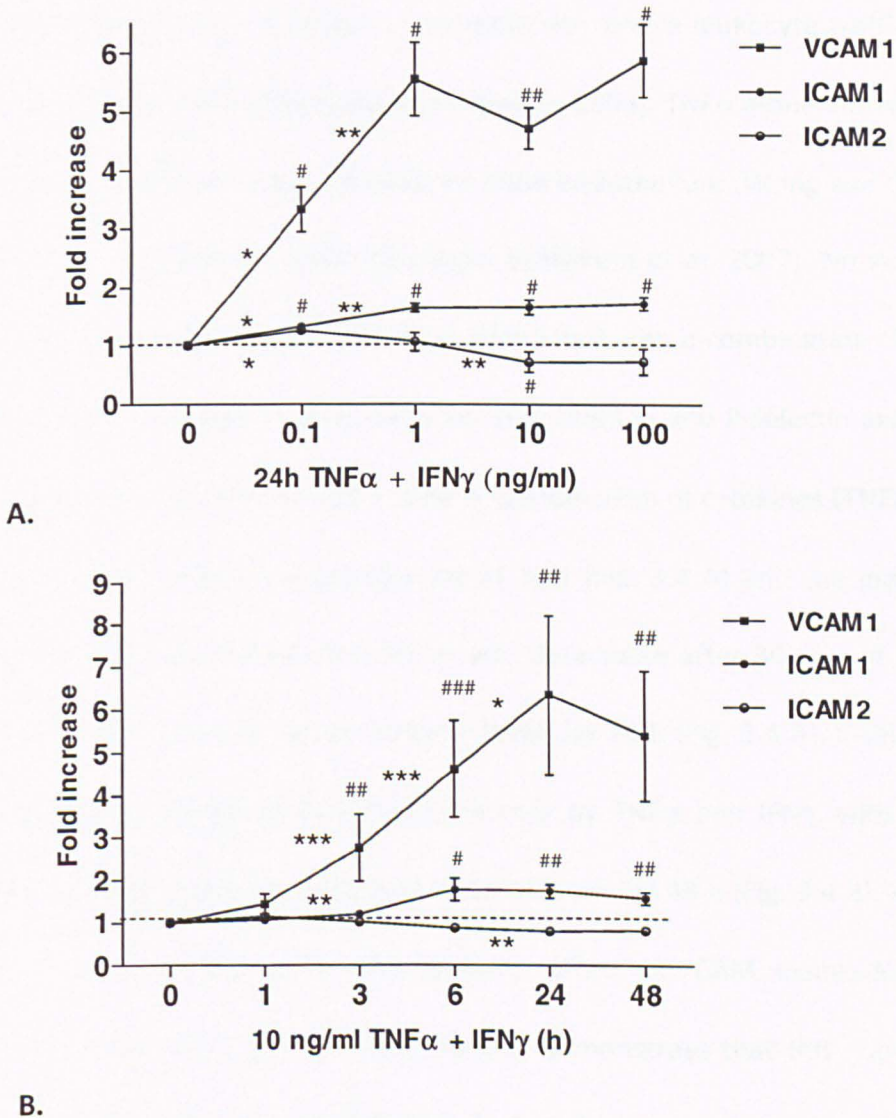
**Fig. 3.3: Combination of cytokines (TNFα and IFNγ) increased VCAM1 and ICAM1, but not ICAM2, expression in hCMEC/D3 cells in a dose- and time-dependent manner. A.** Confluent hCMEC/D3 cell monolayers were treated with TNFα and IFNγ at different concentrations (0, 0.1, 1, 10, 100 ng/ml) for 24 h. **B.** Confluent hCMEC/D3 cell monolayers were treated with TNFα and IFNγ at different times (0, 1, 3, 6, 24, 48 h) at 10 ng/ml. Anti-human VCAM1, ICAM1 and ICAM2 monoclonal antibodies were used to detect VCAM1, ICAM1 and ICAM2 expression levels by ELISA. Experiments were carried out three times with three replicates. Data are mean ±SEM. ($*$,$^{\#}P<0.05$ $**$,$^{\#\#}P<0.01$ $***$,$^{\#\#\#}P<0.001$, $^{\#}$ significantly different vs. unstimulated cells, $*$ significantly different between different doses (A) or treatment times (B)).

### 3.3.4 A combination of cytokines (TNFα and IFNγ) increases E- and P-selectin expression in hCMEC/D3 cells

Selectins are predominantly detected on endothelium of postcapillary venules, as previously described in Chapter 1, the main site where leukocyte trafficking takes place during inflammation (Bevilacqua and Nelson 1993). TNFα alone increased E- and P-selectin expression on primary human cerebral endothelium (Wong and Dorovini-Zis 1996), but not in HBMEC *in vitro* (Oostingh, Schlickum et al. 2007). No studies on E- and P-selectin expression on endothelium stimulated with a combination of TNFα and IFNγ have been published to date. Here we quantified E- and P-selectin expression on 24 h cytokine-stimulated hCMEC/D3 cells. A combination of cytokines (TNFα + IFNγ 10 ng/ml) increased P-selectin expression by >2 fold (Fig. 3.4 A) and the induction was maximal 1 h after stimulation. P-selectin was detectable after 30 min of stimulation and declined after 3-6 h to return to basal levels by 24 h (Fig. 3.4 A). E-selectin levels were significantly increased on hCMEC/D3 cells by TNFα and IFNγ, with a maximal induction (12-fold) at 6 h and returned to basal levels by 48 h (Fig. 3.4 B). VCAM1 was used as a positive control for the cytokine effect on CAM expression in these experiments (Figs. 3.4 A and B). These results demonstrate that this combination of pro-inflammatory cytokines can increase E- and P-selectin expression with different time courses in the human *in vitro* BBB model used.
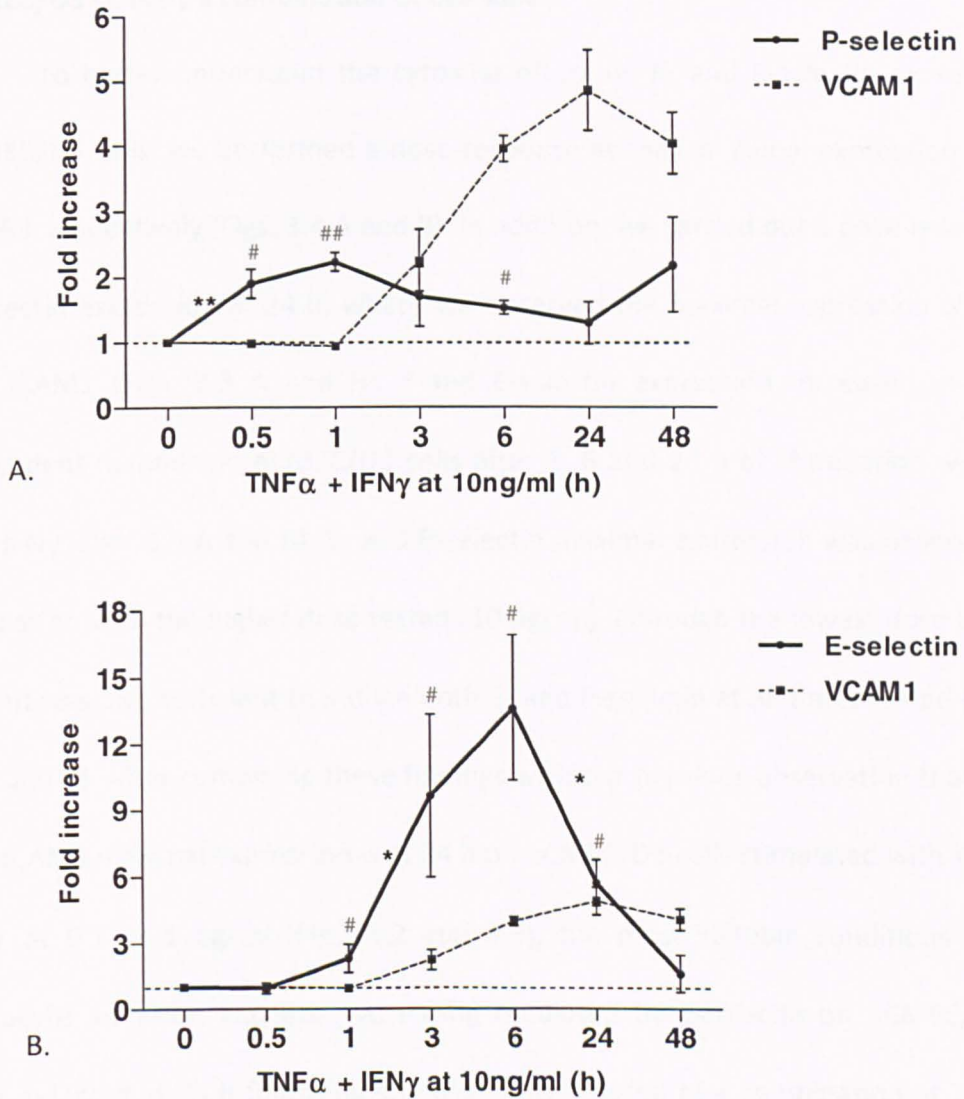
**Fig. 3.4: Combination of cytokines (TNFα and IFNγ) increases E- and P-selectin expression on hCMEC/D3 cells.** Confluent hCMEC/D3 cell monolayers were treated with 10 ng/ml of TNFα and IFNγ in combination for different times (0, 0.5, 1, 3, 6, 24 and 48 h). **A.** Anti-human-P-selectin and -VCAM1 monoclonal antibodies were used to detect P-selectin and VCAM1 expression levels by ELISA. **B.** Anti-human-E-selectin and -VCAM1 monoclonal antibodies were used to detect E-selectin and VCAM1 expression levels by ELISA. Experiments were carried out three times with three replicates. Data are mean ±SEM (*,#P<0.05, ##P<0.01 # significantly different vs. unstimulated cells, * significantly different between different doses).

### 3.3.5 E- and P-selectin expression increase in a dose-dependent manner on hCMEC/D3 cells by a combination of cytokines

To better understand the cytokine effect on P- and E-selectin expression by hCMEC/D3 cells, we performed a dose-response at their maximal expression times, 1 and 6 h respectively (Figs. 3.4 A and B). In addition, we carried out a dose-response for E-selectin expression at 24 h, where we observed the maximal expression of VCAM1 and ICAM1 (Figs. 3.3 A and B). P-and E-selectin expression increased in a dose-dependent manner on hCMEC/D3 cells after 1, 6 and 24 h of stimulation with TNFα and IFNγ (Figs. 3.5 A and B). E- and P-selectin maximal expression was observed after simulation with the higher dose tested (10 ng/ml), although the lowest dose used (0.1 ng/ml) was also sufficient to induce both E- and P-selectin at all times tested (Figs. 3.5 A, B and C). After combining these findings with our previous observation that VCAM1 and ICAM1 maximal expression is at 24 h on hCMEC/D3 cells stimulated with TNFα and IFNγ at 0.1 or 1 ng/ml (Figs. 3.2 and 3.3), the most suitable conditions to study leukocyte adhesion and observe rolling mediated by E-selectin on hCMEC/D3 cells were selected at 24 h following stimulus with 1 ng/ml of a combination of TNFα and IFNγ.
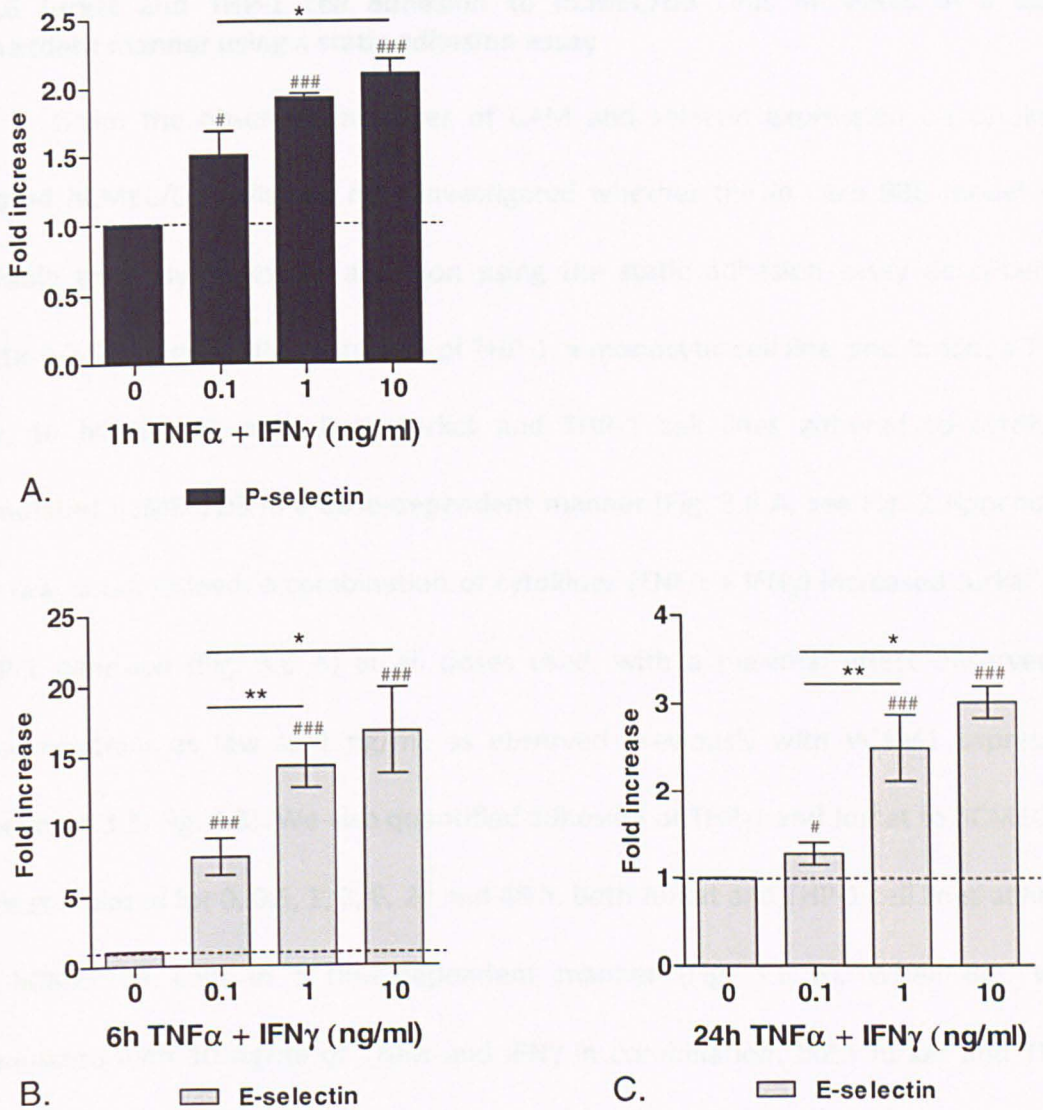
**Fig. 3.5: Combination of cytokines (TNFα and IFNγ) increases E- and P-selectin expression in hCMEC/D3 cells.** Confluent hCMEC/D3 cell monolayers were treated for 1, 6 and 24 h with TNFα and IFNγ in combination at different doses (0, 0.1, 1, 10 ng/ml). **A.** Anti-human-P-selectin monoclonal antibody was used to detect P-selectin expression by ELISA following 1 h cytokine treatment. **B.** and **C.** Anti-human-E-selectin monoclonal antibody was used to detect E-selectin expression levels by ELISA following 6 (B) and 24 (C) h cytokine treatment. Experiments were carried out three times with three replicates. Data are mean ±SEM (*,#$P<0.05$, **$P<0.01$ ***,###$P<0.001$ # significantly different compared to unstimulated cells, * significantly different between cytokine treatments).

### 3.3.6 Jurkat and THP-1 cell adhesion to hCMEC/D3 cells increases in a dose-dependent manner using a static adhesion assay

Given the observed increases of CAM and selectin expression on cytokine-treated hCMEC/D3 cells, we next investigated whether the *in vitro* BBB model was suitable to study leukocyte adhesion using the static adhesion assay described in Section 2.5. We quantified adhesion of THP-1, a monocytic cell line, and Jurkat, a T cell line, to hCMEC/D3 cells. Both Jurkat and THP-1 cell lines adhered to cytokine-stimulated hCMEC/D3 in a dose-dependent manner (Fig. 3.6 A, see Fig. 2 Appendix 4 for raw data). Indeed, a combination of cytokines (TNF$\alpha$ + IFN$\gamma$) increased Jurkat and THP-1 adhesion (Fig. 3.6 A) at all doses used, with a maximal effect observed at concentrations as low as 1 ng/ml, as observed previously with VCAM1 expression (Section 3.3.3, Fig. 3.3). We also quantified adhesion of THP-1 and Jurkat to hCMEC/D3 cells stimulated for 0, 0.5, 1, 3, 6, 24 and 48 h. Both Jurkat and THP-1 cell lines adhered to hCMEC/D3 cells in a time-dependent manner (Fig. 3.6 B). When BEC were stimulated with 10 ng/ml of TNF$\alpha$ and IFN$\gamma$ in combination, both Jurkat and THP-1 adhesion increased significantly at all time points tested (Fig. 3.6 B). Both Jurkat and THP-1 adhesion to unstimulated hCMEC/D3 cells was between 2 and 20% of the input (see Pag. 90), normalized to 1 in result graphs.

However, Jurkat adhesion to cytokine-stimulated endothelium increased to a greater extent compared to THP-1 cells. Both Jurkat and THP-1 maximal adhesion was observed between 6 and 24 h, but 1 h of cytokine stimulation was already sufficient to increase monocyte and T cell adhesion above basal levels (Fig. 3.6 B). Taken together, these results show that pro-inflammatory cytokines (TNF$\alpha$ + IFN$\gamma$) increased both

monocyte and T cell adhesion to hCMEC/D3 cells. Hence the current *in vitro* BBB model is suitable to study leukocyte adhesion under static conditions.



A.



B.
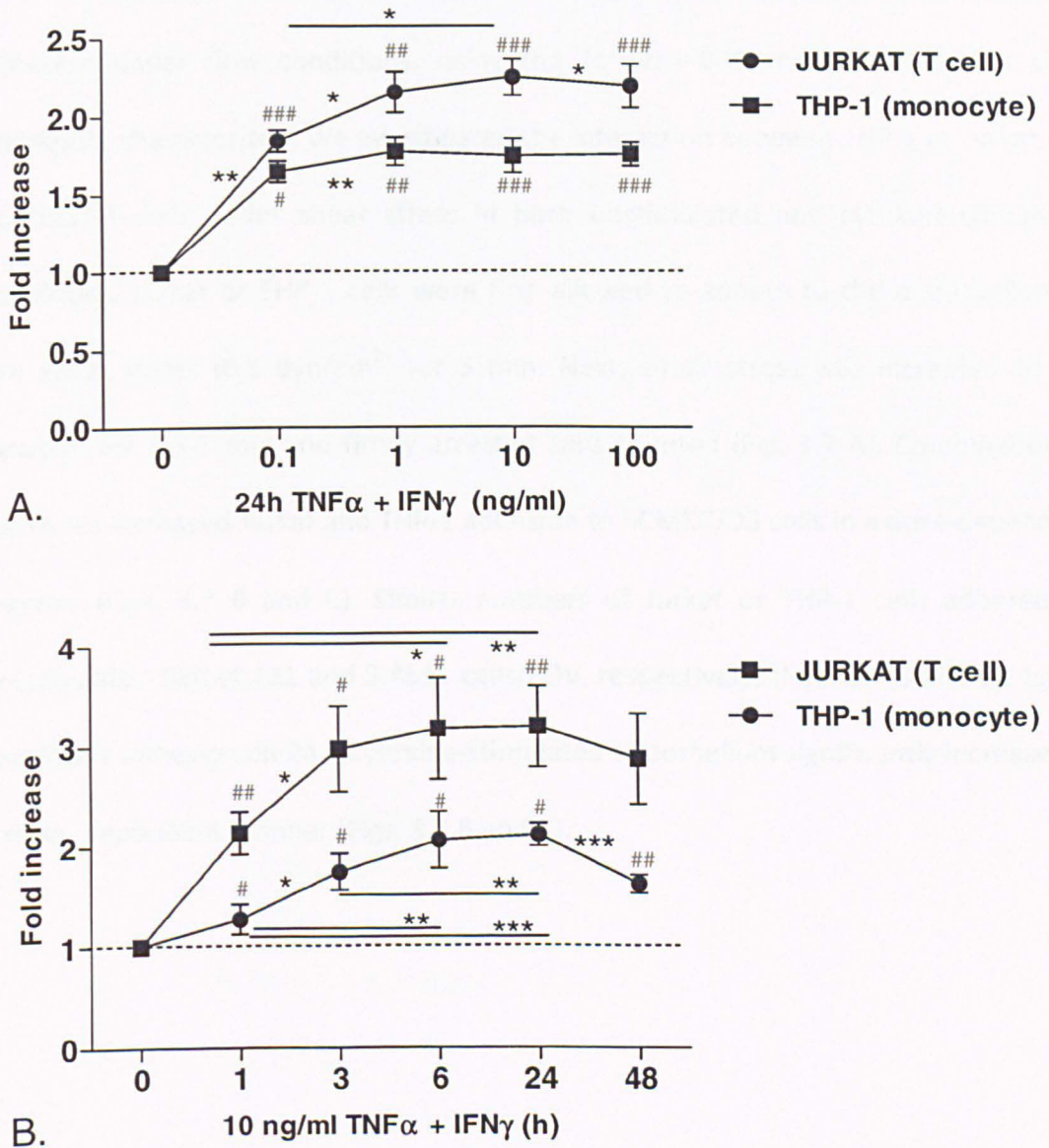
**Fig. 3.6: A combination of cytokines (TNFα and IFNγ) increases adhesion of leukocytes to hCMEC/D3 cells in a dose- and time-dependent manner using a static adhesion assay.** Confluent hCMEC/D3 cell monolayers were treated with TNFα and IFNγ in combination **A.** at different concentrations (0, 0.1, 1, 10, 100 ng/ml) for 24 h or **B.** with 10 ng/ml at different times (0, 1, 3, 6, 24 and 48 h). Fluorescence of adhered THP-1 or Jurkat cells to hCMEC/D3 cell monolayers was quantified at $\lambda_{ex}$= 485nm and $\lambda_{em}$= 525nm. Data are normalized to leukocyte adhesion levels on unstimulated hCMEC/D3 cell monolayers. Experiments were carried out three times with six replicates each. Data are mean ±SEM (*,#$p<0.05$**,##$p<0.01$, ***,###$p<0.001$, # significantly different vs. unstimulated cells, * significantly different between cytokine doses or time points).

### 3.3.7 A combination of cytokines (TNFα and IFNγ) increases Jurkat and THP-1 adhesion on hCMEC/D3 cells under flow in a dose-dependent manner

In addition to the static assay, we set-up a novel system to study leukocyte adhesion under flow conditions, using the *in vitro* BBB model, hCMEC/D3 cells, previously characterized. We investigated the interaction between THP-1 or Jurkat and hCMEC/D3 cells under shear stress in both unstimulated and cytokine-stimulated conditions. Jurkat or THP-1 cells were first allowed to adhere to the endothelium at low shear stress (0.5 dyn/cm$^2$) for 5 min. Next, shear stress was increased to 1.5 dyn/cm$^2$ for 0.5-1 min and firmly arrested cells counted (Fig. 3.7 A). Combination of cytokines increased Jurkat and THP-1 adhesion to hCMEC/D3 cells in a dose-dependent manner (Figs. 3.7 B and C). Similar numbers of Jurkat or THP-1 cells adhered on unstimulated BEC (4.1±1 and 3.46±1 cells/FOV, respectively) (Figs. 3.7 B and C). Jurkat and THP-1 adhesion on 24 h cytokine-stimulated endothelium significantly increased in a dose- dependent manner (Figs. 3.7 B and C).
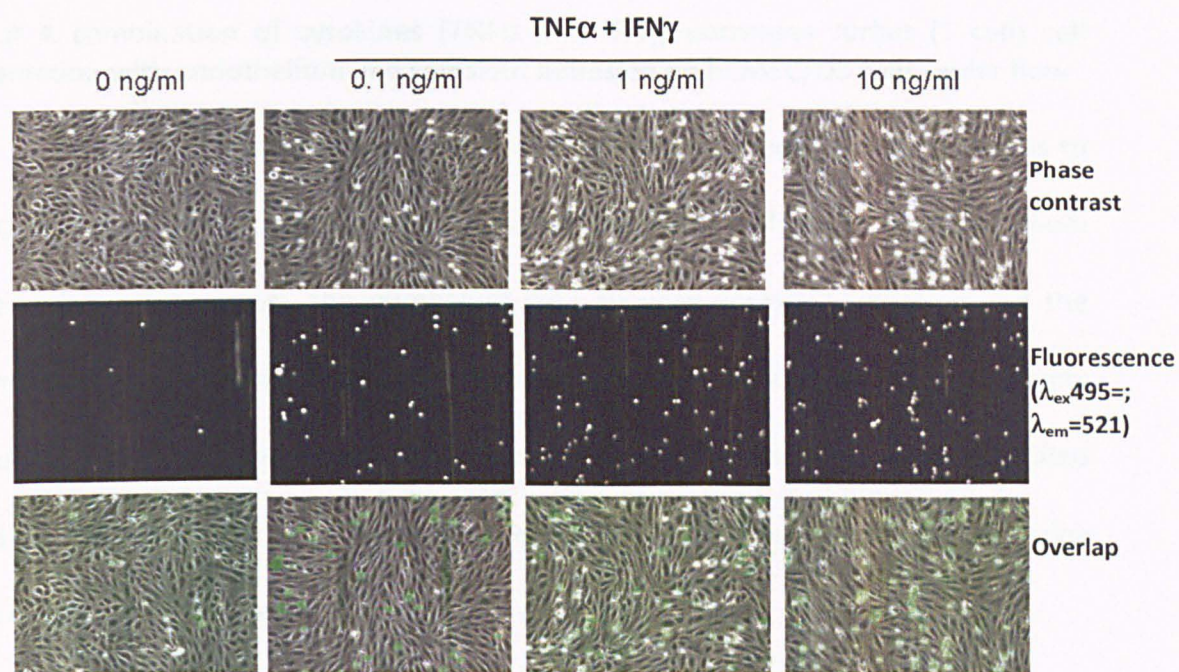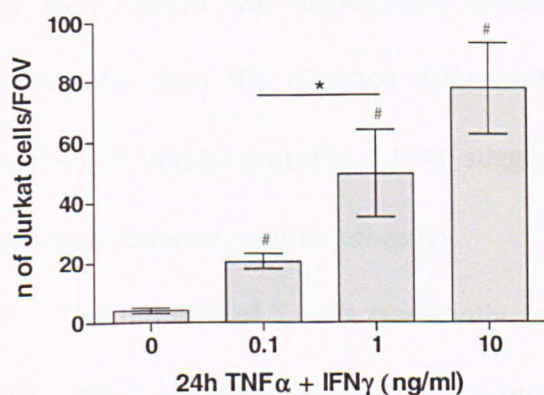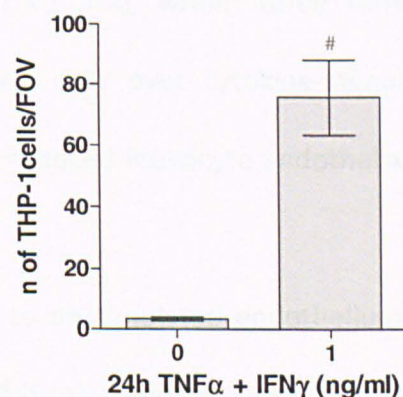
Fig. 3.7: Combination of cytokines (TNFα and IFNγ) increases Jurkat (T cell) and THP-1 (monocyte) adhesion on hCMEC/D3 cells under flow in a dose-dependent manner. Confluent hCMEC/D3 cell monolayers, grown on Ibidí® chambers, were stimulated with TNFα and IFNγ in combination at different concentrations (0, 0.1, 1, 10 ng/ml) for 24 h. A. Representative pictures of firmly adhered Jurkat cells/FOV: (Top) confluent hCMEC/D3 cell monolayers (phase contrast), (Middle) adhered Jurkat cells (fluorescence), (Bottom) overlap of hCMEC/D3 cells (phase contrast) and Jurkat cells (fluorescence). Adhered B. Jurkat and C. THP-1 cells to hCMEC/D3 cell monolayers were counted and results expressed as number of adhered cells per field of vision (FOV). Experiments were carried out three times with five FOV each. Data are mean ±SEM (*,#$p < 0.05$, #significantly different vs. unstimulated cells, * significantly different between cytokine treatments).

### 3.3.8 A combination of cytokines (TNFα and IFNγ) decreases Jurkat (T cell) cell interaction with endothelium and transient adhesion on hCMEC/D3 cells under flow

To better characterise the new *in vitro* flow-based model and its strengths to study leukocyte rolling/adhesion, we measured the distance of leukocyte-endothelium interaction before arrest, the number of cells showing transient adhesion and the number of cells showing firm shear resistant adhesion in a series of experiments involving Jurkat cells and hCMEC/D3 cells under flow. Measurements were quantified and counted using all frames captured along the time of the experimental setup using the Image Pro Plus distance tool.

The cell-cell interaction distance of Jurkat cells over unstimulated endothelium prior to adhesion was significantly greater (350±45 μm), within three different experiments, than the distance covered by Jurkat cells over cytokine-stimulated endothelium (49±13 μm) (Fig. 3.8 A), suggesting a reduced leukocyte-endothelial cell interaction distance prior to adhesion.

The number of T cells transiently adhered to unstimulated endothelium was comparable to or even higher than the number of firmly adhered T cells (Fig. 3.8 B, left), while in cytokine-stimulated conditions, transient adhesion was negligible compared to the number of total shear-resistant firmly adhered T cells (Fig. 3.8 B, right).
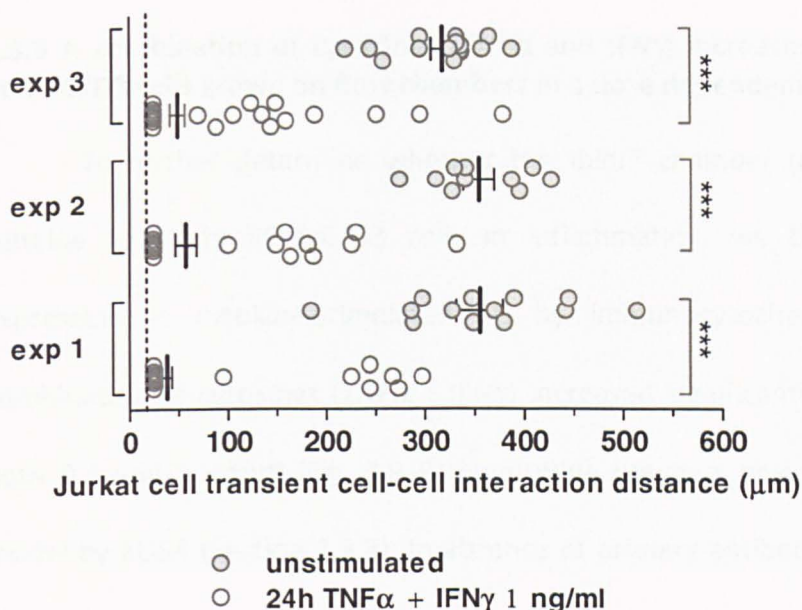
A.
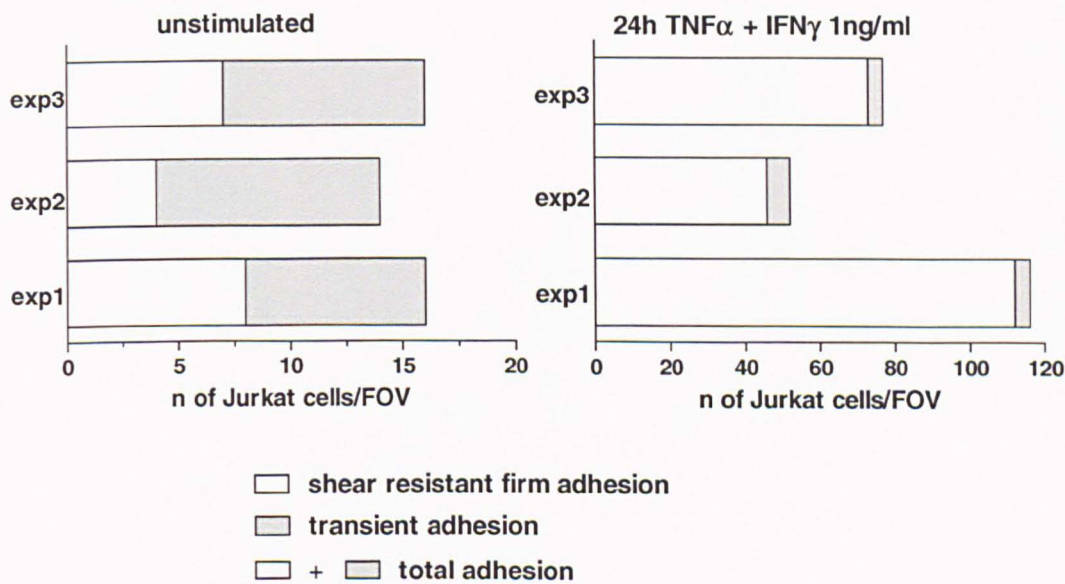


B.

**Fig. 3.8: A combination of cytokines (TNFα and IFNγ) decreases Jurkat (T cell) cell-endothelial cell interaction distance and transient adhesion on hCMEC/D3 cells under flow**. Confluent hCMEC/D3 cell monolayers, were stimulated with TNFα and IFNγ in combination at 1 ng/ml or left untreated for 24 h. **A.** T cell-endothelium interaction distance and **B.** n of transient and firm adhered Jurkat cells were measured and counted in a field of view (FOV= 640 x 480 µm). Experiments were carried out three times. Data are mean ±SEM (***$p<0.001$, * significantly different between unstimulated and cytokine treated).

### 3.3.9 A combination of cytokines (TNFα and IFNγ) increases VCAM1 expression in hCMEC/D3 cells grown on flow chambers in a dose dependent manner

To further determine whether the Ibidí® chamber (described in Fig 2.5) is suitable to study hCMEC/D3 cells in inflammation, we then measured VCAM1 expression in cytokine-stimulated EC by immunocytochemisty (Fig. 3.9 A). A combination of cytokines (TNFα + IFNγ) increased significantly VCAM1 expression at both 0.1 and 1 ng/ml (Fig. 3.9 B) confirming previous observations with the static model by ELISA (Section 3.3.3). In absence of primary antibody, no fluorescent signal was detected.
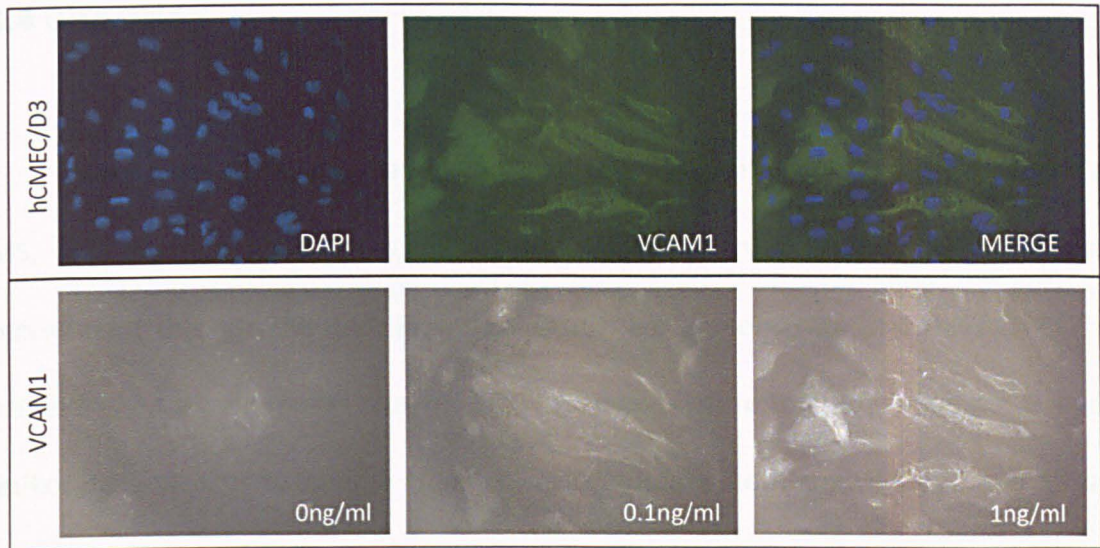
**A.**
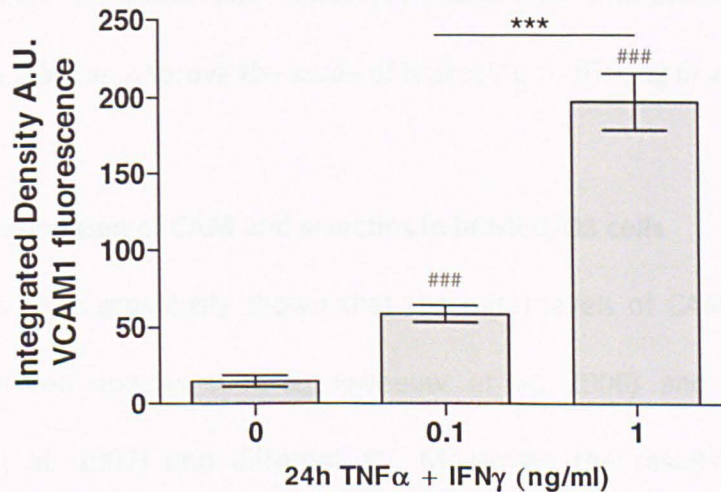


**B.**

**Fig. 3.9: A Combination of cytokines (TNFα and IFNγ) increases VCAM1 expression in hCMEC/D3 cells in a dose dependent manner.** Confluent hCMEC/D3 cell monolayers, grown on Ibidí® chambers, were stimulated with TNFα and IFNγ at different concentrations (0, 0.1, 1 ng/ml) for 24 h. Anti-human-VCAM1 was used to detect VCAM1 expression by immunofluorescence **A.** (Upper panel) Representative picture of DAPI staining cell nuclei (left), VCAM1-FITC fluorescence (middle) and merged fields (right). (Lower panel) Representative pictures of VCAM1-FITC fluorescence B/W on stimulated hCMEC/D3 at 0, 0.1 and 1 ng/ml. **B.** VCAM1-FITC fluorescence quantification by Image J expressed in integrated density (A.U.). Experiments were carried out two times in duplicate with five FOV each. Data are mean ±SEM (***, ###$p<0.001$, #significantly different vs. unstimulated cells, * significantly different between cytokine treatments).

# 3.4 Discussion

Leukocyte trafficking plays a central role in neuroinflammatory diseases such as MS, and the two early steps, rolling and adhesion are crucial for the leukocyte recruitment through the BBB. From our results we demonstrate that the hCMEC/D3 cell line is a suitable model human brain microvasculature to study inflammation and leukocyte adhesion to human brain microvasculature both under static and shear-stress conditions. In addition, we have developed and validated a novel system to study leukocyte adhesion and leukocyte-endothelial interactions under flow, a versatile tool that can improve the study of leukocyte trafficking *in vitro*.

### 3.4.1 Basal expression of CAM and selectins in hCMEC/D3 cells

It has been previously shown that the basal levels of CAM and selectins are variable between species (Coisne, Faveeuw et al. 2006) and organs (Oostingh, Schlickum et al. 2007) and different EC. Moreover, the results on basal selectin expression on endothelium are often contradictory. Weksler et al. studied the basal expression of ICAM1, VCAM1 and ICAM2, but not of selectins, on hCMEC/D3 cells by FACS, reporting that ICAM1 and ICAM2, but not VCAM1, are constitutively expressed by unstimulated endothelium. Our results are in line with Weksler et al. except those for VCAM1, but in line with Stins et al. were VCAM1 is expressed by resting HBMEC. This can be due to the different technique adopted to detect this protein and/or to the different anti-human-VCAM1 monoclonal antibody used in the present study. However, it has been shown that VCAM1 was expressed at low levels on resting

primary culture of human bone marrow endothelial cells and of human brain microvessel EC (HBMEC) while ICAM1 appeared to be expressed at higher levels (van Buul, Mul et al. 2004), in line with our findings. *In vivo*, it has been found that ICAM1 is faintly expressed in human brain microvessels (Lindsberg, Carpen et al. 1996) while another study reported that ICAM1 is not constitutively expressed by human brain EC (Love and Barber 2001).

We also determined by ELISA that hCMEC/D3 cells constitutively expressed low levels of E- and P-selectin. It has been found that P-selectin is expressed by unstimulated hCMEC/D3 cells by FACS (Bahbouhi, Berthelot et al. 2009). In addition, basal P- and E- selectin expression has been observed in other studies using cultured human BEC (Wong and Dorovini-Zis 1996; Wiese, Barthel et al. 2009) and HUVEC (Hattori, Hamilton et al. 1989; Oostingh, Schlickum et al. 2007).

*In vivo*, expression of either P- or E-selectin was not observed on brain tissue of sham rats by immunostaining (Zhang, Chopp et al. 1998), but basal expression of E-selectin was observed on blood vessel walls in C57BL/6 mice (Stielke, Keilhoff et al. 2012). In human brain it has not been detected any P-selectin expression in microvessels (Navratil, Couvelard et al. 1997; Love and Barber 2001).

Selectin expression by BEC is still a strongly debated subject due to the contrasting results obtained across species, both *in vivo* and *in vitro*. Here, our findings are in line with studies using other human BEC lines or primary human BEC (Wong and Dorovini-Zis 1996; Wiese, Barthel et al. 2009), but are in contrast with immunohistochemical studies on human brain microvessels *in* vivo (Navratil, Couvelard et al. 1997; Love and Barber 2001). This can be due to the process of immortalization of human BEC or the conditions used to maintain them *in vitro*. Indeed, it has been

reported that culture conditions influence the expression of many brain endothelial markers, either leading to down-regulation (e.g. tight junctional proteins (Steiner, Coisne et al. 2011)) or up-regulation (e.g. claudin-1, (Fletcher and McKeating 2012)) of specific genes associated with a barrier phenotype. It is thus possible that E- and P-selectin maybe up-regulated by cultured human BEC.

### 3.4.2 Combination of cytokines (TNFα and IFNγ increase synergistically VCAM1 and ICAM1 expression in hCMEC/D3 cells

Previous studies have reported that TNFα either alone or in combination with IFNγ increased VCAM1 and ICAM1 on HCEC (Kallmann, Hummel et al. 2000) and on hCMEC/D3 cells (Weksler, Subileau et al. 2005). Here, we compared the expression of VCAM1 and ICAM1 on hCMEC/D3 cells stimulated with TNFα alone or combined with IFNγ at different doses (0.1 and 10 ng/ml compared to 100 U/ml or 1 ng/ml in previous studies). We observed that TNFα-induced VCAM1, but not ICAM1, expression was enhanced by co-stimulation with INFγ as shown in cultured human macrophages (Tengku-Muhammad, Cryer et al. 1998) and on HUVEC (Ozaki, Ishii et al. 1999).

The synergistic effect of IFNγ to that of TNFα is thought to be mediated by NF-κB. It has been reported that TNFα alone activates NF-κB in hCMEC/D3 cells (Fasler-Kan, Suenderhauf et al. 2010) and that activated NF-κB following translocation to the nucleus is responsible for VCAM1 and ICAM1, but not ICAM2, gene transcription with consequent increases in VCAM1 and ICAM1 protein expression at the plasma membrane level (reviewed in (Pober and Sessa 2007)). IFN-γ may activate NF-κB indirectly, as it induces TNFα and IL-1β production and increases TLR4 receptor expression, thereby up-regulating VCAM1, by STAT1, and ICAM1 expression (reviewed

in (Schroder, Hertzog et al. 2004)). However, we did not observe any significant increases in ICAM1 expression on IFNγ–stimulated hCMEC/D3 cells suggesting that if IFNγ can activate NF-κB indirectly it may only do so in the presence of another stimulus such as TNFα. Nevertheless, we can speculate that the observed synergistic effect of IFNγ with TNFα on VCAM1 expression may occur possibly through potentiation of NF-κB activation. However, TNFα-induced increased ICAM1 expression may require other transcriptional regulators in addition to NF-κB, as IFNγ does not influence ICAM1 expression at the times and doses used in hCMEC/D3 cells. For example, it has been reported that JNK and ERK1 mediate ICAM1 expression via AP-1 activation (reviewed in (Lebedeva, Dustin et al. 2005) and it has been shown that PECAM-1-associated tyrosine phosphatase activity is required for ICAM1 expression in cultured rat BEC (Couty, Rampon et al. 2007). Indeed, ICAM1 expression is regulated by many different molecules of different patways activated either directly or indirectly by other stimuli.

Lopez-Ramirez et al. (2012) have shown that high concentrations (100 ng/ml) of cytokines (TNFα and IFNγ) in combination or alone induced caspase-3/7 activation and apoptotic cell death in hCMEC/D3 cells so we used lower cytokine doses in this study to avoid cell damage. It has been shown that increased apoptosis in rat retinal vascular endothelium is associated with leukocyte rolling and adhesion (Koizumi, Poulaki et al. 2003), and activation of NF-κB in EC (reviewed in (Pober 2002)) with consequent increase in VCAM1 and ICAM1 protein expression at the plasma membrane level. The observed increases in VCAM1 and ICAM1 expression by hCMEC/D3 cells stimulated with 0.1 ng/ml, demonstrate that this dose is sufficient to activate the signalling pathways induced by IFNγ and TNFα without activation of apoptotic mediators.

### 3.4.3 Combination of cytokines (TNFα and IFNγ) increases CAM and selectin expression and leukocyte adhesion on hCMEC/D3 cells

CAM and selectins mediate the early leukocyte trafficking on endothelium in response to inflammatory stimulus (Springer 1994), so the regulation of their presence on the cell surface is crucial for leukocyte adhesion. Here, we observed that increased expression of ICAM1, VCAM1, P- and E-selectin in a time- and dose-dependent manner on TNFα- and IFNγ-stimulated hCMEC/D3 is associated with the changes in T cell and monocyte adhesion. In particular, CAM is consistent with leukocyte rolling/capture preceding firm adhesion. Indeed, hCMEC/D3 cells expressed P-selectin on their surface a few minutes after stimulation as previously reported in hCMEC/D3 cells (Bahbouhi, Berthelot et al. 2009) due to rapid mobilization of the stored P-selectin in the Weibel-Palade bodies to the cell surface of EC as previously demonstrated (Bonfanti, Furie et al. 1989; Johnston, Cook et al. 1989). Up-regulation of P-selectin on cytokine-stimulated hCMEC/D3 cells was detected after 3 and 6 h of induction with the combination TNFα and IFNγ as found in HBEC. These increases of P- selectin are referable to a second regulation mechanism where TNFα is able to stimulate the transcript level and protein level of P-selectin (Weller, Isenmann et al. 1992; Hahne, Jager et al. 1993), as observed in E-selectin. E-selectin, confirming previously observations in TNF-α-stimulated primary human microvessel BEC (Wong and Dorovini-Zis 1996), was up-regulated slightly later, between 6 and 24 h on stimulated endothelium, because it requires *de novo* mRNA and protein synthesis (Bevilacqua, Pober et al. 1987) dependent on transcription factors such as NF-κB and AP-1 (Montgomery, Osborn et al. 1991; Whelan, Ghersa et al. 1991). Moreover, E-selectin is not induced by INFγ (Leeuwenberg, von Asmuth et al. 1990), so probably its increased

expression on hCMEC/D3 cells is exclusively due to the action of TNFα as observed for

ICAM1. TNFα and IFNγ stimulus for 24 h clearly and consistently induced a maximal

monocytic and T cell adhesion on hCMEC/D3 cells using the static model. However, the

monocyte adhesiveness to endothelium was less than that of T cells, possibly due to

THP-1 cells showing a lower avidity for P-selectin, or to them having lower expression

of P-selectin ligands (e.g. PSGL-1), which are essential for monocyte capture

(Kuckleburg, Yates et al. 2011), or of the co-factor CD63, essential for P-selectin

function (Ley K et al 2011).

### 3.4.4 THP-1 and Jurkat cells, models to study leukocyte adhesion

We used resting THP-1 and Jurkat cells which are widely used to study

leukocyte adhesion to endothelium. It has been shown that CCR2 (Chuang, Yang et al.

2011), PSGL-1, and both VLA-4 (Seminario, Sterbinsky et al. 1998) and LFA-1 (Quek, Lim

et al. 2010) integrins are expressed on the surface of THP-1 and Jurkat cells. These two

cell lines were isolated from leukemic patients, therefore an innate activation appears

to be kept even though they are not activated by specific antigens. As previously

described in Chapter 1, both resting THP-1 and Jurkat cells adhere to hCMEC\D3 cells,

this event is due to two different mechanisms. First, increased integrin avidity for the

ligands due to the integrins clusting on the leukocyte surface and, second an increased

intrinsic integrin affinity for its ligands. Hence, THP-1 and Jurkat cells express active

integrins that can mediate firm adhesion.

### 3.4.5 A new *in vitro* model based on hCMEC/D3 cells to study leukocyte-endothelium interaction under flow

Brain endothelial cells *in vivo* are continuously subjected to shear stress, the force generated by blood flow. To preserve this physiological condition during *in vitro* studies of leukocyte adhesion to hCMEC/D3, we used Cellix Vena 8 and Bioflux systems without success (Appendix 1), due to the detachment of the endothelial monolayer and absence of constant leukocyte flow, respectively. Thereafter, we successfully assembled an *in vitro* model to study leukocyte adhesion to hCMEC/D3 cells during inflammation under flow as described before (Section 3.2.2). Ibidi® μ-slideVI 0.4 was selected to assemble the flow-system, where hCMEC/D3 cells were successfully cultured to confluence after an accurate comparison between the three models tested (Table 3.1).

|  | Ibidi® | Cellix | Bioflux |
|---|---|---|---|
| Chamber Set-up | Fairly easy | Easy | Difficult |
| Chamber Sterility | Yes | No | Yes |
| Coating | Collagen | Fibronectin and collagen | Fibronectin and collagen |
| Cell monolayer (static) | 100% properly formed | 100% properly formed | 100% properly formed |
| Cell monolayer (flow) | Shear stress resistant | Cell detachment, 30% cases | Shear stress resistant |
| Transfection | Successful | Successful | Problematic, unsuccessful |
| Leukocyte adhesion | Successful | Successful | Unsuccessful |
| Cost chamber/assay | Low | Medium | High |
| Cost Pumps | Low | High | Very High |
| System Set-up | 100% Manual, Fairly easy | 50% Manual, Fairly easy | 50% Manual, Difficult |
| Transfection Efficiency | ~100% | ~70% | Not efficient |

**Table 3.1: Quality, limitations and conditions of the three flow-based systems tested.**

The flow pattern at the post-capillary level has been defined as a laminar shear flow with a parabolic velocity (Nieto, Frade et al. 1997; Luscinskas, Lim et al. 2001). By contrast, Cucullo et al. argued that the physiological blood flow *in vivo* had a pulsatile nature (Cucullo, McAllister et al. 2002; Desai, Marroni et al. 2002). We perfused the leukocytes through the chambers with endothelial monolayers applying a constant laminar flow without any pulsatory force assuming that the vessel is inelastic, cylindrical and straight and that the blood is a Newtonian fluid.

The shear stress in the post-capillary venules is believed to be between 0.25 and 4 dyn/cm$^2$ (Lawrence, Smith et al. 1990). We pulled leukocytes in culture media at 0.5 dyn/cm$^2$, for the accumulative phase (or so-called bolus phase), and afterwards increased the flow to 1.5 dyn/ cm$^2$ to count the shear-resistant leukocytes adhered to the hCMEC/D3 as in previous flow-based leukocyte adhesion studies (Table 3.2).

| | Cell Type | Dyn/cm$^2$ | Leukocyte | Time of interaction (min) | Washout Time (min) | Reference |
|---|---|---|---|---|---|---|
| HUMAN | HUVEC | 1 | Neutrophils | 4 | 2min | (Burton, Butler et al. 2011) |
| | HUVEC | 1 | PBL or neutrophils | 4 | 2 and 11 | (McGettrick, Buckley et al. 2010) |
| | THBMEC | 0.25 | PBMS from MS patients | 20 | - | (Man, Tucky et al. 2009) |
| | hBMEC-60 | 0.3 to 4.2 | KG1 human hemopoietic Progenitor | Every 15s | - | (Wiese, Barthel et al. 2009) |
| | HDMEC, HBMEC, HUVEC | 1.04 | PBMC from healthy donors | - | - | (Oostingh, Schlickum et al. 2007) |
| | HUVEC | 1 | Neutrophils | 4 | 5 | (Sheikh, Rahman et al. 2005) |
| | HUVEC | 0.75 | PBLs | 40s | 20 mins at 5dyn/ cm$^2$ | (Cinamon, Shinder et al. 2001) |
| | HUVEC | 1.5 | PBMC from healthy donors and Jurkat cells | 1 | - | (Grabovsky, Feigelson et al. 2000) |
| | HUVEC | 1.8 | Human Monocytes | 10 | - | (Luscinskas, Kansas et al. 1994) |
| MOUSE | bEND5 | 0.25 | (PLP)-specific CD4+Thi effector/memory T cell line | 4 | N.A. at 1.5 dyn/ cm$^2$ | (Steiner, Coisne et al. 2011) |
| | pMBMEC | 0.25 | (PLP)-specific CD4+Thi effector/memory T cell line | 4 | N.A. at 1.5 dyn/ cm$^2$ | (Steiner, Coisne et al. 2010) |
| HAMSTER | CHO-E cells | 0.75 to 36 | (PLP)-specific CD4+Thi effector/memory T cell line | 2 at 0.75 | Increasing every 20sec | (Alon, Rossiter et al. 1994) |

**Table 3.2: Parameters of flow-based assays previously used to study endothelium/leukocyte interactions.**

When we counted the shear-resistant adhered THP-1 and Jurkat cells on 24 h TNFα- and IFNγ-stimulated hCMEC/D3 cells, we observed a striking difference between unstimulated and TNFα- and IFNγ-stimulated endothelium compared with the static adhesion results. Moreover, with low doses of cytokines (0.1 and 1 ng/ml) we observed consistent and clear-cut increases of Jurkat and THP-1 adhesion of 5 and 15

times, respectively, compared to basal levels. The flow–based model used enabled us to count the adhered monocytes and T cells on the endothelium very easily.

Furthermore, we quantified transient adhesion (T cell attachment and detachment to and from endothelium) and cell-cell interaction between T cells-endothelium successfully. However, we were not able to study proper leukocyte rolling. On unstimulated hCMEC/D3 cells, the few T cells that interacted with endothelium along the 5 min bolus were in contact for relative long distances and almost 50% of them transiently adhered to detach immediately. In cytokine-stimulated endothelium, a high number of T cells heavily firmly adhered without much cell-cell interaction or detachment, while under basal conditions, there was high cell-cell interaction distances prior to adhesion probably due to low expression of selectins and CAM by brain endothelium. In addition, the low levels of selectin and CAM expression by hCMEC/D3 may not be sufficient to induce firm adhesion between T cells and endothelium, thereby leading to leukocyte detachment after short interaction with BEC. By contrast, in inflammatory conditions, CAM and selectins are overexpressed by brain endothelium and T cells straight firmly adhered with very short cell-cell interaction and rare detachment.

Due to technical limitations of acquisition of images at 1 frame/sec, we were not able to quantify leukocyte rolling. In agreement with our results, it has been reported that the rolling of T lymphocytes on immobilized P-selectin last from 0 to 30 seconds with a displacement of 600 to 800 µm (Lee, Kim et al. 2012), but rolling of leukocyte on HUVEC was estimated to be much faster, at about 10 µm/s (Burton, Butler et al. 2011), whereas *in vivo* leukocyte rolling on mouse post capillary venules and on venules was 70 µm/s (Su, Lei et al. 2012) and 30 µm/s (Westmuckett, Thacker

et al. 2011), respectively, using a setup that acquired 30 frames/sec. Indeed, under inflammatory conditions, most of the leukocyte-endothelial cell interaction distances fell below the threshold of 24.62 μm in our experimental setup. Then, we concluded that in order to confirm whether leukocyte rolling was being determined, further experiments needed to be performed to improve the acquisition system in order to capture 20-30 frame/sec. Nevertheless, cell-cell interaction distances and transient adhesion measurements gave important information about early leukocyte trafficking *in vitro*.

Taken together our results show that cytokines (TNFα and IFNγ) increased VCAM1, ICAM1, and P- and E-selectin expression on hCMEC/D3 cells which is associated with increased THP-1 and Jurkat adhesion on both assays used. The flow-based model, mimicking the physiological conditions characterized by shear stress, results in a more appropriate model to study leukocyte adhesion on human brain endothelium *in vitro*, however far to mimic *in vivo* conditions.

In this chapter we presented evidence that both static and flow-based *in vitro* assays to study leukocyte adhesion on human brain endothelium, using hCMEC/D3 cells, are valuable model systems to study leukocyte trafficking under both basal and cytokine-stimulated conditions with the advantages and disadvantages reported in Table 3.1 and 3.3. However, we obtained more evident and consistent results using the flow-based model mainly due to the continuous passage of leukocytes on EC (shear stress) that reduced weak and unspecific leukocyte adhesion.

| STATIC (96 well plate) | | | FLOW (Ibidi® chamber) | |
|---|---|---|---|---|
| | + | - | + | - |
| Protein expression | High sensitivity (ELISA) | Time-consuming | Fast (immunofluorescence) | Low sensitivity |
| Leukocyte Adhesion | Fast, easy and cheap | High unspecific adhesion, experimental variability | more physiological conditions, high specificity and sensitivity, opportunity to quantify more parameters and detects small changes | Longer, technically more difficult and more expensive |

**Table 3.3: Advantages (+) and disadvantages (-) of static and flow-based adhesion systems.**

## 3.5 Conclusions

Results show that the hCMEC/D3 cell line is an appropriate *in vitro* model of the human BBB to study leukocyte adhesion in neuroinflammation and that the flow-based system represents a significant improvement to study leukocyte trafficking over previous static assays, where cells can be analyzed by fluorescence and harvested for further analysis.

# Chapter 4: The role of endothelial hsa-miR-126 in leukocyte adhesion to human brain endothelium

## 4.1 Introduction

Recent studies have identified miRs as key regulators of a vast number of biological processes including the development of different physiological systems and the maintenance of cellular homeostasis and normal function. Regulatory miRs are also involved in inflammation (Dai and Ahmed 2011) and autoimmunity (Ceribelli, Satoh et al. 2012). Only in the last years have some miRs been characterised as regulators of the endothelial inflammatory response (Zhou, Wang et al. 2011; Rippe, Blimline et al. 2012), leukocyte trafficking (Harris, Yamakuchi et al. 2008; Yoshizaki, Wakita et al. 2008; Schmidt, Spiel et al. 2009) and CAM (Kuehbacher, Urbich et al. 2007; Fish, Santoro et al. 2008). The OU BBB group in collaboration with Drs. Arie Reijekerk and Helga De Vries (VU Medical Centre, Amsterdam, Netherlands) have recently published a study in which miR arrays were used to identify changes in miR levels in cytokine-stimulated and astrocyte-conditioned media-stimulated hCMEC/D3 cells compared to unstimulated cells (Reijekerk, Lopez-Ramirez et al., 2013). Of the miRs most altered by the combination of cytokines (Table 4.1), five miRs were selected, three up-regulated (hsa-miR-155, -146a and b) and two down-regulated (hsa-miR-126 and -30c), to investigate their role in leukocyte adhesion to the human brain endothelium *in vitro*. These were identified as the highest fold change from basal levels (miRs-155, -146a and b, and -30c) or the most abundant endothelial miRs that showed a reduction in levels in response to cytokines (miR-126). Following this initial

screening, this chapter describes the role of miR-126 in leukocyte adhesion to

hCMEC/D3 cells.

| Most abundant miRs in BEC | miRs up-regulated by TNFα+IFNγ and TNFα+ IL | Fold increase following TNFα+IFNγ treatment | miRs down-regulated by TNFα+IFNγ and TNFα+ IL | Fold decrease following TNFα+IFNγ treatment | Highly expressed miRs down-regulated by TNFα+IFNγ and TNFα+ IL | Fold decrease following TNFα+IFNγ treatment |
|---|---|---|---|---|---|---|
| Hsa-miR-720 | **Hsa-miR-155** | 4.5 | **Hsa-miR-30c** | 6.3 | **Hsa-miR-126** | 2.1 |
| Hsa-miR-21 | **Hsa-miR-146b-5p** | 3.0 | Hsa-miR-27b | 5.4 | Hsa-miR-16 | 1.9 |
| Hsa-miR-1274b | **Hsa-miR-146a** | 2.5 | Hsa-miR-324-5p | 5.0 | Hsa-miR-923 | 2.0 |
| **Hsa-miR-126** | Hsa-miR-21* | 2.5 | Hsa-miR-301b | 4.9 | Hsa-miR-7a | 2.4 |
| Hsa-miR-923 | | | Hsa-miR-23b | 4.6 | Hsa-miR-7f | 2.6 |
| Hsa-let-7a | | | Hsa-miR-17* | 4.0 | Hsa-miR-15b | 2.3 |
| Hsa-let-7f | | | Hsa-miR-148b | 3.9 | | |
| Hsa-miR-15b | | | Hsa-miR-31* | 3.9 | | |
| Hsa-miR-7b | | | Hsa-miR-361-5p | 3.8 | | |
| | | | Hsa-miR-128 | 3.8 | | |

**Table 4.1: List of selected miRs up/down-regulated by cytokines in cultured human brain endothelium.** Complete list:
(http://www.ncbi.nlm.nih.gov/projects/geo/query/acc.cgi?acc=GSE44694).

Previous works have shown that the endothelial miR-126 was able (i) to

suppress lung metastasis in breast cancer in mice (Png, Halberg et al. 2012; Zhang,

Yang et al. 2013), (ii) to regulate human hematopoietic stem/progenitor cell trafficking

from the bone marrow to peripheral sites (Salvucci, Jiang et al. 2012), (iii) to decrease

adhesion migratory and invasive capacity of human non-small cell lung cancer cells

(Crawford, Brawner et al. 2008) and (iv) to decrease human neutrophil adhesion to

HUVEC through direct regulation of VCAM1 expression at the posttranscriptional level

(Harris, Yamakuchi et al. 2008). In this study, first, we investigated whether modulating

endothelial hsa-miR-126, either by decreasing or increasing miR-126 expression in

hCMEC/D3 cells could influence the inflammatory response by altering leukocyte

adhesion (T cells, monocytes and PBMC) to brain endothelium. Then, possible

predicted targets of miR-126 involved in leukocyte adhesion were selected using

bioinformatic databases. Finally, whether endothelial hsa-miR-126 modulated

regulated levels of the selected predicted targets was tested potentially providing a mechanism for its effect on leukocyte adhesion.

## 4.2 Aims

First, a suitable method to modulate endothelial miR levels in hCMEC/D3 cells was investigated. Then static leukocyte adhesion assays were employed to determine the role of the five selected miRs on leukocyte adhesion (T cells) to brain endothelium. Finally, the effect of varying levels of miR-126 in BEC on T cell, monocyte and PBMC adhesion to endothelium and its putative mechanism of action were further investigated.

## 4.3 Results

### 4.3.1 Role of seeding cell density on hCMEC/D3 cell confluence

To study cytokine-induced leukocyte adhesion, confluent monolayers of BEC are required whereas modulation of endothelial miRs by lipofection usually requires non-confluent cells in order to achieve maximal transfection efficiency. Therefore, we first investigated the relationship between seeding cell density and confluence at different key time-points. To determine whether hCMEC/D3 cells were able to form confluent monolayers within 22-24 h, 0.5, 1, 1.5 and $2x10^5$ cells/cm$^2$ were seeded as described in Section 2.2.1 in 2 cm$^2$ plates, and, random phase-contrast pictures were taken at 19, 24, 42, 48 and 72 h after seeding. We observed 70-80 % of hCMEC/D3 cell confluence at 24 h when $1.5x10^5$ cells/ cm$^2$ were plated, and at 48 h this density of hCMEC/D3 cells formed a 100% confluent monolayer (Fig. 4.1). At 72 h, this seeding cell density of hCMEC/D3 cells maintained a confluent monolayer. The other tested seeding cell densities, both at 24 and at 48 h, generated either sub-confluent (0.5 and $1x10^5$ cells/cm$^2$) or supra-confluent ($2x10^5$ cells/cm$^2$) hCMEC/D3 monolayers not optimal for transfection of miR modulators (Fig. 4.1).

Therefore, a cell seeding density of $1.5x10^5$ cells/cm$^2$ was used in all further experiments, in order to achieve 70-80% hCMEC/D3 cell confluence at 24 h, optimal for lipofection studies, and 100% hCMEC/D3 confluent monolayer at 48 h, optimal for cell-cell adhesion studies.

**0.5x10⁵cells/cm²**    **1x10⁵cells/cm²**
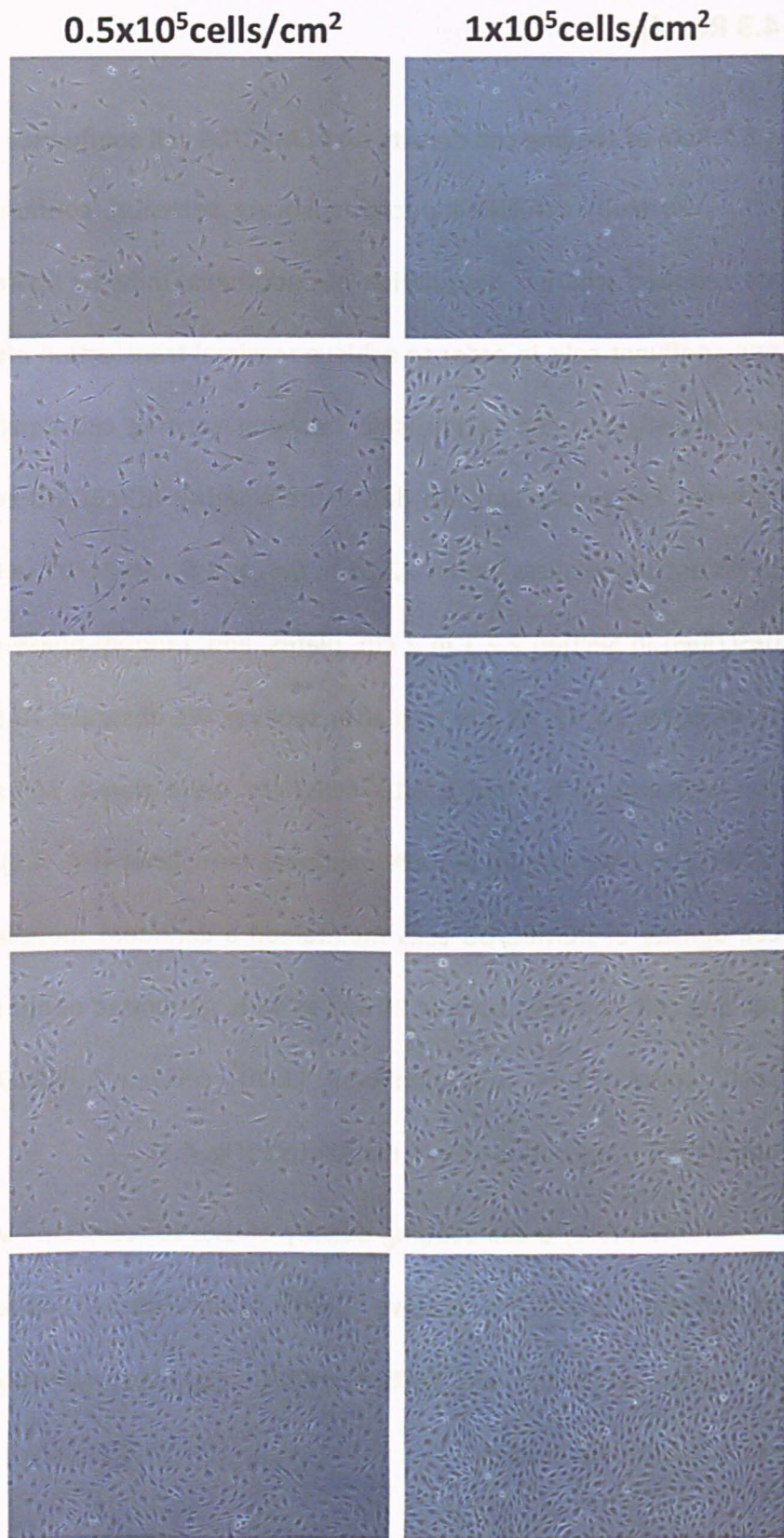


**Fig. 4.1: Cell density of hCMEC/D3 cells at different times after seeding.** hCMEC/D3 cells were seeded at different densities (0.5, 1, 1.5 or $2x10^5$ cells/cm²) and phase-contrast pictures were taken at 19, 24, 42, 48 and 72 h after standard incubation (37°C,
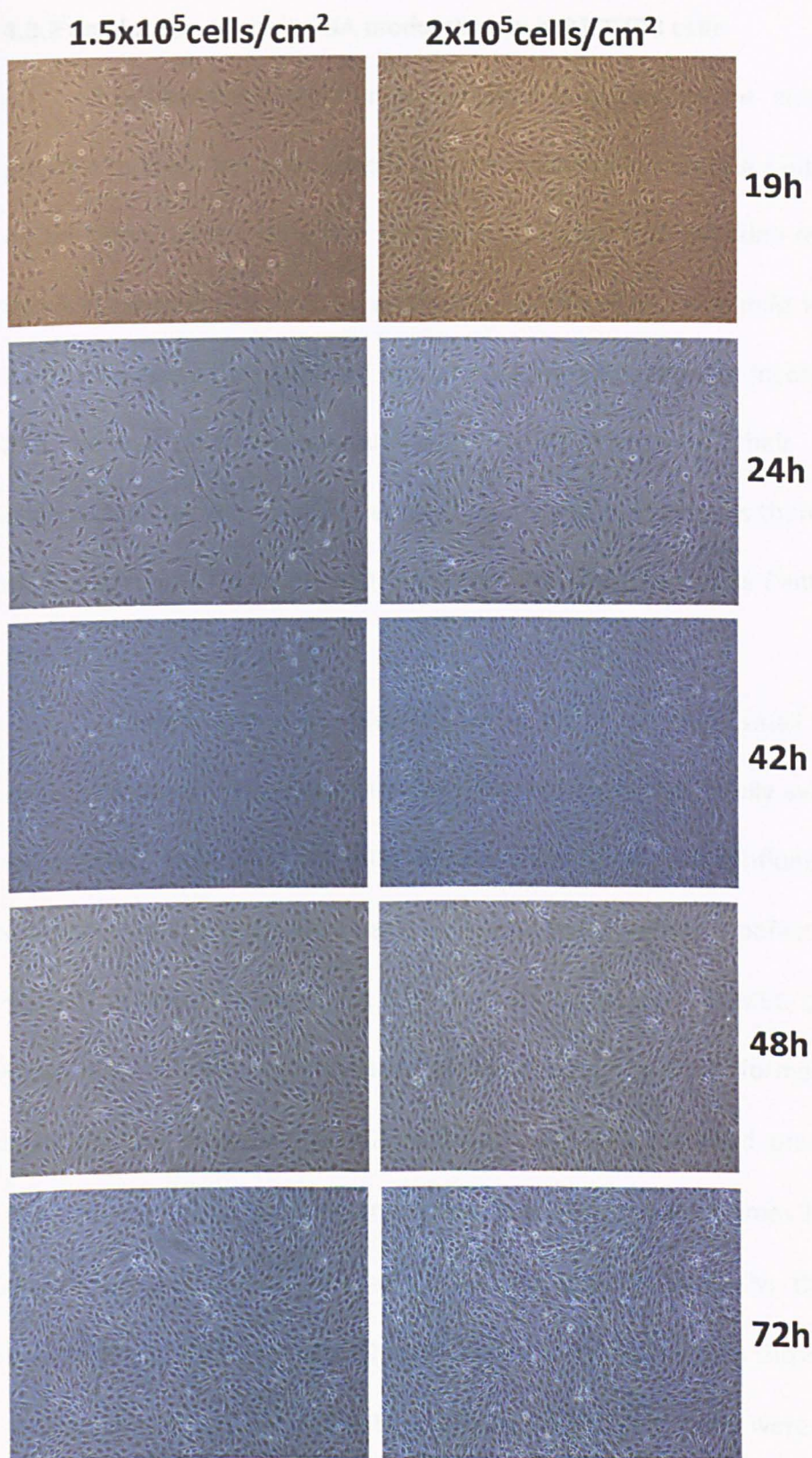
5% CO2) in complete media. hCMEC/D3 cell confluence was studied particularly at 24 h and 48h which are the start and end points of the cell transfection. Results are from three experiments in duplicate. Representative images at magnification x10 are shown.

## 4.3.2 Lipofection of microRNA modulators in hCMEC/D3 cells

It has been shown that miR expression is species-, tissue- and cell-specific. It is possible to modulate endogenous levels of miRs by introducing synthetic miR mimics or inhibitors. Here, to study the role of endothelial cytokine-regulated miRs in leukocyte adhesion *in vitro*, we modulated specific endothelial miRs in hCMEC/D3 cells by transfection either with miR precursors (pre-miRs), that are incorporated into RISC and behave like endogenous miRs hence increasing their levels, or with oligonucleotides with complementary sequence to mature miRs thereby blocking their biological function and/or reducing levels of endogenous miRs ('antagomirs' or anti-miRs).

One of the most efficient approaches to introduce small RNA or miRs into cells to modulate their expression is by lipofection. Commercially available complexes to transfect small RNA or miRs require cells to be sub-confluent. To transiently modulate miRs in hCMEC/D3 cells, we tested two reagents, Lipofectamine® 2000 and Siport™ to transfect both miRs mimics and the inhibitors. hCMEC/D3 cells were four times more efficiently transfected with hsa-pre-miR by Siport-formed complexes than Lipofectamine reagent (Fig. 4.2). Indeed, using a Cy3-labelled pre-miR, the median fluorescence of Siport™ reagent-transfected cells was four times higher than those transfected with Lipofectamine® 2000 (Fig. 4.2 A). Similarly, the percentage of fluorescently-labelled hCMEC/D3 cells was 1.5 fold higher than those transfected with Lipofectamine® (Fig. 4.2 B). In contrast, hCMEC/D3 cells were more efficiently transfected with anti-miR by Lipofectamine® 2000 (Fig. 4.2 B and D). Using Cy3-labelled anti-miR the median fluorescence of cells was seven times higher when cells were transfected with Lipofectamine® 2000 (Fig. 4.2 D), while only a slight but significant

increase in the percentage of transfected cells was observed with the same transfection reagent when compared to Siport™ (Fig. 4.2 D).

In all further experiments Lipofectamine® 2000 and Siport™ were used to transfect hCMEC/D3 cells with anti- and pre-miRs, respectively.
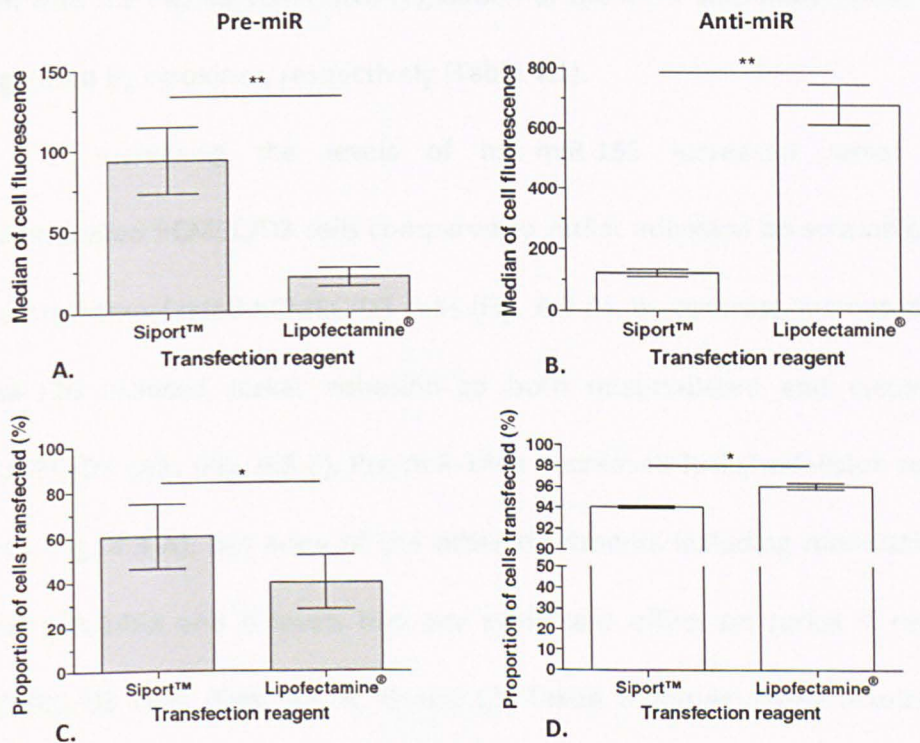


**Fig. 4.2: Siport™ and Lipofectamine® 2000 mediate efficient Pre- and Anti-miR transfection in hCMEC/D3 cells, respectively.** 70% confluent hCMEC/D3 cells were transfected with Cy3-premiR (A and C) or Cy3-antimiR (B and D) using either Siport™ or Lipofectamine® 2000 reagents and 48 h later transfection efficiency was quantified by FACS. **A.** and **B.** Median fluorescence is expressed in arbitrary units. **C.** and **D.** Percentage of fluorescent cells are the positive transfected cells in the sample. Experiments were carried out three times with three or two replicates. Data are mean ±SEM (*$P<0.05$, **$P<0.01$.* significantly different between transfection reagents).

### 4.3.3 Screening of five selected TNFα and IFNγ-regulated endothelial miRs for static Jurkat leukocyte adhesion

To study the role of endothelial miRs in leukocyte adhesion we screened five miRs using the static adhesion assay of Jurkat T cell adhesion to confluent hCMEC/D3 cells. The inflammatory miRs hsa-miR-155, -146a and b were up-regulated in 24 h TNFα and IFNγ-stimulated hCMEC/D3 cells while hsa-miR-30c and -126 were either the miR with the highest fold down-regulation or the most abundant miR which was down regulated by cytokines, respectively (Table 4.1).

Increasing the levels of hsa-miR-155 increased Jurkat adhesion to unstimulated hCMEC/D3 cells compared to Jurkat adhesion on scrambled hsa-pre-miR (control) transfected hCMEC/D3 cells (Fig. 4.3 D). By contrast, increased levels of hsa-miR-126 reduced Jurkat adhesion to both unstimulated and cytokine-stimulated hCMEC/D3 cells (Fig. 4.3 E). Pre-miR-146a decreased Jurkat adhesion to unstimulated cells (Fig. 4.3 A), but none of the other treatments including modulation of miR-30c and miR-146a and b levels had any significant effect on Jurkat T cell adhesion to hCMEC/D3 cells (Figs. 4.3 A, B and C). Taken together, these results showed that modulation of endothelial hsa-miR-126 and -155 levels in endothelium had significant effects on Jurkat adhesion to hCMEC/D3 cells using a static assay. For this reason hsa-miR-126 and 155 merited further studies to determine their role in leukocyte adhesion.
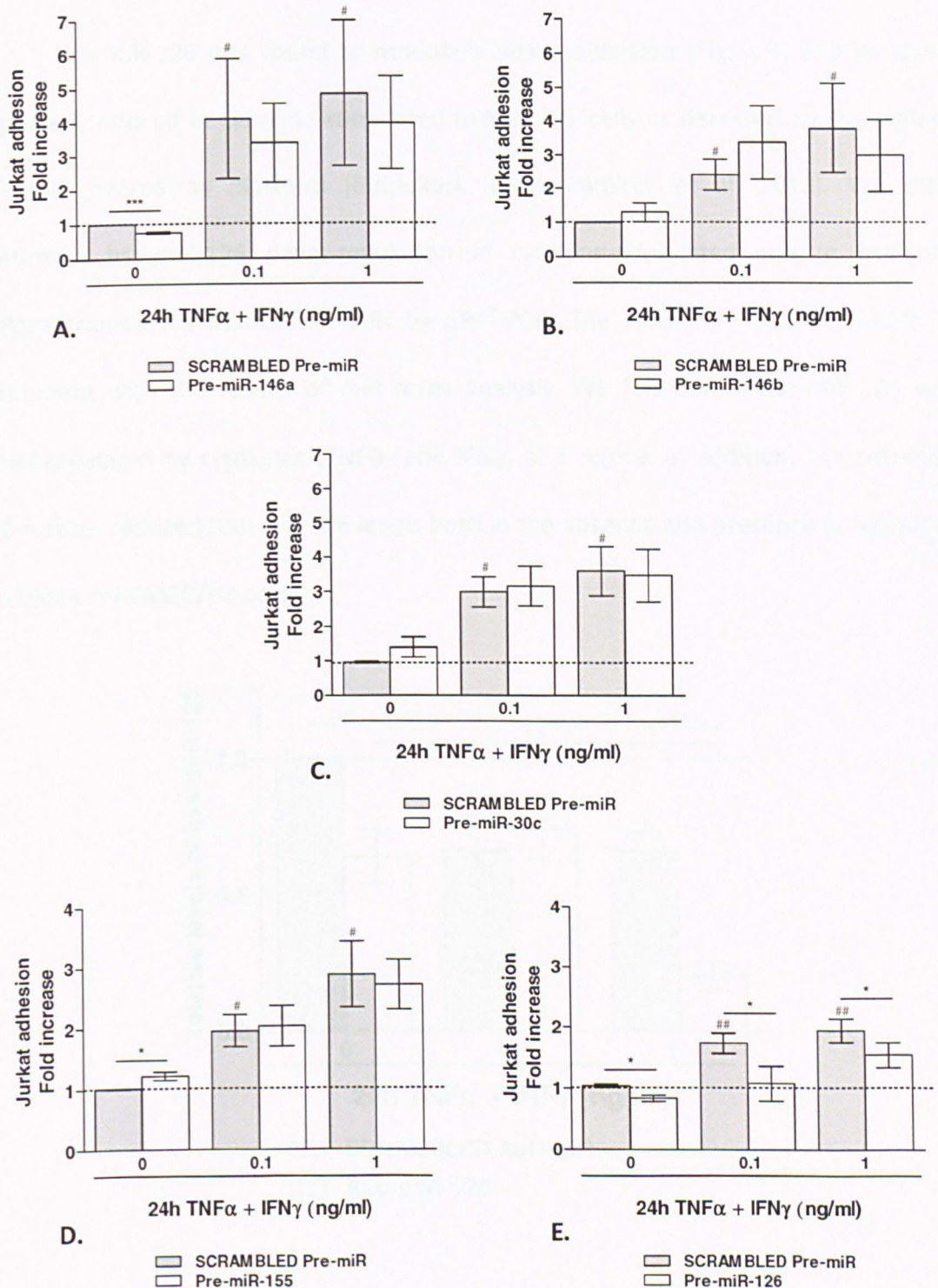
**Fig. 4.3: Increased levels of hsa-miR-126 and hsa-miR-155 affect Jurkat static adhesion on hCMEC/D3 cells.** hCMEC/D3 cells were transfected with scrambled Pre-miR (control) or Pre-miR-, **A.** -146a **B.** -146b, **C.** -30c, **D.** -155 and **E.** -126 followed by treatment with a combination of cytokines (TNFα + IFNγ) at different doses for 24h. Fluorescence of adhered Jurkat is expressed in comparison with unstimulated cells. Data are mean ±SEM (*,#P<0.05**,##P<0.01. # significantly different compared to unstimulated cells *significantly different between Pre-miR and scrambled control).

## 4.3.4 Hsa-miR-126 is down-regulated in TNFα- and IFNγ-stimulated hCMEC/D3 cells

Hsa-miR-126 was found to modulate Jurkat adhesion (Fig. 4.3) and its levels appeared reduced in cytokine-stimulated hCMEC/D3 cells as detected by the Agilent v13 miR microarray platform (Reijerkerk, Lopez-Ramirez et al. 2013). We then confirmed hsa-miR-126 down-regulation in cytokine-stimulated and in hsa-anti-miR126-transfected hCMEC/D3 cells by $qRT^2$-PCR. The results of $qRT^2$-PCR were in agreement with the results of miR array analysis. We found that hsa-miR-126 was down-regulated by cytokines (TNFα- and IFNγ) at 1 ng/ml. In addition, hsa-anti-miR-126 further reduced hsa-miR-126 levels both in the absence and presence (1 ng/ml) of cytokines in hCMEC/D3 cells.
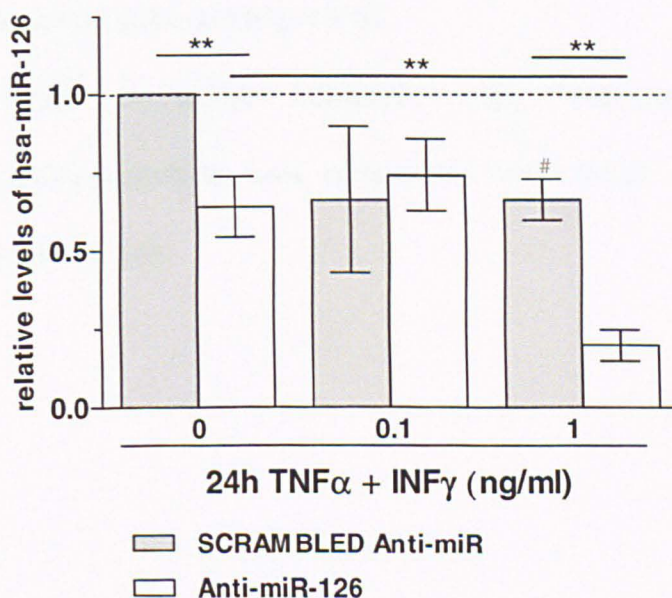


**Fig. 4.4: hsa-miR-126 down-regulation in hCMEC/D3 cells.** hCMEC/D3 cells were transfected with scrambled anti-miR or anti-miR-126 followed by treatment with a combination of cytokines (TNFα + IFNγ) at different doses (0.1, 1 ng/ml) for 24 h. The expression of mature miR-126 was measured by $qRT^2$-PCR. The small nuclear RNA U6 was used as internal control. Experiments were carried out three times with two replicates ([#]$P<0.05$, ** $P<0.01$ [#] significantly different compared to unstimulated cells *significantly different between anti-miR and scrambled control).

## 4.3.5 Hsa-miR-126 modulates Jurkat static adhesion on hCMEC/D3 cells in both control and inflammatory conditions

After confirming that hsa-miR-126 levels are down-regulated in cytokine-treated hCMEC/D3 cells (Fig. 4.4) and finding that hsa-pre-126 reduced Jurkat adhesion on both unstimulated and cytokine stimulated EC (Fig. 4.3, reproduced in Fig. 4.5 A), we investigated Jurkat static adhesion with reduced hsa-miR-126 expression in hCMEC/D3 cells modelling the conditions observed in cytokine-activated cells.

Decreasing hsa-miR-126 levels in resting hCMEC/D3 cells increased Jurkat adhesion under static conditions (Fig. 4.5 B). However, when hCMEC/D3 cells were stimulated with a combination of cytokines (TNFα and IFNγ), further down-regulation of hsa-miR-126 levels by anti-miR transfection did not result in a further increase in cytokines –induced Jurkat adhesion (Fig. 4.5 B).

Jurkat adhesion on control hCMEC/D3 cells, transfected with hsa-pre-scrambled or hsa-anti-scrambled, was comparable with Jurkat adhesion on non transfected cells (see Fig. 3.6).
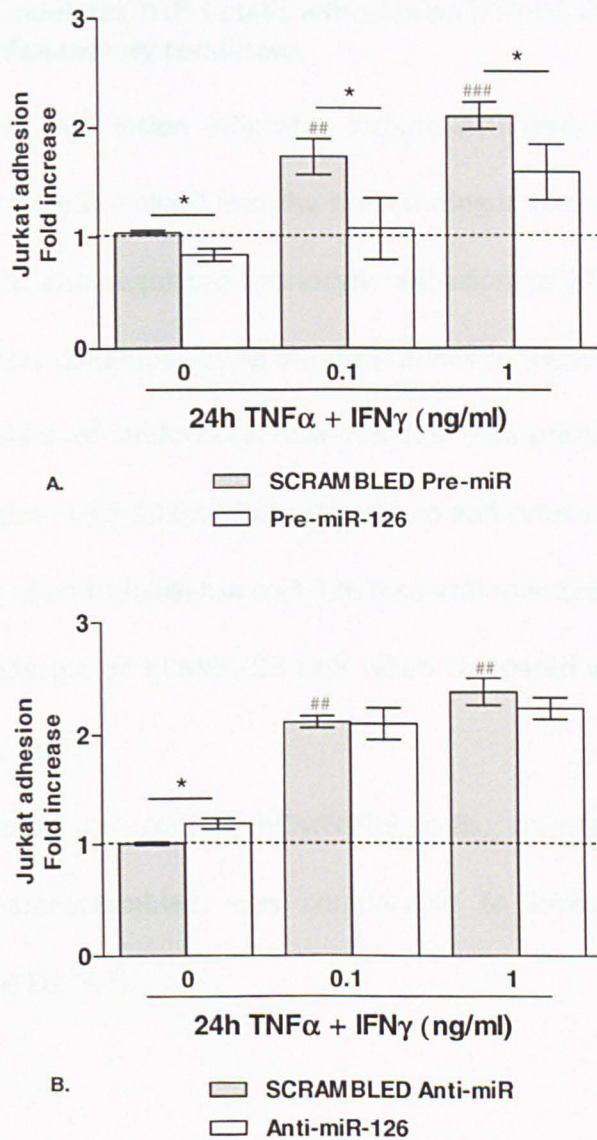
**Fig. 4.5: hsa-miR-126 modulates Jurkat (T cell) static adhesion on hCMEC/D3 cells.** hCMEC/D3 cells were transfected followed by treatment with a combination of cytokines (TNFα + IFNγ) at different doses (0.1, 1 ng/ml) for 24 h. Fluorescence of adhered Jurkat (T cell) is expressed as all conditions over scrambled unstimulated. **A.** Scrambled Pre-miR or Pre-miR-126 were used to transfect hCMEC/D3 cells **B.** Scrambled Anti-miR or Anti-miR-126 were used to transfect hCMEC/D3 cells. Experiments were carried out three times with six replicates. Data are mean ±SEM (*,$P<0.05$, ##$P<0.01$, # significantly different vs. unstimulated cells, * significantly different between scrambled and miR transfections).

### 4.3.6 Hsa-miR-126 modulates THP-1 static adhesion on hCMEC/D3 cells in both physiological and inflammatory conditions

As said above, MS lesion infiltrates include activated macrophages, which adhere and migrate from the blood into the brain during inflammation. We evaluated whether hsa-miR-126 also regulated monocytic adhesion to hCMEC/D3 cells under basal and inflammatory conditions using the static adhesion assay.

Increased levels of endothelial hsa-miR-126 (hsa-pre-miR-126) significantly reduced THP-1 adhesion by 5-10% on both stimulated and cytokine-treated EC (Fig. 4.6 A). Decreased levels of endothelial hsa-miR-126 (hsa-anti-miR-126) did not significantly affect monocytic adhesion on hCMEC/D3 cells when compared with the control (hsa-pre-scrambled) (Fig. 4.6 B).

THP-1 adhesion on control hCMEC/D3 cells, transfected with hsa-pre-scrambled or hsa-anti-scrambled, was comparable to Jurkat adhesion on non transfected cells (see Fig. 3.7).
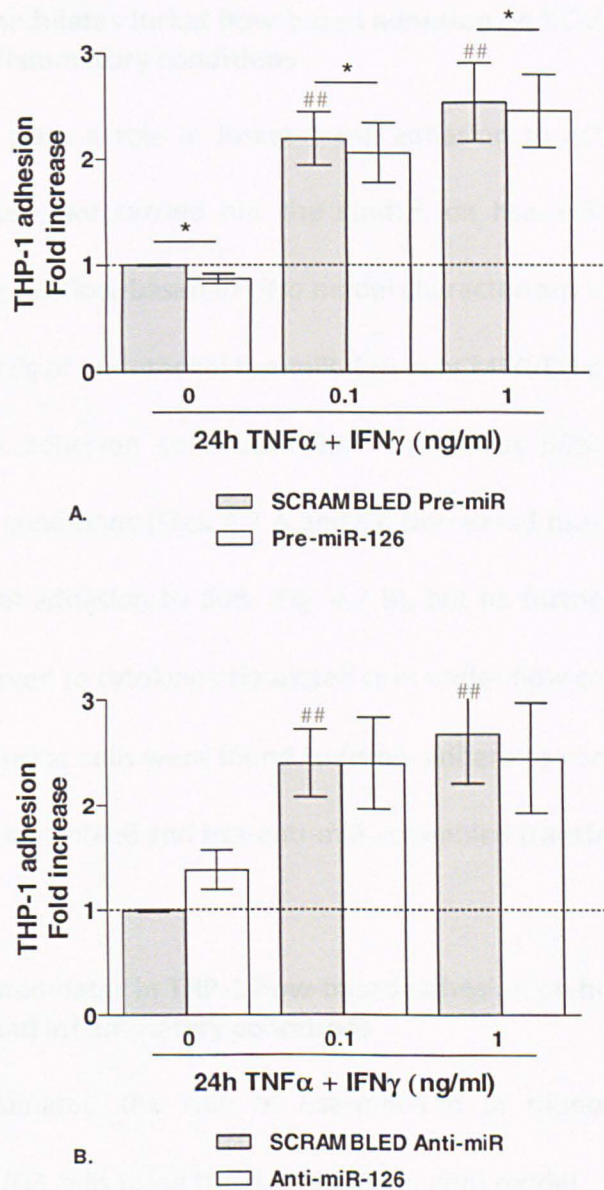
**Fig. 4.6: Hsa-miR-126 modulates THP-1 (monocyte) static adhesion to hCMEC/D3 cells.** hCMEC/D3 cells were transfected followed by treatment of combination of cytokines (TNFα + INFγ) at different doses (0, 0.1, 1 ng/ml) for 24h. Fluorescence of adhered THP-1 is expressed as all conditions over scrambled unstimulated. **A.** Scrambled Pre-miR or Pre-miR-126 were used to transfect hCMEC/D3 cells **B.** Scrambled Anti-miR or Anti-miR-126 were used to transfect hCMEC/D3 cells. Experiments were carried out eight and three times with six replicates, respectively. Data are mean ±SEM (*$P<0.05$, ##$P<0.01$, # significantly different vs. unstimulated cells, * significantly different between scrambled and miR transfections).

### 4.3.7 Hsa-miR-126 modulates Jurkat flow-based adhesion on hCMEC/D3 cells in both physiological and inflammatory conditions

Hsa-miR-126 plays a role in Jurkat T cell adhesion to hCMEC/D3 cells under static conditions. Here, we carried out the studies on hsa-miR-126 in a leukocyte adhesion assay using the flow-based *in vitro* model characterized in Chapter 3.

Increased levels of endothelial hsa-miR-126 in hCMEC/D3 cells prevented shear resistant Jurkat cell adhesion to endothelium by almost 50% in both basal and cytokine-stimulated conditions (Figs. 4.7 A and C). Decreased hsa-miR-126 levels in EC cells, increased Jurkat adhesion by 50% (Fig. 4.7 B), but no further increases in Jurkat adhesion were observed to cytokine-stimulated cells under flow conditions (Fig. 4.7 D). Similar numbers of Jurkat cells were found to firmly adhere to control hCMEC/D3 cells both in hsa-pre-miR-scrambled and hsa-anti-miR-scrambled transfected cells.

### 4.3.8 Hsa-miR-126 modulates in THP-1 flow-based adhesion on hCMEC/D3 cells in both physiological and inflammatory conditions

We also evaluated the role of hsa-miR-126 in monocyte shear-resistant adhesion on hCMEC/D3 cells using the flow-based *in vitro* model.

Increased levels of endothelial hsa-miR-126 in hCMEC/D3 cells prevented shear resistant adhesion of THP-1 cells to endothelium by almost 50% in both basal and cytokine-stimulated conditions (Figs. 4.8 A and C). Decreased endothelial hsa-miR-126 levels promoted monocyte adhesion by 50% (Fig. 4.8 B) and 20% (Fig. 4.8 D) to unstimulated and cytokine-stimulated hCMEC/D3 cells, respectively.
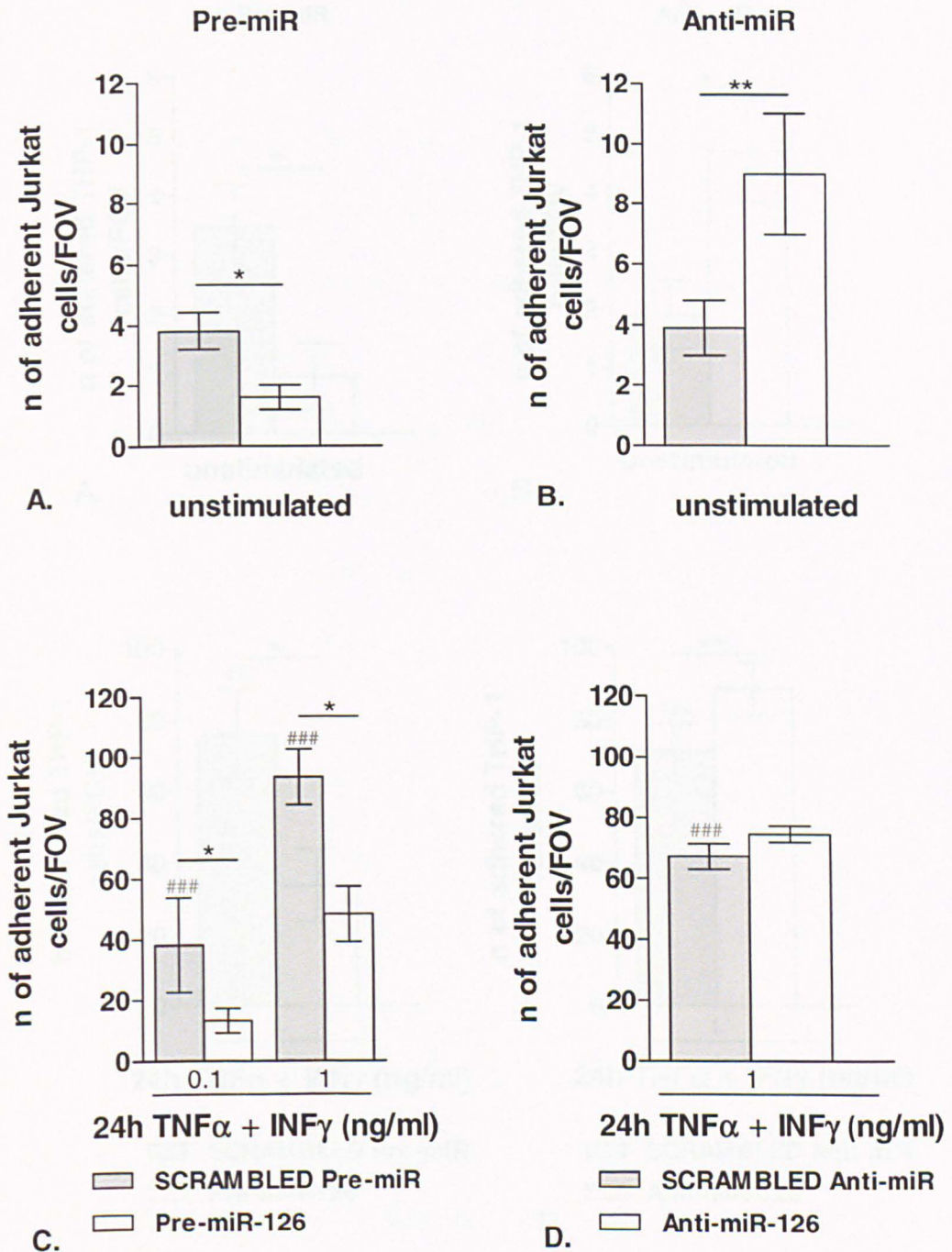
Fig. 4.7: hsa-miR-126 modulates Jurkat flow-based adhesion on hCMEC/D3 cells. hCMEC/D3 cells were transfected followed by treatment with a combination of cytokines at different doses (0, 0.1, 1 ng/ml) for 24 h. Jurkat cells adhered to the hCMEC/D3 cell monolayer were counted/field of view (FOV). A. and C. Scrambled Pre-miR or Pre-miR-126 were used to transfect hCMEC/D3 cells B. and D. Scrambled Anti-miR or Anti-miR-126 were used to transfect hCMEC/D3 cells. Experiments were carried out three to five times with five replicates. Data are mean ±SEM (*,$P<0.05$**$p<0.01$, ###$p<0.001$ # significantly different compared to unstimulated cells, * significantly different between scrambled and miR transfections).
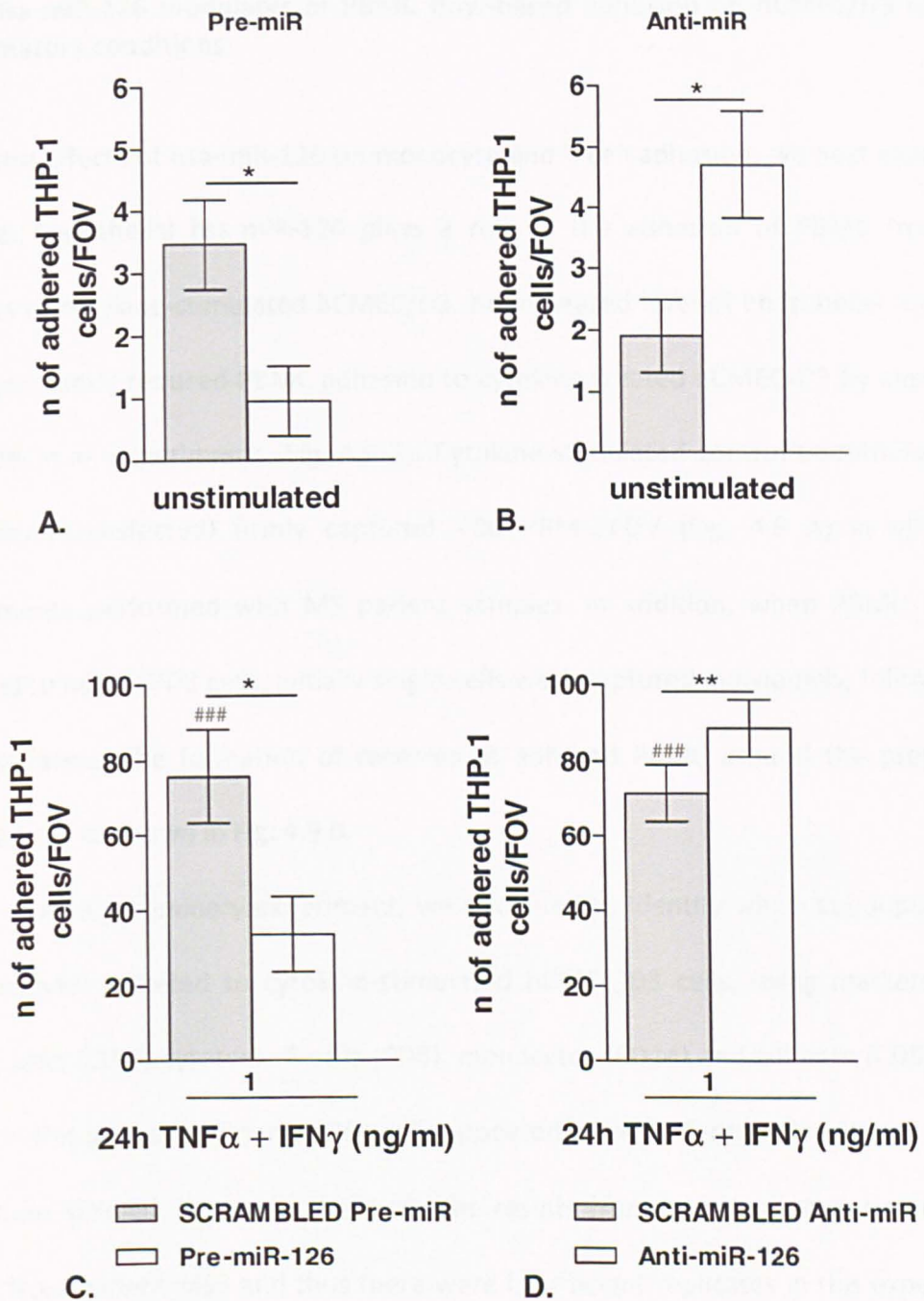
**Fig. 4.8: hsa-miR-126 modulates THP-1 (monocyte) flow-based adhesion on hCMEC/D3 cells.** hCMEC/D3 cells were transfected followed by treatment with a combination of cytokines for 24 h. Adhered THP-1 cells were counted/field of view (FOV). **A.** and **C.** Scrambled Pre-miR or Pre-miR-126 were used to transfect hCMEC/D3 cells. **B.** and **D.** Scrambled Anti-miR or Anti-miR-126 were used to transfect HCMEC/D3 cells Experiments were carried out three times with five replicates. Data are mean ±SEM (*,$P<0.05$, **$P<0.01$, ###$P<0.01$ # significantly different vs. unstimulated cells, * significantly different between scrambled and miR transfections).

### 4.3.9 Hsa-miR-126 modulates in PBMC flow-based adhesion on hCMEC/D3 cells in inflammatory conditions

Given the effects of hsa-miR-126 on monocyte and T cell adhesion, we next examined whether endothelial hsa-miR-126 plays a role in the adhesion of PBMC from MS patients to cytokine-stimulated hCMEC/D3. An increased level of endothelial hsa-miR-126 significantly reduced PBMC adhesion to cytokine-treated hCMEC/D3 by almost 40 and 50% in all experiments (Fig. 4.9 A). Cytokine-stimulated control endothelial cells (scrambled-transfected) firmly captured ~80 PBMC/FOV (Fig. 4.9 A) in all three experiments performed with MS patient samples. In addition, when PBMCs firmly adhered to hCMEC/D3 cells, initially single cells were captured individually, followed by in some areas, the formation of racemes of adhered PBMC around the previously adhered cell as shown in Fig. 4.9 B.

As a preliminary experiment, we also tried to identify which subpopulations of leukocytes adhered to cytokine-stimulated hCMEC/D3 cells, using markers for T helper cells (CD4), cytotoxic T cells (CD8), monocytes (CD14) and NK cells (CD56) (Fig. 4.11). In this pilot experiment, CD8+ cells appeared to be preferentially adherent in the conditions studied. However, these are the results from one single experiment with PBMC from patient MS3 and thus there were insufficient replicates in this experiment to draw firm conclusions.

At the same time the percentages of CD4, CD8, CD14 and CD56 subpopulations in the four PBMC samples were measured by FACS by Dr Laura Edwards (Hospital of Nottingham, UK)(Fig. 4.10). The results showed that all four subpopulations were present in the three samples in approximately the same proportion. Within each sample, the proportion of monocytes was much lower that of T cells and NK cells. In

addition, samples MS1 and MS3 contained a higher proportion of the subpopulations studied than sample MS2.



**A.**
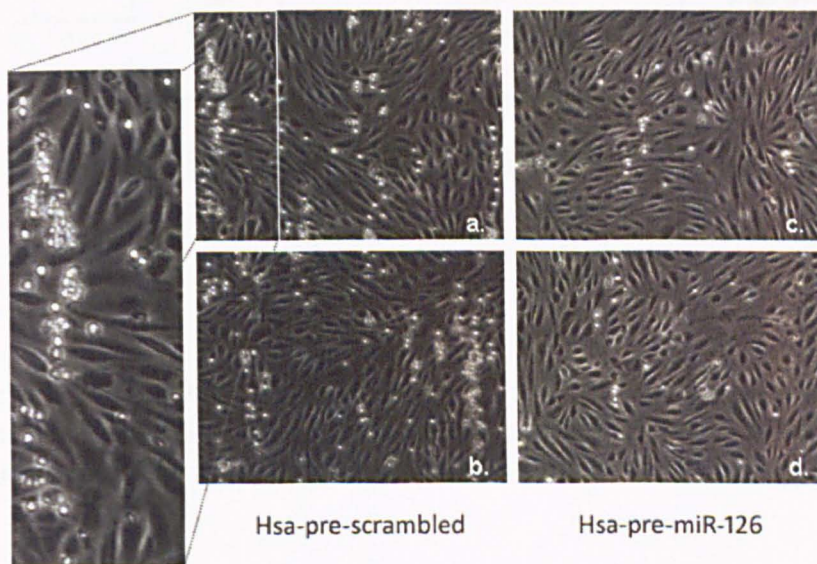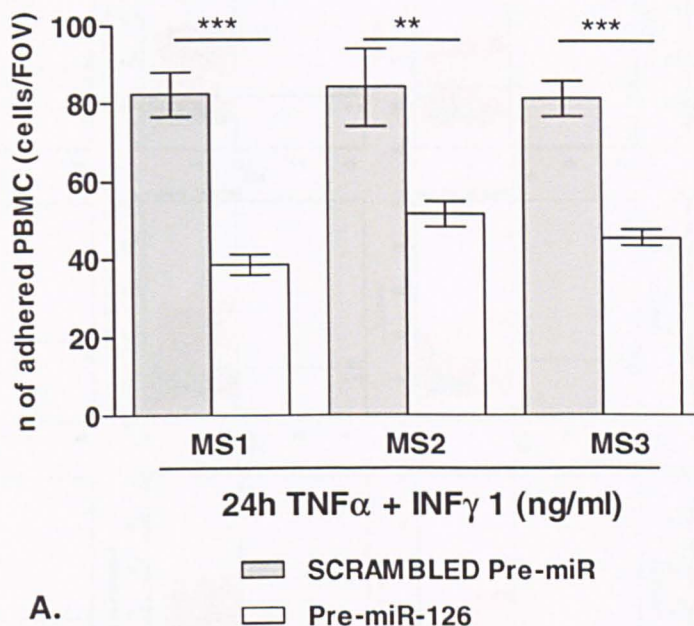


**B.**

**Fig. 4.9: Hsa-miR-126 regulates flow-based adhesion on hCMEC/D3 cells of PBMC from MS patients.** hCMEC/D3 cells were transfected followed by treatment with a combination of cytokines (TNFα + IFNγ) at 1 ng/ml for 24 h. **A.** Adhered PBMC to hCMEC/D3 cell monolayer were counted/field of view (FOV). **B.** Representative pictures of adhered PBMCs on cytokine-stimulated hCMEC/D3 cell monolayers transfected with hsa-pre-miR (c. and d.) or with hsa-pre-scrambled (a. and b.). Experiments were carried out two times with eight FOV. Data are mean ±SEM (***$P<0.001$, * significantly different between scrambled and miR transfections).
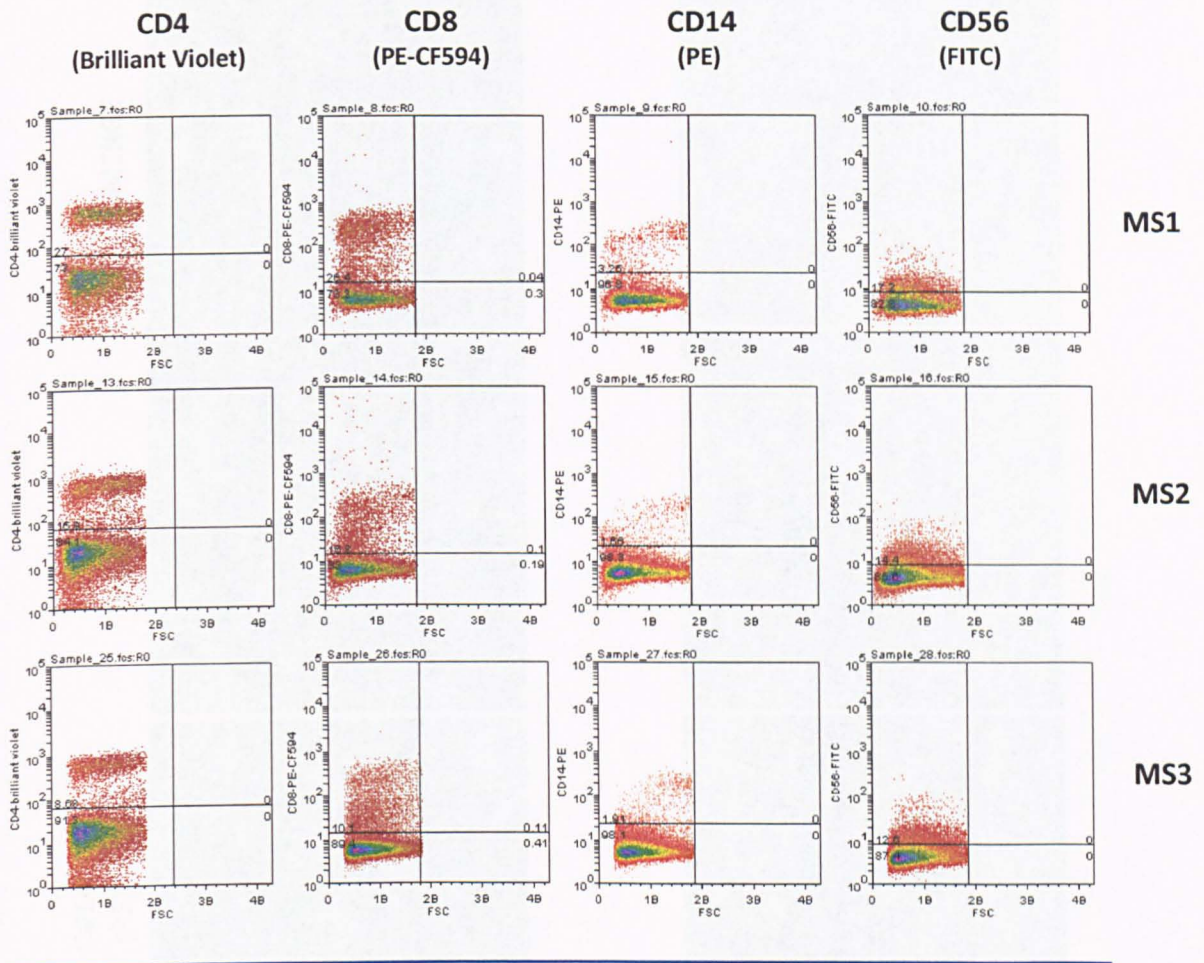
| SAMPLE | CD4+ | CD8+ | CD14+ | CD56+ |
|--------|------|------|-------|-------|
| MS1 | 27% | 26.4% | 3.25% | 17.2% |
| MS2 | 15.9% | 16.8% | 1.66% | 14.4% |
| MS3 | 8.69% | 10.1% | 1.91% | 12.6% |

**Fig. 4.10: Quantification of monocyte, T cell and NK (natural killer) cell subpopulations by FACS in MS patient PBMC (peripheral blood mononuclear cells) and percentages of CD4, CD8, CD14 and CD56 positive cells in the samples.**

**Fig. 4.11 (next page): Identification of monocyte, T cell and NK cell subpopulations in PBMC of MS patient 3 adhered to hCMEC/D3 cells by immunostaining. A.** hCMEC/D3 cells transfected with SCRAMBLED Pre-miR and stimulated with a combination of cytokines (TNFα + IFNγ) at 1 ng/ml and **B.** hCMEC/D3 cells transfected with Pre-miR-126 and stimulated with a combination of cytokines (TNFα + IFNγ) at 1 ng/ml. Bar - 100μm.
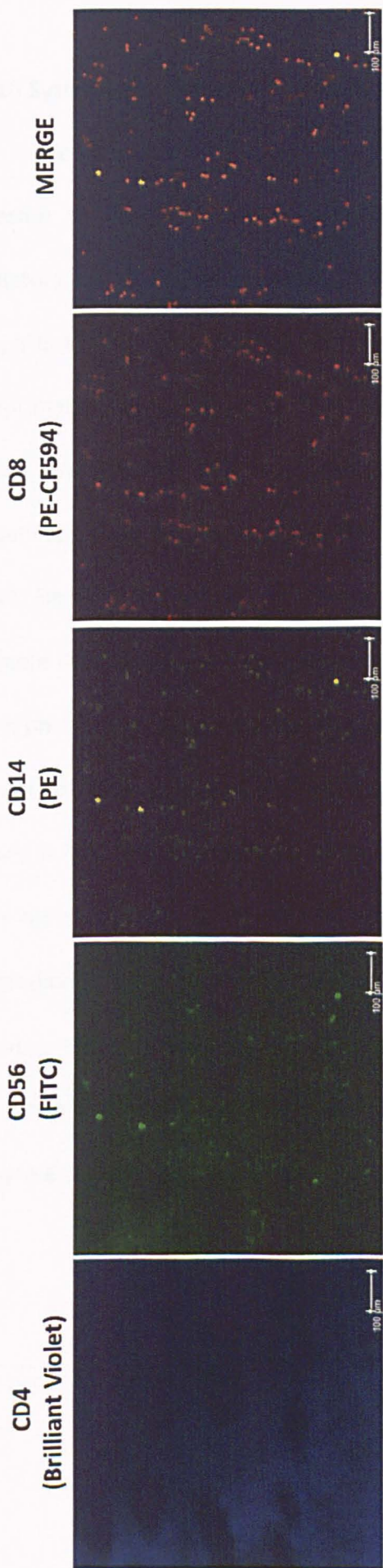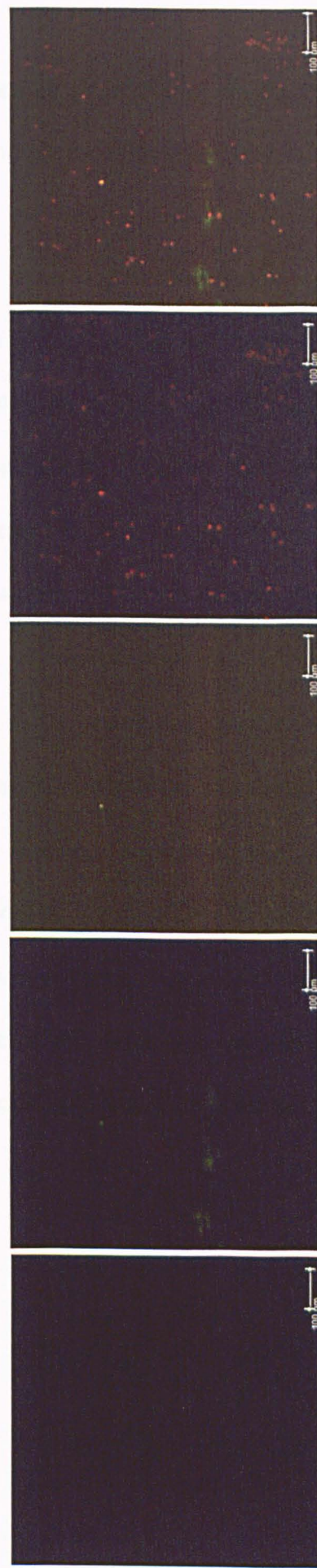
**4.3.10 Systematic collation of hsa-miR-126 predicted targets available on-line**

We observed that hsa-miR-126 plays a role in monocyte, T cell and PBMC adhesion to brain endothelial monolayers, but we do not know the molecular mediators for this observed biological response. Mature miRs sequences become competent following biogenesis to target mRNAs for decay or for translational arrest (Chedrimada 2007, Tjsterman 2004 and Pillai 2007). As described in Section 1.6.4, mRNAs are targeted by the mature miR by base-pairing between the miR seed sequence, nt 2-8 numbered from the 5'-end of the miR, and 3'-UTR of the target mRNA. Here, we systematically collated predicted targets of hsa-miR-126 using on-line available databases based on different algorithms, to predict target gene transcripts. Seven on-line available databases of predicted targets for hsa-miR-126 were consulted and the collated gene targets are listed according to database in alphabetic order (Tables 4.2 A, B and C). We found more than 900 predicted targets for hsa-miR-126 when Mirbase (Table 4.2 A) and Microcosm (Table 4.2 B) were used, while the number of predicted transcripts was hardly reduced when Target Scan, MicroRNA.org, DianaLab-Microt, DianaLab, Pictar, TargetMier and MirDB databases were used. We also listed the twenty predicted and validated hsa-miR-126 targets collected in the Tarbase 6.0 database.

# A.Mirbase

| 38596 | ATP9A | CALML4 | CRISP1 | F8A3 | GRAMD1A | IGSF9 | LOC731944 | NP_079413.3 | PEX5 | Q5TBN0_H | RGS6 | SMCHD1 | TMEM100 | WDR18 |
|---|---|---|---|---|---|---|---|---|---|---|---|---|---|---|
| A1L4H1_ | ATR | CAPN3 | CRKL | FAM104B | GRHL3 | IL13RA1 | LRCH4 | NP_115813.1 | PGM1 | Q5VYG3_H | RGS7 | SMF_H | TMEM126B | WDR37 |
| AAMP | B3GALTL | CAPN9 | CSHL1 | FAM108B1 | GRIA3 | IL17RC | LRRC24 | NP_612147.1 | PGR | Q658K6_H | RGS9 | SNX12 | TMEM161B | WDR49 |
| ABCA12 | BAD | CASK | CSNK1G3 | FAM110A | GRK4 | IL21R | LRRC36 | NP_612362.2 | PHACTR1 | Q694B2_H | RIT1 | SNX13 | TMEM165 | WDR70 |
| ABCB5 | BAG3 | CCDC11 | CSTB | FAM124B | GRM3 | IL31 | LRRC41 | NP_665806.1 | PHOSPHO1 | Q6IQ01_H | RLN3 | SOBP | TMEM178 | WDR8 |
| ABCC10 | BANP | CCDC18 | CTR9 | FAM130A2 | GSG1 | ILK | LRRIQ1 | NP_872380.1 | PHTF2 | Q6PJ53_H | RNF182 | SOX15 | TMEM39B | WIBG |
| ABCE1 | BARX1 | CCDC22 | CUTC | FAM22F | GTF2B | ING2 | LSM7 | NP_954697.1 | PIK3C3 | Q6UWI7_H | ROR2 | SOX17 | TMEM41B | WNT9A |
| ABI1 | BMP8A | CCDC39 | CXCL12 | FAM22G | HAS1 | ING4 | LTB | NP_981967.1 | PIK3R2 | Q6UXU7_H | RPAP1 | SOX2 | TMEM42 | WRNIP1 |
| ACOX2 | BNIPL | CCDC5 | CXCR4 | FAM26B | HBE1 | IRF2 | LUZP4 | NP_995324.1 | PIM3 | Q6ZRB0_H | RPL27A | SOX2 | TMEM69 | XR_016371.1 |
| ACPL2 | BRD1 | CCDC59 | CXorf26 | FAM33B | HCCS | IRF3 | LXN | NP_996778.1 | PIR | Q6ZRX0_H | RPRM | SOX30 | TMPRSS4 | XR_016371.1 |
| ACYP1 | BRUNOL5 | CCDC71 | CYB5R2 | FAM3B | HDAC6 | IRF5 | LYNX1 | NP_997254.2 | PITPNC1 | Q6ZS52_H | RPRML | SPAG11A | TNFRSF10B | XR_016371.1 |
| ADAM23 | BTBD2 | CCDC83 | CYSLTR1 | FAM49B | HDAC8 | IRS1 | MAGEE1 | NP_997260.1 | PKD2 | Q6ZSF8_H | RPS21 | SPAG11B | TNFRSF11B | XR_017795.1 |
| ADAM7 | BUB1B | CCL2 | DCBLD1 | FAP | HEATR1 | IRX2 | MAGI1 | NP_997306.1 | PKD2L2 | Q6ZUE1_H | RTKN | SPAG17 | TNFSF11 | XYLT1 |
| ADAMTS6 | BUD13 | CCNE2 | DCG13_ | FARP1 | HEATR1 | ISCU | MAGIX | NPAS4 | PLA2G7 | Q6ZUU1_H | RTN4R | SPP1 | TOMM7 | YIF1A |
| ADAMTS9 | C10orf18 | CCNL2 | DCST1 | FARP2 | HERC1 | ISOC2 | MAOB | NPAT | PLAC8L1 | Q6ZWB7_H | RUNX1 | SR140_H | TOR1AIP1 | YLPM1 |
| ADAMTSL2 | C10orf35 | CCR6 | DDX25 | FARSA | HERPUD1 | ITPR1 | MAP1S | NPC2 | PLCZ1 | Q8IXE7_H | RXFP1 | STAMBPL1 | TOX2 | ZADH2 |
| ADCK1 | C10orf68 | CCR8 | DDX27 | FBN2 | HES2 | KCNAB3 | MAPKAP1 | NPR2 | PLEKHG3 | Q8N962_H | RYR3 | STAU2 | TPD52L1 | ZC3H14 |
| ADM | C10orf92 | CCT2 | DDX5 | FBXO25 | HGSNAT | KCNQ4 | MARK3 | NR_003239.1 | PLK2 | Q8N9C2_H | SACM1L | STK38 | TPO | ZNF169 |
| AEBP1 | C10orf95 | CD207 | DEFB125 | FBXO7 | HIATL1 | KCTD13 | MATN4 | NR2C2 | PLOD2 | Q8NB26_H | SAE2 | STOML1 | TR112_H | ZNF169 |
| AFF4 | C10orf96 | CD72 | DENND2A | FCGR1A | HIF3A | KCTD4 | MBNL2 | NRSN1 | PLP2 | Q8TBD9_H | SAMD11 | STON1 | TRAV13-2 | ZNF212 |
| AFP | C11orf67 | CD84 | DEPDC4 | FCN1 | HIPK3 | KDELC1 | MCF2 | NSUN6 | PLXNB2 | Q8WUP8_H | SART1 | STX8 | TRAV41 | ZNF215 |
| AGPAT4 | C11orf9 | CD84 | DHH | FCRL5 | HIPK4 | KIAA0040 | MCM5 | NT5C1A | PMM1 | Q8WYG7_H | SAT1 | SUMO1P3 | TRGV1 | ZNF219 |
| AHNAK2 | C12orf41 | CD97 | DHX15 | FERD3L | HISPPD1 | KIAA0196 | MCOLN3 | NT5DC4 | PPAPDC3 | Q8WZ27_H | SATB1 | SUSD1 | TRGV8 | ZNF219 |
| AHSG | C14orf138 | CDC16 | DIAPH1 | FETUB | HIST1H2AK | KIAA0907 | MCTS1 | OGFOD2 | PPFIBP1 | Q96I54_H | SEC13 | SUSD4 | TRIM14 | ZNF219 |
| AKAP14 | C14orf145 | CDK3 | DJBP | FGFR2 | HIST1H3H | KIAA1305 | MDH1 | OPA3 | PPIE | Q96LR6_H | SEMA6D | SUV39H2 | TRIM3 | ZNF224 |
| AKAP5 | C14orf39 | CDKN2A | DLEU7 | FGFR2 | HLA-DRB1 | KIAA1546 | MDS1 | OPRM1 | PPM1D | Q96MU6-2 | SERAC1 | SUZ12 | TRIM67 | ZNF238 |
| ALG14 | C15orf21 | CDKN2AIP | DMGDH | FHAD1 | HLX1 | KIAA1751 | ME3 | OR10R3P | PPP1R16A | Q96NH1_H | SFRS11 | SYDE2 | TRIO | ZNF287 |
| ALS2CR2 | C15orf24 | CENTD1 | DNM1L | FKBP7 | HMGA2 | KIAA1751 | METTL6 | OR2M3 | PPP1R3B | Q9H385_H | SFRS7 | SYT8 | TRM6_H | ZNF365 |
| AMT | C16orf44 | CGRRF1 | DNM3 | FKBPL | HMOX2 | KIAA1946 | MICAL2 | OR4C3 | PQLC2 | Q9H8A7_H | SFTPG | TAF1 | TSGA2 | ZNF365 |
| AMY2B | C17orf68 | CHD1L | DNMT1 | FLCN | HNRPM | KIF13B | MPHOSPH6 | OR51B6 | PRELID1 | Q9HCM3_H | SGIP1 | TBCC | TSPY1_H | ZNF365 |
| ANAPC1 | C18orf18 | CHD5 | DOPEY1 | FOLH1 | HOP_H | KISS1R | MRPL43 | OR51J1 | PRICKLE1 | Q9NW00_H | SGK3 | TCEA3 | TSPYL2 | ZNF462 |
| ANAPC11 | C18orf34 | CHD6 | DPPA4 | FOXO3A | HORMAD1 | KLHL31 | MRPS26 | OR51S1 | PRKACG | Q9NYD3_H | SGK69_H | TCEAL3 | TTC6 | ZNF462 |
| ANGPTL6 | C1orf101 | CHGA | DSCR8 | FTCD | HOXD12 | KLHL4 | MT-CYB | OR5D16 | PRKCB1 | Q9P1G5_H | SGTA | TCEAL5 | TTN | ZNF462 |
| ANKIB1 | C1orf158 | CHMP4B | DSE | FUNDC1 | HP1BP3 | KLK14 | MUC17 | OR5T2 | PRKCD | Q9P1R7_H | SHB | TCEAL8 | TUBAL3 | ZNF536 |
| ANKRA2 | C1orf173 | CHST1 | DUSP27 | FUSIP1 | HPDL | KPNA1 | MYADML | OR8U1 | PRR8 | Q9Y2A2_H | SHH | TCF7L2 | TUBB2B | ZNF599 |
| ANKRD35 | C1orf201 | CHST9 | DUSP8 | FXR2 | HRAS | KR261_H | MYO1B | ORC6L | PRRG2 | Q9Y2I9_H | SHMT2 | TCN1 | TXNDC8 | ZNF613 |
| ANKRD41 | C1orf94 | CILP2 | DVL2 | GAL3ST2 | HRH3 | KRT84 | NANOS2 | OTC | PRRG3 | QDPR | SIPA1L2 | TCP11L2 | TXNL6 | ZNF645 |
| ANKRD44 | C1QC | CIZ1 | DYRK4 | GALNT11 | HS6ST2 | KRTAP19-3 | NAPB | PANK4 | PRTFDC1 | RAB26 | SKIL | TELO2 | TXNRD1 | ZNF650 |
| ANKRD9 | C1QL3 | CKMT2 | EDG3 | GALNTL4 | HSPA12B | KRTAP20-1 | NDUFB6 | PAPD1 | PRTN3 | RAI1 | SLC15A4 | TESC | TXNRD2 | ZNF673 |
| ANKS1A | C20orf26 | CLEC9A | EDG4 | GAP43 | HSPA1B | LARP6 | NFKBIA | PAQR9 | PRY_H | RAI14 | SLC16A8 | TFDP1 | U2AF2 | ZNF738 |
| ANKS1B | C20orf28 | CLPTM1 | EEF1A1 | GAPVD1 | HSPA4L | LATH_H | NIF3L1 | PARP1 | PSL2_H | RANBP3L | SLC1A5 | THAP4 | U773_H | ZNF75A |
| ANP32B | C20orf81 | CLUL1 | EGFL7 | GBA2 | HTR2C | LDHAL6B | NISCH | PARP10 | PSMAL_H | RARRES2 | SLC22A7 | THAP9 | UBE3C | ZNHIT2 |
| APOA4 | C2orf25 | CNTN6 | ELA3A | GCLC | HTR4 | LEO1 | NMI | PARP16 | PSMB9 | RASA2 | SLC24A3 | THOC7 | UBQLN2 | ZNHIT3 |
| ARID4B | C7orf10 | CNTNAP3 | ELL3 | GDF10 | IARS | LEO1 | NOB1 | PARP9 | PSMD5 | RASA3 | SLC26A6 | THSD4 | UBR1 | ZPBP2 |
| ARMCX1 | C7orf33 | CNTNAP4 | ELOVL5 | GFOD2 | ICAM4 | LEPR | NP_001001436.1 | PARVB | PTMA | RASD1 | SLC30A7 | THUMPD1 | UBTD1 | ZPBP2 |
| ARRB1 | C8orf48 | COL4A5 | EN1 | GJA7 | IDH2 | LOC285697 | NP_001004306.1 | PBXIP1 | PTPN21 | RASGEF1C | SLC39A6 | TIAL1 | USP54 | ZRSR1 |
| ATAD3A | C8orf58 | COQ4 | ENOX1 | GNL3 | IDH3G | LOC389844 | NP_001008739.1 | PCDH9 | PTPN9 | RASGRF2 | SLC43A1 | TIGD4 | USP7 | ZSCAN20 |
| ATF2 | C9orf131 | CORT | EPC1 | GNL3L | IDS | LOC390616 | NP_001013662.1 | PCDHB1 | PTPRB | RASSF2 | SLC6A4 | TIMELESS | UXS1 | ZSWIM2 |
| ATF3 | C9orf134 | COX4NB | EPS15L1 | GNRH1 | IFIT2 | LOC441490 | NP_001036038.1 | PCDHB11 | PTPRK | RBM3 | SLC6A9 | TLN2 | VAV1 | ZUBR1 |
| ATP11C | C9orf38 | CP21A_ | EPSTI1 | GOLPH3 | IFNA2 | LOC644994 | NP_001073990.1 | PCDHB2 | PTX3 | RBPJ | SLC7A3 | TLR10 | VCAM1 | |
| ATP1B1 | C9orf68 | CPO | ERBB3 | GON4L | IFT80 | LOC649587 | NP_001074013.1 | PCSK6 | Q15202_H | RER1 | SLC9A6 | TLR9 | VDAC2 | |
| ATP5D | C9orf78 | CR1L | ERV3 | GPR115 | IGFBP7 | LOC729574 | NP_057583.2 | PDCD2 | Q4VXZ3_H | RFC2 | SLCO5A1 | TM6SF1 | VEGFA | |
| ATP5J2 | CABLES1 | CREB5 | EZH2 | GPR151 | IGFBPL1 | LOC729903 | NP_061900.1 | PDGFA | Q5FWF1_H | RFX4 | SMAD6 | TM9SF2 | VPS36 | |
| ATP6AP2 | CACHD1 | CRH | F8A1 | GPR37 | IGKC | | NP_065945.1 | PDSS1 | Q5JQD4_H | RGS16 | SMARCA1 | TMED1 | VPS37D | |
| ATP6V1B1 | CACNA1D | CRIPAK | F8A2 | GPR39 | IGKV1-39 | | NP_078924.1 | PDZRN3 | Q5JST9_H | RGS3 | SMARCAL1 | TMED4 | VPS54 | |

# B.Microcosm

| A1L4H1_H | ATR | CAPN3 | CRKL | F8A2 | GRIA3 | IL21R | LRRC41 | NP_981967.1 | PIK3R2 | Q6UXU7_H | RPAP1 | SOX2 | TMEM42 | WIBG | WIBG |
|---|---|---|---|---|---|---|---|---|---|---|---|---|---|---|---|
| AAMP | B3GALTL | CAPN9 | CSHL1 | F8A3 | GRK4 | IL31 | LRRIQ1 | NP_995324.1 | PIM3 | Q6ZRB0_H | RPL27A | SOX30 | TMEM69 | WNT9A | WNT9A |
| ABCA12 | BAD | CASK | CSNK1G3 | FAM104B | GRM3 | ILK | LSM7 | NP_996778.1 | PIR | Q6ZRX0_H | RPRM | SPAG11A | TMPRSS4 | WRNIP1 | WRNIP1 |
| ABCB5 | BAG3 | CCDC11 | CSTB | FAM108B1 | GSG1 | ING3 | LTB | NP_997254.2 | PITPNC1 | Q6ZS52_H | RPRML | SPAG11B | TNFRSF10B | XR_016371.1 | XR_016371.1 |
| ABCE1 | BANP | CCDC18 | CTR9 | FAM110A | GTF2B | ING4 | LUZP4 | NP_997260.1 | PKD2 | Q6ZSF8_H | RPS21 | SPAG17 | TNFRSF11B | XR_017795.1 | XR_017795.1 |
| ABI1 | BARX1 | CCDC22 | CUTC | FAM130A2 | HAS1 | IRF2 | LXN | NP_997306.1 | PKD2L2 | Q6ZUE1_H | RTKN | SPP1 | TNFSF11 | XYLT1 | XYLT1 |
| ACOX2 | BMP8A | CCDC39 | CXCL12 | FAM22F | HBE1 | IRF3 | LYNX1 | NPAS4 | PLA2G7 | Q6ZUU1_H | RTN4R | SR140_H | TOMM7 | YIF1A | YIF1A |
| ACPL2 | BNIPL | CCDC5 | CXCR4 | FAM22G | HCCS | IRF5 | MAGEE1 | NPAT | PLAC8L1 | Q6ZWB7_H | RUNX1 | STAMBPL1 | TOR1AIP1 | YLPM1 | YLPM1 |
| ACYP1 | BRD1 | CCDC59 | CXorf26 | FAM33B | HDAC6 | IRS1 | MAGI1 | NPC2 | PLCZ1 | Q8IXE7_H | RXFP1 | STAU2 | TOX2 | ZADH2 | ZADH2 |
| ADAM23 | BRUNOL5 | CCDC71 | CXorf26 | FAM3B | HDAC8 | IRX2 | MAGIX | NPR2 | PLEKHG3 | Q8N962_H | RYR3 | STK38 | TPD52L1 | ZC3H14 | ZC3H14 |
| ADAM7 | BTBD2 | CCDC83 | CYB5R2 | FAM49B | HEATR1 | ISCU | MAOB | NR_003239.1 | PLK2 | Q8N9C2_H | SACM1L | STOML1 | TPO | ZNF169 | ZNF169 |
| ADAMTS6 | BUB1B | CCL2 | CYSLTR1 | FAP | HERC1 | ISOC2 | MAP1S | NR2C2 | PLOD2 | Q8NB26_H | SAE2 | STON1 | TR112_H | ZNF212 | ZNF212 |
| ADAMTS9 | BUD13 | CCNE2 | DCBLD1 | FARP1 | HERPUD1 | ITPR1 | MAPKAP1 | NRSN1 | PLP2 | Q8TBD9_H | SAMD11 | STX8 | TRAV13-2 | ZNF215 | ZNF215 |
| ADAMTSL2 | C10orf18 | CCNL2 | DCG13_H | FARP2 | HES2 | KCNAB3 | MARK3 | NSUN6 | PLXNB2 | Q8WUP8_H | SART1 | SUMO1P3 | TRAV41 | ZNF219 | ZNF219 |
| ADCK1 | C10orf35 | CCR6 | DCST1 | FARSA | HGSNAT | KCNQ4 | MATN4 | NT5C1A | PMM1 | Q8WYG7_H | SAT1 | SUSD3 | TRGV1 | ZNF224 | ZNF224 |
| ADM | C10orf68 | CCR8 | DDX25 | FBN2 | HIATL1 | KCTD13 | MBNL2 | NT5DC4 | PPAPDC3 | Q8WZ27_H | SATB1 | SUSD4 | TRGV8 | ZNF238 | ZNF238 |
| AEBP1 | C10orf92 | CCT2 | DDX27 | FBXO25 | HIF3A | KCTD4 | MCF2 | OGFOD2 | PPFIBP1 | Q96I54_H | SEC13 | SUV39H2 | TRIM14 | ZNF287 | ZNF287 |
| AFF4 | C10orf95 | CD207 | DDX5 | FBXO7 | HIPK3 | KDELC1 | MCM5 | OPRM1 | PPIE | Q96LR6_H | SEMA6D | SUZ12 | TRIM3 | ZNF365 | ZNF365 |
| AFP | C10orf96 | CD72 | DEFB125 | FCGR1A | HIPK4 | KIAA0040 | MCOLN3 | OR10R3P | PPM1D | Q96MU6-2 | SERAC1 | SYDE2 | TRIM67 | ZNF462 | ZNF462 |
| AGPAT4 | C11orf67 | CD84 | DENND2A | FCN1 | HISPPD1 | KIAA0196 | MCTS1 | OR2M3 | PPP1R16A | Q96NH1_H | SFRS11 | SYT8 | TRIO | ZNF536 | ZNF536 |
| AHNAK2 | C11orf9 | CD97 | DEPDC4 | FCRL5 | HIST1H2AK | KIAA0907 | MDH1 | OR4C3 | PPP1R3B | Q9H385_H | SFRS7 | SYT8 | TRM6_H | ZNF599 | ZNF599 |
| AHSG | C12orf41 | CDC16 | DHH | FERD3 | HIST1H3H | KIAA1305 | MDS1 | OR51B6 | PQLC2 | Q9H8A7_H | SFTPG | TAF1 | TSGA2 | ZNF613 |  |
| AKAP14 | C14orf138 | CDK3 | DHX15 | FETUB | HLA-DRB1 | KIAA1546 | ME3 | OR51J1 | PRELID1 | Q9HCM3_H | SGIP1 | TBCC | TSPY1_H | ZNF645 |  |
| AKAP5 | C14orf145 | CDKN2A | DIAPH1 | FGFR2 | HLX1 | KIAA1751 | METTL6 | OR51S1 | PRICKLE1 | Q9NW00_H | SGK3 | TCEA3 | TSPYL2 | ZNF650 |  |
| ALG14 | C14orf39 | CDKN2AIP | DJBP_H | FHAD1 | HMGA2 | KIAA1946 | MICAL2 | OR5D16 | PRKACG | Q9NYD3_H | SGK69_H | TCEA5 | TTC6 | ZNF673 |  |
| ALS2CR2 | C15orf21 | CENTD1 | DKN2A | FKBP7 | HMOX2 | KIF13B | MPHOSPH6 | OR5T2 | PRKCB1 | Q9P1G5_H | SGTA | TCEAL5 | TTN | ZNF738 |  |
| AMT | C15orf24 | CENTG1 | DLEU7 | FKBPL | HNRPM | KISS1R | MRPL43 | OR8U1 | PRKCD | Q9P1R7_H | SHB | TCEAL8 | TUBAL3 | ZNF75A |  |
| AMY2B | C16orf44 | CGRRF1 | DMGDH | FLCN | HOP_HUMAN | KLHL31 | MRPS26 | ORC6L | PRR8 | Q9Y2A2_H | SHH | TCF7L2 | TUBB2B | ZNHIT2 |  |
| ANAPC1 | C17orf68 | CHD1L | DNM1L | FOLH1 | HORMAD1 | KLHL4 | MT-CYB | OTC | PRRG3 | Q9Y2I9_H | SHMT2 | TCN1 | TXNDC8 | ZNHIT3 |  |
| ANAPC11 | C18orf18 | CHD5 | DNM3 | FOXO3A | HOXD12 | KLK14 | MUC17 | PANK4 | PRTFDC1 | QDPR | SIPA1L2 | TCP11L2 | TXNL6 | ZPBP2 |  |
| ANGPTL6 | C18orf34 | CHD6 | DNMT1 | FTCD | HP1BP3 | KPNA1 | MYADML | PAPD1 | PRTN3 | RAB26 | SKIL | TELO2 | U2AF2 | ZRSR1 |  |
| ANKIB1 | C1orf101 | CHGA | DOPEY1 | FUNDC1 | HPDL | KR261_H | MYO1B | PAQR9 | PRY_H | RAI1 | SLC15A4 | TESC | U773_H | ZSCAN20 |  |
| ANKRA2 | C1orf158 | CHMP4B | DPPA4 | FUSIP1 | HRAS | KRT84 | NANOS2 | PARP1 | PSL2_H | RAI14 | SLC16A8 | TFDP1 | UBE3C | ZSWIM2 |  |
| ANKRD35 | C1orf173 | CHST1 | DSCR8 | FXR2 | HRH3 | KRTAP19-3 | NAPB | PARP10 | PSMAL_H | RANBP3L | SLC1A5 | THAP4 | UBQLN2 | ZUBR1 |  |
| ANKRD41 | C1orf201 | CHST9 | DSE | GAL3ST2 | HS6ST2 | KRTAP20-1 | NDUFB6 | PARP16 | PSMB9 | RARRES2 | SLC24A3 | THAP9 | UBR1 |  |  |
| ANKRD44 | C1orf94 | CILP2 | DUSP27 | GALNT11 | HSPA12B | LARP6 | NFKBIA | PARP9 | PSMD5 | RASA2 | SLC26A6 | THOC7 | UBTD1 |  |  |
| ANKRD9 | C1QC | CIZ1 | DUSP8 | GALNTL4 | HSPA1B | LATH_H | NIF3L1 | PARVB | PTMA | RASA3 | SLC30A7 | THSD4 | USP54 |  |  |
| ANKS1A | C1QL3 | CKMT2 | DVL2 | GAP43 | HSPA4L | LDHAL6B | NP_001001436.1 | PAXIP1 | PTPN21 | RASD1 | SLC39A6 | THUMPD1 | USP7 |  |  |
| ANKS1B | C20orf26 | CLEC9A | DYRK4 | GAPVD1 | HTR2C | LEO1 | NP_001004306.1 |  | PTPN9 | RASGEF1C | SLC43A1 | TIAL1 | UXS1 |  |  |
| ANP32B | C20orf28 | CLPTM1 | EDG3 | GBA2 | HTR4 | LEPR | NP_001008739.1 |  | PTPRB | RASGRF2 | SLC6A4 | TIGD4 | VAV1 |  |  |
| APOA4 | C20orf85 | CLUL1 | EDG4 | GCLC | IARS | LOC285697 | NP_001013662.1 |  | PTPRK | RASSF2 | SLC6A9 | TIMELESS | VCAM1 |  |  |
| ARID4B | C2orf25 | CNTN6 | EEF1A1 | GDF10 | ICAM4 | LOC389844 | NP_001036038.1 |  | PTX3 | RBM3 | SLC7A3 | TLN2 | VCAM1 |  |  |
| ARMCX1 | C7orf10 | CNTNAP3 | EGFL7 | GFOD2 | IDH2 | LOC390616 | NP_001073990.1 |  | Q15202_H | RBPJ | SLC9A6 | TLR10 | VDAC2 |  |  |
| ARRB1 | C7orf33 | CNTNAP4 | ELA3A | GJA7 | IDH3G | LOC441490 | NP_001074013.1 |  | Q4VXZ3_H | RER1 | SLCO5A1 | TLR9 | VEGFA |  |  |
| ATAD3A | C8orf48 | COL4A5 | ELL3 | GNL3 | IDS | LOC644994 | NP_057583.2 |  | Q5FWF1_H | RFC2 | SMAD6 | TM6SF1 | VPS36 |  |  |
| ATF2 | C8orf58 | COQ4 | ELOVL5 | GNL3L | IFIT2 | LOC649587 | NP_061900.1 |  | Q5JQD4_H | RFX4 | SMARCA1 | TM6SF2 | VPS37D |  |  |
| ATF3 | C9orf131 | CORT | EN1 | GNRH1 | IFNA2 | LOC729574 | NP_065945.1 |  | Q5JST9_H | RGS16 | SMARCAL1 | TMED1 | VPS54 |  |  |
| ATP11C | C9orf134 | COX4NB | ENOX1 | GOLPH3 | IFT80 | LOC729574 | NP_078924.1 |  | Q5TBN0_H | RGS3 | SMCHD1 | TMEM100 | WDR18 |  |  |
| ATP1B1 | C9orf38 | CP21A_H | EPC1 | GON4L | IGFBP7 | LOC729903 | NP_079413.3 |  | Q5VYG3_H | RGS6 | SMF_H | TMEM126B | WDR37 |  |  |
| ATP5D | C9orf68 | CPO | EPS15L1 | GPR115 | IGFBPL1 | LOC730445 | NP_115813.1 |  | Q658K6_H | RGS7 | SNX12 | TMEM161B | WDR49 |  |  |
| ATP5J2 | C9orf78 | CR1L | EPSTI1 | GPR15 | IGKC | LOC731028 | NP_612147.1 |  | Q694B2_H | RGS9 | SNX13 | TMEM165 |  |  |  |
| ATP6AP2 | CABLES1 | CREB5 | ERBB3 | GPR37 | IGKV1-39 | LOC731944 | NP_612362.2 |  | Q6IQ01_H | RIT1 | SOBP |  |  |  |  |
| ATP6V1B1 | CACHD1 | CRH | ERV3 | GPR39 | IGSF9 | LRCH4 | NP_665806.1 |  | Q6PJ53_H | RLN3 | SOX15 |  |  |  |  |
| ATP9A | CACNA1D | CRIPAK | EZH2 | GRAMD1A | IL13RA1 | LRRC24 | NP_872380.1 |  |  | RNF182 |  |  |  |  |  |
|  | CALML4 | CRISP1 | F8A1 | GRHL3 | IL17RC | LRRC36 | NP_954697.1 |  |  |  |  |  |  |  |  |

**C.**

| TargetScanHuman 5.2 | | | Diana Lab Microt | PicTar | Target Miner | MiR DB |
|---|---|---|---|---|---|---|
| ADAM9 | IGF1R | RNF165 | ADAM9 | CARF | NM_000368 | PLXNB2 |
| AGAP2 | IGSF9B | RNF182 | AKAP13 | CRK | NM_018440 | |
| AGPAT3 | IL21R | RPL27A | B4GALT4 | FBXO33 | NM_021961 | |
| AIPL1 | IRS1 | SAMD12 | BAK1 | GOLPH3 | NM_030650 | |
| AKAP13 | IRS2 | SDC2 | BMP1 | HOXA9 | NM_144778 | |
| ALG10B | ITIH5 | SEMA4D | CAMSAP1 | IRS1 | NM_207304 | |
| AMMECR1L | KANK2 | SERPINB13 | CDKN2AIP | ITGA6 | | |
| ANTXR2 | KAZN | SLC12A3 | CRK | KIAA0934 | | |
| APOA5 | KBTBD8 | SLC15A4 | DIP2C | PHF15 | | |
| ARAP2 | KCMF1 | SLC41A2 | EGFL7 | PLK2 | | |
| ARL8A | KCNJ1 | SLC7A5 | FRS2 | PTPN9 | | |
| ARMCX1 | KIAA1456 | SLC7A8 | GOLPH3 | RGS3 | | |
| ARSA | KIAA1715 | SOX2 | HERPUD1 | SLC7A5 | | |
| ATG2B | KIAA1755 | SOX21 | IRS1 | SPRED1 | | |
| ATG7 | KLHL3 | SPG20 | ITGA6 | TOM1 | | |
| B4GALT4 | L2HGDH | SPON1 | KANK2 | | | |
| BCL2 | LARGE | SPRED1 | PHF15 | | | |
| BICD2 | LARP6 | SRSF11 | PLK2 | | | |
| C14orf184 | LPAR2 | STX12 | PLXNB2 | | | |
| C17orf51 | LRP6 | TELO2 | PTPN9 | | | |
| C1orf55 | LYNX1 | THAP6 | QDPR | | | |
| C2orf55 | MAGIX | TMEM132B | RGS3 | | | |
| C2orf69 | MAP3K13 | TMEM40 | RNF165 | | | |
| C5orf47 | MCTS1 | TNFRSF10 | SLC7A5 | | | |
| CAMSAP1 | MGEA5 | TOM1 | SPRED1 | | | |
| CDKN2AIP | MGRN1 | TRAF7 | TRAF7 | | | |
| CHST3 | MICAL3 | TRPC4AP | ZNF131 | | | |
| CHST6 | MMGT1 | TSC1 | ZNF219 | | | |
| CKMT2 | NFASC | TTC22 | | | | |
| CNKSR2 | NOS1 | UBE2Q1 | | | | |
| CNP | NR2F2 | UBQLN2 | | | | |
| CRK | NUAK1 | UNC119B | | | | |
| CTSB | OPA3 | VPS53 | | | | |
| CXorf23 | ORMDL3 | ZADH2 | | | | |
| DFFB | PARP16 | ZNF131 | | | | |
| DIP2C | PARVA | ZNF219 | | | | |
| EFHD2 | PBLD | ZNF470 | | | | |
| EGFL7 | PCDH7 | ZNF611 | | | | |
| EMILIN3 | PEX5 | ZNF709 | | | | |
| EP400 | PHF15 | ZNF784 | | | | |
| ERAP1 | PHF21B | ZNF813 | | | | |
| EVI5 | PHOSPHO1 | | | | | |
| F8A1 | PIK3CD | | | | | |
| FAM118A | PIK3R2 | | | | | |
| FBXL2 | PKD1L1 | | | | | |
| FBXO33 | PKD2 | | | | | |
| FERMT1 | PLA2G12A | | | | | |
| FOXO3 | PLK2 | | | | | |
| FRS2 | PLXNB2 | | | | | |
| GALNT12 | PMM1 | | | | | |
| GATAD2B | PPP3CB | | | | | |
| GNA13 | PTPN18 | | | | | |
| GOLPH3 | PTPN9 | | | | | |
| HEPACAM | QDPR | | | | | |
| HERPUD1 | RGS3 | | | | | |

**D.**

| TARBASE |
|---|
| **Mir DB** |
| CCNE2 |
| CRK |
| E2F1 |
| EGFL7 |
| HOXA9 |
| IRS1 |
| IRS-1 |
| p85beta |
| PIK3R2 |
| PLK2 |
| RGS3 |
| SLC45A3 |
| SOX2 |
| SPRED1 |
| TOM1 |
| TWF1 |
| TWF2 |
| VCAM1 |
| V-CRK |
| VEGFA |

**Table 4.2: Lists of hsa-miR-126 predicted targets (gene names) available on-line grouped by database and sorted in alphabetical order. A.** Mirbase database **B.** Microcosm database **C.** Target Scan, DianaLab Microt, Target Miner and MirDB databases. **D.** Tarbase 6.0, listed all experimentally validated hsa-miR-126 targets **A., B. and C.** List of all genes predicted as target of hsa-miR-126 or hsa-miR-126-3p.

## 4.3.11 Selection of hsa-miR-126 predicted target genes with a role in leukocyte trafficking

In order to select specific predicted hsa-miR-126 targets involved in leukocyte trafficking across hCMEC/D3 cells, we shortlisted all the predicted hsa-mir-126 targets involved in leukocyte rolling or adhesion from all seven databases (Table 4.2). In addition, we selected those genes that are expressed at the mRNA level under physiological and/or inflammatory conditions (Lopez-Ramirez MA, PhD thesis). CAM, selectins and chemokines are molecules produced, expressed and/or released by proinflammatory cytokine-stimulated EC, which promote leukocyte adhesion as described in Section 1.4.4.

HEPACAM (hepatocyte cells adhesion molecule), CCL2, CXCL12, CXCR4, ICAM4 and VCAM1 are predicted targets according to these criteria (Fig. 4.12). The HEPACAM gene encodes the HEPACAM protein which is an immunoglobulin-like cell adhesion molecule and its function is to modulate adhesion and migration in cancer (Zhang, Moh et al. 2010). ICAM-4 is mainly expressed by erythrocytes, promoting sickle red blood cell adhesion to the endothelium (Zennadi, Whalen et al. 2012). CCL2 and CXCL12 are two chemokines. CCL2 recruits monocytes, memory T cells, and dendritic cells to sites of inflammation while CXCL12 stimulates transmigration of CD4(+) and CD8(+) T cells, CD19(+) B cells, and CD14(+) monocytes across the BBB (Liu and Dorovini-Zis 2009; Man, Tucky et al. 2012). Moreover, Increased expression of CCL2 on cerebral endothelium followed by LPS or a combination of TNF-$\alpha$ and IFN-$\gamma$, but not IFN-$\gamma$ alone, suggests an important role for these chemokines in regulating the trafficking of inflammatory cells across the BBB in CNS inflammation (Liu and Dorovini-Zis 2012). VCAM1 is a well-studied adhesion molecule, which has been predicted as a

target for hsa-miR-126 and validated in HUVEC cells (Fig. 4.12 B), but no publications were found about VCAM1 as target of miR-126 in human brain endothelium. For these reasons we selected the VCAM1 and CCL2 genes to evaluate whether their regulation by mature hsa-miR-126 in hCMEC/D3 cells at the post-transcriptional level may be responsible for its role in modulation of leukocyte adhesion.

| Gene | Function | Database | Expression in hCMEC/D3 cells | Selected for further study |
|---|---|---|---|---|
| | | hsa-miR-126 | | |
| HEPACAM | Hepatic and glial cell adh mol | TARGETSCAN | yes | |
| CCL2 | Chemokine ligand 2 | MIRBASE - MICROCOSM | yes | √ |
| CXCL12 | Chemokine ligand 12 | MIRBASE - MICROCOSM | yes | |
| CXCR4 | Chemokine receptor 4 | MIRBASE - MICROCOSM | yes | |
| ICAM4 | Intercellular adhesion molecule 4 | MIRBASE - MICROCOSM | yes | |
| VCAM1 | Vascular adhesion molecule 1 | TARBASE | yes | √ |

**A.**
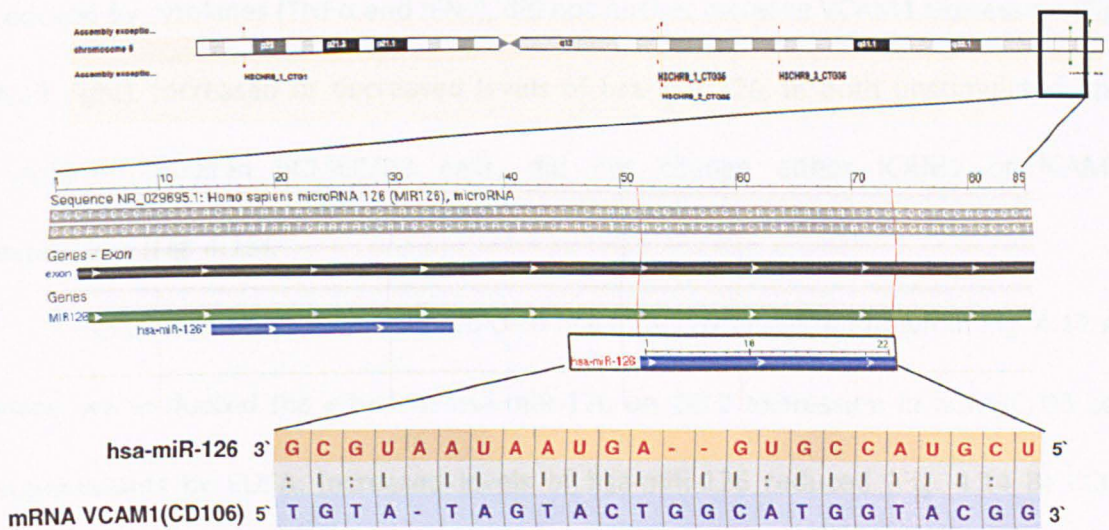


**B.**

**Fig. 4.12: VCAM1 and CCL2 are hsa-miR-126 predicted gene targets. A.** All the genes of proteins involved in leukocyte trafficking and expressed by hCMEC/D3 cells were selected from all predicted targets of hsa-miR-126 listed in Fig.4.11. Amongst these hsa-miR-126 targets, two were further selected as candidates to be further investigated - VCAM1 and CCL2 as the most likely candidates to regulate leukocyte adhesion to human brain endothelium. **B.** hsa-miR126 is partially complementary to a region in the VCAM1 mRNA 3'-UTR.

## 4.3.12 Hsa-miR-126 modulates VCAM1 and CCL2 expression in hCMEC/D3 cells

As shown in Chapter 3, VCAM1 was increased by combination of cytokines (TNFα + IFNγ) in hCMEC/D3 cells in a dose-dependent manner. Here, we evaluated the effect of hsa-miR-126 on VCAM1 expression on hCMEC/D3 cells by ELISA. Furthermore, we investigated whether ICAM1 and ICAM2 expression was affected by hsa-miR-126 by hCMEC/D3 cells, although they were not predicted targets of hsa-miR-126. Increased or decreased levels of hsa-miR-126 significantly reduced (Fig. 4.13 left) or enhanced (Fig. 4.13 right) VCAM1 expression at basal level by 30 % and 10%, respectively. When hCMEC/D3 cells were stimulated with a combination of cytokines (TNFα and IFNγ), VCAM1 was significantly reduced by almost 25% by pre-miR-126 (Fig. 4.13 right). However, further decreased hsa-miR-126 levels by anti-miR-126, already reduced by cytokines (TNFα and IFNγ), did not further increase VCAM1 expression (Fig. 4.13 right). Increased or decreased levels of hsa-miR-126, in both unstimulated and cytokine-stimulated hCMEC/D3 cells, did not change either ICAM1 or ICAM2 expression (Fig. 4.13).

CCL2 is another selected predicted hsa-miR-126 target as shown in Fig. 4.12 A. Here, we evaluated the effect of hsa-miR-126 on CCL2 expression in hCMEC/D3 cell supernatants by ELISA. Increased levels of hsa-miR-126 reduced (Fig. 4.14 B) CCL2 expression in cytokine-stimulated conditions, but no changes were detected in unstimulated cells (Fig. 4.14 A). Decreased levels of hsa-miR-126 did not result in any significant differences in CCL2 expression by hCMEC/D3 cells (Figs. 4.14 C and D right).
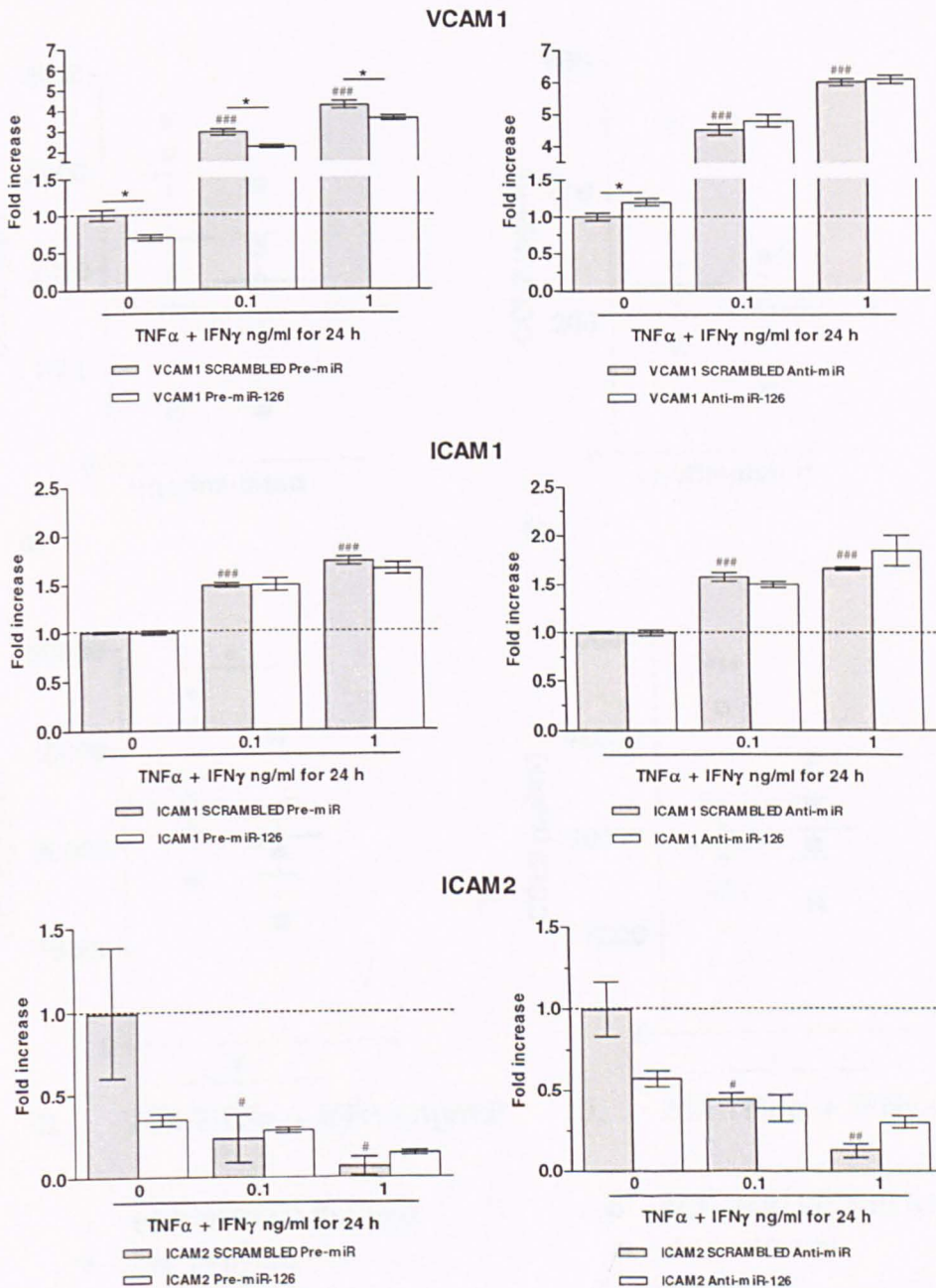
**Fig. 4.13: Hsa-miR-126 modulates VCAM1 expression in hCMEC/D3 cells in both basal and inflammatory conditions.** hCMEC/D3 cells were transfected with the indicated oligonucleotides followed by treatment with a combination of cytokines (TNFα + IFNγ) at different concentrations (0, 0.1 and 1 ng/ml) for 24 h. Anti-human-VCAM1, -ICAM1 and -ICAM2 monoclonal antibodies were used to detect VCAM1, ICAM1 and ICAM2 expression levels by ELISA. Experiments were carried out three times with three replicates. Data are mean ±SEM (*,#$p<0.05$, ##$p<0.01$, ###$p<0.001$, # significantly different vs. unstimulated cells, * significantly different between scrambled and miR transfections).
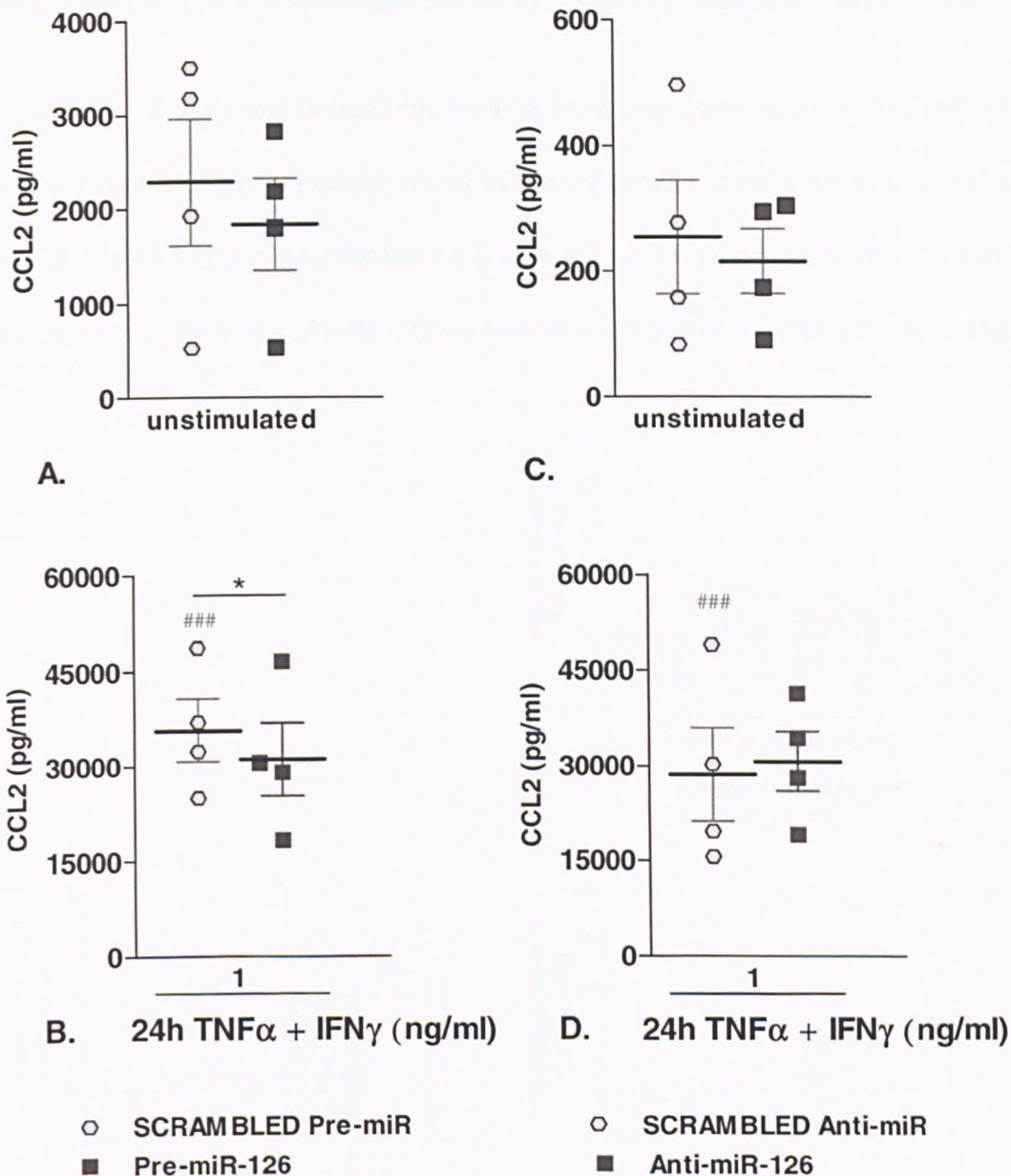
**Fig. 4.14: Hsa-miR-126 modulates CCL2 expression in hCMEC/D3 cells in inflammatory conditions.** hCMEC/D3 cells were transfected with the indicated oligonucleotides followed by treatment with a combination of cytokines (TNFα + IFNγ) at different concentrations (0 and 1 ng/ml) for 24 h. Anti-human-CCL2 monoclonal antibodies were used to detect CCL2 expression levels by sandwich ELISA. Experiments were carried out four times with three replicates. Data are mean ±SEM (*$p<0.05$, ###$p<0.001$, # significantly different vs. unstimulated cells, * significantly different between scrambled and miR transfections).

### 4.3.13 Hsa-miR-126 does not modulate E- and P-selectin expression in hCMEC/D3 cells

In view of their role in leukocyte rolling, here we tested whether hsa-miR-126 regulated E-and P-selectin expression on EC, even though they were not predicted targets of hsa-miR-126 in any databases (Table 4.2). No changes in E- or P- selectin were observed when levels of miR-126 were either increased or decreased (Fig. 4.15).
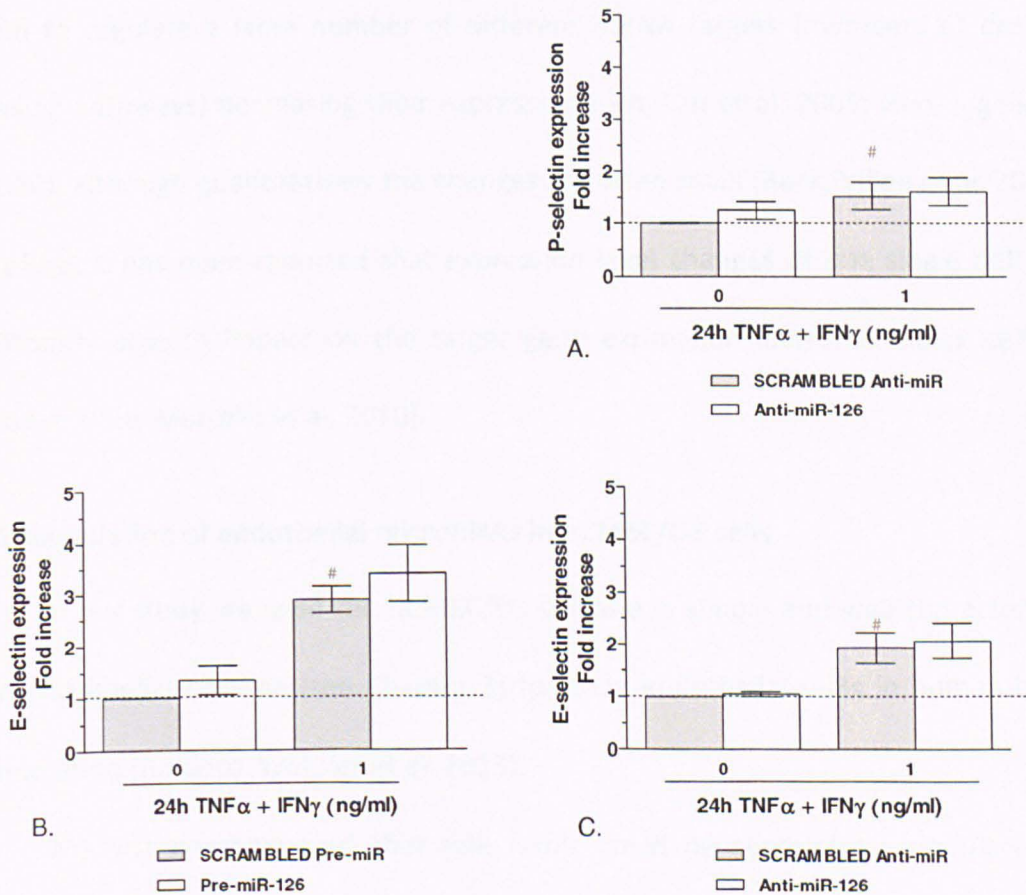


**Fig. 4.15: Hsa-miR-126 does not modulate E- or P-selectin expression in hCMEC/D3 cells under basal or inflammatory conditions.** hCMEC/D3 cells were transfected with the indicated oligonucleotides followed by treatment with a combination of cytokines (TNFα + IFNγ) at different concentrations (0 and 1 ng/ml) for 24 h. **B** and **C** Anti-human-E-selectin and **A** P-selectin monoclonal antibodies were used to detect E- and P-selectin expression levels by ELISA. Experiments were carried out three times with three replicates. Data are mean ±SEM. ($^{\#}p<0.05$, $^{\#}$ significantly different vs. unstimulated cells).

## 4.4 Discussion

Leukocyte adhesion at the BBB level is believed to be a critical step in leukocyte extravasation that characterizes neuroinflammatory diseases. Recently, miRs have been shown to regulate multiple aspects of endothelial biology, including inflammation, vascular disease and autoimmunity (Dai and Ahmed 2011 ; Urbich, Kuehbacher et al. 2008; Qin, Yang et al. 2012; Schroen and Heymans 2012). MiRs are known to regulate a large number of different mRNA targets (members of distinct signalling pathways) decreasing their expression (Lim, Lau et al. 2005; Guo, Ingolia et al. 2010), although quantitatively the changes are often small (Baek, Villen et al. 2008). Therefore, it has been reported that expression level changes of one single miR are significantly able to impact on the target gene expression and/or complex cellular processes (Inui, Martello et al. 2010).

### 4.4.1 Modulation of endothelial microRNAs in hCMEC/D3 cells

In our study we used the hCMEC/D3 cell line, a simple and well characterised brain endothelial cell line (see Chapter 3) to study endothelial miRs in human brain inflammation (Romero, Weksler et al. 2013).

We first demonstrated that miR levels could be successfully modulated in hCMEC/D3 cells, by transient transfection of either miR inhibitors or precursors, following specific times and reagent doses adapted from the supplier's protocol. When incubation times suggested by the manufacturer's protocol were used, we observed a low cytotoxic effects with the Lipofectamine® 2000 reagent (not shown), possibly due to the high sensitivity to cationic liposomes of this cell line. For this reason, we used the experimental timeline depicted in Section 2.6. Another issue was to obtain a high

transfection efficiency suitable for the experimental assay (>80%). For this purpose, we adopted different reagents to transfect anti- and pre-miR, Lipofectamine and Siport, respectively, with different transfection efficiencies perhaps due to the different oligonucleotide size and/or shape of these miR modulators.

### 4.4.2 Deregulation of hsa-miR-126 in endothelium

Brain endothelial hsa-miR-126 is down-regulated in cytokine-stimulated hCMEC/D3 cells at 24 h post stimulation. MiR-126 has been described as an important player in inflammation and in particular in vascular inflammation. When this project started, only Harris at al. had reported that miR-126 was involved in vascular inflammation in HUVEC cells, in particular in the modulation of neutrophil adhesion to these endothelial cells (Harris, Yamakuchi et al. 2008). Since then, miR-126 has been proved to be involved in inflammation in mouse kidney microvasculature (Asgeirsdottir, van Solingen et al. 2012), airway tissue (Collison, Herbert et al. 2011) and in human aortic EC (Kin, Miyagawa et al. 2012, Rippe, Blimline et al. 2012), in HUVEC (Dentelli, Rosso et al. 2010), colonic epithelial cells (Wu, Zikusoka et al. 2008), adipocytes (Arner, Mejhert et al. 2012) and circulating blood as marker for cardiovascular diseases, such as coronary artery disease and myocardial infarction (Fichtlscherer, De Rosa et al. 2010; Zampetaki, Willeit et al. 2012). Our data are in accordance with previous studies showing that hsa-miR-126 is reduced by cytokines (TNFα) in HUVEC (Harris, Yamakuchi et al. 2008) and in coronary artery disease, type 2 diabetes (Zampetaki, Kiechl et al. 2010) and other inflammatory and/or autoimmune diseases triggered by pro-inflammatory cytokines such as TNF-α, IL-6, IL-3 and chamokines such as CCL2 (Suarez, Wang et al. 2010). However, this is not the case for

other immune-related conditions since in airway tissue miR-126 was found increased during chronic asthma (Collison, Herbert et al. 2011).

In the context of the MS, miR-126 is decreased in peripheral blood of MS patients (Cox, Cairns et al. 2010) while it appears to be up-regulated in inactive MS lesions (Junker, Krumbholz et al. 2009). It is well known that in MS cerebral white matter there is an increase in blood vessel density and EC proliferation (Holley 2010, Zhong, Li et al. 2012), for this reason we can speculate that miR-126 was found increased because there were an increased vessel density due to angiogenesis, not because there was an actual up-regulation of miR levels within each EC. In addition, it has been reported that also CD4+ T cells express miR-126 (Zhao, Wang et al. 2011), then the miR-126 up-regulation in inactive MS lesions can be due to the increase of infiltrated T cells although leukocyte activation within these lesions is minimal. An alternative explanation involves an increase in miR-126 levels exclusively in blood vessels without perivascular infiltrates. In any case these observations imply that miR-126 is an important regulator in the early stage and in the chronic phase of inflammation, but possibly playing different roles within each phase.

### 4.4.3 Role of endothelial hsa-miR-126 in leukocyte adhesion

The role of brain endothelial hsa-miR-126 has not been described in leukocyte adhesion to human CNS endothelium before. We demonstrated that hsa-miR-126 is involved in the regulation of Jurkat and THP-1 adhesion to a human immortalized BEC line. Previously, it has been shown that increased levels hsa-miR-126 in HUVEC prevented HL-60 (human promyelocytic cell line) adhesion (Harris, Yamakuchi et al. 2008). In cancer, a high level of hsa-miR-126 in human microvascular endothelial cells

170

has been shown to prevent primary human bronchial epithelial cell adhesion, migration and invasion (Crawford, Brawner et al. 2008). As a result, endothelial miR-126 has been defined to play a dual role as a metastatic suppressor and a tumour suppressor in breast cancer, by reducing adhesion and migration of MDA-MB-231 breast cancer cells towards mouse lung epithelium *in vitro* and *in vivo* (Li, Shen et al. 2009; Png, Halberg et al. 2012).

We have detected changes in leukocyte adhesion due to modulation of hsa-miR-126 in hCMEC/D3 cells using static conditions (described in Chapter 3). However we did not measured by real time PCR the miR-126 increase in hCMEC/D3 cells by pre-miR-126 transfection, Dr. Lopez and Dr. Wu detected by $RT^2$-PCR an increase of miR expression by thousand times following pre-miR trasfection (personal communication). We used a flow-based *in vitro* model (characterised in Chapter 3) to increase the sensitivity of the leukocyte adhesion assay, to observe small changes in adhesion due to modulation of miR levels and to mimic the characteristic shear stress that occurs *in vivo*. Therefore, the flow-based assay revealed changes in adhesion due to the endothelial hsa-miR-126, which were not detectable using the static assay. We presented for the first time an *in vitro* system to study leukocyte trafficking under flow, where brain endothelial miRs are modulated exogenously.

### 4.4.4 Hsa-miR-126 plays a significant role in leukocyte adhesion on unstimulated brain endothelium

Taking into account the observation that in cytokine-stimulated hCMEC/D3 cells hsa-miR-126 is down-regulated, decreased hsa-miR-126 levels, to simulate the cytokines effect, in resting hCMEC/D3 cells led to increased adhesion of both T cells and monocytes and to increased endothelial VCAM1 basal expression, but not P- or E-

selectin nor CCL2 and ICAM1. Furthermore, we reported for the first time that increasing hsa-miR-126 levels prevented T cell and monocyte adhesion to resting hCMEC/D3 cells and reduced basal VCAM1 expression, but not ICAM1, CCL2 and E-selectin.

VCAM1 has been shown to be a hsa-miR-126 target in non-brain endothelial cells (Harris, Yamakuchi et al. 2008). Our observation that VCAM1 expression is modulated in BEC by hsa-miR-126 is in accordance with previous studies on HUVEC and hematopoietic stem/progenitor cells (Salvucci, Jiang et al. 2012; Harris, Yamakuchi et al. 2008). These findings suggest that hsa-miR-126 may be involved in leukocyte adhesion to endothelium, by modulating VCAM1, but probably not in rolling which mainly occurs via E-selectin (Sperandio, Pickard et al. 2006). This is in accordance with another previous study reporting that E-selectin is not regulated by hsa-miR-126 in renal microvasculature (Asgeirsdottir, van Solingen et al. 2012). However, miR-126-mediated modulation of leukocyte adhesion could be due to other molecules involved in rolling and adhesion such as chemokines and CAM not studied here, that can be direct (Fig. 4.12) or indirect targets of hsa-miR-126. hCMEC/D3 cells, in addition to VCAM1, CCL2 and selectins, express ALCAM (activated leukocyte cell adhesion molecule), ICAM1-5, MADCAM1 (mucosal vascular addressin cell adhesion molecule 1) and PECAM1 adhesion molecules known to be involved in the early step on leukocyte trafficking (Ley, Laudanna et al. 2007).

Chemokines CCL3-5, -17, -19-21 and -22, CXCL9, -10 and -12, CX3CL1 and CXCR3 and -4 receptors, which trigger lymphocyte adhesion to brain endothelium (Piali, Weber et al. 1998; Matsumiya, Ota et al. 2010)(see for reviews (Laudanna, Kim et al. 2002; Charo and Ransohoff 2006; Constantin 2008), are all expressed by hCMEC/D3

cells and up-regulated by cytokines (http://www.ncbi.nlm.nih.gov/projects/geo /query/acc.cgi?acc=GSE44694). Both CXCR4 and its ligand CXCL12 (SDF-1) were putative targets for miR-126 and their regulation/expression play a critical role in CD4+ and CD8+ T cell adhesion to and migration across human BEC (Liu and Dorovini-Zis 2009). In addition, it has been proposed that miRs can control signal transduction, targeting signalling pathway components, thereby potentially regulating indirectly the expression of endothelial cell surface molecules involved in leukocyte adhesion (Inui, Martello et al.2010). Indeed, it has been shown that Spred1 is a direct target of miR-126 (Fish, Santoro et al. 2008), and it is a protein phosphorylated by tyrosine kinases upstream of the signalling cascade of NF-κB, JNK and ERK (Mennicken, Maki et al. 1999; Phoenix and Temple 2010; Meng, Cao et al. 2012). NF-κB and JNK are known transcription factors for E-selectin and CAM (VCAM1 and ICAM1) (Meager 1999; Zhong, Li et al. 2012) and therefore the expression of these CAM may be indirectly affected by modulation of endothelial miR-126 levels, either promoting or repressing their levels through directly targeting Spred1. However, we did not observed any change in E-selectin expression at 24 h due to miR-126, in addiction Spred1 has been considered to be involved mainly in angiogenesis and vascular remodelling but not in leukocyte adhesion to endothelium.

MiR-126 gene targets may be targeted by other miRs expressed by the cell (see Reijekerk et al 2013 for a full list of miRs, which expression was changed by cytokines in human brain endothelium) that can also affect the expression of molecules involved in adhesion acting positively or negatively on pathways related to adhesion. For example VCAM1 is targeted by other 33 miRs in addition to miR-126 in Homo sapiens (http://www.ebi.ac.uk/enright-srv/microcosm/cgi-bin/targets/v5/      detail_view.pl?

transcript_id=ENST00000294728). Finally, it has been shown that shear stress can modulate miR and gene expression in endothelium (Chapter 1), but since our experimental setup is mainly based on static conditions, it is debatable whether five minutes of 0.5 dyn/cm$^2$ flow to study leukocyte adhesion, could influence the endothelium in such a way to change expression of CAM and chemokines. Indeed, the earliest observable changes in cell surface molecule expression such as VCAM1 in cultured mouse endothelium subject to shear stress appeared at 1 h after applied flow (Ohtsuka, Ando et al. 1993).

Modulation of leukocyte adhesion by hsa-miR-126 under basal conditions may also indicate a role for this miR in immunosurveillance mainly (but not exclusively) via interactions between endothelial VCAM1 and its cognate integrin on leukocytes (VLA-4), which have been implicated in leukocyte adhesion to brain endothelium of healthy individuals (Kleine and Benes 2006).

### 4.4.5 Effect of miR-126 on leukocyte adhesion to cytokine-activated brain endothelium

In cytokine-treated hCMEC/D3 cells, sustained levels of hsa-miR-126 prevented T cell, monocyte and PBMC adhesion to hCMEC/D3 cells and this effect was associated with decreased VCAM1 and CCL2, but not E-selectin, levels.

These findings are in line with the literature reporting the hsa-miR-126 modulates VCAM1 and CCL2 expression by directly binding to the 3`UTR of VCAM1 (Harris, Yamakuchi et al. 2008) and CCL2 (Arner, Mejhert et al. 2012; Zhang, Yang et al. 2013) mRNAs in mesenchymal stem cells and adipocites. Our study further demonstrates that these two important leukocyte adhesion-regulating molecules appear to be targets for miR-126 in human BEC. In addition, we have shown almost

50% decrease in PBMC adhesion in cytokine-stimulated BEC. Indeed, the inhibitory effect of miR-126 on adhesion of PBMC from MS patients appeared to be greater than that observed with leukocytic cell lines. In addition, most of the adhered PBMC appeared to be CD8+ T cells, corroborating the observations that in RRMS patients, where there was a selective increase of infiltrated CD8+ T cells compared to CD4+ T cells (Battistini, Piccio et al. 2003). These findings are promising for future *in vivo* or more complex *ex vivo* tests. However, further studies will still be required to understand the complex molecular mechanisms of miR-126 in relation to leukocyte trafficking.

Further decreases of hsa-miR-126 induced by pro-inflammatory cytokines, induced further increases in monocytic adhesion, but not in T cell adhesion and VCAM1, ICAM1, P- and E- selectin, CCL2 expression to and by endothelium. Monocytes and T cells express different integrins (Meager 1999; Pribila, Quale et al. 2004) and adhere/extravasate at different times due to differential chemokines expression to different adhesion molecules expressed by the endothelium in inflammatory conditions (Yonekawa and Harlan 2005). Thus the differences observed between T cell and monocyte adhesion could depend on selectins and/or CAM and/or chemokines expression by hCMEC/D3 cells, therefore we were not able to observe further increase in T cells adhesion.

## 4.5 Conclusions

Here, we report that human brain endothelial miR-126 regulates leukocyte adhesion to the human brain endothelium *in vitro* by a mechanism possibly involving thought its targets VCAM1 and CCL2.

## Chapter 5: The role of endothelial hsa-miR 126*
## in leukocyte adhesion to human brain endothelium

## 5.1 Introduction

The miR* species are not as well studied as the leading miR species, but in recent years research in the field of miRs has started to unravel the role of miR*s in post-trascriptional regulation of gene expression. In particular, many studies have examined whether miR*s are conserved across different species (Okamura, Phillips et al. 2008). It has also been shown that miR* species play an important role in inflammation. For example, miR-155* is the most induced miR in cytokine-activated astrocytes and it shares a proinflammatory function with miR-155 (Tarassishin, Loudig et al. 2011). In addition, miR-27a* and -27b* were also found to be involved in inflammation through modulation of the NK-κB pathway in macrophages (Thulasingam, Massilamany et al. 2011; Cheng, Kuang et al. 2012).

At the beginning of this part of the project aimed at investigating the role of hsa-miR-126* in leukocyte adhesion to brain endothelial cells, only three publications had been published on the subject. miR-126* has been studied by different groups focused on erythropoiesis (Huang, Gschweng et al. 2011), cancer cell motility (Meister and Schmidt 2010) and prostate cancer (Musiyenko, Bitko et al. 2008). Subsequently, two studies on miR-126* have been published. Zhang et al. recently found that in breast cancer epithelial cells miR-126* is down-regulated and promotes monocyte recruitment through increased level production of miR-126*'s targets Sdf-1a (CXCL12) (Zhang, Yang et al. 2013), a chemokine known to mediate monocyte recruitment. Felli

et al. reported that in a metastatic melanoma cell line miR-126* is down-regulated, but restoring miR-126* levels to those of non-malignant melanocytes plays an antineoplastic role by targeting ADAM9 and MMP7, pivotal regulators of melanoma progression (Felli, Felicetti et al. 2013).

## 5.2 Aims

In this chapter, we aimed to study the role of endothelial hsa-miR-126* in T cell and monocyte adhesion to hCMEC/D3 cells. We then systematically searched for hsa-miR-126* predicted targets and selected two, that has been previously shown to be involved in leukocyte trafficking. Finally, we determined whether the expression of these two proteins was regulated by hsa-miR-126* in BEC.

## 5.3 Results

### 5.3.1 TNFα and IFNγ down-regulate hsa-miR-126* expression in hCMEC/D3 cells

The miR array data performed on hCMEC/D3 cells (Reijerkerk, Lopez-Ramirez et al. 2013) showed that the non-leading hsa-miR-126 strand, hsa-miR-126*, was also down-regulated by a combination of cytokines (TNFα and IFNγ) in hCMEC/D3 cells. Here, we confirmed by RT²-qPCR that cytokine treatment for 24 h decreased hsa-miR-126* levels in hCMEC/D3 cells by approximately 60% (Fig. 5.1 grey). Transfection with hsa- anti-miR-126* further reduced miR-126* expression in both unstimulated and cytokine-stimulated cells (Fig. 5.1 white).

### 5.3.2 hsa-miR-126* mediates monocyte adhesion, but not T cell adhesion to hCMEC/D3 cells in both unstimulated and inflammatory conditions using a static assay

We investigated the role of hsa-miR-126* in leukocyte adhesion, which was also down regulated in cytokine-treated hCMEC/D3 cells in a similar fashion to hsa-miR-126 (Chapter 4, Section 4.3.4).

Decreasing levels of endothelial hsa-miR-126* to simulate inflammatory conditions did not affect Jurkat adhesion to hCMEC/D3 cells either in non-stimulated and cytokine-stimulated hCMEC/D3 cells (Fig. 5.2 A). By contrast, low levels of hsa-miR-126* slightly increased, but significantly, THP-1 adhesion to EC under both basal (~20%) and cytokine-stimulated conditions (~10%) (Fig. 5.2 B). These results suggest

that hsa-miR-126* is involved in the regulation of monocyte adhesion to human brain

endothelium.
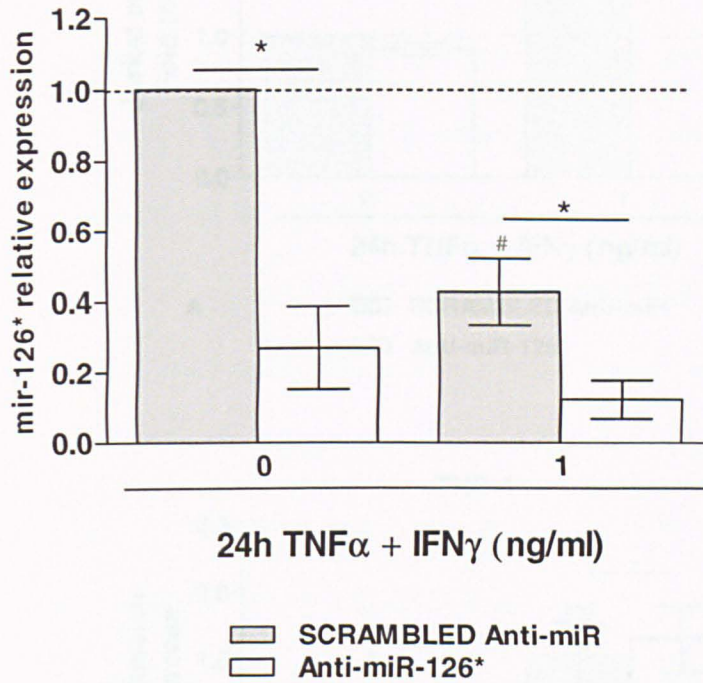


**Fig. 5.1: Cytokine- and anti-miR-induced hsa-miR-126\* down-regulation in hCMEC/D3 cells.** hCMEC/D3 cells were transfected with scrambled Anti-miR or Anti-miR-126* followed by treatment with a combination of cytokines (TNFα + IFNγ) at 0 and 1 ng/ml for 24 h. The expression of mature miR-126* was measured by $qRT^2$-PCR. U6 was used as internal control. Experiments were carried out three times with two replicates. Data are mean ±SEM. (*,#$P<0.05$, #significantly different compared to unstimulated cells * significantly different when compared with scrambled Anti-miR).
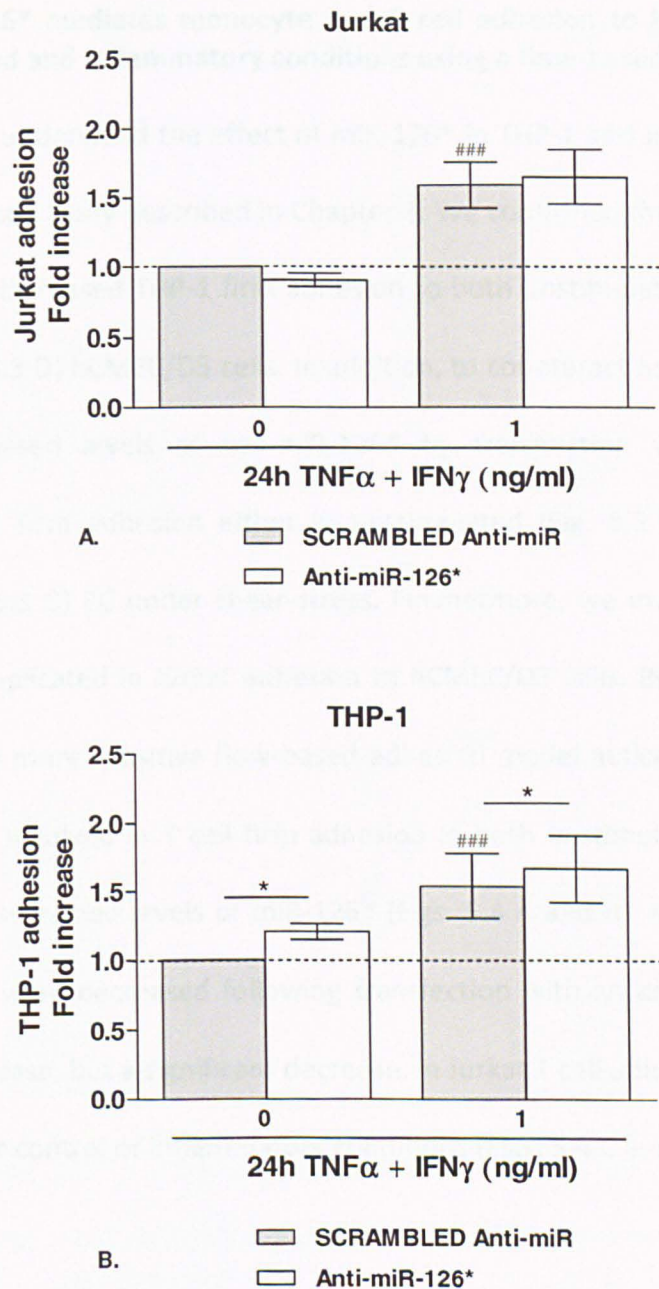
**Fig. 5.2: hsa-miR-126* modulates THP-1 (monocyte), but not Jurkat, static adhesion on hCMEC/D3 cells.** hCMEC/D3 cells were transfected followed by treatment of combination of cytokines (TNFα + IFNγ) at 0 and 1 ng/ml for 24 h. Fluorescence of adhered THP-1 (monocyte), is expressed as fold increase over unstimulated cells transfected with scrambled oligonucleotides. **A.** Scrambled Pre-miR or Pre-miR-126 were used to transfect hCMEC/D3 cells **B.** Scrambled Anti-miR or Anti-miR-126 were used to transfect hCMEC/D3 cells Experiments were carried out four times with six replicates. Data are mean ±SEM. (*P<0.05, ###P<0.001 # significantly different vs. unstimulated cells, * significantly different when compared with scrambled Anti-miR).

### 5.3.3 hsa-miR-126\* mediates monocyte and T cell adhesion to hCMEC/D3 cells in both unstimulated and inflammatory conditions using a flow-based assay

To better understand the effect of miR-126\* in THP-1 and Jurkat adhesion, we used the flow-based assay described in Chapter 3. We confirmed that decreased levels of hsa-miR-126\* increased THP-1 firm adhesion to both unstimulated (Fig. 5.3 C) and stimulated (Fig. 5.3 D) hCMEC/D3 cells. In addition, to counteract hsa-miR-126\* down-regulation, increased levels of hsa-miR-126\* by transfection with pre-miR-126\* prevented THP-1 firm adhesion either in unstimulated (Fig. 5.3 A) or in cytokine-stimulated (Fig. 5.3 B) EC under shear-stress. Furthermore, we investigated whether miR-126\* was implicated in Jurkat adhesion to hCMEC/D3 cells. By contrast with the static model, the more sensitive flow-based adhesion model indicated that miR-126\* was significantly involved in T cell firm adhesion in both unstimulated and cytokine-treated EC with sustained levels of miR-126\* (Figs. 5.4 A and B). However, when the miR-126\* levels were decreased following transfection with an anti-miR, we did not observe any increase, but a significant decrease, in Jurkat T cell adhesion to hCMEC/D3 cells under either control or inflammatory conditions (Figs. 5.4 C and D).
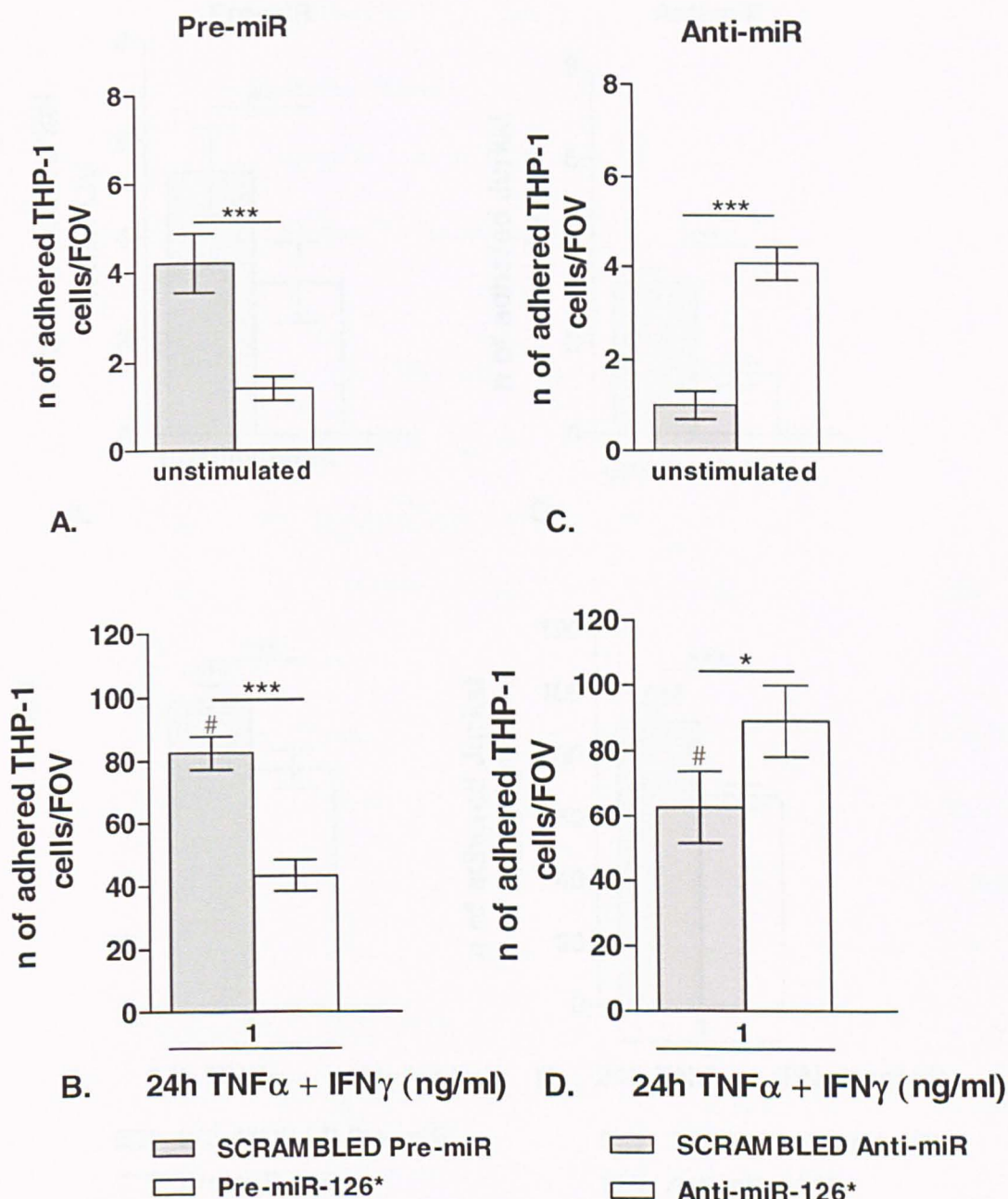
**Fig. 5.3: hsa-miR-126\* regulates THP-1 (monocyte) flow-based adhesion on hCMEC/D3 cells.** hCMEC/D3 cells were transfected followed by treatment of combination of cytokines (TNFα + IFNγ) at 0 and 1 ng/ml for 24 h. Firmly adhered THP-1 cells to hCMEC/D3 cell monolayer were counted/field of view (FOV). Scrambled **A.** Pre- or **C.** Anti-miR and **B.** Pre- or **D.** Anti-miR-126\* were used to transfect hCMEC/D3 cells. Experiments were carried out three times with five replicates. Data are mean ±SEM (\*,#$P<0.05$,\*\*\*$P<0.001$ # significantly different vs. unstimulated cells, \* significantly different when compared with scrambled Pre- or Anti-miR).
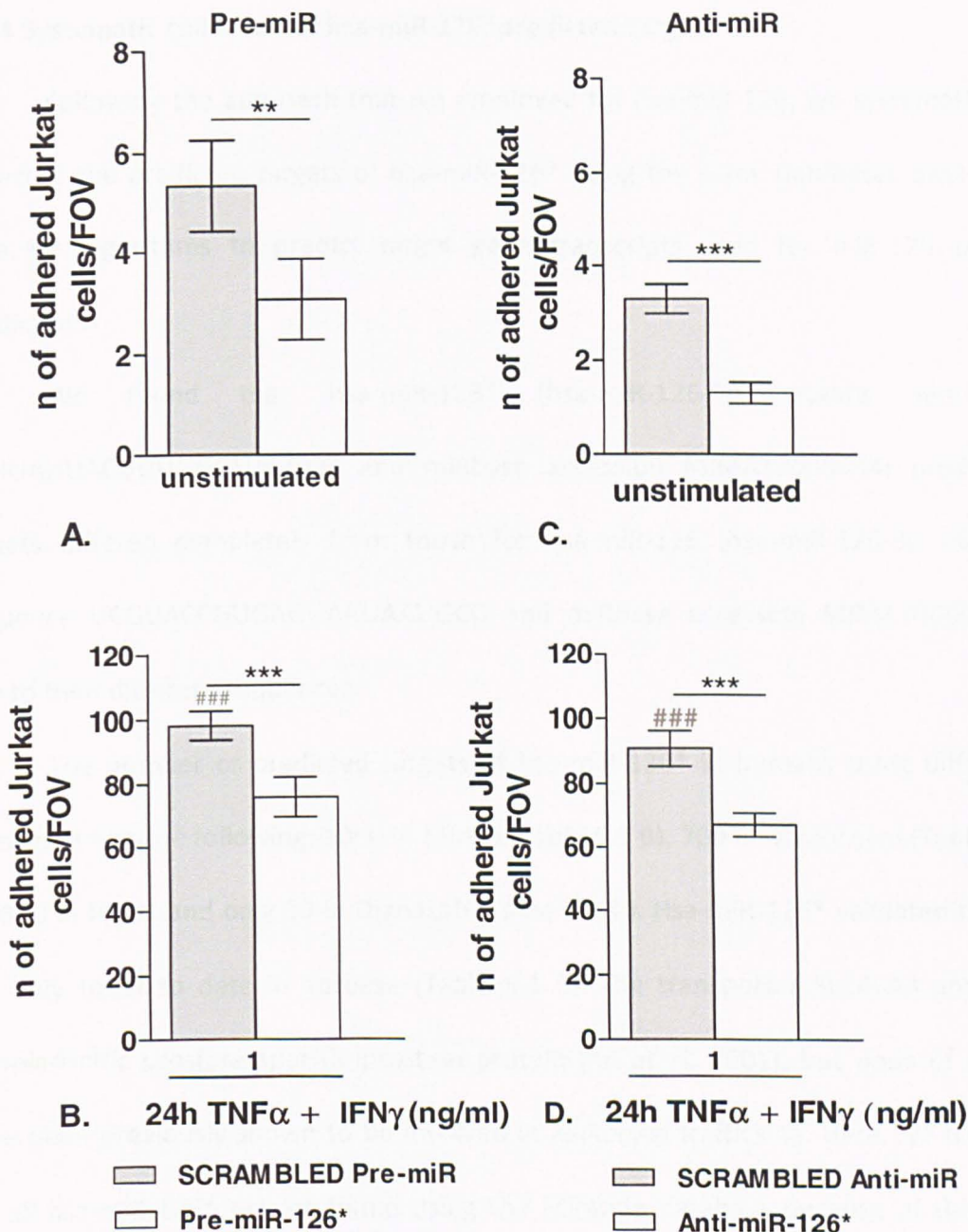
**Fig. 5.4: hsa-miR-126\* regulates Jurkat (T cell) flow-based adhesion to hCMEC/D3 cells.** hCMEC/D3 cells were transfected followed by treatment with a combination of cytokines (TNFα + IFNγ) at 0 and 1 ng/ml for 24 h. Firmly adhered Jurkat cells to hCMEC/D3 cell monolayer were counted/field of view (FOV). Scrambled **A.** Pre- or **C.** Anti-miR and **B.** Pre- or **D.** Anti-miR-126\* were used to transfect hCMEC/D3 cells. Experiments were carried out three times with five replicates. Data are mean ±SEM (\*\*$P<0.01$, \*\*\*, ###$P<0.001$ # significantly different vs. unstimulated cells, \* significantly different when compared with scrambled Pre- or Anti-miR).

## 5.3.4 Systematic collection of hsa-miR-126*predicted targets

Following the approach that we employed for hsa-miR-126, we systematically collected the predicted targets of hsa-miR-126* using the same databases based on different algorithms to predict target gene transcripts used for miR-126 target prediction.

We found that hsa-miR-126* (hsa-miR-126-5p mature sequence CAUUAUUACUUUUGGUACGCG and miRbase accession MIMAT0000444) predicted targets differed completely from those for hsa-miR-126 (hsa-miR-126-3p mature sequence UCGUACCGUGAGUAAUAAUGCG and miRbase accession MIMAT0000445) due to their different sequences.

The number of predicted targets of hsa-miR-126* in humans using different databases was the following: 1000 in MirBD (Table 5.1 B), 700 in Microcosm (Table 5.1 A), 300 in Pictar and only 30 in DianaLab (Table 5.1 C). Hsa-miR-126* validated target are only three to date in Tarbase (Table 5.1 C): the transporter SLC45A3 and the cytoplasmatic prostate specific prostein protein (Xu et al. 2001), but none of these have been previously shown to be involved in leukocyte trafficking. Here, we did not list all hsa-miR-126* targets found using the Miranda database because of the vast number, 8000 targets.

## A. Microcosm

| | | | | | | | | | | | | | | |
|---|---|---|---|---|---|---|---|---|---|---|---|---|---|---|
| A1L4H1_H | BIRC2 | CAMK4 | CYP2A7 | FAM111A | IGHV(III)-22-2 | MAP2K1IP1 | NIT1 | OR52E8 | PRSS22 | Q9UHU9_H | SCYL2 | SYNPO2L | TUBB2A | ZNF684 |
| AASS | BOLL | CAT | CYP39A1 | FAM18B | IGHV3-72 | MAP9 | NOX3 | OR52H1 | PSCDBP | Q9UHZ6_H | SDCCAG1 | TAF13 | TXNDC3 | ZNF687 |
| ABCA6 | BRIP1 | CCDC13 | CYP7B1 | FAM26A | IGSF11 | MAPKAPK5 | NP_001011724.1 | OR8A1 | PSIP1 | RAB9A | SETD6 | TAF1B | TYRP1 | ZNF703 |
| ABCC2 | BRP44L | CCDC22 | DB136_H | FAM26D | IL17F | MARS | NP_001013770.1 | ORC3L | PSMA5 | RAG2 | SETX | TAF9 | UAP1 | |
| ABCD3 | BTF3 | CCDC29 | DBNDD2 | FAM48A | IL1F9 | MCTP1 | NP_001030177.1 | OSTF1 | PSMAL_H | RALGPS1 | SF3B4 | TAF9 | UBTD2 | |
| ACOX2 | BUD13 | CCDC32 | DBP | FAM81B | IL6 | MDH1 | NP_001032308.1 | OSTN | PSMC6 | RASAL2 | SFRS11 | TBC1D15 | UBXD6 | |
| ACSM1 | C10orf119 | CCDC38 | DDX43 | FGF21 | INADL | MED11 | NP_001074319.1 | P2RY10 | PSMD5 | RASGEF1B | SFT2D1 | TCEA3 | UGT2B17 | |
| ACYP2 | C10orf58 | CCDC44 | DEPDC1 | FGFBP1 | INPP1 | MELK | NP_056350.1 | P2RY12 | PSPC1 | RC3H2 | SI | TCEA3 | UHRF2 | |
| ADAM7 | C11orf65 | CCDC45 | DIRC2 | FGG | INSL5 | MFSD8 | NP_056409.1 | PAFAH1B2 | PTGER3 | REG3G | SLC26A7 | TCHHL1 | UMOD | |
| AFF4 | C12orf26 | CCDC53 | DISP2 | FGL1 | IPO7 | MLANA | NP_057209.3 | PAIP1 | PTH | REV3L | SLC35A2 | TEP1 | USP15 | |
| AIG1 | C12orf39 | CCDC85B | DJBP_H | FPGT | IRS4 | MLF1 | NP_057487.2 | PALMD | PTPRQ | REXO1L1 | SLC35E3 | TFCP2 | USP45 | |
| AKR1CL1 | C12orf56 | CCL7 | DMRT2 | FRY | IRX3 | MMACHC | NP_060101.2 | PAPPA2 | PTTG1 | REXO1L2P | SLC39A12 | TFE3 | USP48 | |
| ALB | C12orf57 | CCNA2 | DNAH5 | FSHR | IRX5 | MMP10 | NP_060404.3 | PARD6G | PYGL | REXO1L5P | SLC46A3 | THEX1 | UTP18 | |
| ALDH1A1 | C12orf64 | CCNB3 | DNAL1 | GABRA2 | ISCU | MMP12 | NP_060761.2 | PCDHB13 | PYHIN1 | REXO1L6P | SLC5A11 | THSD1 | UTS2D | |
| ALG10B | C13orf31 | CCT4 | DNMT1 | GBA3 | JARID1D | MMP20 | NP_079189.3 | PCGF5 | Q3LIC9_H | REXO1L7P | SLC7A4 | TMCO3 | VANGL1 | |
| ALS2CR4 | C14orf102 | CD52 | DOCK7 | GBP7 | KARS | MMP3 | NP_115813.1 | PCSK5 | Q3MIB7_H | RFTN2 | SLCO6A1 | TMCO4 | VGLL1 | |
| ANK3 | C14orf135 | CDH9 | DRD3 | GFRAL | KCNA4 | MORG1_H | NP_115813.1 | PDF | Q5T5W8_H | RGR | SLITRK2 | TMCO4 | VIL1 | |
| ANKRD32 | C14orf153 | CENPE | DSG3 | GLMN | KCNH2 | MORN2 | NP_612147.1 | PENK | Q5VVG4_H | RGS10 | SMARCA5 | TMEM176A | VNN2 | |
| ANKRD7 | C14orf37 | CFHR3 | DTD1 | GLRX2 | KCNMB3 | MORN2 | NP_612420.1 | PEX5L | Q6NSF3_H | RGS18 | SNAPC3 | TMEM26 | VPREB3 | |
| ANXA7 | C14orf39 | CFHR4 | DTWD1 | GOLGB1 | KDELC1 | MPP6 | NP_620158.2 | PGBD1 | Q6NZ63_H | RGS9BP | SNRPA1 | TMEM27 | VPS45 | |
| APOOL | C18orf17 | CFI | DUSP28 | GPR137B | KERA | MPV17L | NP_620158.2 | PGC | Q6PDB4_H | RHAG | SNRPD2 | TMEM33 | VRK1 | |
| ARHGAP9 | C1GALT1C1 | CHD1L | DYM | GPR177 | KIF27 | MRPL13 | NP_659455.2 | PGM3 | Q6ZMK7_H | RHAG | SNRPEL1 | TMEM41B | WDR78 | |
| ARL17P1 | C1orf19 | CHIRNA5 | DYNLT3 | GPR31 | KIF3A | MRPL42 | NP_690872.2 | PHC3 | Q6ZN80_H | RIBC1 | SNX24 | TMEM5 | WFDC8 | |
| ARPC1B | C1orf31 | CHRNB1 | EAF2 | GPR98 | KIFAP3 | MRPL43 | NP_710154.1 | PHKA1 | Q6ZNV2_H | RKHD3 | SP7 | TMEM63B | XR_019154.1 | |
| ARPC3 | C1orf41 | CIB1 | EBNA1BP2 | GTF2B | KLHL7 | MRPS26 | NP_777590.1 | PIGL | Q6ZP06_H | RNF13 | SPACA1 | TMEM67 | XRCC2 | |
| ARPM1_H | C1orf67 | CLDN14 | EBPL | GUCY2E | KRR1 | MRPS30 | NP_991111.1 | PIGO | Q6ZRM4_H | RNF170 | SPAG11A | TMSL8 | ZBTB2 | |
| ART3 | C2 | CLEC7A | ECHDC2 | HAS1 | KSR1 | MSH2 | NP_995324.1 | PIGV | Q6ZTZ0_H | RPAIN | SPAG11B | TNFRSF10B | ZCCHC5 | |
| ARV1 | C20orf107 | CMPK | EFR1_H | HEATR5B | L2HGDH | MSH4 | NP_997254.2 | PILRA | Q6ZU57_H | RPL14 | SPAG9 | TNFRSF19 | ZCRB1 | |
| ASMT | C20orf196 | CNBD1 | EIF1AP1 | HIBCH | LCE4A | MT1G | NPY6R | PLA2G4B | Q6ZUF4_H | RPL23 | SPATA6 | TOP2B | ZDHHC9 | |
| ATAD2 | C20orf26 | CNGA1 | EIF2A | HIF1A | LILRB5 | MT1H | NR0B1 | PLOD2 | Q6ZVX8_H | RPL26L1 | SPIC | TOR3A | ZFP2 | |
| ATBF1 | C20orf51 | CNGB3 | EIF3S1 | HIST1H2BJ | LOC145853 | MTHFD1 | NR2E3 | PLXNA4A | Q6ZW50_H | RPSAP15 | SPINK2 | TPM4 | ZIC5 | |
| ATN1 | C21orf88 | COBLL1 | ELL3 | HIST1H3H | LOC402120 | MTHFD2L | NR2F1 | POLI | Q71M28_H | RSBN1 | SPO11 | TPP2 | ZMYM5 | |
| ATP5H | C2orf25 | COLEC12 | ENDOG | HIST2H2BA | LOC646871 | MTO1 | NRBF2 | POLR2K | Q86TS2_H | RSHL2 | SPTB | TPX2 | ZNF287 | |
| ATP6V1G2 | C2orf42 | COMMD10 | ENOX1 | HNRPA3 | LOC728378 | MYO16 | NRP1 | POPDC3 | Q86XQ1_H | RYK | SPTLC3 | TRAF6 | ZNF334 | |
| ATP7A | C2orf46 | COMMD6 | ENPP3 | HOXB2 | LOC728403 | NCAPD3 | NSUN2 | POTE2_H | Q8IVR1_H | S100A11 | SRFBP1 | TRAV8-2 | ZNF354A | |
| ATR | C3orf41 | COX4I1 | ENST00000311104 | HOXD8 | LOC730602 | NCOA6 | NT5DC4 | POU1F1 | Q8IVY7_H | S100A8 | SRGAP1 | TRBV11-1 | ZNF354C | |
| ATXN1 | C3orf60 | COX7C | ENST00000367310 | HPS1 | LOX | NCOA6 | NTF5 | POU3F2 | Q8N1B8_H | S11Y_H | SSBP3 | TRBV15 | ZNF407 | |
| AXIN1 | C4BPA | CPA6 | EPHA8 | HRSP12 | LPHN3 | NCOR1 | NUP160 | PPA1 | Q8N1Y7_H | SAMSN1 | ST8SIA3 | TREML1 | ZNF428 | |
| AYTL1 | C5orf34 | CRBN | EPOR | HSD11B1 | LRIG3 | NDUFA9 | NXT1 | PPM1A | Q96QE0_H | SAP30 | STAG2 | TRIM42 | ZNF507 | |
| BAG3 | C7orf16 | CRSP6 | EPYC | HSD11B1 | LRRC3B | NDUFB5 | O95108_H | PRDM8 | Q9BVM4_H | SBDS | STAU2 | TRIP6 | ZNF583 | |
| BAI3 | C7orf46 | CSF2 | ERCC1 | HSFY2 | LRRC42 | NEDD9 | OLFML1 | PRIM2A | Q9H7S7_H | SCAP | STON1 | TSC22D4 | ZNF606 | |
| BAT5_H | C9orf134 | CSF2RA | EXOSC9 | HTR2B | LXN | NEK3 | OPN1SW | PRLR | Q9NWP0_H | SCEL | SULT1C4 | TSHB | ZNF613 | |
| BCAR3 | C9orf138 | CTGLF7 | F9 | HYDIN | MAGEE2 | NFE2L3 | OR2L13 | PROCR | Q9P145_H | SCLT1 | SUPT7L | TTC15 | ZNF622 | |
| BCCIP | C9orf25 | CYorf15B | FABP3 | ICT1 | MAK10 | NFX1 | OR4M1 | PRPF8 | Q9P1H6_H | SCN7A | SVEP1 | TTY11_H | ZNF642 | |
| BDH2 | C9orf46 | CYP2A13 | FAF1 | IFI44 | MAP2 | NGFRAP1L1 | OR4M2 | PRSS12 | Q9P1K0_H | SCRG1_H | SYCP3 | | | ZNF669 |

*Chapter 5: Role of endothelial hsa-miR-126\* in leukocyte adhesion to human brain endothelium*

## B. MirDB

| | | | | | | | | | | | | | | |
|---|---|---|---|---|---|---|---|---|---|---|---|---|---|---|
| A2LD1 | ARL4C | C14orf129 | CALCOCO2 | CHST7 | DCAF13 | ENO4 | FKTN | GPR88 | IL15 | KRAS | MAP9 | MPP7 | NPHS1 | PDCD2 |
| A2ML1 | ARL5A | C14orf39 | CALHM1 | CHUK | DCAF7 | ENOX2 | FLT1 | GPSM1 | IL17D | KRR1 | MAPK10 | MR1 | NPR3 | PDCL |
| AAK1 | ARPC3 | C15orf29 | CALHM3 | CHURC1 | DCAF8L1 | ENPP5 | FLT4 | GRHL2 | IL6 | KSR1 | MAPK1IP1L | MRP63 | NPTXR | PDE3B |
| AASDHPPT | ARSK | C15orf40 | CALU | CISH | DCK | EPHB1 | FMO2 | GRIA2 | IL7 | L2HGDH | MAPK9 | MRPL13 | NR1D2 | PDE4D |
| AASS | ASB4 | C15orf41 | CAMK2A | CLCN5 | DCLK3 | EPOR | FNDC3B | GRIA4 | IMPA1 | L3MBTL4 | MARCKS | MRPL42 | NR2C1 | PDE7B |
| ABCA1 | ASCC3 | C15orf43 | CASK | CLDN11 | DCP2 | EPT1 | FNDC9 | GRIK1 | IMPAD1 | LACC1 | MARK1 | MRPL43 | NR2C2 | PDGFD |
| ABCB10 | ASMT | C15orf61 | CASP3 | CLDN22 | DCUN1D3 | ERBB2IP | FOLH1B | GRIK2 | ING3 | LAMTOR3 | MAT2B | MRS2 | NR3C1 | PDGFRA |
| ABCD3 | ASPH | C16orf72 | CAST | CLEC12B | DENND1B | ERCC6 | FOXO1 | GRIN2A | INHBE | LARP4 | MBL2 | MS4A1 | NRXN3 | PDLIM5 |
| ABCE1 | ASPHD2 | C17orf75 | CBWD1 | CLEC16A | DGKB | EREG | FPGT | GRIN3A | INO80D | LDHA | MBLAC2 | MSR1 | NSL1 | PDZRN4 |
| ABRA | ASPN | C18orf32 | CBWD2 | CLEC1A | DHFR | ERGIC2 | FPGT | GRM8 | INPP1 | LDLRAD2 | MBNL3 | MSRB3 | NSRP1 | PELI3 |
| ACAN | ATAD2 | C19orf52 | CBWD3 | CLLU1 | DHX35 | ERO1L | FRYL | GSK3B | INPP5D | LIN9 | MBOAT1 | MTAP | NT5DC1 | PERP |
| ACN9 | ATF1 | C19orf69 | CBWD6 | CLTC | DIMT1 | ESM1 | FRZB | GUCY1A3 | INSC | LMO7 | MBP | MTCH2 | NUAK1 | PEX5L |
| ACTR10 | ATN1 | C1GALT1 | CCBP2 | CMYA5 | DIRC2 | ESRRG | FSD1L | GUF1 | INTS6 | LOC100130451 | MCART6 | MTFR1 | NUDT12 | PGBD1 |
| ADAM22 | ATP2B1 | C1GALT1C1 | CCDC122 | CNOT4 | DLG1 | ETV1 | FSHR | GXYLT1 | IRS2 | LOC100130705 | MCHR2 | MTL5 | NUDT16L1 | PGC |
| ADAM8 | ATRN | C1orf109 | CCDC13 | CNPY1 | DLK1 | EVI2A | FSIP1 | H3F3A | ISPD | LOC100131091 | MCMBP | MTMR10 | NUDT7 | PGM2L1 |
| ADAM9 | ATXN1L | C1orf27 | CCDC148 | CNTN5 | DMBX1 | EXD2 | FUT9 | HBP1 | ITGB8 | LOC100500938 | MCTP2 | MTUS1 | NUP153 | PGM3 |
| ADAMTS4 | AXIN1 | C1orf52 | CCDC149 | COBLL1 | DMD | EXPH5 | FXN | HBS1L | IVD | LOC100506255 | MCTS1 | MYD88 | NUP43 | PHACTR2 |
| ADAMTS6 | B2M | C1orf55 | CCDC15 | COG6 | DMRT2 | EYA4 | FYB | HCFC2 | JARID2 | LOC100509575 | MCU | MYEF2 | NWD1 | PHAX |
| ADCY7 | B3GNT7 | C1QTNF7 | CCDC36 | COL11A1 | DMXL1 | EYS | FYCO1 | HCN4 | JKAMP | LOC100652825 | MDH1 | MYT1 | NXT1 | PHC3 |
| ADCYAP1 | B4GALT4 | C1RL | CCDC50 | COL5A2 | DNAH14 | F5 | FZD2 | HDAC4 | JMY | LOC100653112 | MDM4 | MYZAP | NXT2 | PHF14 |
| ADH4 | BACE1 | C21orf62 | CCDC53 | COLEC12 | DNAH5 | F9 | GABRA4 | HECTD2 | JPH1 | LOC100653325 | ME2 | N4BP2L1 | OCLN | PHKA1 |
| ADK | BAG3 | C21orf7 | CCDC82 | COMMD10 | DNAJB4 | FABP3 | GABRA5 | HIF1A | JRKL | LOC389831 | MED11 | NAA50 | ODF2L | PHKB |
| AFF4 | BAI3 | C21orf91 | CCNT2 | COMMD2 | DNAJB9 | FAF1 | GABRB2 | HINT3 | KAT2B | LOC400682 | MED14 | NAALAD2 | OGT | PHLPP1 |
| AGPS | BAIAP2L1 | C22orf39 | CCP110 | CPD | DNAJC3 | FAM105B | GALNT4 | HIPK2 | KBTBD10 | LOC646851 | MED17 | NACC2 | OLFM3 | PI15 |
| AIG1 | BBS12 | C2CD4A | CCPG1 | CPEB4 | DOK6 | FAM111 | GATA3 | HIVEP3 | KBTBD6 | LONRF2 | MED21 | NADKD1 | OLFML1 | PIAS2 |
| AIMP1 | BCAP29 | C2orf69 | CCR1 | CPNE8 | DPP8 | FAM116A | GBP1 | HLF | KCMNB | LOX | METAP1 | NAF1 | OPTN | PIGK |
| AK2 | BCAR3 | C3orf15 | CCRL1 | CRBN | DPY19L2 | FAM129A | GBP3 | HMCN1 | KCNA1 | LPHN2 | METTL10 | NALCN | OR51E2 | PIKFYVE |
| AKIRIN1 | BCCIP | C3orf17 | CD200R1 | CRCP | DSC2 | FAM135A | GBP4 | HMGXB4 | KCNJ16 | LPHN3 | METTL17 | NAPG | ORC3 | PIP4K2A |
| ALDH1A1 | BCL11B | C3orf23 | CD2AP | CREB1 | DSEL | FAM165B | GBP6 | HN1L | KCNMA1 | LPIN2 | METTL21D | NAT1 | OSMR | PIP4K2C |
| ALG10B | BCL2L2 | C4orf26 | CD44 | CREB3L2 | DSG1 | FAM172A | GBP7 | HNRNPU | KCNN3 | LPP | METTL2A | NCALD | OSTF1 | PITPNB |
| AMACR | BCLAF1 | C4orf34 | CD84 | CRLS1 | DTD1 | FAM175B | GFM1 | HOMEZ | KCNQ5 | LPPR5 | MEX3A | NCAN | OTUD3 | PKHD1 |
| AMFR | BDH2 | C5orf30 | CDC14B | CRNKL1 | DTL | FAM189A1 | GGA1 | HOOK3 | KCTD3 | LRCH2 | MEX3B | NCOA4 | OTUD4 | PKIA |
| AMMECR1L | BEND4 | C5orf34 | CDC7 | CRTAM | DTX3L | FAM190A | GGT6 | HOXA13 | KDELC2 | LRP1 | MFAP4 | NCOA7 | OTUD6B | PLA2G12A |
| ANAPC7 | BEND6 | C5orf47 | CDCA7 | CRY1 | DUXA | FAM198B | GHR | HOXB5 | KDM6A | LRP1B | MFSD11 | NCOR1 | OXNAD1 | PLAG1 |
| ANGPTL1 | BICD2 | C5orf51 | CDH9 | CRYZ | DYNLT3 | FAM199X | GINS1 | HOXB6 | KIAA0355 | LRP2BP | MGAT3 | NDUFA9 | P2RY12 | PLCB1 |
| ANKIB1 | BMP3 | C6orf118 | CDK13 | CSF1 | DYRK2 | FAM27E3 | GJB2 | HOXC6 | KIAA0430 | LRRC19 | MGAT4A | NDUFAF3 | PAFAH1B2 | PLEKHB2 |
| ANKRD12 | BMPR1B | C6orf168 | CDK19 | CSF2RA | E2F6 | FAM63B | GJC1 | HOXD8 | KIAA0564 | LRRC3B | MGP | NDUFB5 | PALM2 | PLEKHF1 |
| ANKRD20A3 | BRAF | C7orf42 | CEACAM8 | CSRNP3 | E2F7 | FAM76A | GK | HPGD | KIAA1024 | LRRC57 | MIB1 | NDUFS1 | PALMD | PLEKHF2 |
| ANKRD33B | BRD1 | C7orf46 | CELF2 | CTAGE5 | EARS2 | FAM76B | GLE1 | HPS5 | KIAA1033 | LRRC8B | MID1 | NEGR1 | PANX1 | PLEKHG7 |
| ANKRD34B | BRD3 | C7orf57 | CEP170 | CTBS | EBF1 | FAM78A | GLIPR1 | HPSE | KIAA1377 | LSAMP | MIPOL1 | NETO1 | PAPD5 | PLEKHH2 |
| ANO3 | BRP44L | C7orf58 | CEPT1 | CTR9 | EBPL | FAM84A | GLRA2 | HRH4 | KIAA1430 | LTN1 | MITF | NEU3 | PAPPA | PLEKHM3 |
| ANO5 | BRWD3 | C8orf34 | CFTR | CUBN | EDA2R | FAM8A1 | GLYAT | HS3ST3B1 | KIAA1456 | LUC7L2 | MLL | NFAT5 | PARP11 | PLOD2 |
| ANTXR2 | BTBD1 | C8orf37 | CHAMP1 | CUL2 | EFCAB7 | FANCL | GNB4 | HS6ST3 | KIAA1468 | LYRM2 | MLLT10 | NFIA | PARP12 | PLXDC1 |
| AP1G1 | BTC | C8orf44 | CHD1L | CX3CR1 | EFHA2 | FBN2 | GNE | HSD11B1 | KIAA1644 | LZTFL1 | MLPH | NFIB | PATE1 | PNLIPRP3 |
| AP1S3 | BTF3L4 | C8orf46 | CHD9 | CYB561D1 | EFR3A | FBRSL1 | GNG12 | HSPB8 | KIAA1826 | MAB21L1 | MMAA | NFX1 | PAX2 | PNN |
| AP3B1 | BZW1 | C9orf5 | CHIC1 | CYP20A1 | EGLN1 | FBXL14 | GNG2 | IAH1 | KIF3A | MACC1 | MMACHC | NFYA | PAX6 | PNPLA8 |
| APOPT1 | C10orf32 | C9orf72 | CHL1 | CYP39A1 | EIF1AX | FBXO25 | GNL1 | IAPP | KITLG | MAGEF1 | MME | NHLRC2 | PCBD2 | PNRC1 |
| ARF6 | C11orf82 | CA1 | CHM | CYS1 | EIF2A | FBXO35 | GOSR1 | ICK | KL | MAGI3 | MMP16 | NHSL1 | PCDHB13 | POC1B-GALNT4 |
| ARHGAP28 | C11orf87 | CA13 | CHMP5 | CYTIP | EIF3J | FBXO6 | GPBP1 | IDS | KLF17 | MAK | MMRN1 | NIT1 | PCDHB16 | PODXL |
| ARHGAP32 | C12orf23 | CA3 | CHODL | DAB2IP | EIF4A2 | FGF12 | GPC6 | IFI44 | KLHDC10 | MAN1A1 | MMS22L | NLGN4X | PCDHB7 | POFUT1 |
| ARID1A | C12orf4 | CACNA1A | CHRAC1 | DAPP1 | ELAVL3 | FGF2 | GPCRLTM7 | IGFBP3 | KLHL32 | MAN1A2 | MOB1B | NLGN4Y | PCGF5 | POLK |
| ARID2 | C12orf40 | CACNB4 | CHRNA5 | DBF4 | ELK4 | FGF7 | GPR137B | IGSF1 | KLHL4 | MANEA | MOB3B | NLN | PCLO | POLR2K |
| ARL11 | C12orf48 | CADM1 | CHRNB1 | DBR1 | ELL3 | FGFRL1 | GPR64 | IGSF11 | KLHL7 | MAP3K2 | MOG | NOVA1 | PCNX | POPDC3 |
| ARL13B | C12orf65 | CALCB | CHST11 | DCAF10 | EMP2 | FGG | GPR85 | IKZF2 | KLLN | MAP3K7 | MORC1 | NOX1 | PCSK2 | POU2F1 |

| | | | | | | | |
|---|---|---|---|---|---|---|---|
| PPARGC1A | RAPGEF6 | SAA2 | SLC35B4 | ST8SIA1 | TMEM41B | UPRT | ZFY |
| PPAT | RASAL2 | SAE1 | SLC35G1 | ST8SIA3 | TMEM47 | USP10 | ZFYVE16 |
| PPFIA1 | RASSF6 | SAMD13 | SLC39A9 | STAM2 | TMEM56 | USP12 | ZIC2 |
| PPFIA2 | RBAK | SAMD4A | SLC41A2 | STC1 | TMEM65 | USP14 | ZIC4 |
| PPIL1 | RBL2 | SAMSN1 | SLC46A1 | STEAP2 | TMEM70 | USP15 | ZMYM6 |
| PPIL6 | RBM12 | SAR1B | SLC47A2 | STK17B | TMOD2 | USP45 | ZNF10 |
| PPP1R10 | RBM19 | SCAI | SLC4A10 | SULT6B1 | TMPRSS11D | USP47 | ZNF135 |
| PPP1R12B | RBM41 | SCAMP1 | SLC4A5 | SUPT7L | TMPRSS11E | USP53 | ZNF148 |
| PPP1R15B | RCBTB1 | SCAP | SLC4A7 | SYNJ2BP | TMX1 | UTRN | ZNF192 |
| PPP2R5E | RDH11 | SCEL | SLC5A3 | SYNPO2 | TMX3 | UTS2D | ZNF193 |
| PPP4R4 | RDX | SCN3A | SLC6A15 | SYNPR | TMX4 | UTY | ZNF197 |
| PPP6R3 | REEP3 | SCRN1 | SLC7A14 | SYT10 | TNC | VAMP4 | ZNF212 |
| PRAMEF1 | REEP5 | SDPR | SLCO1C1 | SYT14 | TNFAIP2 | VAPA | ZNF264 |
| PRAMEF13 | REG3G | SEC61A1 | SLFN13 | TAF13 | TNFAIP8L3 | VCPIP1 | ZNF333 |
| PRAMEF14 | REV3L | SEC62 | SLITRK4 | TAF1D | TNFRSF19 | VGLL1 | ZNF33A |
| PRDM8 | REXO1L1 | SECISBP2L | SMAD4 | TAF9 | TNFSF4 | VGLL3 | ZNF33B |
| PRKACB | RFT1 | SELE | SMARCC1 | TAOK3 | TNIK | VPS13A | ZNF354C |
| PRKCA | RFTN2 | SELT | SMCHD1 | TBC1D15 | TNKS2 | VPS13C | ZNF407 |
| PRKX | RFX4 | SEMA5A | SMS | TBC1D19 | TNNI3K | VPS4B | ZNF434 |
| PROCR | RG9MTD2 | SEMA6D | SMYD1 | TBC1D20 | TOB1 | VTA1 | ZNF507 |
| PRPF8 | RGAG1 | SEMA7A | SNAI2 | TBC1D9B | TOMM34 | WAPAL | ZNF519 |
| PRRG2 | RGMB | SEPSECS | SNAPC1 | TBL1XR1 | TPD52L3 | WDR35 | ZNF549 |
| PRTG | RGPD4 | SEPT14 | SNCA | TCEA1 | TRAF3 | WDR5B | ZNF566 |
| PRUNE2 | RGPD5 | SEPT7 | SNRPN | TCFL5 | TRAF6 | WEE1 | ZNF567 |
| PSAT1 | RGPD6 | SERF1A | SNURF | TCP10L2 | TRAFD1 | WFDC13 | ZNF568 |
| PSG1 | RGPD8 | SERF1B | SNX1 | TDG | TRAM1 | WHSC1 | ZNF572 |
| PSMA8 | RGR | SESTD1 | SNX13 | TEAD1 | TRDN | WNK1 | ZNF576 |
| PSMB2 | RGS10 | SETBP1 | SNX4 | TECPR2 | TRIM33 | WWC1 | ZNF615 |
| PTGFR | RGS14 | SETD5 | SOCS3 | TEP1 | TRIM8 | XIRP2 | ZNF622 |
| PTGS2 | RGS18 | SETD8 | SOCS6 | TET1 | TRIP6 | XKRY | ZNF624 |
| PTPN11 | RGS5 | SF3A1 | SOX13 | TET2 | TRNAU1AP | XKRY2 | ZNF626 |
| PTPN12 | RGS9BP | SFRP4 | SOX6 | TFEC | TRPS1 | YIPF6 | ZNF627 |
| PTPN14 | RHOBTB3 | SGCB | SP1 | TFPI | TSC22D4 | ZAK | ZNF687 |
| PTPN20A | RIMS1 | SGK3 | SP5 | TGFBR1 | TSHZ1 | ZBTB1 | ZNF695 |
| PTPN20B | RINL | SGPP1 | SPAG16 | THAP3 | TSHZ3 | ZBTB2 | ZNF74 |
| PTPN21 | RMI1 | SGTB | SPAST | THEMIS | TSPAN13 | ZBTB38 | ZNF777 |
| PTPRC | RNASEL | SH3BGR | SPATA18 | THSD7A | TTC22 | ZBTB41 | ZNF793 |
| PTPRD | RNF141 | SH3BGRL2 | SPATA2 | TLR4 | TTC3 | ZBTB6 | ZNF81 |
| PTPRO | RNF19A | SH3TC2 | SPATA6 | TM4SF18 | TTC39C | ZBTB7B | ZNF829 |
| PUS10 | ROCK1 | SHANK3 | SPATS2L | TMCO4 | TTC7B | ZBTB7C | ZNF83 |
| PWWP2A | RORA | SHROOM3 | SPCS3 | TMED5 | TTC9 | ZBTB8A | ZPLD1 |
| QRSL1 | RP2 | SKAP2 | SPICE1 | TMED7 | TTF2 | ZC3H12B | ZRANB1 |
| RAB11FIP2 | RPF1 | SLC16A9 | SPOPL | TMEFF1 | U2SURP | ZC3H6 | ZSCAN30 |
| RAB30 | RPL17 | SLC17A8 | SPRED1 | TMEM135 | UBE2V2 | ZC3H7B | ZWILCH |
| RAB33B | RPL26L1 | SLC25A12 | SPRY3 | TMEM168 | UBFD1 | ZCCHC5 | ZXDA |
| RAB3IP | RPRD1A | SLC25A24 | SPRY4 | TMEM170B | UBN2 | ZDHHC15 | |
| RAB8B | RPSA | SLC26A4 | SRD5A3 | TMEM182 | UBR5 | ZDHHC21 | |
| RAB9B | RSBN1 | SLC26A7 | SREK1IP1 | TMEM188 | UBXN4 | ZEB2 | |
| RABGEF1 | RTKN2 | SLC2A11 | SRFBP1 | TMEM209 | UGGT1 | ZFAND5 | |
| RABL3 | RTN4RL1 | SLC2A13 | SRSF11 | TMEM215 | UGT2A3 | ZFC3H1 | |
| RAG1 | RUFY3 | SLC33A1 | SRSF12 | TMEM237 | UGT2B17 | ZFHX4 | |
| RALGPS1 | RUNX1T1 | SLC34A2 | SS18L1 | TMEM26 | UHRF1BP1L | ZFP14 | |
| RALGPS2 | RWDD4 | SLC35A3 | SSX2IP | TMEM27 | UNC5D | ZFR | |
| RAPGEF3 | S1PR3 | SLC35A5 | ST6GALNAC1 | TMEM33 | UPP2 | ZFX | |

**Table 5.1: lists of hsa-miR-126* predicted targets (gene names) available on-line grouped for databases and sorted in alphabetical order. A. Microcosm database B. MiRDB C. Pictat, Dianalab, Targetscan and D. Tarbase (validated targets).**

C.

D.

| Pictar | | | | | | Diana Lab | Targerscan | Tarbase |
|---|---|---|---|---|---|---|---|---|
| ABCB11 | CLASP1 | FLRT2 | MARCH-III | PPARGC1A | TGFBI | AP001005.6-2 | No prediction | SLC45A3 |
| ABCC12 | CLEC1 | FNDC3 | MAT2A | PPM1B | THRAP1 | ATXN7L1 | | prostein |
| ABCG4 | CLPX | FURIN | MAT2B | PPP1CB | TMEM33 | BCL11B | | |
| ABHD6 | CNOT7 | FUSIP1 | MDM1 | PPP1R10 | TOX | CUGBP2 | | |
| ACSL6 | COBLL1 | FUT8 | MEF2D | PPP2R5E | TRIM8 | DCP1A | | |
| ACTR1B | COL1A1 | GABRA5 | MGC23401 | PRDM8 | TRPC5 | ERBB2IP | | |
| ACYP1 | COLEC12 | GGTL3 | MGC35558 | PRKCE | TRPS1 | ESRRG | | |
| ADAM9 | COLEC12 | GMPPB | MGC48972 | PRO0149 | TXNDC | FOXN3 | | |
| ADCYAP1 | CPEB2 | GNB1 | MGC8974 | PSMC6 | UBE2G1 | GABRB2 | | |
| AFURS1 | CREB3L1 | GPHN | MLSTD2 | PTER | UPP2 | GJC1 | | |
| AKNA | CREBBP | GPR116 | MTCH2 | PTPN12 | USP3 | HECTD2 | | |
| AP1G1 | CTAGE5 | GPR85 | MYEF2 | PTPRT | VCIP135 | HMGXB4 | | |
| APRIN | CTCF | GRIK1 | MYLIP | PTX1 | WDR44 | HOXA13 | | |
| ARF6 | CUGBP2 | HDAC4 | MYT1 | PURB | WDR47 | KAT2B | | |
| ARID1A | CUL2 | HMG2L1 | NAV3 | RAB1A | XPR1 | KIAA1468 | | |
| ARK5) | CYP26A1 | HMGB1 | NCOA3 | RAP1B | YAP1 | KIAA2018 | | |
| ARNT | CYP26A1 | HFGFR2 | NDFIP1 | RASAL2 | YES1 | KLHL32 | | |
| ARNT | DAB2IP | HomoOGT | NEUROG2 | RBBP6 | ZADH2 | KZF2 | | |
| ATOH7 | DACH1 | HOXB2 | NOMO3 | RFX4 | ZBTB2 | NPAS2 | | |
| ATP2B1 | DAG1 | HS3ST3B1 | NOVA1 | RGS4 | ZDHHC17 | PLCB1 | | |
| ATRN | DDR1 | HSF1 | NPAS2 | RNF103 | ZFHX4 | PPAPR5 | | |
| AXIN1 | DIRC2 | IFIT5 | NR2E1 | RNF138 | ZIC4 | PPARGC1A | | |
| BACE1 | DKFZP564J0123 | ILF3 | NR5A2 | RNF152 | ZNF265 | RAB8B | | |
| BACH2 | DKFZP566B183 | ILF3. | OGT | RNP24. | ZNF281 | RABL3 | | |
| BAI3 | DKFZp761B1514 | IMMT | OSBP | ROCK2 | ZNF354C | REV3L | | |
| BCL11A | DKFZp761C169 | ING3 | PCAF | SAMD8 | ZNF533 | SETD5 | | |
| BCL11B | DKK2. | INPP5D | PCANAP6 | SCAP2. | ZNF537 | TRPS1 | | |
| BCL2L2 | DMRT2 | INSIG1 | PCDH9 | SCN3A | ZNF583 | UBN2 | | |
| BET1 | DVL3 | JARID2 | PCDHA1 | SCRT1 | ZNF81 | ZNF583 | | |
| BLCAP | DYRK1 | KCND2 | PCDHA10 | SDCCAG33 | | ZNF608 | | |
| BRP44L | DYRK1A | KCNH2 | PCDHA11 | SEMA6D | | | | |
| BZW1 | E2F6. | KCNJ3 | PCDHA12 | SF | | | | |
| C11orf23 | EIF1AX | KIAA0261 | PCDHA13 | SF1 | | | | |
| C15orf27 | EIF3S1 | KIAA0828 | PCDHA2 | SFRS1 | | | | |
| C8orf4 | EIF4A2 | KIAA1033) | PCDHA3 | SLC16A9 | | | | |
| C9orf10 | ELAVL4 | KIAA1128 | PCDHA4 | SLC25A27 | | | | |
| C9orf25 | ELF1 | KIAA1285 | PCDHA5 | SLC38A2 | | | | |
| CABP7 | EPHA7 | KIAA1409 | PCDHA6 | SMC4L1 | | | | |
| CARD6 | ERBB2IP | KIAA1434 | PCDHA7 | SP192 | | | | |
| CAV2 | ESRRG | KIAA1468 | PCDHA8 | SP3 | | | | |
| CBFA2T1 | EYA1 | KIAA1853 | PCDHA9 | SPAG9 | | | | |
| CBFA2T2 | EZH2 | KLF12 | PCDHAC1 | SPFH1 | | | | |
| CCPG1 | FBXO3# | KPNA4 | PCDHAC2 | SPFH2 | | | | |
| CDC10 | FGD4 | LDB2 | PCSK2 | SPG4 | | | | |
| CDC14B | FGF7 | LIN9 | PDE7B | SRRM1 | | | | |
| CDC42 | FGFR2 | LNK | PFN2 | SSB4 | | | | |
| CDCA7 | FLJ10154 | LOC51234 | PLAC2 | SSBP3 | | | | |
| CDYL | FLJ20859 | LPP | PLAG1 | STAG2 | | | | |
| CGI-109 | FLJ22104 | LRP1 | PLEKHB2 | STC1 | | | | |
| CHCHD3 | FLJ30046 | LRRC3B | PLEKHE1 | STK24 | | | | |
| CHD1L | FLJ34969 | M6PR | PLXNA2 | STRN3 | | | | |
| CHD7 | FLJ42200 | MAFB | PNN | SURF4 | | | | |
| CHES1 | FLJ45187 | MAK | PNRC1 | SYAP1 | | | | |
| CHUK | FLJ46156 | MAN1A1 | POU4F1 | TAP2 | | | | |

### 5.3.5 Selection of hsa-miR-126*predicted targets with a putative role in leukocyte trafficking

Here, we shortlisted hsa-miR-126* predicted target gene names of proteins that have been shown to be related to adhesion such as chemokines, CAM and selectins (Carlos and Harlan 1994; Muller 2003; Ley and Kansas 2004; Engelhardt and Ransohoff 2005) (Table 5.2).

| Gene | Description | Database | Expression in hCMEC/D3 cells | Selected for further study |
|------|-------------|----------|------------------------------|----------------------------|
| | | hsa-miR-126* | | |
| CX3CR1 | Chemokine receptor 1 | MIR DB | yes | |
| SCAMP1 | Secretory carrier membrane protein 1 | MIR DB | yes | |
| CEACAM8 | Carcinoembryon antigen-rel cell adhesion molecule 8 | MIR DB | yes | |
| CHL1 | Cell adhesion molecule with homology to L1CAM | MIR DB | yes | |
| SELE | E-selectin or ELAM-1 | MIR DB | yes | √ |
| CD44 | Cell surface glycoprotein involved in cell-cell adhesion | MIR DB | yes | |
| CD200 | Receptor 1 ox-2 membrane glycoprotein containing 2 immuglobulin domains | MIR DB | yes | |
| CD2 | CD2 is a surface antigen of the human T-lymphocyte lineage that is expressed on all peripheral blood T cells or LFA-2 | MIR DB | yes | |
| CCL7 | Chemokine ligand 7 | MICROCOSM | yes | √ |
| CADM1 | Cell adhesion molecule 1 | MIR DB | yes | |

**Table 5.2: Selected hsa-miR-126* predicted targets for further study.**

We found eleven predicted target expressed by hCMEC/D3 cells, related to cellular adhesion or trafficking, and out of these we selected E-selectin (SELE) and CCL7. The chemokine CCL7 is a small cytokine previously known as monocyte-specific chemokine 3 (MCP3). CCL7 has been reported to mediate firm adhesion to endothelium by CD4+ T lymphocytes (Loetscher, Seitz et al. 1994) and monocytes (Gerard and Rollins 2001; Mackay 2001).

E-selectin also known as CD62E, ELAM-1, or leukocyte-endothelial cell adhesion molecule 2 (LECAM2) is a cell adhesion molecule expressed only on EC and it plays an

important part in inflammation, in particular in leukocyte rolling on endothelium as described in 1.4.4.

Because CCL7 and E-selectin were most likely to be involved in inflammation and leukocyte trafficking, we have chosen to study these proteins further as potential hsa-miR-126* targets in BEC.

### 5.3.6 E-selectin expression is modulated by hsa-miR-126* in hCMEC/D3 cells

E-selectin was a predicted target of hsa-miR-126* that was selected for further investigation. Here we studied whether hsa-miR-126* was able to regulate E-selectin expression on hCMEC/D3 cells both in unstimulated and cytokine-stimulated endothelium. We observed that decreasing the levels of miR-126*, and mimicking inflammatory conditions, caused a small, but significant increase in E-selectin under control conditions (Fig. 5.5). Due to decrease of miR-126* with cytokines, E-selectin expression was increased. When miR-126* was increased, no differences were observed in E-selectin expression in all conditions tested.
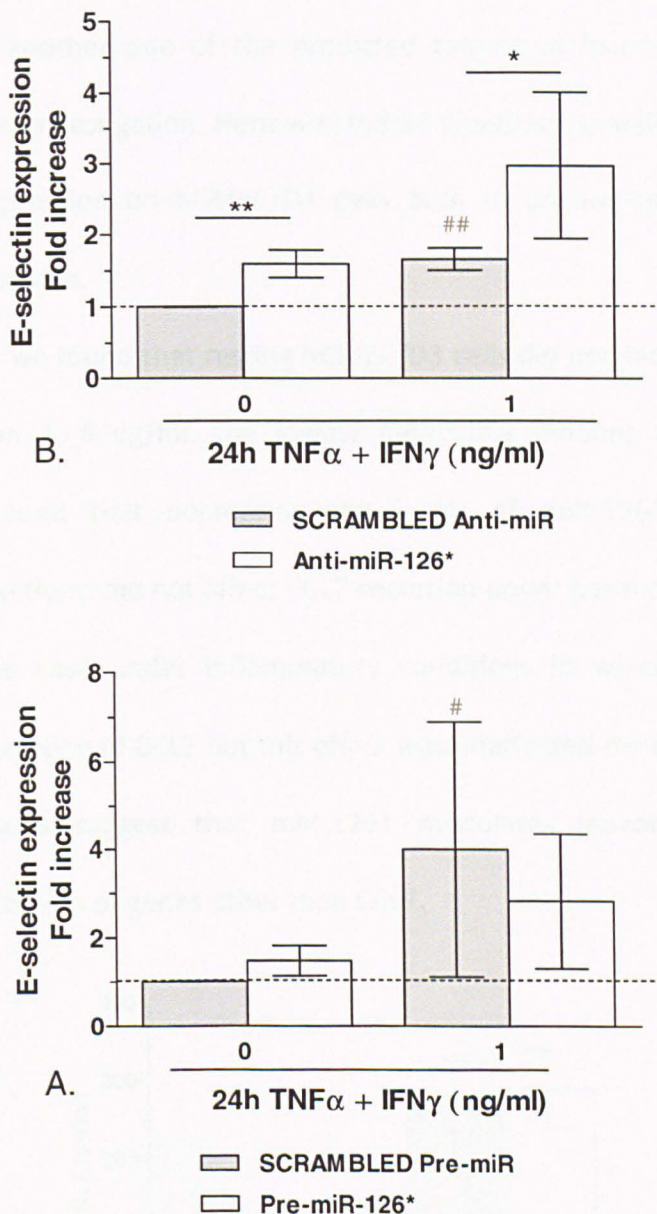
Fig. 5.5: Hsa-miR-126* modulates E-selectin expression in hCMEC/D3 cells in basal or inflammatory conditions. hCMEC/D3 cells were transfected with A. Pre-miR-126* and B. Anti-miR-126* followed by treatment with a combination of cytokines (TNFα + IFNγ) at 0 and 1 ng/ml for 24 h. Anti-human-E-selectin monoclonal antibody was used to detect E-selectin expression levels by ELISA. Experiments were carried out three times with three replicates. Data are mean ±SEM ([#,*]p<0.05 [##,] **p<0.01 [#] significantly different vs. unstimulated cells,* significantly different when compared with scrambled Pre- or Anti-miR).

### 5.3.7 CCL7 expression is not modulated by hsa-miR-126* in hCMEC/D3 cells

CCL7 was another one of the predicted targets of hsa-miR-126* that was selected for further investigation. Here we studied whether hsa-miR-126* was able to regulate CCL7 expression on hCMEC/D3 cells both in unstimulated and cytokine-stimulated endothelium.

First of all, we found that resting hCMEC/D3 cells did not secrete CCL7, or they secreted less than 15.6 pg/ml, the lowest detectable amount above the assay's threshold. We found that decreasing the levels of miR-126*, and mimicking inflammatory conditions, did not affect CCL7 secretion under basal conditions (Fig 5.6). This was also the case under inflammatory conditions in which hCMEC/D3 cells increased their secretion of CCL7 but this effect was unaffected my modulation of miR-126*. These results suggest that miR-126* modulates leukocyte adhesion via regulation of expression of genes other than CCL7.
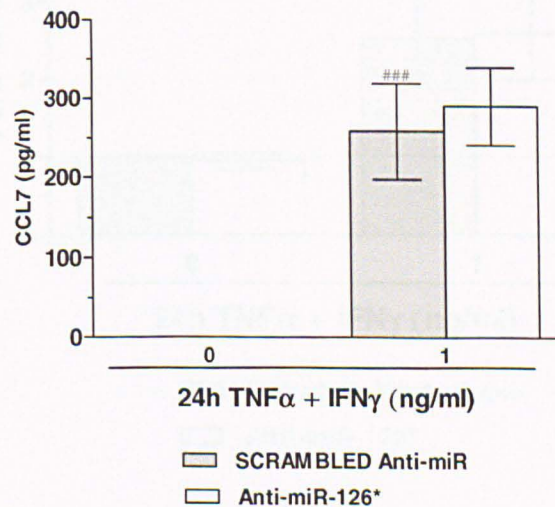


**Fig. 5.6: Hsa-miR-126* does not modulate CCL7 expression in hCMEC/D3 cells.** hCMEC/D3 cells were transfected followed by treatment with a combination of cytokines (TNF$\alpha$ + IFN$\gamma$) at 0 and 1 ng/ml for 24 h. Anti-human-CCL7 monoclonal antibody was used to detect CCL7 expression levels by ELISA. Experiments were carried out three times with three replicates. Data are mean ±SEM ([###]$P<0.001$ [#] significantly different vs. unstimulated cells).

### 5.3.8 VCAM1 expression is not modulated by hsa-miR-126* in hCMEC/D3 cells

VCAM1 was a validated target of hsa-miR-126 in HUVEC, and we confirmed its regulation of expression by this miR in hCMEC/D3 cells. However, VCAM1 is not a directly predicted target for miR-126*, however ROCK2 is a predicted target gene of miR-126* (Table 5.1), which has been implicated in the regulation of VCAM1 expression by lysophosphatidic acid (LPA) in HUVEC (Shimada and Rajagopalan 2010). Therefore, we tested whether the levels of VCAM1 expression by hCMEC/D3 cells could be indirectly affected by decreased levels of miR-126* in hCMEC/D3 cells. As expected, VCAM1 expression by hCMEC/D3 cells was not modulated by hsa-miR-126* (Fig. 5.7).
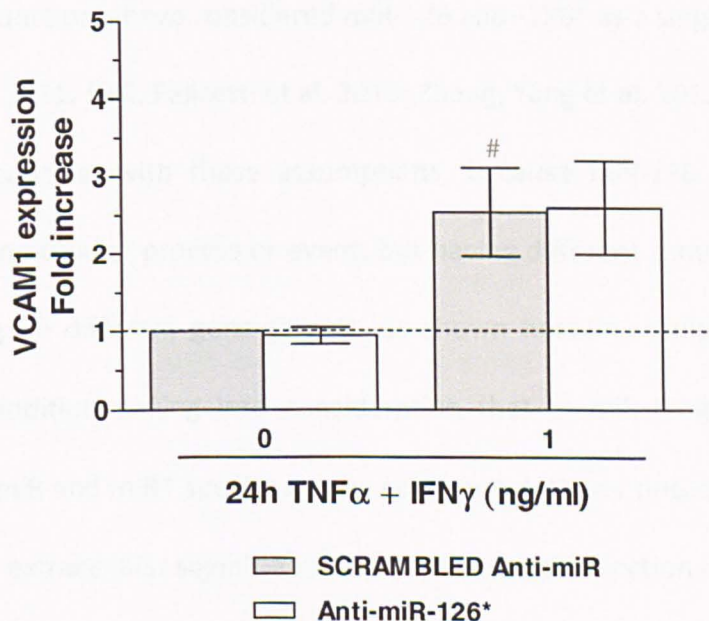


**Fig. 5.7: Hsa-miR-126* does not modulate VCAM1 expression in hCMEC/D3 cells.** hCMEC/D3 cells were transfected followed by treatment with a combination of cytokines (TNFα + IFNγ) at 0 and 1 ng/ml for 24 h. Anti-human-VCAM1 monoclonal antibody was used to detect VCAM1 expression levels by ELISA. Experiments were carried out three times with three replicates. Data are mean ±SEM ([#]$P<0.05$ [#] significantly different vs. unstimulated cells).

## 5.4 Discussion

### 5.4.1 The role of the non leading strand microRNA in leukocyte adhesion

In Chapter 4 we showed that miR-126 regulates monocyte and T cell adhesion (Harris, Yamakuchi et al. 2008). Here we demonstrated that hsa-miR-126*, the complement of hsa-miR-126 was involved in the regulation of leukocyte adhesion. Overexpression of hsa-miR-126* prevented both T cell and monocyte adhesion which was comparable to hsa-miR-126 (shown in Chapter 4). These observations could suggest that miR-126 and -126* have the same role and function in leukocyte adhesion because they originate from the same gene and pri-miR precursor, although they have different sequences. Probably for these reasons most studies, assuming that both miRs have the same functions, have considered miR-126 and -126* as a single entity (Huang, Gschweng et al. 2011; Felli, Felicetti et al. 2013; Zhang, Yang et al. 2013). However, our results are in contrast with these assumptions, because miR-126 and -126* may regulate the same cellular process or event, but having different sequences, they may do so by acting on different gene targets, as shown here in results section and in Chapter 4. In addition, taking into consideration that (i) miR biogenesis is tissue-dependent, (ii) miR and miR* species can be co-accumulated or not, depending on the cell type and/or extracellular signals and that (iii) the target selection mechanism is not standard (Ro, Park et al. 2007), it is expected that miR-126 and -126* can be expressed in a tissue-specific way and may have different regulatory functions as shown in human BEC in this study and in HUVEC and prostate cancer cells (Musiyenko, Bitko et al. 2008). It has been previously shown that miR/miR* can play opposite roles, as is the case for miR-155* and -155 in human dendritic cells where are inversely regulated by

type I interferons (Zhou, Huang et al. 2010), or a similar function, as is the case for miR-155* and -155 in human astrocytes where both miRs are co-regulated by cytokines and have the same proinflammatory function (Tarassishin, Loudig et al. 2011). As reported by Byrd et al., miR-30c and its passenger strand (mir-30c2*) are both expressed by fibroblast cells, but only mir-30c2* regulates the endoplasmic reticulum by targeting the specific gene XBP1 gene (Byrd, Aragon et al. 2012). The results from these studies suggest that miR star species, in addition to their own regulatory activity, may have antagonistic or supportive regulatory functions when compared with their leading strand (Yang, Phillips et al. 2011).

## 5.4.2 Different role of mir-126* in T cell and monocyte adhesion

Our results demonstrate for the first time that hsa-miR-126* modulated THP-1, but not Jurkat, adhesion to brain endothelium in static conditions. When the flow-based assay was used, a significant modulation by hsa-miR-126* on both Jurkat and THP-1 cells firm adhesion was observed. However, we observed contrasting results about T cell adhesion when inflammation was mimicked (miR-126* down-regulation). When hsa-miR-126* expression levels were decreased in BEC, T cell adhesion was unexpectedly prevented in a similar manner to the effect observed when hsa-miR-126* expression levels were increased. Jurkat cell adhesion to BEC may be more sensitive than THP-1 cells to a fine balance in the levels of miR-126* and its leading strand. It is possible that miR-126* can indirectly or directly target genes involved in intracellular pathways or adhesion molecules, which mediate selectively monocyte and T cell adhesion. For example, CCL7 is a predicted target of miR-126*, which has been reported to mediate preferentially monocyte adhesion (Gerard and Rollins 2001;

Mackay 2001), although to our knowledge CCL7 was not regulated by miR-126*. Regarding the observation that decreased levels of hsa-miR-126* lead to reduced T cell adhesion, we can speculate that decreasing miR-126* induces transcriptional activation of the *egfl7* gene (where miR-126 and -126* originate), increasing the endogenous levels of both miR-126 species (miR-126 and -126*) leading to reduced T cell adhesion. Indeed, miR-126* levels were reduced by transfection with anti-miR-126* but we observed in preliminary data that miR-126* down-regulation led to increased levels of miR-126 in hCMEC/D3 cells. This suggests a compensatory regulation or autoregulatory feedback that it taking place in miR responses which has been previously observed in different cell types of different species (Shen-Orr, Milo et al. 2002; Tsang, Zhu et al. 2007) such as miRs being involved in transcriptional control (Martinez, Ow et al. 2008). However, we have not produced any evidence of this regulatory mechanism for miR-126/-126* of transcription factors, nor on the effect of a possible complete depletion of miR126* on cell signalling. We can speculate that decreased level of miR-126* enhanced a positive feedback on production and expression of miR-126 which targets specific genes involved in T cell recruitment such as CXCL12, possibly leading to the prevention of T cell adhesion observed in hCMEC/D3 cells in Fig 5.4.

### 5.4.3 Effect of miR-126* modulation on its predicted targets in hCMEC/D3 cells

When a computational search to identify all possible miR-126* targets was performed, these targets were totally different from those for miR-126 due to the differences in the miR sequences. Two genes were chosen for further studies because they are known to be mediators of inflammation and leukocyte trafficking on brain

endothelium: CCL7 (Takeshita and Ransohoff 2012) and E-selectin (Wiese, Barthel et al. 2009). MiR-126* down-regulation led to a small increase in E-selectin protein expression on BEC, which may have mediated, at least partially, the observed increase in monocyte capture and firm adhesion. In addition, VCAM1 expression was not modulated by hsa-miR-126*, then THP-1 adhesion was probably mediated by other proteins likely modulated by hsa-miR-126* neither directly nor indirectly indicating that this CAM was not involved in the modulatory effect of hsa-miR-126* on leukocyte adhesion. By contrast, increased concentration of endothelial miR-126* prevented T cell and monocyte adhesion, but it did not significantly decrease E-selectin expression on hCMEC/D3 cells nor were cytokine-induced CCL7 levels affected. It is possible that CCL7 is not a direct target of miR-126* in hCMEC/D3 cells or that the effect of miR-126* on CCL7 is not sufficient to counteract the strong cytokine-inducing effect on CCL7 in hCMEC/D3 cells. Thus, it is likely that other endothelial gene targets than the ones investigated here are modulated by miR-126* such as fractalkine receptor, CD200 or CD44, which are known to promote adhesion.

## 5.5 Conclusions

Here, we report that human brain endothelial miR-126* regulates leukocyte adhesion to the human brain endothelium *in vitro* by a mechanism possibly involving partially E-selectin. In this study we reported for the first time that miR-126* plays a role in both monocytic and T cell adhesion.

## Chapter 6: The role of endothelial hsa-miR-155 in leukocyte adhesion to human brain endothelium

### 6.1 Introduction

miR-155 is a multifunctional miR (Faraoni, Antonetti et al. 2009) and plays a crucial role in both physiological processes (Kluiver, Poppema et al. 2005; Vigorito, Perks et al. 2007) such as innate immunity (Leng, Pan et al. 2011) and in pathologies such as cancer (Tili, Croce et al. 2009; Mattiske, Suetani et al. 2012), and inflammation (Leah 2011). In addition, miR-155 has been defined as a pro-inflammatory miR (O'Connell, Rao et al. 2012) induced by inflammatory cytokines including TNF$\alpha$ and IFN$\gamma$ and its expression was found either up/down-regulated in monocytes, macrophages, dendritic cells and epithelial cells (Kutty, Nagineni et al. 2010; Ponomarev, Veremeyko et al. 2013).

Hsa-miR-155 is up-regulated in human EC (Suarez, Wang et al. 2010) and in hCMEC/D3 cells (M.A. Lopez PhD thesis) by cytokines. Pulkkinen et al. reported that hsa-miR-155 expression in EC is triggered by TNF$\alpha$ via NF-$\kappa$B (Pulkkinen, Yla-Herttuala et al. 2011). In addition, hsa-miR-155 is up-regulated in brain lesions from MS patients (Junker, Krumbholz et al. 2009) and in human brain microvessels of ALMS (M.A. Lopez PhD thesis 2012).

Recent studies reported that miR-155 is indirectly involved in adhesion and migration. High expression of hsa-miR-155 in angiotensin II-activated HUVEC cells attenuated Jurkat T cell adhesion (Zhu, Zhang et al. 2011), while in gastric cancer cells (Li, Nie et al. 2012), ovarian cancer-initiating cells (Qin, Ren et al. 2013) and human cardiomyocyte progenitor cells (Liu, van Mil et al. 2012), has-miR-155 suppressed cell-cell adhesion and invasion by targeting SMAD2, claudin-1 and MMP-16, respectively.

## 6.2 Aims

To the best of our knowledge, no studies on the role of brain endothelial miR-155 in leukocyte adhesion have been previously reported in the literature. As shown previously, hsa-miR-155 was up-regulated in cytokine-treated hCMEC/D3 cells. In the screening at the beginning of Chapter 4, miR-155 modulated Jurkat adhesion under basal conditions. Here, we further investigated the role of hsa-miR-155 in leukocyte adhesion using the flow-based assay.

## 6.3 Results

### 6.3.1 Hsa-miR-155 modulates Jurkat and THP-1 static adhesion on hCMEC/D3 cells at basal level

As shown in Fig. 4.3, increased hsa-miR-155 levels in hCMEC/D3 cells, to simulate inflammatory conditions, led to increased with Jurkat cells. Here we observed increases THP-1 adhesion to resting hCMEC/D3 cells (Figs. 6.1 A and 6.2 A) but not in cytokine-activated EC (at 1 ng/ml). Lower concentration of cytokines (0.1 ng/ml), which still increased Jurkat T cell adhesion to hCMEC/D3 cells, did not induce any further increase in adhesion suggesting that either cytokine-induced increase in miR-155 levels are already sufficient to increase Jurkat and THP-1 adhesion or that the miR-155-mediated increase in cytokine-induced leukocyte adhesion is too small to be detected using a static assay.

Decreased levels of miR-155 by transfection with anti-hsa-miR-155 slightly reduced Jurkat (Fig. 6.1 B), but not THP-1 (Fig. 6.2 B) adhesion to endothelium under resting conditions. In cytokine-stimulated endothelium, down-regulation of hsa-miR-155 levels did not lead to significant differences in Jurkat or THP-1 adhesion to hCMEC/D3 cells (Figs. 6.1 and 6.2). These results would suggest that either cytokine-induced increases in miR-155 levels are not involved in the cytokine-induced increase in Jurkat and/or THP-1 adhesion or that the miR-155-mediated increase in cytokine-induced leukocyte adhesion is again too small to be detected using a static assay.
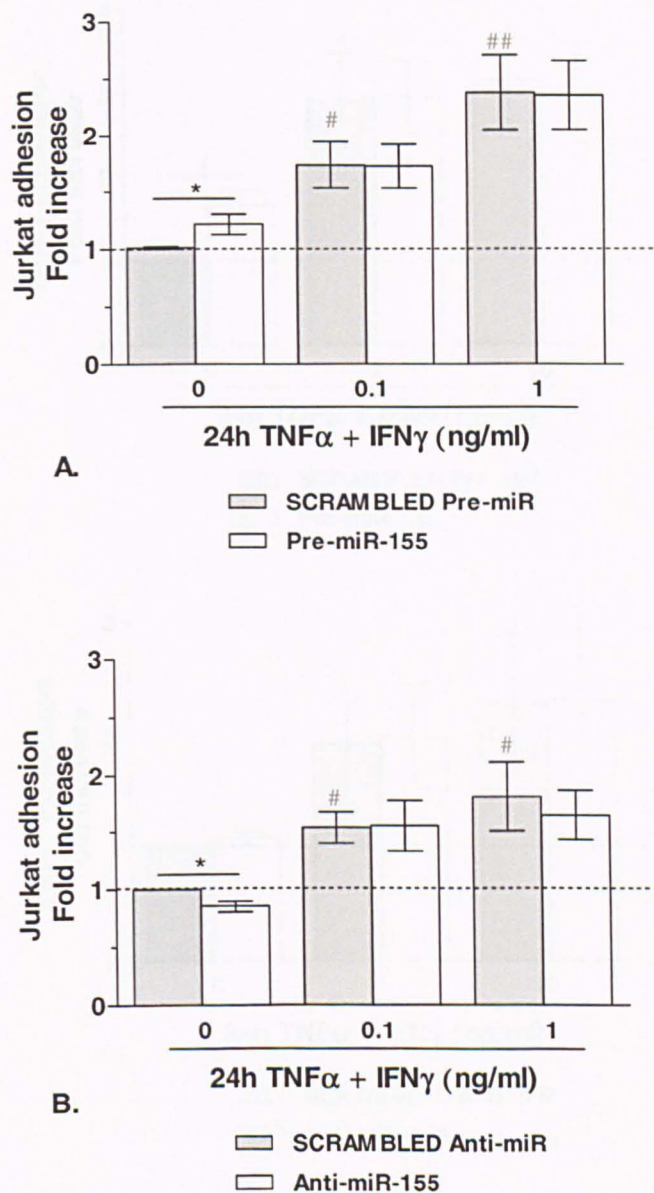
**Fig. 6.1: Hsa-miR-155 modulates Jurkat static adhesion on hCMEC/D3 cells.** hCMEC/D3 cells were transfected followed by treatment with a combination of cytokines (TNFα + IFNγ) at 0.1 and 1 ng/ml for 24 h. Results are expressed as fold increase over scrambled-transfected unstimulated cells. **A.** Scrambled Pre-miR or Pre-miR-155 were used to transfect hCMEC/D3 cells **B.** Scrambled Anti-miR or Anti-miR-155 were used to transfect hCMEC/D3 cells. Experiments were carried out three **A.** and four **B.** times with six replicates each. Data are mean ±SEM (*,#$P<0.05$, ##$P<0.01$, # significantly different vs. unstimulated cells, * significantly different when compared with scrambled Pre- or Anti-miR).
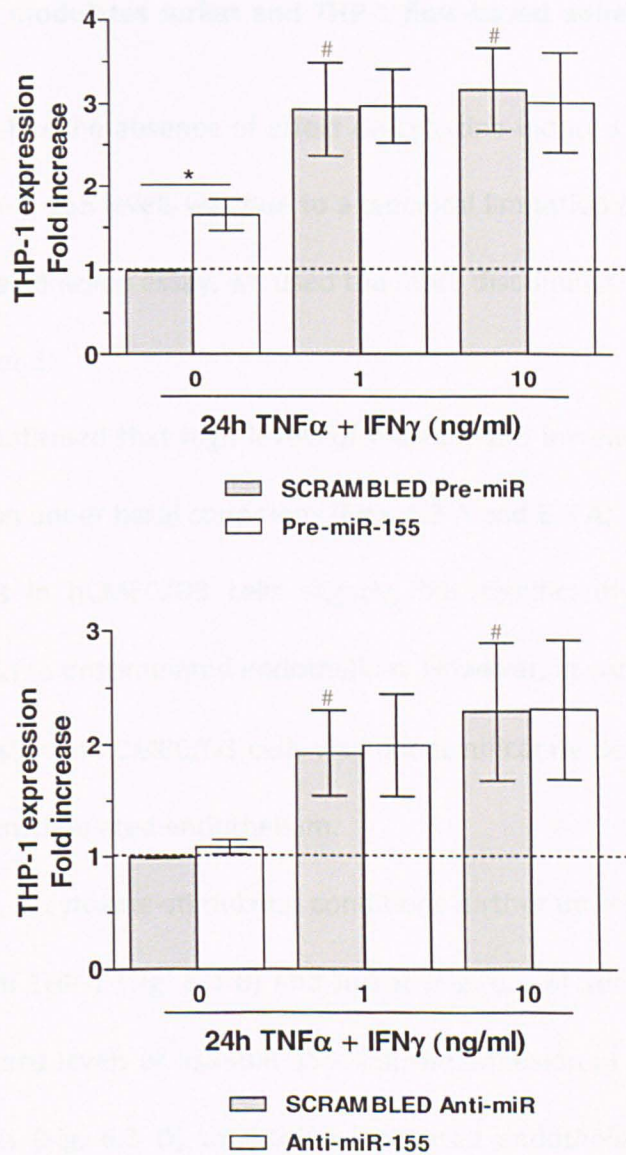
**Fig. 6.2: Hsa-miR-modulates THP-1 static adhesion on hCMEC/D3 cells.** hCMEC/D3 cells were transfected followed by treatment with a combination of cytokines (TNFα + IFNγ) at 1 and 10 ng/ml for 24 h. Fluorescence of adhered THP-1 cells (monocyte), is expressed as fold increase over scrambled-transfected unstimulated cells. **A.** Scrambled Pre-miR or Pre-miR-155 were used to transfect hCMEC/D3 cells **B.** Scrambled Anti-miR or Anti-miR-155 were used to transfect hCMEC/D3 cells. Experiments were carried out **A.** three and **B.** four times with six replicates each. Data are mean ±SEM (*,#P<0.05, ##P<0.01 # significantly different vs. unstimulated cells, * significantly different when compared with scrambled Pre- or Anti-miR).

## 6.3.2 Hsa-miR-155 modulates Jurkat and THP-1 flow-based adhesion on hCMEC/D3 cells

To determine whether the absence of effect on cytokine-induced leukocyte adhesion by modulation of miR-155 levels was due to a teecnical limitation of the method used, the static leukocyte adhesion assay, we used the more discriminating flow-based assay described in Chapter 3.

First, we confirmed that high levels of hsa-miR-155 increased both Jurkat and THP-1 firm adhesion under basal conditions (Figs. 6.3 A and 6.4 A). Moreover, reducing hsa-miR-155 levels in hCMEC/D3 cells slightly, but significantly, decreased THP-1 adhesion (Fig. 6.4 C) to unstimulated endothelium. However, in contrast with the static assay, Jurkat adhesion to hCMEC/D3 cells was not significantly decreased by reducing miR-155 levels in unstimulated endothelium.

In addition, in cytokine-stimulated conditions further up-regulation of hsa-miR-155 increased both THP-1 (Fig. 6.4 B) and Jurkat (Fig. 6.3 B) adhesion to hCMEC/D3 cells, while decreased levels of hsa-miR-155 reduced adhesion of both THP-1 (Fig. 6.4 D) and Jurkat cells (Fig. 6.3 D) to cytokine-activated endothelial cells under shear stress, by almost 50%.
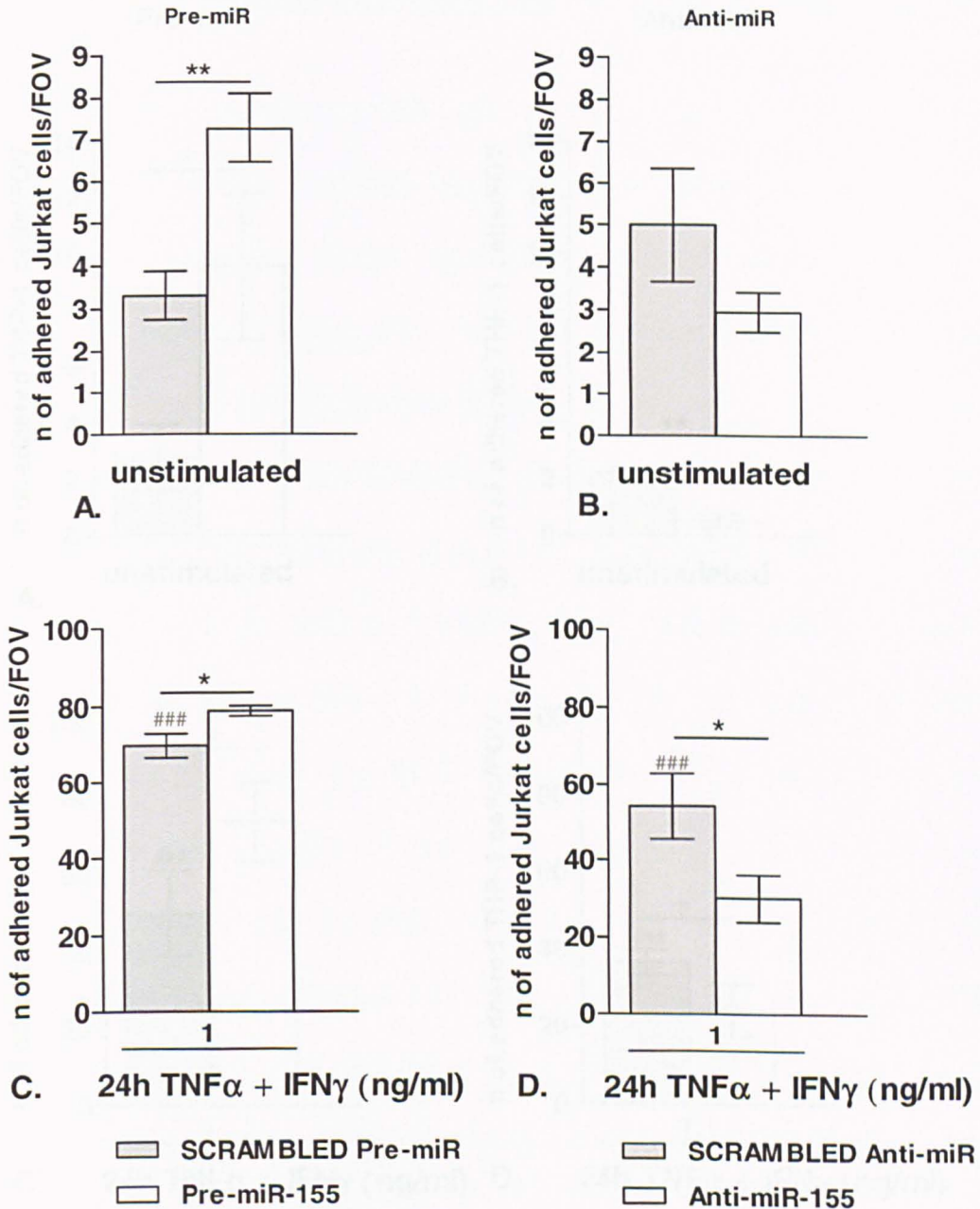
**Fig. 6.3: Hsa-miR-155 modulates Jurkat flow-based adhesion on hCMEC/D3 cells.** hCMEC/D3 cells were transfected followed by treatment with a combination of cytokines (TNFα + IFNγ) at 1 ng/ml for 24 h. Firmly adhered Jurkat cells to hCMEC/D3 cell monolayers were counted/field of view (FOV). **A.** and **C.** Scrambled Pre-miR or Pre-miR-155 were used to transfect hCMEC/D3 cells **B.** and **D.** Scrambled Anti-miR or Anti-miR-155 were used to transfect hCMEC/D3 cells. Experiments were carried out **C.** and **D.** three, **B.** four and **A.** six times with five replicates each. Data are mean ±SE (*$p<0.05$**$p<0.01$,###$p<0.001$ # significantly different vs. unstimulated cells, * significantly different when compared with scrambled Pre- or Anti-miR).
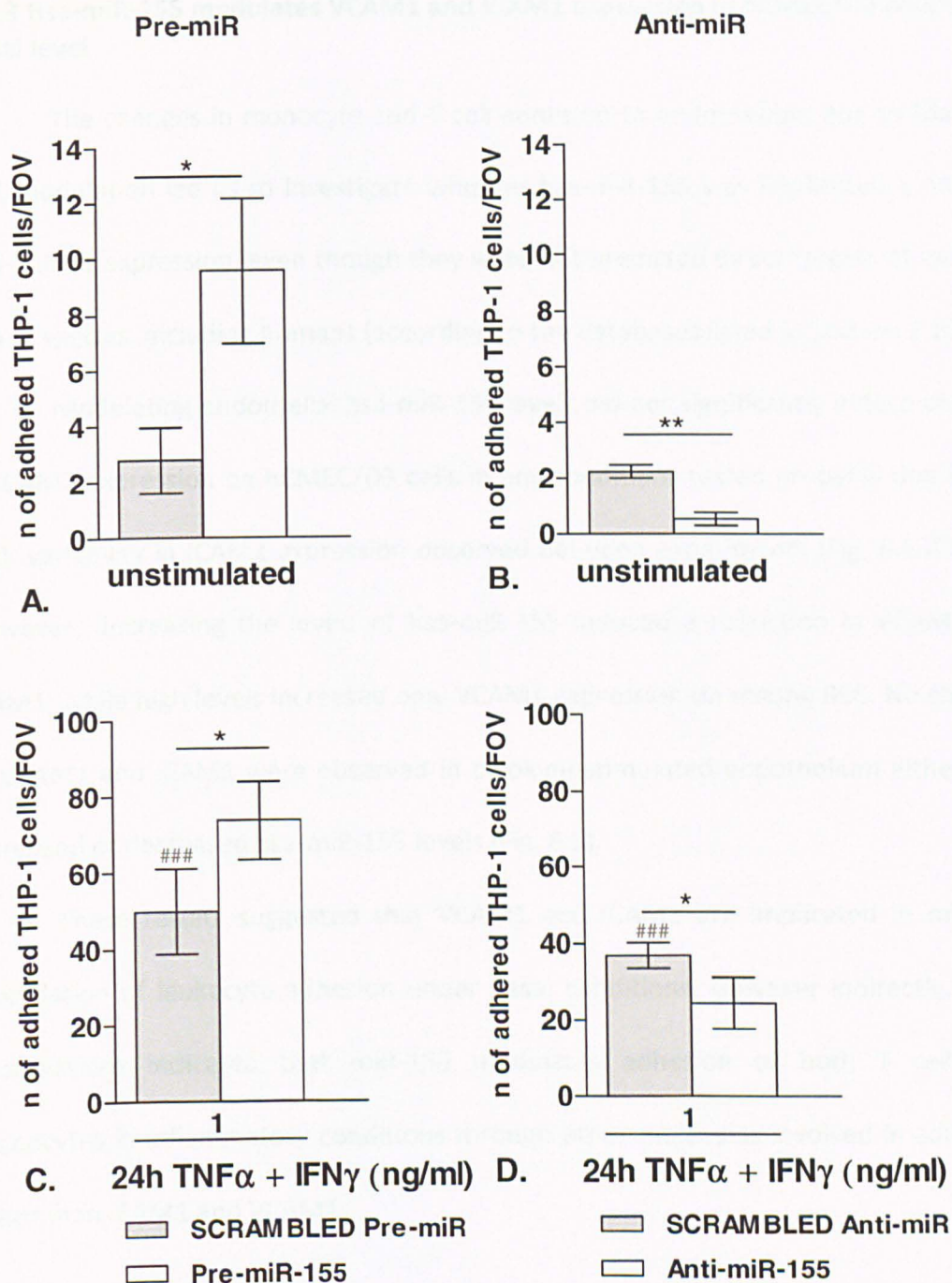
Fig. 6.4: Hsa-miR-155 modulates THP-1 flow-based adhesion to hCMEC/D3 cells. hCMEC/D3 cells were transfected followed by treatment with a combination of cytokines (TNFα + IFNγ) at 1 ng/ml for 24 h. Adhered THP-1 cells to hCMEC/D3 cell monolayers were counted/field of view (FOV). **A.** and **C.** Scrambled Pre-miR or Pre-miR-155 were used to transfect hCMEC/D3 cells **B.** and **D.** Scrambled Anti-miR or Anti-miR-155 were used to transfect hCMEC/D3 cells. Experiments were carried out **B.** three and **A., C.** and **D.** four times with five replicates each. Data are mean ±SEM (*$p<0.05$**$p<0.01$,###$p<0.001$ # significantly different vs. unstimulated cells, * significantly different when compared with scrambled Pre- or Anti-miR).

## 6.3.3 Hsa-miR-155 modulates VCAM1 and ICAM1 expression in hCMEC/D3 cells at basal level

The changes in monocyte and T cell adhesion to endothelium due to hsa-miR-155 modulation led us to investigate whether hsa-miR-155 was implicated in VCAM1 and ICAM1 expression, even though they were not predicted direct targets of miR-155 in any species, including humans (according to the databases listed in Section 2.10).

Modulating endothelial hsa-miR-155 levels did not significantly induce changes in ICAM2 expression on hCMEC/D3 cells in any conditions tested probably due to the high variability in ICAM2 expression observed between experiments (Fig. 6.5 ICAM2). However, decreasing the levels of hsa-miR-155 induced a reduction in VCAM1 and ICAM1, while high levels increased only VCAM1 expression on resting BEC. No changes in VCAM1 and ICAM1 were observed in cytokine-stimulated endothelium either with increased or decreased hsa-miR-155 levels (Fig. 6.5).

These results suggested that VCAM1 and ICAM1 are implicated in miR-155 modulation of leukocyte adhesion under basal conditions. However indirectly, these observations indicated that miR-155 modulates adhesion of both T cells and monocytes in inflammatory conditions through other molecules involved in adhesion, other than ICAM1 and VCAM1.
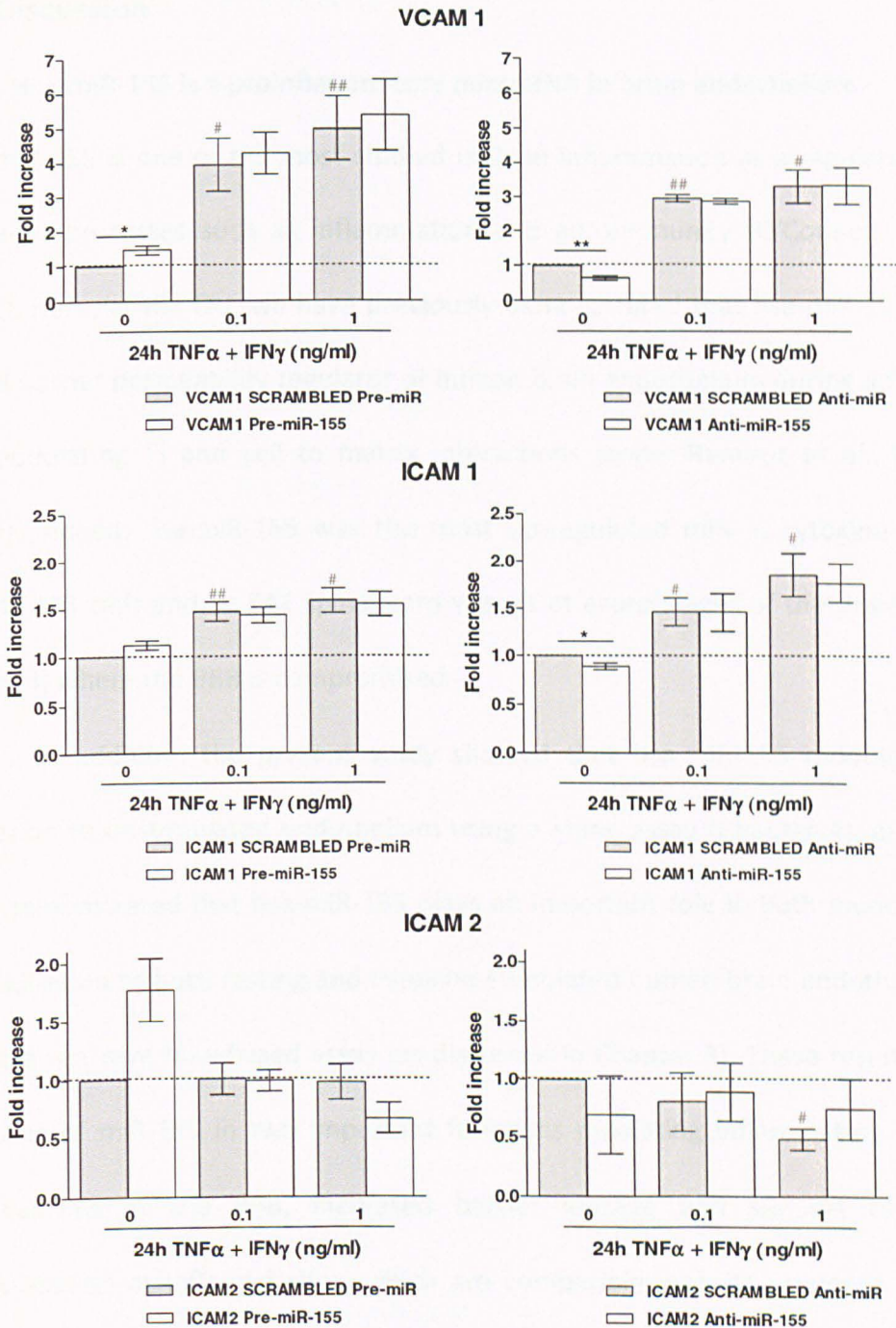
**Fig. 6.5: Hsa-miR-155 modulates VCAM1 and ICAM1 expression in hCMEC/D3 cells at basal level.** hCMEC/D3 cells were transfected followed by treatment with a combination of cytokines (TNFα + IFNγ) at different concentrations (0, 0.1 and 1 ng/ml) for 24 h. Anti-human-VCAM1, - ICAM1 and ICAM2 monoclonal antibodies were used to detect VCAM1, ICAM1 and ICAM2 expression levels by ELISA. Experiments were carried out three times with three replicates each. Data are mean ±SEM (*,#p<0.05**,##p<0.01 # significantly different vs. unstimulated cells, * significantly different when compared with scrambled Pre- or Anti-miR).

## 6.4 Discussion

### 6.4.1 Hsa-miR-155 is a proinflammatory microRNA in brain endothelium

hsa-miR-155 is one of the most studied miRs in inflammation as a regulator of many different processes such as inflammation and autoimmunity (O'Connell, Rao et al. 2012). Here, at the OU, we have previously demonstrated that hsa-miR-155 acts as a novel barrier permeability regulator of human brain endothelium during inflammation by modulating TJ and cell to matrix interactions (Lopez-Ramirez et al., PhD thesis 2012). Indeed, hsa-miR-155 was the most up-regulated miR in cytokine-stimulated hCMEC/D3 cells and, in EAE spinal cord vessels at acute stages of the disease (clinical score, 4) where the BBB is compromised.

In addition, the present study showed that hsa-miR-155 modulated Jurkat adhesion to unstimulated endothelium using a static assay (Chapter 4), and here we also demonstrated that hsa-miR-155 plays an important role in both monocyte and T cell adhesion to both resting and cytokine-stimulated human brain endothelium using a more sensitive flow-based assay (as discussed in Chapter 3). These results reinforce the role of miR-155 in two important functions mediating inflammatory pathogenic mechanisms at the BBB, increased barrier leakage and support of leukocyte extravasation at inflamed sites, which are compatible with its proposed function in contributing to the initiation of immune responses (Rodriguez, Vigorito et al. 2007; Vigorito, Perks et al. 2007; Kurowska-Stolarska, Alivernini et al. 2011).

## 6.4.2 Hsa-miR-155 promotes leukocyte adhesion and increased CAM expression in brain endothelium

We have shown that elevation of hsa-miR-155 levels in unstimulated human brain endothelium leads to increased expression of VCAM1 and ICAM1, probably leading to the small increases in T cell and monocye adhesion to these cells. Indeed, ICAM1 and VCAM1 are well know endothelial mediators of leukocyte adhesion in inflammation (Rijcken, Krieglstein et al. 2002; Engelhardt 2006). Interestingly, preliminary results carried out by our collaborators in Ottawa (Drs Danica Snatnimirovic and Arsalan Haqqani) using proteomic analysis of membrane proteins in hCMEC/D3 cells transfected with scrambled pre-miR oligonucleotides or pre-miR-155 confirmed VCAM1 and ICAM1 increased expression induced by elevated levels of miR-155 together with a decrease in ICAM2 expression (see Table in Appendix 2). However, our findings are in contrast with those of Zhu et al. who reported that increased levels of miR-155 prevented Jurkat adhesion to angiotensin II-stimulated HUVEC, and decreased VCAM1 and CCL2 mRNA relative expression (Zhu, Zhang et al. 2011).

Several factors may have been involved in the apparent discrepancy between our study and that of (Zhu, Zhang et al. 2011). First, Zhu et al. used a static leukocyte adhesion assay which we found to be less sensitive than the flow-based assay in discriminating miR actions on leukocyte adhesion. It is worth noting here that the experiments by Zhu et al. did not include unstimulated cells transfected with pre- or anti-miR-155, the only conditions in which an effect of miR-155 on leukocyte adhesion could be demonstrated using the static assay. Second, the effects of miR-155 may be cell-type specific, which may include endothelium from different vascular beds (HUVEC). It is well known that the modulatory actions of miRs on cell function depend

on the existence and/or abundance of their mRNA targets in a particular cell type (Lagos-Quintana, Rauhut et al. 2002). In addition, BEC are unique in their phenotype compared to endothelium from other vascular beds (Aird 2007). Hence, it is possible that different mRNA targets co-exist with miR-155 in HUVEC and brain endothelium.

Finally, the actions of miR-155 may also be specific to the stimulus used to activate endothelium. Angiotensin II induces endothelial dysfunction by increasing ICAM1 and VCAM1 expression (Nakashima, Suzuki et al. 2006) as does TNF$\alpha$. However, their signalling pathways and induced transcription factor activity are different (as discussed below) and could lead to different modulation of CAM expression by miR-155. Angiotensin II activates two signalling pathways related to vascular inflammation. First, it induces RhoA-mediated NF-$\kappa$B activation which is resposible for the trascription of molecules such as VCAM1, ICAM1 and IL-6, and second, the secreted IL-6 induces STAT3 to transcribe CCL2 (reviewed in (Han, Runge et al. 1999; Brasier 2010). Indeed, RhoA is a validated miR-155 target in murine mammary gland epithelial cells (Kong, Yang et al. 2008). By contrast, TNF$\alpha$ induces VCAM1, ICAM1 and E-selectin expression via either AP1 or the canonical NF-$\kappa$B pathway involving I$\kappa$B degradation, but not RhoA activation (Pober and Sessa 2007; Montgomery and Bowers 2012).

In addition, angiotensin-II receptor itself is a target for miR-155 in HUVEC (Martin, Lee et al. 2006) and it is likely that miR-155 may act as a negative feedback modulator of the angiotensin-induced response whereas miR-155 may still be a pro-inflammatory mediator in the presence of cytokines. All together, our findings are in line with all the literature supporting the theory that in neuroinflammatory conditions, miR-155 is up-regulated and regulates many pro-inflammatory processes (O'Connell, Rao et al. 2012).

## 6.4.3 Possible pro-inflammatory intracellular patwhays regulated by hsa-miR-155 in brain endothelium

MiRs can act directly or indirectly on transcription factors (Martinez, Ow et al. 2008; Zhou, Wang et al. 2011). Ets-1 is a transcription factor responsible for angiogenesis, vascular remodelling, inflammation (Sato 2001; Zhan, Brown et al. 2005) and adhesion in ECs . However, in resting hCMEC/D3 cells Est-1 seems barely expressed, although it increased eight times in cytokine-treated BEC (http://www.ncbi.nlm.nih.gov /projects/geo/query/acc.cgi?acc=GSE44694), so some of the differences in leukocyte adhesion observed between unstimulated and cytokine-treated endothelium may be due to the differential expression of this miR-155 target. Moreover, we can also speculate that Ets-1 targeting by miR-155 may lead to other functional consequences (Zhu, Zhang et al. 2011). Indeed, Ets-1 down-regulation decreases transactivation of egfl7 and leads to miR-126/-126* down-regulation (Harris, Yamakuchi et al. 2010), which would lead to increased VCAM1 expression and leukocyte adhesion as we observed in Chapters 4 and 5. Therefore, we cannot exlude that miR-155 acts indirectly on VCAM1 expression, by targeting different signalling pathways involved in leukocyte adhesion.

RhoA has been shown to be a target of miR-155 in epithelial cells (Kong, Yang et al. 2008), and of RhoA and PKC crosstalk in inflammatory conditions has been shown to be critical for TJ maintenance in BEC (He, Yin et al. 2012). In addition, it has been shown that ICAM1 crosslinking (mimicking interactions with LFA-1) activates Rho and induces actin cytoskeletal reorganization via PKC (Etienne, Adamson et al. 1998; Etienne-Manneville, Manneville et al. 2000). Taken together, these observations may suggest an anti-inflammatory role for miR-155 in the context of leukocyte adhesion.

However, it is important to stress here that, as with many so-called pro-inflammatory cytokines, miR-155 may be involved in different functions depending on disease state.

## 6.5 Conclusions

Here, we report that human brain endothelial miR-155 regulates leukocyte adhesion to the human brain endothelium *in vitro* possibly related to an indirect regulation of VCAM1 and ICAM1 expression.

# Chapter 7: General discussion

Neurodegenerative and autoimmune diseases such as MS are characterised by inflammation with subsequent increase of immune cell adhesion and infiltration from the blood to the CNS across the BBB. Immune cell adhesion to the BBB has been deeply studied. However, its molecular regulation remains to be fully elucidated. The overall aim of this thesis was to study whether brain endothelial miRs which expression was changed by TNFα and IFNγ-stimulation in hCMEC/D3 cells were involved in leukocyte adhesion and, if so, through which gene target/s.

Our results have shown that:

i) The hCMEC/D3 cells line is a suitable human *in vitro* model to study leukocyte adhesion to brain endothelium and to investigate brain endothelial miRs and their potential as novel therapeutic target to prevent leukocyte adhesion/infiltration in the CNS in disorders such as MS.

ii) A novel flow-based *in vitro* system, to mimic the blood flow in the brain microvasculature, coupled to a live cell imaging technique was successfully set up, to model leukocyte interactions with the human BBB, using the hCMEC/D3 cell line.

iii) We propose that out of the five more either up or down-rugulated miRs in cytokine-stimulated hCMEC/D3 cells tested, miR-126, miR-126* and miR-155 are significantly involved in the regulation of leukocyte adhesion by mechanisms that may involve, at least partially, endothelial CAM and chemokines.

## 7.1 A new flow-based *in vitro* system to study leukocyte adhesion to the human blood-brain barrier, using the hCMEC/D3 cell line as model

While focusing on leukocyte trafficking from the blood to tissues *in vitro*, mimicking the blood flow is one of the most challenging elements. Nevertheless, a variety of models have been set up in the past (Chapter 1, section 1.8.1), but all of them have limitations in term of cell culture treatments and number of cells required. However, we successfully developed a new flow-based system to mimic the microvasculature *in vivo* (Chapter 3). The system is based on commercially available six-channel chambers and hCMEC/D3 cells, in which we modulated intracellular miR levels by transfection. Compared to other commercially and custom-made available flow based systems to study adhesion, ours was easy to assemble, cost-effective and hCMEC/D3 cells formed proper monolayers and were easily transfected with synthetic miR sequences using small volumes. This flow-based system has allowed us to study leukocyte adhesion to brain endothelium, minimizing unspecific adhesion due to the discrimination of the flow. In addition, it was possible to detect small, but significant, changes in leukocyte adhesion due to regulation by miRs. The chamber allows six parallel experiments to be carried out simultaneously, and from each experiment/channel it was possible to capture more than ten FOV within the same experiment. In leukocyte trafficking research, flow-based *in vitro* systems and/or models have become necessary to better mimic *in vivo* conditions and to understand the fine mechanisms of immune cell trafficking across endothelium. Few *in vitro* systems have been established to study cell trafficking at the BBB, and no one to date has studied endothelial miRs. We believe that this new system can contribute to better understanding of the biology of both human brain microvasculature and leukocyte

trafficking, while improving the specificity, accuracy and quality of the research data. Although this system was developed in order to study leukocyte rolling, adhesion, crawling and migration under flow in a flexible, consistent and very accurate way, there are still many way to improve the chamber, tubing and the time-lapse microscopy/software. The chamber is not optimal to investigate migration/transmigration, because it lacks a lower part where migrated cells could physically be separated from the endothelium and be better quantified/studied. In addition, co-cultures or 3D cultures cannot be performed with this chamber. The closed system of tubing which connects syringes and chambers has connectors and tubing, that could be subjected to accumulation of pulled cells and/or bacterial contamination if used for long periods of time. To overcome this problem, silicone tubing with moulded fittings and connectors, custom designed, connected to a sterile closed container with silicone bottle stoppers and a sealing system could be used but to the expense of a higher cost. In addition, a de-bubbler between the chamber and the leukocyte bottle could be very helpful to avoid bubbles from entering the experimental channel.

To quantify the length of leukocyte-endothelial cell interactions prior to firm adhesion we captured one frame per second, which was the maximal capacity of our camera/software. To study rolling properly, it has been reported that twenty frames/second are required to be able to analyse rolling distances and speed, which requires a more powerful computer and camera.

## 7.2 Endothelial microRNAs as modulators of leukocyte adhesion to the human blood-brain barrier: miR-126, miR-126* and miR-155

The results of the current study show that the brain endothelial miR-126*, miR-126 and miR-155 regulate monocyte and T cell adhesion *in vitro* targeting molecules such as E-selectin VCAM1 and CCL2, either directly or indirectly (Fig 7.1). Prior to this work, Harris et al. reported that endothelial miR-126 regulates leukocyte adhesion in HUVEC via VCAM1 down-regulation (Harris, Yamakuchi et al. 2008) whereas another study showed miRs targeting another key cell adhesion molecule, ICAM1, where miR-222 and miR-339 promoted resistance of cancer cells to cytotoxic T lymphocytes via ICAM1 down-regulation (Ueda, Kohanbash et al. 2009). Our findings help to unravel miR regulation of leukocyte adhesion to endothelium, a field that to date is poorly understood. In particular, our finding - if confirmed *in vivo* - can improve understanding of the molecular regulation of leukocyte adhesion to human brain endothelium in inflammation. Furthermore, leukocyte adhesion is crucial event for neuroinflammatory diseases, then our approach might be translated into a possible molecular therapy, targeted at modulating the expression of up-/down-regulated miR in brain endothelium, such as miR-126, -126* and -155 (see Section 7.3).

We found that miR-126, -126* and -155 have a significant role in the regulation of leukocyte adhesion targeting different gene directly and indirectly. Overall, the results about miRs shown in this thesis are novel in the fields of BBB and neuroinflammation, introducing new brain endothelial players in monocyte and T cell adhesion in acute inflammation. However, *in vivo* studies need to be performed to investigate whether miR-126 and -126* are down-regulated in MS lesions with acute inflammation when compared to normal appearing white matter (NAWM) (Appendix

3). In addition, it would be interesting to perform further experiments to investigate which populations of PBMC from MS patients selectively adhere to BEC *in vitro*, and whether the modulation of miR-126, -126* and miR-155 specifically prevent adhesion of a particular leukocyte population. Furthermore, it would be interesting to modulate the levels of all three miRs in BEC in combination in order to dtermine whether synergistic effects occur when down-regulation of miR-126 and -126* and up-regulation of miR-155 occur concomitantly. In addition, modulation of miR levels that countreact the changes induced by cytokines would be informative to determine the relative contribution of these miR to the effect induced by cytokines.
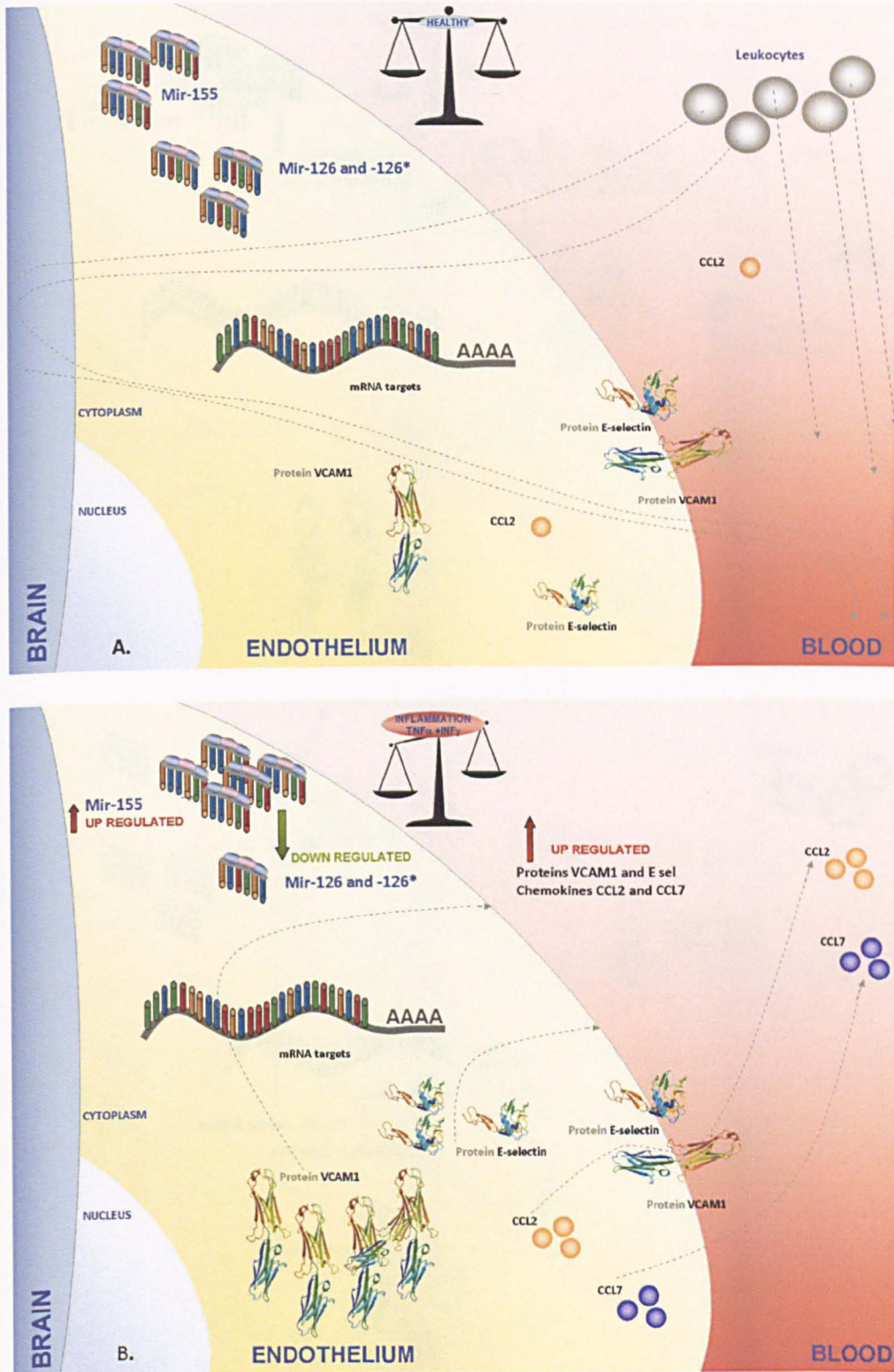
**Fig. 7.1: MiR-126, -126\*and -155 may prove therapeutic targets for leukocyte adhesion related disorders. A.** In healty conditions brain endothelium express normal levels of miRs, and proteins, while blood immune cells (leukocytes) exert their role of immunosurveillance. **B.** In inflammatory conditions (TNFα + IFNγ) the brain endothelium is activated, up-regulating the expression of VCAM1, E-selectin,CCL2 and CCL7 proteins and miR-155 and decreasing the level of miR-126 and -126\*. **C.** Cytokine-

activated endothelium leads to an increase in leukocyte adhesion to endothelium and possible migration to the brain triggering neuroinflammatory disease. **D.** Ectopic modulation of miR-155, -126 and -126* in brain endothelium, to couteract the cytokines effects, prevents leukocyte adhesion via VCAM1, CCL2 and E-selectin.
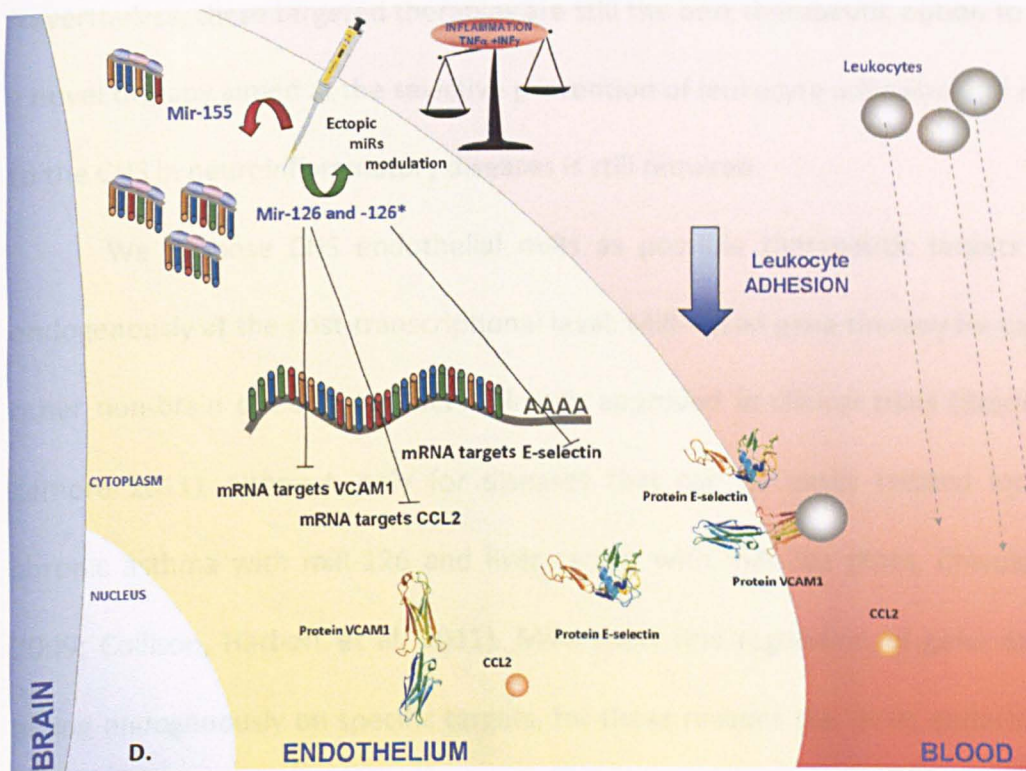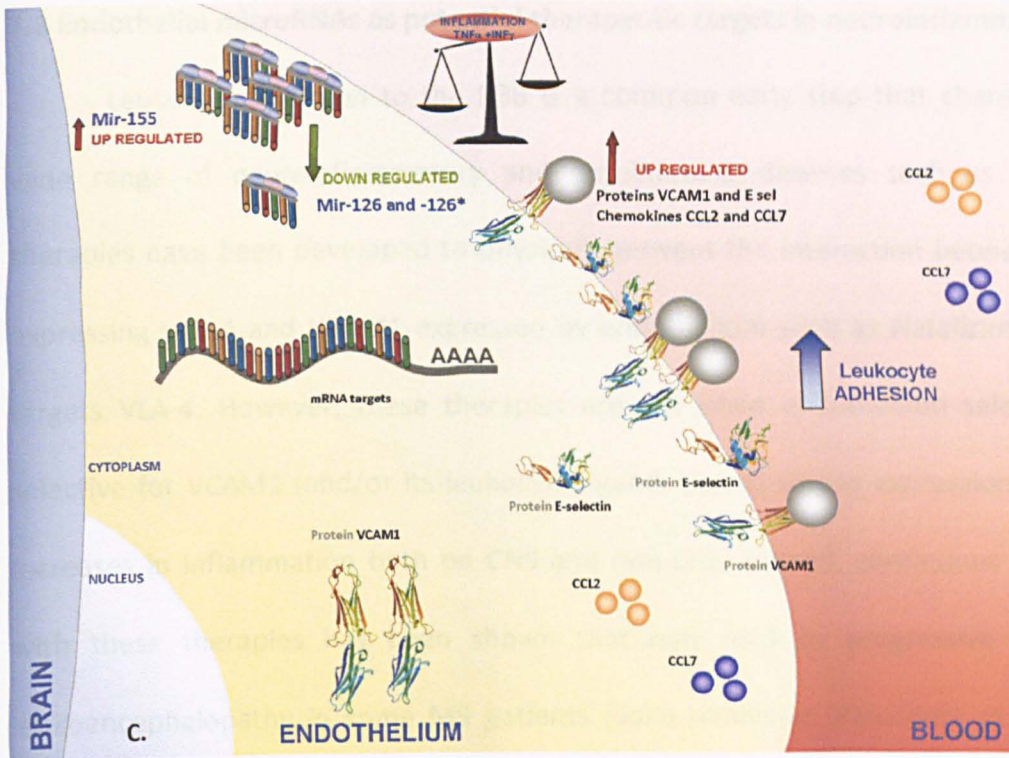
## 7.3 Endothelial microRNAs as potential therapeutic targets in neuroinflammation

Leukocyte adhesion to the BBB is a common early step that characterises a wide range of neuroinflammatory and autoimmune diseases such as MS. New therapies have been developed to physically prevent the interaction between T cells expressing VLA-4 and VCAM1 expressed by endothelium such as Natalizumab which targets VLA-4. However, these therapies are not brain endothelium selective, but selective for VCAM1 (and/or its leukocyte ligand, VLA-4) whose expression generally increases in inflammation both on CNS and non-CNS. Indeed, continuous treatment with these therapies has been shown that may lead to progressive multifocal leukoencephalopathy in some MS patients (Soilu-Hanninen, Paivarinta et al. 2013). Nevertheless, these targeted therapies are still the best therapeutic option to date but a novel therapy aimed at the selective prevention of leukocyte adhesion and migration to the CNS in neuroinflammatory diseases is still required.

We propose CNS endothelial miRs as possible therapeutic targets that act endogenously at the post-transcriptional level. MiR-based gene therapy for cancer and other non-brain diseases has been already approved in clinical trials (Broderick and Zamore 2011), although only for diseases that can be easily treated locally such chronic asthma with miR-126 and liver cancer with miR-26a (Kota, Chivukula et al. 2009; Collison, Herbert et al. 2011). MiRs exert fine regulation of gene expression, acting endogenously on specific targets, for these reasons the three endothelial miRs identified in the present study could be targeted in combination as a potential therapy to decrease leukocyte adhesion in autoimmune diseases such as MS, that is, by specifically increasing miR-126 and 126* with mimetics and decreasing miR-155 with antagomiRs in CNS endothelium. However, to prove their potential *in vivo*, an

adequate delivery system would still be required. Some of the miR delivery systems *in vivo* are based on recombinant adeno-associated viruses (Christensen, Larsen et al. 2010), rabies virus glycoprotein-disulphite linked PEI nanocarriers (Hwang do, Son et al. 2011), cationic lipoplexes injected systemically (Wu, Crawford et al. 2013), but no specific miR-delivery tools for BEC have been tested *in vivo*. Since miRs are species-specific and tissue-specific, further work may look for more specific miR targets belonging to endothelial pathways involved in leukocyte adhesion to inflamed CNS endothelium.

# Chapter 8: References

**Ehrlich**, P. (1885) Das Sauerstoff-Bedu¨rfnis des Organismus. Eine farbenanalytische Studie. [On the oxygen consumption of the body. A study using intravital dyes.], Verlag von August Hirschwald, Berlin

**Lewandowski**, M. (1900) Zur Lehre von der Cerebrospinalflu¨ssigkeit.[On the cerebrospinal fluid.]. Z. Klein Forsch. 40, 480–494

**Goldmann**, E. (1913) Vitalfa¨rbungen am Zentralnervensystem. Beitrag zur Physio-Pathologie des Plexus Choroideus und der Hirnha¨ute. [Intravital labelling of the central nervous system. A study on the pathophysiology of the choroid plexus and the meninges.] Abhandlungen der ko¨niglich preußischen Akademie der Wissenschaften. Physikalisch-Mathematische Classe 1, 1–64

Abbassi, O., T. K. Kishimoto, et al. (1993). "E-selectin supports neutrophil rolling in vitro under conditions of flow." J Clin Invest **92**(6): 2719-2730.

Abbott, N. J. (2000). "Inflammatory Mediators and Modulation of Blood–Brain Barrier Permeability." Cellular and Molecular Neurobiology **20**(2): 131-147.

Abbott, N. J., A. A. Patabendige, et al. (2010). "Structure and function of the blood-brain barrier." Neurobiol Dis **37**(1): 13-25.

Abbott, N. J., L. Ronnback, et al. (2006). "Astrocyte-endothelial interactions at the blood-brain barrier." Nat Rev Neurosci **7**(1): 41-53.

Aird, W. C. (2007). "Phenotypic heterogeneity of the endothelium: I. Structure, function, and mechanisms." Circ Res **100**(2): 158-173.

Aird, W. C. (2007). "Phenotypic heterogeneity of the endothelium: II. Representative vascular beds." Circ Res **100**(2): 174-190.

Alexander, J. S., R. Zivadinov, et al. (2011) "Multiple sclerosis and cerebral endothelial dysfunction: Mechanisms." Pathophysiology In Press, Corrected Proof.

Allan, S. M. and N. J. Rothwell (2001). "Cytokines and acute neurodegeneration." Nat Rev Neurosci **2**(10): 734-744.

Aloisi, F., F. Ria, et al. (1999). "Relative efficiency of microglia, astrocytes, dendritic cells and B cells in naive CD4+ T cell priming and Th1/Th2 cell restimulation." Eur J Immunol **29**(9): 2705-2714.

Aloisi, F., F. Ria, et al. (1998). "Microglia are more efficient than astrocytes in antigen processing and in Th1 but not Th2 cell activation." J Immunol **160**(10): 4671-4680.

Alon, R., H. Rossiter, et al. (1994). "Distinct cell surface ligands mediate T lymphocyte attachment and rolling on P and E selectin under physiological flow." J Cell Biol **127**(5): 1485-1495.

Alsam, S., K. S. Kim, et al. (2003). "Acanthamoeba interactions with human brain microvascular endothelial cells." Microbial Pathogenesis **35**(6): 235-241.

Alvarez, J. I., R. Cayrol, et al. 2011 "Disruption of central nervous system barriers in multiple sclerosis." Biochimica et Biophysica Acta (BBA) - Molecular Basis of Disease

Ando, J., H. Tsuboi, et al. (1994). "Shear stress inhibits adhesion of cultured mouse endothelial cells to lymphocytes by downregulating VCAM-1 expression." Am J Physiol 267(3 Pt 1): C679-687.

Ando, J. and K. Yamamoto (2013). "Flow detection and calcium signaling in vascular endothelial cells." Cardiovasc Res.

Armulik, A., G. Genove, et al. (2010). "Pericytes regulate the blood-brain barrier." Nature 468(7323): 557-561.

Arner, E., N. Mejhert, et al. (2012). "Adipose tissue microRNAs as regulators of CCL2 production in human obesity." Diabetes 61(8): 1986-1993.

Asgeirsdottir, S. A., C. van Solingen, et al. (2012). "MicroRNA-126 contributes to renal microvascular heterogeneity of VCAM-1 protein expression in acute inflammation." Am J Physiol Renal Physiol 302(12): F1630-1639.

Baek, D., J. Villen, et al. (2008). "The impact of microRNAs on protein output." Nature 455(7209): 64-71.

Baggiolini, M. (1998). "Chemokines and leukocyte traffic." Nature 392(6676): 565-568.

Bahbouhi, B., L. Berthelot, et al. (2009). "Peripheral blood CD4+ T lymphocytes from multiple sclerosis patients are characterized by higher PSGL-1 expression and transmigration capacity across a human blood-brain barrier-derived endothelial cell line." J Leukoc Biol 86(5): 1049-1063.

Bahra, P., G. E. Rainger, et al. (1998). "Each step during transendothelial migration of flowing neutrophils is regulated by the stimulatory concentration of tumour necrosis factor-alpha." Cell Adhes Commun 6(6): 491-501.

Bandyopadhyay, S. and R. Mitra (2009). "TargetMiner: microRNA target prediction with systematic identification of tissue-specific negative examples." Bioinformatics 25(20): 2625-2631.

Banks, W. A. and M. A. Erickson (2010) "The blood-brain barrier and immune function and dysfunction." Neurobiology of Disease 37(1): 26-32.

Barczyk, M., S. Carracedo, et al. (2010). "Integrins." Cell Tissue Res 339(1): 269-280.

Bartel, D. P. (2004). "MicroRNAs: Genomics, Biogenesis, Mechanism, and Function." Cell 116(2): 281-297.

Bartel, D. P. (2009). "MicroRNAs: Target Recognition and Regulatory Functions." Cell 136(2): 215-233.

Bartholomaus, I., N. Kawakami, et al. (2009). "Effector T cell interactions with meningeal vascular structures in nascent autoimmune CNS lesions." Nature 462(7269): 94-98.

Battistini, L., L. Piccio, et al. (2003). "CD8+ T cells from patients with acute multiple sclerosis display selective increase of adhesiveness in brain venules: a critical role for P-selectin glycoprotein ligand-1." Blood 101(12): 4775-4782.

Bazzoni, G. and E. Dejana (2004). "Endothelial cell-to-cell junctions: molecular organization and role in vascular homeostasis." Physiol Rev 84(3): 869-901.

Bechmann, I., I. Galea, et al. (2007). "What is the blood-brain barrier (not)?" Trends Immunol 28(1): 5-11.

Begley, D. J. (2003). "Understanding and circumventing the blood-brain barrier." Acta Paediatr Suppl 92(443): 83-91.

Begley, D. J. (2004). ABC Transporters and the Blood-Brain Barrier. Current Pharmaceutical Design, Bentham Science Publishers Ltd. 10: 1295-1312.

Bell, R. D., E. A. Winkler, et al. (2010). "Pericytes control key neurovascular functions and neuronal phenotype in the adult brain and during brain aging." Neuron 68(3): 409-427.

Benoit, M. R., C. G. Conant, et al. (2010). "New device for high-throughput viability screening of flow biofilms." Appl Environ Microbiol 76(13): 4136-4142.

Bernstein, E., A. A. Caudy, et al. (2001). "Role for a bidentate ribonuclease in the initiation step of RNA interference." Nature 409(6818): 363-366.

Beste, M. T. and D. A. Hammer (2008). "Selectin catch-slip kinetics encode shear threshold adhesive behavior of rolling leukocytes." Proc Natl Acad Sci U S A 105(52): 20716-20721.

Betz, A. L. (1986). "Transport of ions across the blood-brain barrier." Fed Proc 45(7): 2050-2054.

Bevilacqua, M. P. and R. M. Nelson (1993). "Selectins." J Clin Invest 91(2): 379-387.

Bevilacqua, M. P., J. S. Pober, et al. (1987). "Identification of an inducible endothelial-leukocyte adhesion molecule." Proc Natl Acad Sci U S A 84(24): 9238-9242.

Bi, Y., G. Liu, et al. (2009). "MicroRNAs: Novel Regulators During the Immune Response." Journal of Cellular Physiology 218(3): 467-472.

Bodenheimer, T. S. and M. W. Brightman (1968). "A blood-brain barrier to peroxidase in capillaries surrounded by perivascular spaces." Am J Anat 122(2): 249-267.

Boehm, U., T. Klamp, et al. (1997). "Cellular responses to interferon-gamma." Annu Rev Immunol 15: 749-795.

Bonfanti, R., B. C. Furie, et al. (1989). "PADGEM (GMP140) is a component of Weibel-Palade bodies of human endothelial cells." Blood 73(5): 1109-1112.

Bouïs, D., G. Hospers, et al. (2001). "Endothelium in vitro: A review of human vascular endothelial cell lines for blood vessel-related research." Angiogenesis 4(2): 91-102.

Brachvogel, B., F. Pausch, et al. (2007). "Isolated Anxa5+/Sca-1+ perivascular cells from mouse meningeal vasculature retain their perivascular phenotype in vitro and in vivo." Experimental Cell Research 313(12): 2730-2743.

Bradl, M. and H. Lassmann (2009). "Progressive multiple sclerosis." Seminars in Immunopathology 31(4): 455-465.

Bradley, J. R., S. Thiru, et al. (1995). "Disparate localization of 55-kd and 75-kd tumor necrosis factor receptors in human endothelial cells." Am J Pathol 146(1): 27-32.

Brasier, A. R. (2010). "The nuclear factor-kappaB-interleukin-6 signalling pathway mediating vascular inflammation." Cardiovasc Res 86(2): 211-218.

Brightman, M. W. and T. S. Reese (1969). "Junctions between intimately apposed cell membranes in the vertebrate brain." J Cell Biol 40(3): 648-677.

Broderick, J. A. and P. D. Zamore (2011). "MicroRNA therapeutics." Gene Ther 18(12): 1104-1110.

Brown, D. C. and R. S. Larson (2001). "Improvements to parallel plate flow chambers to reduce reagent and cellular requirements." BMC Immunol 2: 9.

Brunk, D. K. and D. A. Hammer (1997). "Quantifying rolling adhesion with a cell-free assay: E-selectin and its carbohydrate ligands." Biophys J 72(6): 2820-2833.

Burton, V. J., L. M. Butler, et al. (2011). "Delay of migrating leukocytes by the basement membrane deposited by endothelial cells in long-term culture." Exp Cell Res 317(3): 276-292.

Butcher, E. C. (1991). "Leukocyte-endothelial cell recognition: Three (or more) steps to specificity and diversity." Cell **67**(6): 1033-1036.

Butt, A. M., H. C. Jones, et al. (1990). "Electrical resistance across the blood-brain barrier in anaesthetized rats: a developmental study." J Physiol **429**: 47-62.

Byrd, A. E., I. V. Aragon, et al. (2012). "MicroRNA-30c-2* limits expression of proadaptive factor XBP1 in the unfolded protein response." J Cell Biol **196**(6): 689-698.

Calabresi, P. A., A. Prat, et al. (2001). "T lymphocytes conditioned with Interferon beta induce membrane and soluble VCAM on human brain endothelial cells." J Neuroimmunol **115**(1-2): 161-167.

Carissimi, C., V. Fulci, et al. (2009). "MicroRNAs: Novel regulators of immunity." Autoimmunity Reviews **8**(6): 520-524.

Carlos, T. and J. Harlan (1994). "Leukocyte-endothelial adhesion molecules." Blood **84**(7): 2068-2101.

Carlos, T., N. Kovach, et al. (1991). "Human monocytes bind to two cytokine-induced adhesive ligands on cultured human endothelial cells: endothelial-leukocyte adhesion molecule-1 and vascular cell adhesion molecule-1." Blood **77**(10): 2266-2271.

Carrithers, M. D., I. Visintin, et al. (2000). "Differential adhesion molecule requirements for immune surveillance and inflammatory recruitment." Brain **123** ( Pt 6): 1092-1101.

Carthew, R. and E. Sontheimer (2009). "Origins and mechanisms of miRNAs and siRNAs." Cell **136**(4): 642-655.

Cassatella, M. A., S. Gasperini, et al. (1997). "Regulated production of the interferon-gamma-inducible protein-10 (IP-10) chemokine by human neutrophils." Eur J Immunol **27**(1): 111-115.

Cayrol, R., K. Wosik, et al. (2008). "Activated leukocyte cell adhesion molecule promotes leukocyte trafficking into the central nervous system." Nat Immunol **9**(2): 137-145.

Celie, J. W., R. H. Beelen, et al. (2009). "Heparan sulfate proteoglycans in extravasation: assisting leukocyte guidance." Front Biosci **14**: 4932-4949.

Ceribelli, A., M. Satoh, et al. (2012). "MicroRNAs and autoimmunity." Curr Opin Immunol **24**(6): 686-691.

Chakravorty, S. J., H. M. McGettrick, et al. (2006). "An in vitro model for analysing neutrophil migration into and away from the sub-endothelial space: Roles of flow and CD31." Biorheology **43**(1): 71-82.

Chan, J. R., S. J. Hyduk, et al. (2001). "Chemoattractants induce a rapid and transient upregulation of monocyte alpha4 integrin affinity for vascular cell adhesion molecule 1 which mediates arrest: an early step in the process of emigration." J Exp Med **193**(10): 1149-1158.

Chandrasekharan, U. M., M. Siemionow, et al. (2007). "Tumor necrosis factor alpha (TNF-alpha) receptor-II is required for TNF-alpha-induced leukocyte-endothelial interaction in vivo." Blood **109**(5): 1938-1944.

Charles, W. W., L. H. Karen, et al. (1997). "TNF-Î± and IL-1 Upregulate Membrane-Bound and Soluble E-Selectin through a Common Pathway." The Journal of surgical research **73**(2): 107-112.

Charo, I. F. and R. M. Ransohoff (2006). "The many roles of chemokines and chemokine receptors in inflammation." N Engl J Med **354**(6): 610-621.

Chen, T., Z. Huang, et al. (2009). "MicroRNA-125a-5p partly regulates the inflammatory response, lipid uptake, and ORP9 expression in oxLDL-stimulated monocyte/macrophages." Cardiovasc Res **83**(1): 131-139.

Cheng, Y., W. Kuang, et al. (2012). "Downregulation of miR-27a* and miR-532-5p and upregulation of miR-146a and miR-155 in LPS-induced RAW264.7 macrophage cells." Inflammation **35**(4): 1308-1313.

Chigaev, A., G. Zwartz, et al. (2003). "Alpha4beta1 integrin affinity changes govern cell adhesion." J Biol Chem **278**(40): 38174-38182.

Christensen, M., L. A. Larsen, et al. (2010). "Recombinant Adeno-Associated Virus-Mediated microRNA Delivery into the Postnatal Mouse Brain Reveals a Role for miR-134 in Dendritogenesis in Vivo." Front Neural Circuits **3**: 16.

Chuang, S. Y., S. H. Yang, et al. (2011). "Cilostazol reduces MCP-1-induced chemotaxis and adhesion of THP-1 monocytes by inhibiting CCR2 gene expression." Biochem Biophys Res Commun **411**(2): 402-408.

Chun, H. B., M. Scott, et al. (2011). "The proteome of mouse brain microvessel membranes and basal lamina." J Cereb Blood Flow Metab **31**(12): 2267-2281.

Cinamon, G. and R. Alon (2003). "A real time in vitro assay for studying leukocyte transendothelial migration under physiological flow conditions." J Immunol Methods **273**(1-2): 53-62.

Cinamon, G., V. Shinder, et al. (2001). "Shear forces promote lymphocyte migration across vascular endothelium bearing apical chemokines." Nat Immunol **2**(6): 515-522.

Coisne, C., C. Faveeuw, et al. (2006). "Differential expression of selectins by mouse brain capillary endothelial cells in vitro in response to distinct inflammatory stimuli." Neurosci Lett **392**(3): 216-220.

Coisne, C., R. Lyck, et al. (2013). "Live cell imaging techniques to study T cell trafficking across the blood-brain barrier in vitro and in vivo." Fluids Barriers CNS **10**(1): 7.

Collison, A., C. Herbert, et al. (2011). "Altered expression of microRNA in the airway wall in chronic asthma: miR-126 as a potential therapeutic target." BMC Pulm Med **11**: 29.

Coman, I., M. S. Aigrot, et al. 2006 "Nodal, paranodal and juxtaparanodal axonal proteins during demyelination and remyelination in multiple sclerosis." Brain **129**(12): 3186-3195.

Comerford, I. and S. R. McColl (2011). "Mini-review series: focus on chemokines." Immunol Cell Biol **89**(2): 183-184.

Compston, A. and A. Coles (2008). "Multiple sclerosis." The Lancet **372**(9648): 1502-1517.

Constantin, G. (2008). "Chemokine signaling and integrin activation in lymphocyte migration into the inflamed brain." J Neuroimmunol **198**(1-2): 20-26.

Constantinescu, A. A., H. Vink, et al. (2003). "Endothelial cell glycocalyx modulates immobilization of leukocytes at the endothelial surface." Arterioscler Thromb Vasc Biol **23**(9): 1541-1547.

Constantinescu, C. S. and B. Gran (2010). "Multiple sclerosis: autoimmune associations in multiple sclerosis." Nat Rev Neurol **6**(11): 591-592.

Couty, J. P., C. Rampon, et al. (2007). "PECAM-1 engagement counteracts ICAM-1-induced signaling in brain vascular endothelial cells." J Neurochem **103**(2): 793-801.

Cox, M. B., M. J. Cairns, et al. (2010). "MicroRNAs miR-17 and miR-20a inhibit T cell activation genes and are under-expressed in MS whole blood." PLoS One **5**(8): e12132.

Crawford, M., E. Brawner, et al. (2008). "MicroRNA-126 inhibits invasion in non-small cell lung carcinoma cell lines." Biochem Biophys Res Commun **373**(4): 607-612.

Cucullo, L., P. O. Couraud, et al. (2008). "Immortalized human brain endothelial cells and flow-based vascular modeling: a marriage of convenience for rational neurovascular studies." J Cereb Blood Flow Metab **28**(2): 312-328.

Cucullo, L., M. Hossain, et al. (2011). "The role of shear stress in Blood-Brain Barrier endothelial physiology." BMC Neurosci **12**: 40.

Cucullo, L., M. Hossain, et al. (2013). "A new dynamic in vitro modular capillaries-venules modular system: cerebrovascular physiology in a box." BMC Neurosci **14**: 18.

Cucullo, L., N. Marchi, et al. (2011). "A dynamic in vitro BBB model for the study of immune cell trafficking into the central nervous system." J Cereb Blood Flow Metab **31**(2): 767-777.

Cucullo, L., M. S. McAllister, et al. (2002). "A new dynamic in vitro model for the multidimensional study of astrocyte-endothelial cell interactions at the blood-brain barrier." Brain Res **951**(2): 243-254.

Czech, B., R. Zhou, et al. (2009). "Hierarchical rules for Argonaute loading in Drosophila." Mol Cell **36**(3): 445-456.

Dai, R. and S. A. Ahmed (2011) "MicroRNA, a new paradigm for understanding immunoregulation, inflammation, and autoimmune diseases." Translational Research **157**(4): 163-179.

Daneman, R., L. Zhou, et al. (2010). "Pericytes are required for blood-brain barrier integrity during embryogenesis." Nature **468**(7323): 562-566.

Dasgupta, S., M. Yanagisawa, et al. (2007). "Tumor necrosis factor-alpha up-regulates glucuronosyltransferase gene expression in human brain endothelial cells and promotes T-cell adhesion." J Neurosci Res **85**(5): 1086-1094.

Davson, H. and W. H. Oldendorf (1967). "Symposium on membrane transport. Transport in the central nervous system." Proceedings of the Royal Society of Medicine **60**(4): 326-329.

de Fougerolles, A. R., S. A. Stacker, et al. (1991). "Characterization of ICAM-2 and evidence for a third counter-receptor for LFA-1." J Exp Med **174**(1): 253-267.

de Vries, H. E., M. C. Blom-Roosemalen, et al. (1996). "The influence of cytokines on the integrity of the blood-brain barrier in vitro." J Neuroimmunol **64**(1): 37-43.

Dentelli, P., A. Rosso, et al. (2010). "microRNA-222 controls neovascularization by regulating signal transducer and activator of transcription 5A expression." Arterioscler Thromb Vasc Biol **30**(8): 1562-1568.

Desai, S. Y., M. Marroni, et al. (2002). "Mechanisms of endothelial survival under shear stress." Endothelium **9**(2): 89-102.

Diacovo, T. G., S. J. Roth, et al. (1996). "Interactions of human alpha/beta and gamma/delta T lymphocyte subsets in shear flow with E-selectin and P-selectin." J Exp Med **183**(3): 1193-1203.

Diaz, R., J. Silva, et al. (2008). "Deregulated expression of miR-106a predicts survival in human colon cancer patients." Genes Chromosomes Cancer **47**(9): 794-802.

Dong, Y. and E. N. Benveniste (2001). "Immune function of astrocytes." Glia **36**(2): 180-190.

Dore-Duffy, P. (2008). Pericytes: Pluripotent Cells of the Blood Brain Barrier. Current Pharmaceutical Design, Bentham Science Publishers Ltd. **14**: 1581-1593.

Dore-Duffy, P. and K. Cleary (2011). "Morphology and properties of pericytes." Methods Mol Biol **686**: 49-68.

Dueck, A. and G. Meister (2010) "MicroRNA processing without Dicer." Genome Biology **11**(6): 123.

Dyment, D. A., G. C. Ebers, et al. (2004). "Genetics of multiple sclerosis." The Lancet Neurology **3**(2): 104-110.

Ebnet, K. (2008). "Organization of multiprotein complexes at cell-cell junctions." Histochem Cell Biol **130**(1): 1-20.

Efremov, A. and J. Cao (2011). "Bistability of cell adhesion in shear flow." Biophys J **101**(5): 1032-1040.

Engelhardt, B. (2006). "Molecular mechanisms involved in T cell migration across the blood-brain barrier." J Neural Transm **113**(4): 477-485.

Engelhardt, B. (2006). "Regulation of immune cell entry into the central nervous system." Cell Communication in Nervous and Immune System: 259-280.

Engelhardt, B. (2008). "Immune cell entry into the central nervous system: Involvement of adhesion molecules and chemokines." Journal of the Neurological Sciences **274**(1-2): 23-26.

Engelhardt, B. and C. Coisne (2011). "Fluids and barriers of the CNS establish immune privilege by confining immune surveillance to a two-walled castle moat surrounding the CNS castle." Fluids Barriers CNS **8**(1): 4.

Engelhardt, B. and R. M. Ransohoff (2005). "The ins and outs of T-lymphocyte trafficking to the CNS: anatomical sites and molecular mechanisms." Trends Immunol **26**(9): 485-495.

Engelhardt, B. and R. M. Ransohoff (2012). "Capture, crawl, cross: the T cell code to breach the blood-brain barriers." Trends Immunol **33**(12): 579-589.

Engelhardt, B. and L. Sorokin (2009). "The blood–brain and the blood–cerebrospinal fluid barriers: function and dysfunction." Seminars in Immunopathology **31**(4): 497-511.

Enright, A. J., B. John, et al. (2003). "MicroRNA targets in Drosophila." Genome Biol **5**(1): R1.

Faraoni, I., F. R. Antonetti, et al. (2009). "miR-155 gene: a typical multifunctional microRNA." Biochim Biophys Acta **1792**(6): 497-505.

Fasanaro, P., Y. D'Alessandra, et al. (2008). "MicroRNA-210 modulates endothelial cell response to hypoxia and inhibits the receptor tyrosine kinase ligand Ephrin-A3." J Biol Chem **283**(23): 15878-15883.

Fasler-Kan, E., C. Suenderhauf, et al. (2010). "Cytokine signaling in the human brain capillary endothelial cell line hCMEC/D3." Brain Res **1354**: 15-22.

Feghali, C. A. and T. M. Wright (1997). "Cytokines in acute and chronic inflammation." Front Biosci **2**: d12-26.

Felli, N., F. Felicetti, et al. (2013). "miR-126&126* Restored Expressions Play a Tumor Suppressor Role by Directly Regulating ADAM9 and MMP7 in Melanoma." PLoS One 8(2): e56824.

Feng, R., X. Chen, et al. (2010). "miR-126 functions as a tumour suppressor in human gastric cancer." Cancer Lett 298(1): 50-63.

Fichtlscherer, S., S. De Rosa, et al. (2010). "Circulating microRNAs in patients with coronary artery disease." Circ Res 107(5): 677-684.

Filipowicz, W., S. N. Bhattacharyya, et al. (2008). "Mechanisms of post-transcriptional regulation by microRNAs: are the answers in sight?" Nat Rev Genet 9(2): 102-114.

Fish, J. E., M. M. Santoro, et al. (2008). "miR-126 regulates angiogenic signaling and vascular integrity." Dev Cell 15(2): 272-284.

Fletcher, N. F. and J. A. McKeating (2012). "Hepatitis C virus and the brain." J Viral Hepat 19(5): 301-306.

Friedman, J. M. and P. A. Jones (2009). "MicroRNAs: critical mediators of differentiation, development and disease." Swiss Med Wkly 139(33-34): 466-472.

Friedman, R. C., K. K. Farh, et al. (2009). "Most mammalian mRNAs are conserved targets of microRNAs." Genome Res 19(1): 92-105.

Frijns, C. J. and L. J. Kappelle (2002). "Inflammatory cell adhesion molecules in ischemic cerebrovascular disease." Stroke 33(8): 2115-2122.

Frijns, C. J. M. and L. J. Kappelle (2002). "Inflammatory Cell Adhesion Molecules in Ischemic Cerebrovascular Disease." Stroke 33(8): 2115-2122.

Fu, B. M., R. H. Adamson, et al. (2005). "Determination of microvessel permeability and tissue diffusion coefficient of solutes by laser scanning confocal microscopy." J Biomech Eng 127(2): 270-278.

Furuse, M., T. Hirase, et al. (1993). "Occludin: a novel integral membrane protein localizing at tight junctions." J Cell Biol 123(6 Pt 2): 1777-1788.

Garberg, P., M. Ball, et al. (2005). "In vitro models for the blood-brain barrier." Toxicology in Vitro 19(3): 299-334.

Gerard, C. and B. J. Rollins (2001). "Chemokines and disease." Nat Immunol 2(2): 108-115.

Ghildiyal, M., J. Xu, et al. (2010). "Sorting of Drosophila small silencing RNAs partitions microRNA* strands into the RNA interference pathway." RNA 16(1): 43-56.

Giagulli, C., L. Ottoboni, et al. (2006). "The Src family kinases Hck and Fgr are dispensable for inside-out, chemoattractant-induced signaling regulating beta 2 integrin affinity and valency in neutrophils, but are required for beta 2 integrin-mediated outside-in signaling involved in sustained adhesion." J Immunol 177(1): 604-611.

Gonzalez-Mariscal, L., A. Betanzos, et al. (2003). "Tight junction proteins." Prog Biophys Mol Biol 81(1): 1-44.

Gough, D. J., D. E. Levy, et al. (2008). "IFNgamma signaling-does it mean JAK-STAT?" Cytokine Growth Factor Rev 19(5-6): 383-394.

Graber, N., T. V. Gopal, et al. (1990). "T cells bind to cytokine-activated endothelial cells via a novel, inducible sialoglycoprotein and endothelial leukocyte adhesion molecule-1." J Immunol 145(3): 819-830.

Grabovsky, V., S. Feigelson, et al. (2000). "Subsecond induction of alpha4 integrin clustering by immobilized chemokines stimulates leukocyte tethering and rolling on endothelial vascular cell adhesion molecule 1 under flow conditions." J Exp Med **192**(4): 495-506.

Greenwood, J., Y. Wang, et al. (1995). "Lymphocyte adhesion and transendothelial migration in the central nervous system: the role of LFA-1, ICAM-1, VLA-4 and VCAM-1. off." Immunology **86**(3): 408.

Griffiths-Jones, S., R. J. Grocock, et al. (2006). "miRBase: microRNA sequences, targets and gene nomenclature." Nucleic Acids Res **34**(Database issue): D140-144.

Griffiths-Jones, S., H. K. Saini, et al. (2008). "miRBase: tools for microRNA genomics." Nucleic Acids Res **36**(Database issue): D154-158.

Grunewald, J. K. and A. J. Ridley (2010). "CD73 represses pro-inflammatory responses in human endothelial cells." J Inflamm (Lond) **7**(1): 10.

Guo, H., N. T. Ingolia, et al. (2010). "Mammalian microRNAs predominantly act to decrease target mRNA levels." Nature **466**(7308): 835-840.

Hahne, M., U. Jager, et al. (1993). "Five tumor necrosis factor-inducible cell adhesion mechanisms on the surface of mouse endothelioma cells mediate the binding of leukocytes." J Cell Biol **121**(3): 655-664.

Hamann, I., F. Zipp, et al. (2008). "Therapeutic targeting of chemokine signaling in Multiple Sclerosis." J Neurol Sci **274**(1-2): 31-38.

Hammer, D. A. and S. M. Apte (1992). "Simulation of cell rolling and adhesion on surfaces in shear flow: general results and analysis of selectin-mediated neutrophil adhesion." Biophys J **63**(1): 35-57.

Han, J., Y. Lee, et al. (2006). "Molecular basis for the recognition of primary microRNAs by the Drosha-DGCR8 complex." Cell **125**(5): 887-901.

Han, Y., M. S. Runge, et al. (1999). "Angiotensin II induces interleukin-6 transcription in vascular smooth muscle cells through pleiotropic activation of nuclear factor-kappa B transcription factors." Circ Res **84**(6): 695-703.

Harris, T. A., M. Yamakuchi, et al. (2008). "MicroRNA-126 regulates endothelial expression of vascular cell adhesion molecule 1." Proceedings of the National Academy of Sciences **105**(5): 1516-1521.

Hattori, R., K. K. Hamilton, et al. (1989). "Stimulated secretion of endothelial von Willebrand factor is accompanied by rapid redistribution to the cell surface of the intracellular granule membrane protein GMP-140." J Biol Chem **264**(14): 7768-7771.

Hawkins, B. T. and T. P. Davis (2005). "The Blood-Brain Barrier/Neurovascular Unit in Health and Disease." Pharmacological Reviews **57**(2): 173-185.

Hickey, W. F. (1991). "Migration of Hematogenous Cells Through the Blood-Brain Barrier and the Initiation of CNS Inflammation." Brain Pathology **1**(2): 97-105.

Hillyer, P., E. Mordelet, et al. (2003). "Chemokines, chemokine receptors and adhesion molecules on different human endothelia: discriminating the tissue-specific functions that affect leucocyte migration." Clin Exp Immunol **134**(3): 431-441.

Hirsch, S., J. Reichold, et al. (2012). "Topology and hemodynamics of the cortical cerebrovascular system." J Cereb Blood Flow Metab **32**(6): 952-967.

Hisano, T., T. Namba, et al. (2005). "Inhibition of E-selectin-mediated leukocyte adhesion by volatile anesthetics in a static condition." J Anesth **19**(1): 1-6.

Hohlfeld, R. (1999). "Therapeutic strategies in multiple sclerosis. I. Immunotherapy." Philosophical transactions of the Royal Society of London. Series B, Biological sciences 354(1390): 1697-1710.

Holman, D. W., R. S. Klein, et al. (2011). "The blood-brain barrier, chemokines and multiple sclerosis." Biochim Biophys Acta 1812(2): 220-230.

Huang, M. T., J. C. Mason, et al. (2005). "Endothelial intercellular adhesion molecule (ICAM)-2 regulates angiogenesis." Blood 106(5): 1636-1643.

Huang, X., E. Gschweng, et al. (2011). "Regulated expression of microRNAs-126/126* inhibits erythropoiesis from human embryonic stem cells." Blood 117(7): 2157-2165.

Hudetz, A. G., G. Feher, et al. (1996). "Heterogeneous autoregulation of cerebrocortical capillary flow: evidence for functional thoroughfare channels?" Microvasc Res 51(1): 131-136.

Huizinga, R., C. Linington, et al. (2008). "Resistance is futile: antineuronal autoimmunity in multiple sclerosis." Trends in Immunology 29(2): 54-60.

Hulshof, S., E. S. van Haastert, et al. (2003). "CX3CL1 and CX3CR1 expression in human brain tissue: noninflammatory control versus multiple sclerosis." J Neuropathol Exp Neurol 62(9): 899-907.

Huntzinger, E. and E. Izaurralde (2011). "Gene silencing by microRNAs: contributions of translational repression and mRNA decay." Nat Rev Genet 12(2): 99-110.

Huynh, H. and K. Dorovini-Zis (1993). "Effects of interferon-gamma on primary cultures of human brain microvessel endothelial cells." Am J Pathol 142(4): 1265-1278.

Hwang do, W., S. Son, et al. (2011). "A brain-targeted rabies virus glycoprotein-disulfide linked PEI nanocarrier for delivery of neurogenic microRNA." Biomaterials 32(21): 4968-4975.

Hyduk, S. J., J. Oh, et al. (2004). "Paxillin selectively associates with constitutive and chemoattractant-induced high-affinity alpha4beta1 integrins: implications for integrin signaling." Blood 104(9): 2818-2824.

Inui, M., G. Martello, et al. (2010) "MicroRNA control of signal transduction." Nature Reviews Molecular Cell Biology 11(4): 252-263.

Ito, H., I. Kanno, et al. (2003). "Changes in human cerebral blood flow and myocardial blood flow during mental stress measured by dual positron emission tomography." Ann Nucl Med 17(5): 381-386.

Ivanov, K. P., M. K. Kalinina, et al. (1981). "Blood flow velocity in capillaries of brain and muscles and its physiological significance." Microvasc Res 22(2): 143-155.

Jiang, Y., J. F. Zhu, et al. (1994). "MCP-1-stimulated monocyte attachment to laminin is mediated by beta 2-integrins." Am J Physiol 267(4 Pt 1): C1112-1118.

Johnston, G. I., R. G. Cook, et al. (1989). "Cloning of GMP-140, a granule membrane protein of platelets and endothelium: sequence similarity to proteins involved in cell adhesion and inflammation." Cell 56(6): 1033-1044.

Junker, A., R. Hohlfeld, et al. (2011). "The emerging role of microRNAs in multiple sclerosis." Nat Rev Neurol 7(1): 56-59.

Junker, A., M. Krumbholz, et al. (2009). "MicroRNA profiling of multiple sclerosis lesions identifies modulators of the regulatory protein CD47." Brain 132(12): 3342-3352.

Kakalacheva, K., C. Münz, et al. (2011) "Viral triggers of multiple sclerosis." Biochimica et Biophysica Acta (BBA) - Molecular Basis of Disease In Press, Corrected Proof.

Kallmann, B. A., V. Hummel, et al. (2000). "Cytokine-induced modulation of cellular adhesion to human cerebral endothelial cells is mediated by soluble vascular cell adhesion molecule-1." Brain **123 ( Pt 4)**: 687-697.

Kamouchi, M., T. Ago, et al. (2011). "Brain pericytes: emerging concepts and functional roles in brain homeostasis." Cell Mol Neurobiol **31**(2): 175-193.

Kawamata, T. and Y. Tomari (2010). "Making RISC." Trends Biochem Sci **35**(7): 368-376.

Keller, A., P. Leidinger, et al. (2009). "Multiple Sclerosis: MicroRNA Expression Profiles Accurately Differentiate Patients with Relapsing-Remitting Disease from Healthy Controls." PLoS ONE **4**(10): e7440.

Kerfoot, S. M. and P. Kubes (2002). "Overlapping Roles of P-Selectin and {alpha}4 Integrin to Recruit Leukocytes to the Central Nervous System in Experimental Autoimmune Encephalomyelitis." J Immunol **169**(2): 1000-1006.

Kim, M., C. V. Carman, et al. (2003). "Bidirectional transmembrane signaling by cytoplasmic domain separation in integrins." Science **301**(5640): 1720-1725.

Kim, S. and H. Iwao (2000). "Molecular and cellular mechanisms of angiotensin II-mediated cardiovascular and renal diseases." Pharmacol Rev **52**(1): 11-34.

Kin, K., S. Miyagawa, et al. (2012). "Tissue- and plasma-specific MicroRNA signatures for atherosclerotic abdominal aortic aneurysm." J Am Heart Assoc **1**(5): e000745.

Kleine, T. O. and L. Benes (2006). "Immune surveillance of the human central nervous system (CNS): different migration pathways of immune cells through the blood-brain barrier and blood-cerebrospinal fluid barrier in healthy persons." Cytometry A **69**(3): 147-151.

Kluiver, J., S. Poppema, et al. (2005). "BIC and miR-155 are highly expressed in Hodgkin, primary mediastinal and diffuse large B cell lymphomas." J Pathol **207**(2): 243-249.

Koizumi, K., V. Poulaki, et al. (2003). "Contribution of TNF-alpha to leukocyte adhesion, vascular leakage, and apoptotic cell death in endotoxin-induced uveitis in vivo." Invest Ophthalmol Vis Sci **44**(5): 2184-2191.

Kong, W., H. Yang, et al. (2008). "MicroRNA-155 is regulated by the transforming growth factor beta/Smad pathway and contributes to epithelial cell plasticity by targeting RhoA." Mol Cell Biol **28**(22): 6773-6784.

Korenaga, R., J. Ando, et al. (1997). "Negative transcriptional regulation of the VCAM-1 gene by fluid shear stress in murine endothelial cells." Am J Physiol **273**(5 Pt 1): C1506-1515.

Kota, J., R. R. Chivukula, et al. (2009). "Therapeutic microRNA delivery suppresses tumorigenesis in a murine liver cancer model." Cell **137**(6): 1005-1017.

Koutsiaris, A. G., S. V. Tachmitzi, et al. (2007). "Volume flow and wall shear stress quantification in the human conjunctival capillaries and post-capillary venules in vivo." Biorheology **44**(5-6): 375-386.

Koutsiaris, A. G., S. V. Tachmitzi, et al. (2010). "Blood velocity pulse quantification in the human conjunctival pre-capillary arterioles." Microvasc Res **80**(2): 202-208.

Kraft, A. D., C. A. McPherson, et al. (2009). "Heterogeneity of microglia and TNF signaling as determinants for neuronal death or survival." NeuroToxicology **30**(5): 785-793.

Krek, A., D. Grun, et al. (2005). "Combinatorial microRNA target predictions." Nat Genet **37**(5): 495-500.

Kubes, P. and P. A. Ward (2000). "Leukocyte recruitment and the acute inflammatory response." Brain Pathol 10(1): 127-135.

Kuckleburg, C. J., C. M. Yates, et al. (2011). "Endothelial cell-borne platelet bridges selectively recruit monocytes in human and mouse models of vascular inflammation." Cardiovasc Res 91(1): 134-141.

Kuehbacher, A., C. Urbich, et al. (2007). "Role of Dicer and Drosha for endothelial microRNA expression and angiogenesis." Circ Res 101(1): 59-68.

Kuhnert, F., M. R. Mancuso, et al. (2008). "Attribution of vascular phenotypes of the murine Egfl7 locus to the microRNA miR-126." Development 135(24): 3989-3993.

Kurowska-Stolarska, M., S. Alivernini, et al. (2011). "MicroRNA-155 as a proinflammatory regulator in clinical and experimental arthritis." Proc Natl Acad Sci U S A 108(27): 11193-11198.

Kutty, R. K., C. N. Nagineni, et al. (2010). "Inflammatory cytokines regulate microRNA-155 expression in human retinal pigment epithelial cells by activating JAK/STAT pathway." Biochem Biophys Res Commun 402(2): 390-395.

Lagos-Quintana, M., R. Rauhut, et al. (2002). "Identification of tissue-specific microRNAs from mouse." Curr Biol 12(9): 735-739.

Lai, C.-H., K.-H. Kuo, et al. (2005). "Critical role of actin in modulating BBB permeability." Brain Research Reviews 50(1): 7-13.

Larsson, E., C. Sander, et al. (2010). "mRNA turnover rate limits siRNA and microRNA efficacy." Mol Syst Biol 6: 433.

Lassmann, H., W. Bruck, et al. (2001). "Heterogeneity of multiple sclerosis pathogenesis: implications for diagnosis and therapy." Trends Mol Med 7(3): 115-121.

Lassmann, H., W. Brück, et al. (2007). "The Immunopathology of Multiple Sclerosis: An Overview." Brain Pathology 17(2): 210-218.

Laudanna, C., J. Y. Kim, et al. (2002). "Rapid leukocyte integrin activation by chemokines." Immunol Rev 186: 37-46.

Lawrence, M. B., G. S. Kansas, et al. (1997). "Threshold levels of fluid shear promote leukocyte adhesion through selectins (CD62L,P,E)." J Cell Biol 136(3): 717-727.

Lawrence, M. B., L. V. McIntire, et al. (1987). "Effect of flow on polymorphonuclear leukocyte/endothelial cell adhesion." Blood 70(5): 1284-1290.

Lawrence, M. B., C. W. Smith, et al. (1990). "Effect of venous shear stress on CD18-mediated neutrophil adhesion to cultured endothelium." Blood 75(1): 227-237.

Lawrence, M. B. and T. A. Springer (1991). "Leukocytes roll on a selectin at physiologic flow rates: distinction from and prerequisite for adhesion through integrins." Cell 65(5): 859-873.

Leah, E. (2011). "Rheumatoid arthritis: miR-155 mediates inflammation." Nat Rev Rheumatol 7(8): 437.

Lebedeva, T., M. L. Dustin, et al. (2005). "ICAM-1 co-stimulates target cells to facilitate antigen presentation." Curr Opin Immunol 17(3): 251-258.

Ledeen, R. W. and G. Chakraborty (1998). "Cytokines, Signal Transduction, and Inflammatory Demyelination: Review and Hypothesis." Neurochemical Research 23(3): 277-289.

Lee, D., J. Kim, et al. (2012). "Diacylglycerol kinase zeta negatively regulates CXCR4-stimulated T lymphocyte firm arrest to ICAM-1 under shear flow." Integr Biol (Camb) **4**(6): 606-614.

Lee, K. M., E. J. Choi, et al. (2011). "microRNA-7 increases radiosensitivity of human cancer cells with activated EGFR-associated signaling." Radiother Oncol **101**(1): 171-176.

Lee, R. C., R. L. Feinbaum, et al. (1993). "The C. elegans heterochronic gene lin-4 encodes small RNAs with antisense complementarity to lin-14." Cell **75**(5): 843-854.

Lee, S. J. and E. N. Benveniste (1999). "Adhesion molecule expression and regulation on cells of the central nervous system." J Neuroimmunol **98**(2): 77-88.

Lee, Y., M. Kim, et al. (2004). "MicroRNA genes are transcribed by RNA polymerase II." EMBO J **23**(20): 4051-4060.

Leeuwenberg, J. F., E. J. von Asmuth, et al. (1990). "IFN-gamma regulates the expression of the adhesion molecule ELAM-1 and IL-6 production by human endothelial cells in vitro." J Immunol **145**(7): 2110-2114.

Leng, R. X., H. F. Pan, et al. (2011). "Role of microRNA-155 in autoimmunity." Cytokine Growth Factor Rev **22**(3): 141-147.

Lewis, B. P., R. E. Green, et al. (2003). "Evidence for the widespread coupling of alternative splicing and nonsense-mediated mRNA decay in humans." Proc Natl Acad Sci U S A **100**(1): 189-192.

Ley, K. and G. S. Kansas (2004). "Selectins in T-cell recruitment to non-lymphoid tissues and sites of inflammation." Nat Rev Immunol **4**(5): 325-335.

Ley, K., C. Laudanna, et al. (2007). "Getting to the site of inflammation: the leukocyte adhesion cascade updated." Nat Rev Immunol **7**(9): 678-689.

Li, C. L., H. Nie, et al. (2012). "microRNA-155 is downregulated in gastric cancer cells and involved in cell metastasis." Oncol Rep **27**(6): 1960-1966.

Li, Q.-J., J. Chau, et al. (2007). "miR-181a Is an Intrinsic Modulator of T Cell Sensitivity and Selection." Cell **129**(1): 147-161.

Li, Q., X. W. Song, et al. (2010). "Attenuation of microRNA-1 derepresses the cytoskeleton regulatory protein twinfilin-1 to provoke cardiac hypertrophy." J Cell Sci **123**(Pt 14): 2444-2452.

Li, X., G. Gibson, et al. (2011). "MicroRNA-146a is linked to pain-related pathophysiology of osteoarthritis." Gene **480**(1-2): 34-41.

Li, X., Y. Shen, et al. (2009). "Regulation of miRNA expression by Src and contact normalization: effects on nonanchored cell growth and migration." Oncogene **28**(48): 4272-4283.

Li, Z., J. Lu, et al. (2008). "Distinct microRNA expression profiles in acute myeloid leukemia with common translocations." Proc Natl Acad Sci U S A **105**(40): 15535-15540.

Lim, L. P., N. C. Lau, et al. (2005). "Microarray analysis shows that some microRNAs downregulate large numbers of target mRNAs." Nature **433**(7027): 769-773.

Lim, Y. C., K. Snapp, et al. (1998). "Important contributions of P-selectin glycoprotein ligand-1-mediated secondary capture to human monocyte adhesion to P-selectin, E-selectin, and TNF-alpha-activated endothelium under flow in vitro." J Immunol **161**(5): 2501-2508.

Lindberg, R. L., F. Hoffmann, et al. (2010). "Altered expression of miR-17-5p in CD4+ lymphocytes of relapsing-remitting multiple sclerosis patients." Eur J Immunol **40**(3): 888-898.

Lindsberg, P. J., O. Carpen, et al. (1996). "Endothelial ICAM-1 expression associated with inflammatory cell response in human ischemic stroke." Circulation **94**(5): 939-945.

Lipowsky, H. H. and A. Lescanic (2013). "Shear-dependent adhesion of leukocytes and lectins to the endothelium and concurrent changes in thickness of the glycocalyx of post-capillary venules in the low-flow state." Microcirculation **20**(2): 149-157.

Lipowsky, H. H., S. Usami, et al. (1980). "In vivo measurements of "apparent viscosity" and microvessel hematocrit in the mesentery of the cat." Microvasc Res **19**(3): 297-319.

Liu, J., A. van Mil, et al. (2012). "MiR-155 inhibits cell migration of human cardiomyocyte progenitor cells (hCMPCs) via targeting of MMP-16." J Cell Mol Med.

Liu, K. K. and K. Dorovini-Zis (2009). "Regulation of CXCL12 and CXCR4 expression by human brain endothelial cells and their role in CD4+ and CD8+ T cell adhesion and transendothelial migration." J Neuroimmunol **215**(1-2): 49-64.

Liu, K. K. and K. Dorovini-Zis (2012). "Differential Regulation of CD4+ T Cell Adhesion to Cerebral Microvascular Endothelium by the &#946;-Chemokines CCL2 and CCL3." Int J Mol Sci **13**(12): 16119-16140.

Livak, K. J. and T. D. Schmittgen (2001). "Analysis of relative gene expression data using real-time quantitative PCR and the 2(-Delta Delta C(T)) Method." Methods **25**(4): 402-408.

Lobb, R. R., G. Antognetti, et al. (1995). "A direct binding assay for the vascular cell adhesion molecule-1 (VCAM1) interaction with alpha 4 integrins." Cell Adhes Commun **3**(5): 385-397.

Lock, C., G. Hermans, et al. (2002). "Gene-microarray analysis of multiple sclerosis lesions yields new targets validated in autoimmune encephalomyelitis." Nat Med **8**(5): 500-508.

Loeffler, C., K. Dietz, et al. (2011). "Immune surveillance of the normal human CNS takes place in dependence of the locoregional blood-brain barrier configuration and is mainly performed by CD3(+)/CD8(+) lymphocytes." Neuropathology **31**(3): 230-238.

Loetscher, P., M. Seitz, et al. (1994). "Monocyte chemotactic proteins MCP-1, MCP-2, and MCP-3 are major attractants for human CD4+ and CD8+ T lymphocytes." FASEB J **8**(13): 1055-1060.

Lombardi, A., G. Cantini, et al. (2009). "Molecular mechanisms underlying the pro-inflammatory synergistic effect of tumor necrosis factor alpha and interferon gamma in human microvascular endothelium." Eur J Cell Biol **88**(12): 731-742.

Long, J., Y. Wang, et al. (2010). "Identification of microRNA-93 as a novel regulator of vascular endothelial growth factor in hyperglycemic conditions." J Biol Chem **285**(30): 23457-23465.

Lopez-Ramirez, M. A., R. Fischer, et al. (2012). "Role of caspases in cytokine-induced barrier breakdown in human brain endothelial cells." J Immunol **189**(6): 3130-3139.

Love, S. and R. Barber (2001). "Expression of P-selectin and intercellular adhesion molecule-1 in human brain after focal infarction or cardiac arrest." <u>Neuropathol Appl Neurobiol</u> **27**(6): 465-473.

Lucchinetti, C., W. Brück, et al. (2000). "Heterogeneity of multiple sclerosis lesions: implications for the pathogenesis of demyelination." <u>Annals of Neurology</u> **47**(6): 707-717.

Lund, E., S. Guttinger, et al. (2004). "Nuclear export of microRNA precursors." <u>Science</u> **303**(5654): 95-98.

Luscinskas, F. W., H. Ding, et al. (1995). "P-selectin and vascular cell adhesion molecule 1 mediate rolling and arrest, respectively, of CD4+ T lymphocytes on tumor necrosis factor alpha-activated vascular endothelium under flow." <u>J Exp Med</u> **181**(3): 1179-1186.

Luscinskas, F. W., G. S. Kansas, et al. (1994). "Monocyte rolling, arrest and spreading on IL-4-activated vascular endothelium under flow is mediated via sequential action of L-selectin, beta 1-integrins, and beta 2-integrins." <u>J Cell Biol</u> **125**(6): 1417-1427.

Luscinskas, F. W., Y. C. Lim, et al. (2001). "Wall shear stress: the missing step for T cell transmigration?" <u>Nat Immunol</u> **2**(6): 478-480.

Luster, A. D., R. Alon, et al. (2005). "Immune cell migration in inflammation: present and future therapeutic targets." <u>Nat Immunol</u> **6**(12): 1182-1190.

Luu, N. T., G. E. Rainger, et al. (2003). "CD31 regulates direction and rate of neutrophil migration over and under endothelial cells." <u>J Vasc Res</u> **40**(5): 467-479.

Lyck, R. and B. Engelhardt (2012). "Going against the tide--how encephalitogenic T cells breach the blood-brain barrier." <u>J Vasc Res</u> **49**(6): 497-509.

Ma, Y. P., A. Koo, et al. (1974). "On-line measurement of the dynamic velocity of erythrocytes in the cerebral microvessels in the rat." <u>Microvasc Res</u> **8**(1): 1-13.

Mackay, C. R. (2001). "Chemokines: immunology's high impact factors." <u>Nat Immunol</u> **2**(2): 95-101.

Mahad, D., M. K. Callahan, et al. (2006). "Modulating CCR2 and CCL2 at the blood-brain barrier: relevance for multiple sclerosis pathogenesis." <u>Brain</u> **129**(Pt 1): 212-223.

Malfitano, A. M., M. C. Proto, et al. (2008). "Cannabinoids in the management of spasticity associated with multiple sclerosis." <u>Neuropsychiatric disease and treatment</u> **4**(5): 847-853.

Man, S., B. Tucky, et al. (2009). "alpha4 Integrin/FN-CS1 mediated leukocyte adhesion to brain microvascular endothelial cells under flow conditions." <u>J Neuroimmunol</u> **210**(1-2): 92-99.

Man, S., B. Tucky, et al. (2012). "CXCL12-induced monocyte-endothelial interactions promote lymphocyte transmigration across an in vitro blood-brain barrier." <u>Sci Transl Med</u> **4**(119): 119ra114.

Man, S., E. E. Ubogu, et al. (2008). "Human brain microvascular endothelial cells and umbilical vein endothelial cells differentially facilitate leukocyte recruitment and utilize chemokines for T cell migration." <u>Clin Dev Immunol</u> **2008**: 384982.

Marelli-Berg, F. M., E. Peek, et al. (2000). "Isolation of endothelial cells from murine tissue." <u>J Immunol Methods</u> **244**(1-2): 205-215.

Maria Malfitano, A., G. Matarese, et al. (2005). From Cannabis to Endocannabinoids in Multiple Sclerosis: A Paradigm of Central Nervous System Autoimmune

Diseases. <u>Current Drug Targets - CNS & Neurological Disorders</u>, Bentham Science Publishers Ltd. **4:** 667-675.

Martin, M. M., E. J. Lee, et al. (2006). "MicroRNA-155 regulates human angiotensin II type 1 receptor expression in fibroblasts." <u>J Biol Chem</u> **281**(27): 18277-18284.

Martinez, N. J., M. C. Ow, et al. (2008). "A C. elegans genome-scale microRNA network contains composite feedback motifs with high flux capacity." <u>Genes Dev</u> **22**(18): 2535-2549.

Marx, N., F. Mach, et al. (2000). "Peroxisome proliferator-activated receptor-gamma activators inhibit IFN-gamma-induced expression of the T cell-active CXC chemokines IP-10, Mig, and I-TAC in human endothelial cells." <u>J Immunol</u> **164**(12): 6503-6508.

Matsumiya, T., K. Ota, et al. (2010). "Characterization of synergistic induction of CX3CL1/fractalkine by TNF-alpha and IFN-gamma in vascular endothelial cells: an essential role for TNF-alpha in post-transcriptional regulation of CX3CL1." <u>J Immunol</u> **184**(8): 4205-4214.

Mattiske, S., R. J. Suetani, et al. (2012). "The oncogenic role of miR-155 in breast cancer." <u>Cancer Epidemiol Biomarkers Prev</u> **21**(8): 1236-1243.

Maus, U., S. Henning, et al. (2002). "Role of endothelial MCP-1 in monocyte adhesion to inflamed human endothelium under physiological flow." <u>Am J Physiol Heart Circ Physiol</u> **283**(6): H2584-2591.

McCandless, E. E., B. Zhang, et al. (2008). "CXCR4 antagonism increases T cell trafficking in the central nervous system and improves survival from West Nile virus encephalitis." <u>Proc Natl Acad Sci U S A</u> **105**(32): 11270-11275.

McCarty, J. H. (2009). "Cell adhesion and signaling networks in brain neurovascular units." <u>Current opinion in hematology</u> **16**(3): 209-214.

McGettrick, H. M., C. D. Buckley, et al. (2010). "Stromal cells differentially regulate neutrophil and lymphocyte recruitment through the endothelium." <u>Immunology</u> **131**(3): 357-370.

McLaughlin, F., B. P. Hayes, et al. (1998). "Tumor necrosis factor (TNF)-alpha and interleukin (IL)-1beta down-regulate intercellular adhesion molecule (ICAM)-2 expression on the endothelium." <u>Cell Adhes Commun</u> **6**(5): 381-400.

Meager, A. (1999). "Cytokine regulation of cellular adhesion molecule expression in inflammation." <u>Cytokine Growth Factor Rev</u> **10**(1): 27-39.

Meister, J. and M. H. Schmidt (2010). "miR-126 and miR-126*: new players in cancer." <u>ScientificWorldJournal</u> **10**: 2090-2100.

Meng, S., J. T. Cao, et al. (2012). "Downregulation of microRNA-126 in endothelial progenitor cells from diabetes patients, impairs their functional properties, via target gene Spred-1." <u>J Mol Cell Cardiol</u> **53**(1): 64-72.

Mennicken, F., R. Maki, et al. (1999). "Chemokines and chemokine receptors in the CNS: a possible role in neuroinflammation and patterning." <u>Trends Pharmacol Sci</u> **20**(2): 73-78.

Michell, D. L., K. L. Andrews, et al. (2011). "Imaging leukocyte adhesion to the vascular endothelium at high intraluminal pressure." <u>J Vis Exp</u>(54).

Minagar, A. and J. S. Alexander (2003). "Blood-brain barrier disruption in multiple sclerosis." <u>Mult Scler</u> **9**(6): 540-549.

Montgomery, K. F., L. Osborn, et al. (1991). "Activation of endothelial-leukocyte adhesion molecule 1 (ELAM-1) gene transcription." Proc Natl Acad Sci U S A **88**(15): 6523-6527.

Montgomery, S. L. and W. J. Bowers (2012). "Tumor necrosis factor-alpha and the roles it plays in homeostatic and degenerative processes within the central nervous system." J Neuroimmune Pharmacol **7**(1): 42-59.

Morlando, M., M. Ballarino, et al. (2008). "Primary microRNA transcripts are processed co-transcriptionally." Nat Struct Mol Biol **15**(9): 902-909.

Muller, W. A. (2003). "Leukocyte-endothelial-cell interactions in leukocyte transmigration and the inflammatory response." Trends Immunol **24**(6): 327-334.

Muller, W. A. (2011). "Mechanisms of leukocyte transendothelial migration." Annu Rev Pathol **6**: 323-344.

Murphy, A., A. Long, et al. (2000). "Cross-linking of LFA-1 induces secretion of macrophage inflammatory protein (MIP)-1&agr; and MIP-1&bgr; with consequent directed migration of activated lymphocytes." European Journal of Immunology **30**(10): 3006-3011.

Muruganandam, A., L. M. Herx, et al. (1997). "Development of immortalized human cerebromicrovascular endothelial cell line as an in vitro model of the human blood-brain barrier." FASEB J **11**(13): 1187-1197.

Musiyenko, A., V. Bitko, et al. (2008). "Ectopic expression of miR-126*, an intronic product of the vascular endothelial EGF-like 7 gene, regulates prostein translation and invasiveness of prostate cancer LNCaP cells." J Mol Med (Berl) **86**(3): 313-322.

Nahid, M. A., K. M. Pauley, et al. (2009). "miR-146a Is Critical for Endotoxin-induced Tolerance." Journal of Biological Chemistry **284**(50): 34590-34599.

Naik, P. and L. Cucullo (2012). "In vitro blood-brain barrier models: current and perspective technologies." J Pharm Sci **101**(4): 1337-1354.

Nakashima, H., H. Suzuki, et al. (2006). "Angiotensin II regulates vascular and endothelial dysfunction: recent topics of Angiotensin II type-1 receptor signaling in the vasculature." Curr Vasc Pharmacol **4**(1): 67-78.

Nandi, A., P. Estess, et al. (2004). "Bimolecular complex between rolling and firm adhesion receptors required for cell arrest; CD44 association with VLA-4 in T cell extravasation." Immunity **20**(4): 455-465.

Navikas, V. and H. Link (1996). "Review: cytokines and the pathogenesis of multiple sclerosis." J Neurosci Res **45**(4): 322-333.

Navratil, E., A. Couvelard, et al. (1997). "Expression of cell adhesion molecules by microvascular endothelial cells in the cortical and subcortical regions of the normal human brain: an immunohistochemical analysis." Neuropathol Appl Neurobiol **23**(1): 68-80.

Neuwelt, E., N. J. Abbott, et al. (2008). "Strategies to advance translational research into brain barriers." The Lancet Neurology **7**(1): 84-96.

Neuwelt, E. A., B. Bauer, et al. (2011). "Engaging neuroscience to advance translational research in brain barrier biology." Nat Rev Neurosci **12**(3): 169-182.

Nicoletti, F., F. Patti, et al. (1996). "Elevated serum levels of interleukin-12 in chronic progressive multiple sclerosis." J Neuroimmunol **70**(1): 87-90.

Nieto, M., J. M. Frade, et al. (1997). "Polarization of chemokine receptors to the leading edge during lymphocyte chemotaxis." <u>J Exp Med</u> **186**(1): 153-158.

Nitta, T., M. Hata, et al. (2003). "Size-selective loosening of the blood-brain barrier in claudin-5-deficient mice." <u>The Journal of cell biology</u> **161**(3): 653-660.

Nortamo, P., R. Li, et al. (1991). "The expression of human intercellular adhesion molecule-2 is refractory to inflammatory cytokines." <u>Eur J Immunol</u> **21**(10): 2629-2632.

Noseworthy, J. H., C. Lucchinetti, et al. (2000). "Multiple sclerosis." <u>N Engl J Med</u> **343**(13): 938-952.

Nourshargh, S., P. L. Hordijk, et al. (2010) Breaching multiple barriers: leukocyte motility through venular walls and the interstitium. <u>Nature Reviews Molecular Cell Biology</u>. **11:** 366-378.

Nusrat, A., G. T. Brown, et al. (2005). "Multiple protein interactions involving proposed extracellular loop domains of the tight junction protein occludin." <u>Mol Biol Cell</u> **16**(4): 1725-1734.

O'Connell, R. M., D. S. Rao, et al. (2012). "microRNA regulation of inflammatory responses." <u>Annu Rev Immunol</u> **30**: 295-312.

Oglesby, I. K., I. M. Bray, et al. (2010). "miR-126 is downregulated in cystic fibrosis airway epithelial cells and regulates TOM1 expression." <u>J Immunol</u> **184**(4): 1702-1709.

Ohmori, Y., R. D. Schreiber, et al. (1997). "Synergy between interferon-gamma and tumor necrosis factor-alpha in transcriptional activation is mediated by cooperation between signal transducer and activator of transcription 1 and nuclear factor kappaB." <u>J Biol Chem</u> **272**(23): 14899-14907.

Ohtsuka, A., J. Ando, et al. (1993). "The effect of flow on the expression of vascular adhesion molecule-1 by cultured mouse endothelial cells." <u>Biochem Biophys Res Commun</u> **193**(1): 303-310.

Ohtsuki, S. and T. Terasaki (2007). "Contribution of carrier-mediated transport systems to the blood-brain barrier as a supporting and protecting interface for the brain; importance for CNS drug discovery and development." <u>Pharm Res</u> **24**(9): 1745-1758.

Okamura, K., M. D. Phillips, et al. (2008). "The regulatory activity of microRNA* species has substantial influence on microRNA and 3' UTR evolution." <u>Nat Struct Mol Biol</u> **15**(4): 354-363.

Olena, A. F. and J. G. Patton (2010). "Genomic organization of microRNAs." <u>J Cell Physiol</u> **222**(3): 540-545.

Olson, T. S. and K. Ley (2002). "Chemokines and chemokine receptors in leukocyte trafficking." <u>Am J Physiol Regul Integr Comp Physiol</u> **283**(1): R7-28.

Oostingh, G. J., S. Schlickum, et al. (2007). "Impaired induction of adhesion molecule expression in immortalized endothelial cells leads to functional defects in dynamic interactions with lymphocytes." <u>J Invest Dermatol</u> **127**(9): 2253-2258.

Osborn, L., C. Hession, et al. (1989). "Direct expression cloning of vascular cell adhesion molecule 1, a cytokine-induced endothelial protein that binds to lymphocytes." <u>Cell</u> **59**(6): 1203-1211.

Otaegui, D., S. E. Baranzini, et al. (2009). "Differential micro RNA expression in PBMC from multiple sclerosis patients." <u>PLoS One</u> **4**(7): e6309.

Otsubo, T., Y. Akiyama, et al. (2011). "MicroRNA-126 inhibits SOX2 expression and contributes to gastric carcinogenesis." PLoS One 6(1): e16617.

Ousman, S. S. and P. Kubes (2012). "Immune surveillance in the central nervous system." Nat Neurosci 15(8): 1096-1101.

Owens, T., I. Bechmann, et al. (2008). "Perivascular spaces and the two steps to neuroinflammation." J Neuropathol Exp Neurol 67(12): 1113-1121.

Ozaki, H., K. Ishii, et al. (1999). "Cutting edge: combined treatment of TNF-alpha and IFN-gamma causes redistribution of junctional adhesion molecule in human endothelial cells." J Immunol 163(2): 553-557.

Pan, W. and A. J. Kastin (2007). "Tumor necrosis factor and stroke: role of the blood-brain barrier." Prog Neurobiol 83(6): 363-374.

Papaioannou, T. G. and C. Stefanadis (2005). "Vascular wall shear stress: basic principles and methods." Hellenic J Cardiol 46(1): 9-15.

Pardridge, W. (2005). "Molecular biology of the blood-brain barrier." Molecular Biotechnology 30(1): 57-69.

Pasquinelli, A. E., B. J. Reinhart, et al. (2000). "Conservation of the sequence and temporal expression of let-7 heterochronic regulatory RNA." Nature 408(6808): 86-89.

Pauley, K. M. and E. K. Chan (2008). "MicroRNAs and Their Emerging Roles in Immunology." Annals of the New York Academy of Sciences 1143(1): 226-239.

Peppiatt, C. M., C. Howarth, et al. (2006). "Bidirectional control of CNS capillary diameter by pericytes." Nature 443(7112): 700-704.

Persidsky, Y., S. Ramirez, et al. (2006). "Blood–brain Barrier: Structural Components and Function Under Physiologic and Pathologic Conditions." Journal of Neuroimmune Pharmacology 1(3): 223-236.

Peters, L. and G. Meister (2007). "Argonaute proteins: mediators of RNA silencing." Mol Cell 26(5): 611-623.

Phan, U. T., T. T. Waldron, et al. (2006). "Remodeling of the lectin-EGF-like domain interface in P- and L-selectin increases adhesiveness and shear resistance under hydrodynamic force." Nat Immunol 7(8): 883-889.

Phoenix, T. N. and S. Temple (2010). "Spred1, a negative regulator of Ras-MAPK-ERK, is enriched in CNS germinal zones, dampens NSC proliferation, and maintains ventricular zone structure." Genes Dev 24(1): 45-56.

Piali, L., C. Weber, et al. (1998). "The chemokine receptor CXCR3 mediates rapid and shear-resistant adhesion-induction of effector T lymphocytes by the chemokines IP10 and Mig." Eur J Immunol 28(3): 961-972.

Piccio, L., B. Rossi, et al. (2002). "Molecular mechanisms involved in lymphocyte recruitment in inflamed brain microvessels: critical roles for P-selectin glycoprotein ligand-1 and heterotrimeric G(i)-linked receptors." J Immunol 168(4): 1940-1949.

Piccio, L., W. Vermi, et al. (2005). "Adhesion of human T cells to antigen-presenting cells through SIRP{beta}2-CD47 interaction costimulates T-cell proliferation." Blood 105(6): 2421-2427.

Pillai, R. S., S. N. Bhattacharyya, et al. (2007). "Repression of protein synthesis by miRNAs: how many mechanisms?" Trends Cell Biol 17(3): 118-126.

Png, K. J., N. Halberg, et al. (2012). "A microRNA regulon that mediates endothelial recruitment and metastasis by cancer cells." Nature 481(7380): 190-194.

Pober, J. S. (2002). "Endothelial activation: intracellular signaling pathways." <u>Arthritis Res</u> **4 Suppl 3**: S109-116.

Pober, J. S. and W. C. Sessa (2007). "Evolving functions of endothelial cells in inflammation." <u>Nat Rev Immunol</u> **7**(10): 803-815.

Poller, B., H. Gutmann, et al. (2008). "The human brain endothelial cell line hCMEC/D3 as a human blood-brain barrier model for drug transport studies." <u>Journal of Neurochemistry</u> **107**(5): 1358-1368.

Ponomarev, E. D., T. Veremeyko, et al. (2013). "MicroRNAs are universal regulators of differentiation, activation, and polarization of microglia and macrophages in normal and diseased CNS." <u>Glia</u> **61**(1): 91-103.

Pribila, J. T., A. C. Quale, et al. (2004). "Integrins and T cell-mediated immunity." <u>Annu Rev Immunol</u> **22**: 157-180.

Pulkkinen, K. H., S. Yla-Herttuala, et al. (2011). "Heme oxygenase 1 is induced by miR-155 via reduced BACH1 translation in endothelial cells." <u>Free Radic Biol Med</u> **51**(11): 2124-2131.

Qin, B., H. Yang, et al. (2012). "Role of microRNAs in endothelial inflammation and senescence." <u>Mol Biol Rep</u> **39**(4): 4509-4518.

Qin, W., Q. Ren, et al. (2013). "MicroRNA-155 is a novel suppressor of ovarian cancer-initiating cells that targets CLDN1." <u>FEBS Lett</u>.

Qin, X., X. Wang, et al. (2010). "MicroRNA-19a mediates the suppressive effect of laminar flow on cyclin D1 expression in human umbilical vein endothelial cells." <u>Proc Natl Acad Sci U S A</u> **107**(7): 3240-3244.

Quan, N. and W. A. Banks (2007). "Brain-immune communication pathways." <u>Brain, Behavior, and Immunity</u> **21**(6): 727-735.

Quek, B. Z., Y. C. Lim, et al. (2010). "CD137 enhances monocyte-ICAM-1 interactions in an E-selectin-dependent manner under flow conditions." <u>Mol Immunol</u> **47**(9): 1839-1847.

Reese, T. S. and M. J. Karnovsky (1967). "Fine structural localization of a blood-brain barrier to exogenous peroxidase." <u>J Cell Biol</u> **34**(1): 207-217.

Reijerkerk, A., M. A. Lopez-Ramirez, et al. (2013). "MicroRNAs Regulate Human Brain Endothelial Cell-Barrier Function in Inflammation: Implications for Multiple Sclerosis." <u>J Neurosci</u> **33**(16): 6857-6863.

Reinhart, B. J., F. J. Slack, et al. (2000). "The 21-nucleotide let-7 RNA regulates developmental timing in Caenorhabditis elegans." <u>Nature</u> **403**(6772): 901-906.

Rejdak, K., S. Jackson, et al. "Multiple sclerosis: a practical overview for clinicians." <u>British Medical Bulletin</u> **95**(1): 79-104.

Renno, T., M. Krakowski, et al. (1995). "TNF-alpha expression by resident microglia and infiltrating leukocytes in the central nervous system of mice with experimental allergic encephalomyelitis. Regulation by Th1 cytokines." <u>J Immunol</u> **154**(2): 944-953.

Rijcken, E., C. F. Krieglstein, et al. (2002). "ICAM-1 and VCAM-1 antisense oligonucleotides attenuate in vivo leucocyte adherence and inflammation in rat inflammatory bowel disease." <u>Gut</u> **51**(4): 529-535.

Rippe, C., M. Blimline, et al. (2012). "MicroRNA changes in human arterial endothelial cells with senescence: relation to apoptosis, eNOS and inflammation." <u>Exp Gerontol</u> **47**(1): 45-51.

Ro, S., C. Park, et al. (2007). "Tissue-dependent paired expression of miRNAs." <u>Nucleic Acids Res</u> **35**(17): 5944-5953.

Rodriguez, A., S. Griffiths-Jones, et al. (2004). "Identification of mammalian microRNA host genes and transcription units." <u>Genome Res</u> **14**(10A): 1902-1910.

Rodriguez, A., E. Vigorito, et al. (2007). "Requirement of bic/microRNA-155 for normal immune function." <u>Science</u> **316**(5824): 608-611.

Rose, D. M., R. Alon, et al. (2007). "Integrin modulation and signaling in leukocyte adhesion and migration." <u>Immunol Rev</u> **218**: 126-134.

Rosell, A., E. Cuadrado, et al. (2008). "MMP-9-positive neutrophil infiltration is associated to blood-brain barrier breakdown and basal lamina type IV collagen degradation during hemorrhagic transformation after human ischemic stroke." <u>Stroke</u> **39**(4): 1121-1126.

Rosenberg, G. A. (2002). "Matrix metalloproteinases in neuroinflammation." <u>Glia</u> **39**(3): 279-291.

Ross, J. (1995). "mRNA stability in mammalian cells." Microbiol Rev **59**(3): 423-450.

Rothlein, R., M. L. Dustin, et al. (1986). "A human intercellular adhesion molecule (ICAM-1) distinct from LFA-1." <u>J Immunol</u> **137**(4): 1270-1274.

Sallusto, F. and M. Baggiolini (2008). "Chemokines and leukocyte traffic." <u>Nat Immunol</u> **9**(9): 949-952.

Salvucci, O., K. Jiang, et al. (2012). "MicroRNA126 contributes to granulocyte colony-stimulating factor-induced hematopoietic progenitor cell mobilization by reducing the expression of vascular cell adhesion molecule 1." <u>Haematologica</u> **97**(6): 818-826.

Sana, T. R., M. J. Janatpour, et al. (2005). "Microarray analysis of primary endothelial cells challenged with different inflammatory and immune cytokines." <u>Cytokine</u> **29**(6): 256-269.

Santaguida, S., D. Janigro, et al. (2006). "Side by side comparison between dynamic versus static models of blood-brain barrier in vitro: a permeability study." <u>Brain Res</u> **1109**(1): 1-13.

Sassen, S., E. Miska, et al. (2008). "MicroRNA—implications for cancer." <u>Virchows Archiv</u> **452**(1): 1-10.

Sato, Y. (2001). "Role of ETS family transcription factors in vascular development and angiogenesis." <u>Cell Struct Funct</u> **26**(1): 19-24.

Satoh, J. i., H. Tabunoki, et al. (2007). "Human astrocytes express aquaporin-1 and aquaporin-4 in vitro and in vivo." <u>Neuropathology</u> **27**(3): 245-256.

Schall, T. J. and K. B. Bacon (1994). "Chemokines, leukocyte trafficking, and inflammation." <u>Current Opinion in Immunology</u> **6**(6): 865-873.

Scherrmann, J. M. (2002). "Drug delivery to brain via the blood-brain barrier." <u>Vascul Pharmacol</u> **38**(6): 349-354.

Schmidt, W. M., A. O. Spiel, et al. (2009). "In vivo profile of the human leukocyte microRNA response to endotoxemia." <u>Biochem Biophys Res Commun</u> **380**(3): 437-441.

Schoenborn, J. R., C. B. Wilson, et al. (2007). Regulation of Interferon[hyphen (true graphic)][gamma] During Innate and Adaptive Immune Responses. <u>Advances in Immunology</u>, Academic Press. **Volume 96:** 41-101.

Schroder, K., P. J. Hertzog, et al. (2004). "Interferon-gamma: an overview of signals, mechanisms and functions." <u>J Leukoc Biol</u> **75**(2): 163-189.

Schroen, B. and S. Heymans (2012). "Small but smart--microRNAs in the centre of inflammatory processes during cardiovascular diseases, the metabolic syndrome, and ageing." <u>Cardiovasc Res</u> **93**(4): 605-613.

Selmaj, K., C. S. Raine, et al. (1991). "Anti-tumor necrosis factor therapy abrogates autoimmune demyelination." <u>Ann Neurol</u> **30**(5): 694-700.

Seminario, M. C., S. A. Sterbinsky, et al. (1998). "Beta 1 integrin-dependent binding of Jurkat cells to fibronectin is regulated by a serine-threonine phosphatase." <u>J Leukoc Biol</u> **64**(6): 753-758.

Sessa, R., G. Seano, et al. (2012). "The miR-126 regulates angiopoietin-1 signaling and vessel maturation by targeting p85beta." <u>Biochim Biophys Acta</u> **1823**(10): 1925-1935.

Setiadi, H., G. Sedgewick, et al. (1998). "Interactions of the cytoplasmic domain of P-selectin with clathrin-coated pits enhance leukocyte adhesion under flow." <u>J Cell Biol</u> **142**(3): 859-871.

Shamri, R., V. Grabovsky, et al. (2005). "Lymphocyte arrest requires instantaneous induction of an extended LFA-1 conformation mediated by endothelium-bound chemokines." <u>Nat Immunol</u> **6**(5): 497-506.

Sharief, M. K. and R. Hentges (1991). "Association between tumor necrosis factor-alpha and disease progression in patients with multiple sclerosis." <u>N Engl J Med</u> **325**(7): 467-472.

Sheikh, S., Z. Gale, et al. (2004). "Methods for exposing multiple cultures of endothelial cells to different fluid shear stresses and to cytokines, for subsequent analysis of inflammatory function." <u>J Immunol Methods</u> **288**(1-2): 35-46.

Sheikh, S., M. Rahman, et al. (2005). "Differing mechanisms of leukocyte recruitment and sensitivity to conditioning by shear stress for endothelial cells treated with tumour necrosis factor-alpha or interleukin-1beta." <u>Br J Pharmacol</u> **145**(8): 1052-1061.

Shen-Orr, S. S., R. Milo, et al. (2002). "Network motifs in the transcriptional regulation network of Escherichia coli." <u>Nat Genet</u> **31**(1): 64-68.

Shen, J., F. W. Luscinskas, et al. (1992). "Fluid shear stress modulates cytosolic free calcium in vascular endothelial cells." <u>Am J Physiol</u> **262**(2 Pt 1): C384-390.

Shen, W. F., Y. L. Hu, et al. (2008). "MicroRNA-126 regulates HOXA9 by binding to the homeobox." <u>Mol Cell Biol</u> **28**(14): 4609-4619.

Shimada, H. and L. E. Rajagopalan (2010). "Rho kinase-2 activation in human endothelial cells drives lysophosphatidic acid-mediated expression of cell adhesion molecules via NF-kappaB p65." <u>J Biol Chem</u> **285**(17): 12536-12542.

Sidorenko, T., E. KOLYAK, et al. (2009). "Natalizumab: a new way for MS treatment." <u>Žurnal nevrologii i psihiatrii imeni SS Korsakova</u> **109**(7): 122-128.

Sirs, J. A. (1991). "The flow of human blood through capillary tubes." <u>J Physiol</u> **442**: 569-583.

Smith, D. F., T. L. Deem, et al. (2006). "Leukocyte phosphoinositide-3 kinase {gamma} is required for chemokine-induced, sustained adhesion under flow in vivo." <u>J Leukoc Biol</u> **80**(6): 1491-1499.

Snapp, K. R., C. E. Heitzig, et al. (2002). "Attachment of the PSGL-1 cytoplasmic domain to the actin cytoskeleton is essential for leukocyte rolling on P-selectin." <u>Blood</u> **99**(12): 4494-4502.

Soe, M. and N. Michael "Axonal Damage in Leukodystrophies." Pediatric neurology 42(4): 239-242.

Soilu-Hanninen, M., M. Paivarinta, et al. (2013). "[Progressive multifocal leukoencephalopathy as a complication of natalizumab therapy]." Duodecim 129(7): 765-770.

Solito, E., I. A. Romero, et al. (2000). "Annexin 1 binds to U937 monocytic cells and inhibits their adhesion to microvascular endothelium: involvement of the alpha 4 beta 1 integrin." J Immunol 165(3): 1573-1581.

Song, J., P. Liu, et al. (2012). "MiR-155 negatively regulates c-Jun expression at the post-transcriptional level in human dermal fibroblasts in vitro: implications in UVA irradiation-induced photoaging." Cell Physiol Biochem 29(3-4): 331-340.

Sospedra, M. and R. Martin (2005). "Immunology of multiple sclerosis." Annu Rev Immunol 23: 683-747.

Sperandio, M., J. Pickard, et al. (2006). "Analysis of leukocyte rolling in vivo and in vitro." Methods Enzymol 416: 346-371.

Springer, T. A. (1994). "Traffic signals for lymphocyte recirculation and leukocyte emigration: the multistep paradigm." Cell 76(2): 301-314.

Srigunapalan, S., C. Lam, et al. (2011). "A microfluidic membrane device to mimic critical components of the vascular microenvironment." Biomicrofluidics 5(1): 13409.

Stamatovic, S. M., R. F. Keep, et al. (2008). "Brain endothelial cell-cell junctions: how to "open" the blood brain barrier." Curr Neuropharmacol 6(3): 179-192.

Steiner, O., C. Coisne, et al. (2010). "Differential roles for endothelial ICAM-1, ICAM-2, and VCAM-1 in shear-resistant T cell arrest, polarization, and directed crawling on blood-brain barrier endothelium." J Immunol 185(8): 4846-4855.

Steiner, O., C. Coisne, et al. (2011). "Comparison of immortalized bEnd5 and primary mouse brain microvascular endothelial cells as in vitro blood-brain barrier models for the study of T cell extravasation." J Cereb Blood Flow Metab 31(1): 315-327.

Steinman, L. (2009). "A molecular trio in relapse and remission in multiple sclerosis." Nat Rev Immunol 9(6): 440-447.

Stielke, S., G. Keilhoff, et al. (2012). "Adhesion molecule expression precedes brain damages of lupus-prone mice and correlates with kidney pathology." J Neuroimmunol 252(1-2): 24-32.

Stins, M. F., F. Gilles, et al. (1997). "Selective expression of adhesion molecules on human brain microvascular endothelial cells." J Neuroimmunol 76(1-2): 81-90.

Stolp, H. B. and K. M. Dziegielewska (2009). "Review: Role of developmental inflammation and blood–brain barrier dysfunction in neurodevelopmental and neurodegenerative diseases." Neuropathology and Applied Neurobiology 35(2): 132-146.

Stolpen, A. H., E. C. Guinan, et al. (1986). "Recombinant tumor necrosis factor and immune interferon act singly and in combination to reorganize human vascular endothelial cell monolayers." Am J Pathol 123(1): 16-24.

Su, Y., X. Lei, et al. (2012). "The role of endothelial cell adhesion molecules P-selectin, E-selectin and intercellular adhesion molecule-1 in leucocyte recruitment induced by exogenous methylglyoxal." Immunology 137(1): 65-79.

Suarez, Y., C. Wang, et al. (2010). "Cutting edge: TNF-induced microRNAs regulate TNF-induced expression of E-selectin and intercellular adhesion molecule-1 on human endothelial cells: feedback control of inflammation." J Immunol **184**(1): 21-25.

Subileau, E. A., P. Rezaie, et al. (2009). "Expression of chemokines and their receptors by human brain endothelium: implications for multiple sclerosis." J Neuropathol Exp Neurol **68**(3): 227-240.

Sugihara-Seki, M. (2001). "Flow around cells adhered to a microvessel wall II: comparison to flow around adherent cells in channel flow." Biorheology **38**(1): 3-13.

Sugihara-Seki, M. and G. W. Schmid-Schonbein (2003). "The fluid shear stress distribution on the membrane of leukocytes in the microcirculation." J Biomech Eng **125**(5): 628-638.

Sundd, P., M. K. Pospieszalska, et al. (2011). "Biomechanics of leukocyte rolling." Biorheology **48**(1): 1-35.

Takeshita, Y. and R. M. Ransohoff (2012). "Inflammatory cell trafficking across the blood-brain barrier: chemokine regulation and in vitro models." Immunol Rev **248**(1): 228-239.

Tarassishin, L., O. Loudig, et al. (2011). "Interferon regulatory factor 3 inhibits astrocyte inflammatory gene expression through suppression of the proinflammatory miR-155 and miR-155*." Glia **59**(12): 1911-1922.

Tengku-Muhammad, T. S., A. Cryer, et al. (1998). "Synergism between interferon gamma and tumour necrosis factor alpha in the regulation of lipoprotein lipase in the macrophage J774.2 cell line." Cytokine **10**(1): 38-48.

Thornhill, M. H., S. M. Wellicome, et al. (1991). "Tumor necrosis factor combines with IL-4 or IFN-gamma to selectively enhance endothelial cell adhesiveness for T cells. The contribution of vascular cell adhesion molecule-1-dependent and -independent binding mechanisms." J Immunol **146**(2): 592-598.

Thulasingam, S., C. Massilamany, et al. (2011). "miR-27b*, an oxidative stress-responsive microRNA modulates nuclear factor-kB pathway in RAW 264.7 cells." Mol Cell Biochem **352**(1-2): 181-188.

Tili, E., C. M. Croce, et al. (2009). "miR-155: on the crosstalk between inflammation and cancer." Int Rev Immunol **28**(5): 264-284.

Tsang, J., J. Zhu, et al. (2007). "MicroRNA-mediated feedback and feedforward loops are recurrent network motifs in mammals." Mol Cell **26**(5): 753-767.

Tsou, C. L., W. Peters, et al. (2007). "Critical roles for CCR2 and MCP-3 in monocyte mobilization from bone marrow and recruitment to inflammatory sites." J Clin Invest **117**(4): 902-909.

Tsunoda, I., T. Tanaka, et al. (2007). "Contrasting Roles for Axonal Degeneration in an Autoimmune versus Viral Model of Multiple Sclerosis: When Can Axonal Injury Be Beneficial?" Am J Pathol **170**(1): 214-226.

Tunkel, A. R., S. W. Rosser, et al. (1991). "Blood-brain barrier alterations in bacterial meningitis: development of an in vitro model and observations on the effects of lipopolysaccharide." In Vitro Cell Dev Biol **27A**(2): 113-120.

Ueda, R., G. Kohanbash, et al. (2009). "Dicer-regulated microRNAs 222 and 339 promote resistance of cancer cells to cytotoxic T-lymphocytes by down-regulation of ICAM-1." Proc Natl Acad Sci U S A **106**(26): 10746-10751.

245

Ukkonen, M., K. Wu, et al. (2007). "Cell surface adhesion molecules and cytokine profiles in primary progressive multiple sclerosis." Mult Scler 13(6): 701-707.

Ul Hussain, M. (2012). "Micro-RNAs (miRNAs): genomic organisation, biogenesis and mode of action." Cell Tissue Res 349(2): 405-413.

Ulfman, L. H., P. H. Kuijper, et al. (1999). "Characterization of eosinophil adhesion to TNF-alpha-activated endothelium under flow conditions: alpha 4 integrins mediate initial attachment, and E-selectin mediates rolling." J Immunol 163(1): 343-350.

Urbich, C., A. Kuehbacher, et al. (2008). "Role of microRNAs in vascular diseases, inflammation, and angiogenesis." Cardiovascular Research 79(4): 581-588.

Vajkoczy, P., M. Laschinger, et al. (2001). "Alpha4-integrin-VCAM-1 binding mediates G protein-independent capture of encephalitogenic T cell blasts to CNS white matter microvessels." J Clin Invest 108(4): 557-565.

van Buul, J. D., F. P. Mul, et al. (2004). "ICAM-3 activation modulates cell-cell contacts of human bone marrow endothelial cells." J Vasc Res 41(1): 28-37.

Vandenabeele, P., W. Declercq, et al. (1995). "Two tumour necrosis factor receptors: structure and function." Trends Cell Biol 5(10): 392-399.

Vasa-Nicotera, M., H. Chen, et al. (2011). "miR-146a is modulated in human endothelial cell with aging." Atherosclerosis 217(2): 326-330.

Vasudevan, S., Y. Tong, et al. (2007). "Switching from repression to activation: microRNAs can up-regulate translation." Science 318(5858): 1931-1934.

Vergoulis, T., I. S. Vlachos, et al. (2012). "TarBase 6.0: capturing the exponential growth of miRNA targets with experimental support." Nucleic Acids Res 40(Database issue): D222-229.

Verma, S., M. Kumar, et al. (2010). "Reversal of West Nile virus-induced blood-brain barrier disruption and tight junction proteins degradation by matrix metalloproteinases inhibitor." Virology 397(1): 130-138.

Verma, S., R. Nakaoke, et al. (2006). "Release of cytokines by brain endothelial cells: A polarized response to lipopolysaccharide." Brain Behav Immun 20(5): 449-455.

Vigorito, E., K. L. Perks, et al. (2007). "microRNA-155 regulates the generation of immunoglobulin class-switched plasma cells." Immunity 27(6): 847-859.

Vilcek, J. and T. H. Lee (1991). "Tumor necrosis factor. New insights into the molecular mechanisms of its multiple actions." Journal of Biological Chemistry 266(12): 7313-7316.

Walsh, T. G., R. P. Murphy, et al. (2011). "Stabilization of brain microvascular endothelial barrier function by shear stress involves VE-cadherin signaling leading to modulation of pTyr-occludin levels." J Cell Physiol 226(11): 3053-3063.

Wang, S., A. B. Aurora, et al. (2008). "The endothelial-specific microRNA miR-126 governs vascular integrity and angiogenesis." Dev Cell 15(2): 261-271.

Weihong, P. and A. J. Kastin (2008). Cytokine Transport Across the Injured Blood-Spinal Cord Barrier. Current Pharmaceutical Design, Bentham Science Publishers Ltd. 14: 1620-1624.

Weinbaum, S., J. M. Tarbell, et al. (2007). "The structure and function of the endothelial glycocalyx layer." Annu Rev Biomed Eng 9: 121-167.

Weiner, H. L. (2009). "The challenge of multiple sclerosis: How do we cure a chronic heterogeneous disease?" Annals of Neurology 65(3): 239-248.

Weiss, N., F. Miller, et al. (2009). "The blood-brain barrier in brain homeostasis and neurological diseases." <u>Biochim Biophys Acta</u> **1788**(4): 842-857.

Weksler, B., I. A. Romero, et al. (2013). "The hCMEC/D3 cell line as a model of the human blood brain barrier." <u>Fluids Barriers CNS</u> **10**(1): 16.

Weksler, B. B., E. A. Subileau, et al. (2005). "Blood-brain barrier-specific properties of a human adult brain endothelial cell line." <u>FASEB J.</u>: 04-3458fje.

Weksler, B. B., E. A. Subileau, et al. (2005). "Blood-brain barrier-specific properties of a human adult brain endothelial cell line." <u>FASEB J</u> **19**(13): 1872-1874.

Weller, A., S. Isenmann, et al. (1992). "Cloning of the mouse endothelial selectins. Expression of both E- and P-selectin is inducible by tumor necrosis factor alpha." <u>J Biol Chem</u> **267**(21): 15176-15183.

Westmuckett, A. D., K. M. Thacker, et al. (2011). "Tyrosine sulfation of native mouse Psgl-1 is required for optimal leukocyte rolling on P-selectin in vivo." <u>PLoS One</u> **6**(5): e20406.

Whelan, J., P. Ghersa, et al. (1991). "An NF kappa B-like factor is essential but not sufficient for cytokine induction of endothelial leukocyte adhesion molecule 1 (ELAM-1) gene transcription." <u>Nucleic Acids Res</u> **19**(10): 2645-2653.

Wiese, G., S. R. Barthel, et al. (2009). "Analysis of physiologic E-selectin-mediated leukocyte rolling on microvascular endothelium." <u>J Vis Exp</u>(24).

Wightman, B., I. Ha, et al. (1993). "Posttranscriptional regulation of the heterochronic gene lin-14 by lin-4 mediates temporal pattern formation in C. elegans." <u>Cell</u> **75**(5): 855-862.

Willis, C. L. and T. P. Davis (2008). Chronic Inflammatory Pain and the Neurovascular Unit: A Central Role for Glia in Maintaining BBB Integrity? <u>Current Pharmaceutical Design</u>, Bentham Science Publishers Ltd. **14**: 1625-1643.

Wittchen, E. S. (2009). "Endothelial signaling in paracellular and transcellular leukocyte transmigration." <u>Front Biosci</u> **14**: 2522-2545.

Wolburg, H. and A. Lippoldt (2002). "Tight junctions of the blood-brain barrier: development, composition and regulation." <u>Vascul Pharmacol</u> **38**(6): 323-337.

Wolburg, H., S. Noell, et al. (2009). "Brain endothelial cells and the glio-vascular complex." <u>Cell Tissue Res</u> **335**(1): 75-96.

Wong, D. and K. Dorovini-Zis (1996). "Regualtion by cytokines and lipopolysaccharide of E-selectin expression by human brain microvessel endothelial cells in primary culture." <u>J Neuropathol Exp Neurol</u> **55**(2): 225-235.

Wong, D., R. Prameya, et al. (2007). "Adhesion and migration of polymorphonuclear leukocytes across human brain microvessel endothelial cells are differentially regulated by endothelial cell adhesion molecules and modulate monolayer permeability." <u>J Neuroimmunol</u> **184**(1-2): 136-148.

Wosik, K., K. Biernacki, et al. (2007). "Death receptor expression and function at the human blood brain barrier." <u>J Neurol Sci</u> **259**(1-2): 53-60.

Wu, F., Z. Yang, et al. (2009). "Role of specific microRNAs for endothelial function and angiogenesis." <u>Biochemical and Biophysical Research Communications</u> **386**(4): 549-553.

Wu, F., M. Zikusoka, et al. (2008). "MicroRNAs are differentially expressed in ulcerative colitis and alter expression of macrophage inflammatory peptide-2 alpha." <u>Gastroenterology</u> **135**(5): 1624-1635 e1624.

Wu, L. and J. G. Belasco (2008). "Let me count the ways: mechanisms of gene regulation by miRNAs and siRNAs." <u>Mol Cell</u> **29**(1): 1-7.

Wu, Y., M. Crawford, et al. (2013). "Therapeutic Delivery of MicroRNA-29b by Cationic Lipoplexes for Lung Cancer." <u>Mol Ther Nucleic Acids</u> **2**: e84.

Xia, H., Y. Qi, et al. (2009). "microRNA-146b inhibits glioma cell migration and invasion by targeting MMPs." <u>Brain Res</u> **1269**: 158-165.

Xiao, C., D. P. Calado, et al. (2007). "MiR-150 Controls B Cell Differentiation by Targeting the Transcription Factor c-Myb." <u>Cell</u> **131**(1): 146-159.

Xiao, C. and K. Rajewsky (2009). "MicroRNA Control in the Immune System: Basic Principles." <u>Cell</u> **136**(1): 26-36.

Xu, G., C. Fewell, et al. (2010). "Transcriptome and targetome analysis in MIR155 expressing cells using RNA-seq." <u>RNA</u> **16**(8): 1610-1622.

Yang, J. S., M. D. Phillips, et al. (2011). "Widespread regulatory activity of vertebrate microRNA* species." <u>RNA</u> **17**(2): 312-326.

Yonekawa, K. and J. M. Harlan (2005). "Targeting leukocyte integrins in human diseases." <u>J Leukoc Biol</u> **77**(2): 129-140.

Yoshida, M., W. F. Westlin, et al. (1996). "Leukocyte adhesion to vascular endothelium induces E-selectin linkage to the actin cytoskeleton." <u>J Cell Biol</u> **133**(2): 445-455.

Yoshizaki, K., H. Wakita, et al. (2008). "Conditional expression of microRNA against E-selectin inhibits leukocyte-endothelial adhesive interaction under inflammatory condition." <u>Biochemical and Biophysical Research Communications</u> **371**(4): 747-751.

Zakrzewicz, A., M. Grafe, et al. (1997). "L-selectin-dependent leukocyte adhesion to microvascular but not to macrovascular endothelial cells of the human coronary system." <u>Blood</u> **89**(9): 3228-3235.

Zampetaki, A., S. Kiechl, et al. (2010). "Plasma microRNA profiling reveals loss of endothelial miR-126 and other microRNAs in type 2 diabetes." <u>Circ Res</u> **107**(6): 810-817.

Zampetaki, A., P. Willeit, et al. (2012). "Prospective study on circulating MicroRNAs and risk of myocardial infarction." <u>J Am Coll Cardiol</u> **60**(4): 290-299.

Zarbock, A., T. Kempf, et al. (2012). "Leukocyte integrin activation and deactivation: novel mechanisms of balancing inflammation." <u>J Mol Med (Berl)</u> **90**(4): 353-359.

Zarbock, A., K. Ley, et al. (2011). "Leukocyte ligands for endothelial selectins: specialized glycoconjugates that mediate rolling and signaling under flow." <u>Blood</u> **118**(26): 6743-6751.

Zeng, Y., E. J. Wagner, et al. (2002). "Both natural and designed micro RNAs can inhibit the expression of cognate mRNAs when expressed in human cells." <u>Mol Cell</u> **9**(6): 1327-1333.

Zeng, Y., R. Yi, et al. (2005). "Recognition and cleavage of primary microRNA precursors by the nuclear processing enzyme Drosha." <u>EMBO J</u> **24**(1): 138-148.

Zennadi, R., E. J. Whalen, et al. (2012). "Erythrocyte plasma membrane-bound ERK1/2 activation promotes ICAM-4-mediated sickle red cell adhesion to endothelium." <u>Blood</u> **119**(5): 1217-1227.

Zhan, Y., C. Brown, et al. (2005). "Ets-1 is a critical regulator of Ang II-mediated vascular inflammation and remodeling." <u>J Clin Invest</u> **115**(9): 2508-2516.

Zhang, J., Y. Y. Du, et al. (2008). "The cell growth suppressor, mir-126, targets IRS-1." <u>Biochem Biophys Res Commun</u> **377**(1): 136-140.
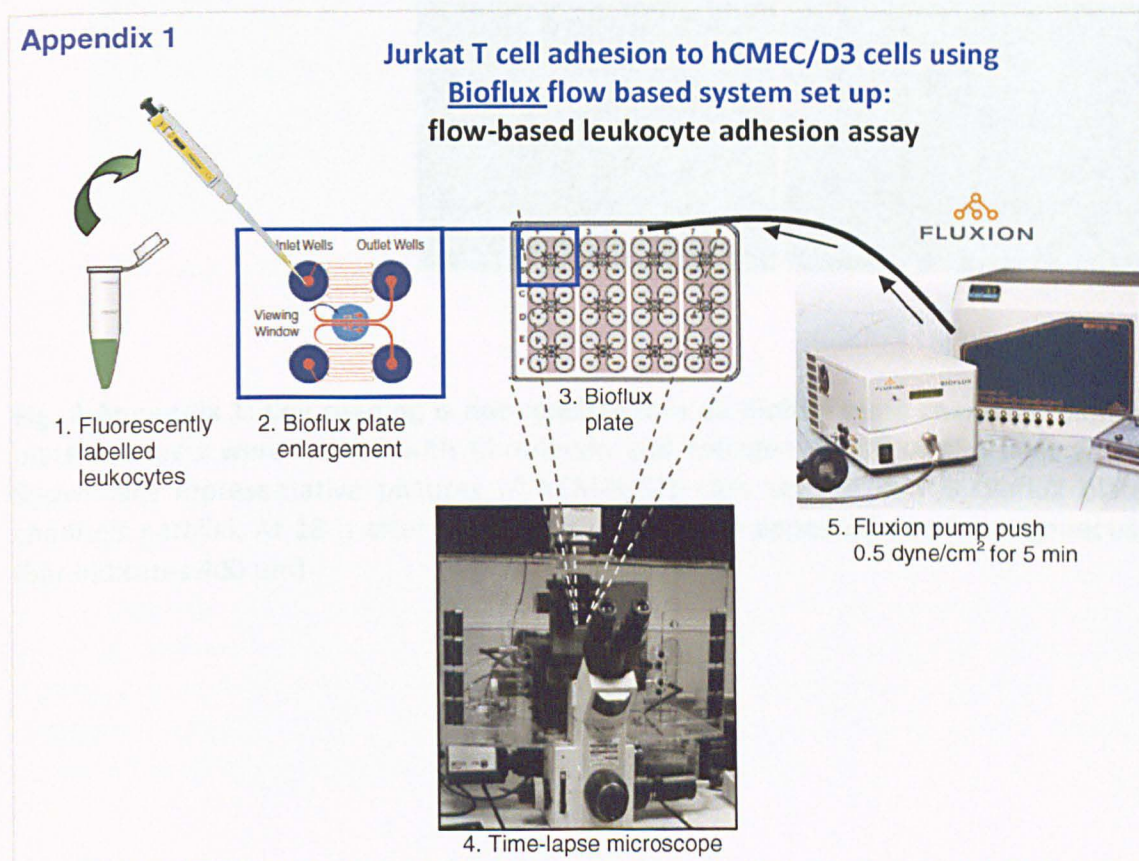
Zhang, R., M. Chopp, et al. (1998). "The expression of P- and E-selectins in three models of middle cerebral artery occlusion." Brain Res 785(2): 207-214.

Zhang, T., M. C. Moh, et al. (2010). "The immunoglobulin-like cell adhesion molecule hepaCAM is cleaved in the human breast carcinoma MCF7 cells." Int J Oncol 37(1): 155-165.

Zhang, Y., P. Yang, et al. (2013). "miR-126 and miR-126(*) repress recruitment of mesenchymal stem cells and inflammatory monocytes to inhibit breast cancer metastasis." Nat Cell Biol 15(3): 284-294.

Zhao, S., Y. Wang, et al. (2011). "MicroRNA-126 regulates DNA methylation in CD4+ T cells and contributes to systemic lupus erythematosus by targeting DNA methyltransferase 1." Arthritis Rheum 63(5): 1376-1386.

Zhao, T., J. Li, et al. (2010). "MicroRNA-34a induces endothelial progenitor cell senescence and impedes its angiogenesis via suppressing silent information regulator 1." Am J Physiol Endocrinol Metab 299(1): E110-116.

Zheng, L., C. C. Xu, et al. (2010). "MicroRNA-155 regulates angiotensin II type 1 receptor expression and phenotypic differentiation in vascular adventitial fibroblasts." Biochem Biophys Res Commun 400(4): 483-488.

Zhong, X., X. Li, et al. (2012). "Omentin inhibits TNF-alpha-induced expression of adhesion molecules in endothelial cells via ERK/NF-kappaB pathway." Biochem Biophys Res Commun 425(2): 401-406.

Zhou, H., X. Huang, et al. (2010). "miR-155 and its star-form partner miR-155* cooperatively regulate type I interferon production by human plasmacytoid dendritic cells." Blood 116(26): 5885-5894.

Zhou, J., K. C. Wang, et al. (2011). "MicroRNA-21 targets peroxisome proliferators-activated receptor-alpha in an autoregulatory loop to modulate flow-induced endothelial inflammation." Proc Natl Acad Sci U S A 108(25): 10355-10360.

Zhu, N., D. Zhang, et al. (2011). "Endothelial enriched microRNAs regulate angiotensin II-induced endothelial inflammation and migration." Atherosclerosis 215(2): 286-293.

Zhu, N., D. Zhang, et al. (2011). "Endothelial-specific intron-derived miR-126 is down-regulated in human breast cancer and targets both VEGFA and PIK3R2." Mol Cell Biochem 351(1-2): 157-164.

Zlokovic, B. V. (2005). "Neurovascular mechanisms of Alzheimer's neurodegeneration." Trends Neurosci 28(4): 202-208.

Zou, J., W. Q. Li, et al. (2011). "Two functional microRNA-126s repress a novel target gene p21-activated kinase 1 to regulate vascular integrity in zebrafish." Circ Res 108(2): 201-209.

# Appendix 1

Appendix 1 is supported by a CD-ROM attached to the thesis, with a Power Point presentation of the set-up and videos of the three flow-based systems tested in this project to study leukocyte adhesion.
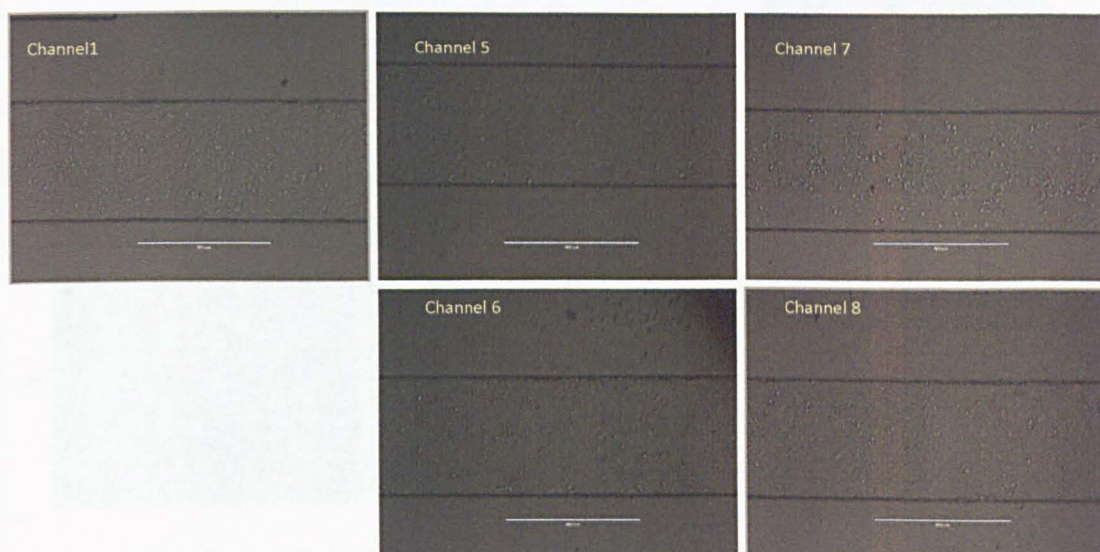
Here, a hard copy of Figs. 1-5 Appendix 1.



**Appendix 1**

**Jurkat T cell adhesion to hCMEC/D3 cells using Bioflux flow based system set up:**
**flow-based leukocyte adhesion assay**

1. Fluorescently labelled leukocytes
2. Bioflux plate enlargement
   - Inlet Wells   Outlet Wells
   - Viewing Window
3. Bioflux plate
4. Time-lapse microscope
5. Fluxion pump push 0.5 dyne/cm² for 5 min

FLUXION

**Fig. 1 Appendix 1: Bioflux flow-based adhesion assay set-up.** hCMEC/D3 cells were seeded in the Bioflux plate (3) and treated with TNFα + IFNγ proinflammatory cytokines. Fluorescent labelled leukocytes (1) were added to the inlet wells (2), then the bioflux plate (3) was sealed, connected to the pump (5) and positioned on the platform of a time-lapse microscope (4). The leukocyte suspension in the inlet wells was pushed at 0.5 dyne/cm2 for 5 min towards the outlet wells.

## Appendix 1

### Jurkat T cell adhesion to hCMEC/D3 cells using Bioflux flow based system set up: cell seeding is not consistent in all Bioflux plate channels



**Fig. 2 Appendix 1: Cell seeding is not consistent in all Bioflux plate channels.** Bioflux plate channels were coated with fibronectin and collagen added to the inlet wells. Shown are representative pictures of hCMEC/D3 cells seeded in the Bioflux plate channels parallel. At 18 h after seeding, EC confluence appeared non homogeneous. (bar indicates 400 µm)

**Appendix 1**
**Jurkat T cell adhesion to hCMEC/D3 cells using Bioflux flow based system set up:**
**High number of cells is required for confluent monolayers in 24h,**
**and transfection is not consistent**
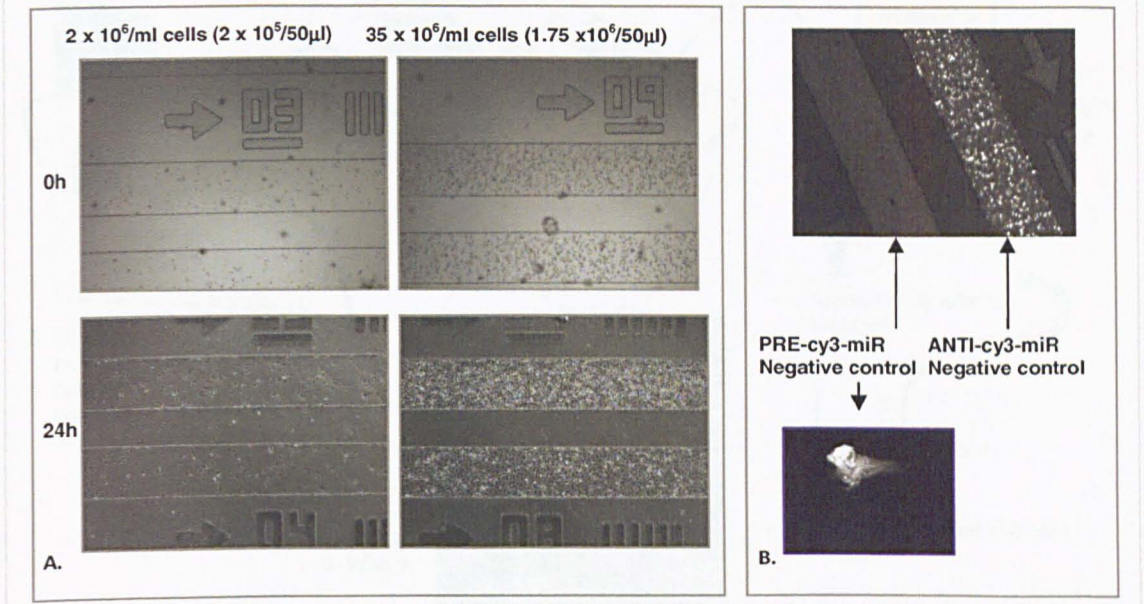
**Fig. 3 Appendix 1: Cell seeding and transfection of Bioflux plate channels. A.** Bioflux plate channels were seeded with different concentrations of hCMEC/D3 cells. Representative pictures of hCMEC/D3 cells at 0 and 24 h after seeding are shown. In order to obtain a confluent monolayer at 24 h, a seeding density of 35x106 /ml cells is required. **B.** Transfection with fluorescent negative control miRs (anti- and pre-miR) was performed on 70% confluent hCMEC/D3 cell monolayers. Representative pictures showing different transfection efficiencies are included. Left channel shows cells transfected with pre-miR which was unreliable (lower panel picture shows fluorescent aggregates trapped in the inlet well of the plate), while transfection with anti-miR appeared to be highly efficient as shown in the right channel.

**Video 1 Appendix 1:** Representative video of T cell Jurkat adhesion to hCMEC/D3 cells performed with the system described in Fig. 1 Appendix 1.
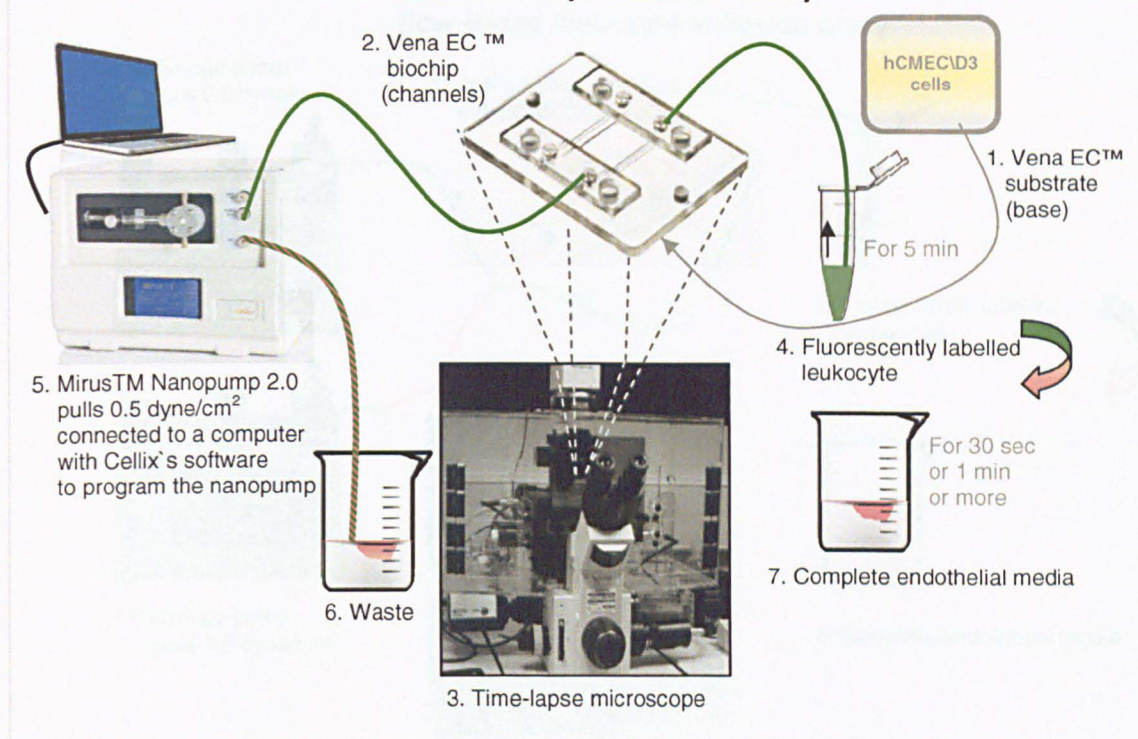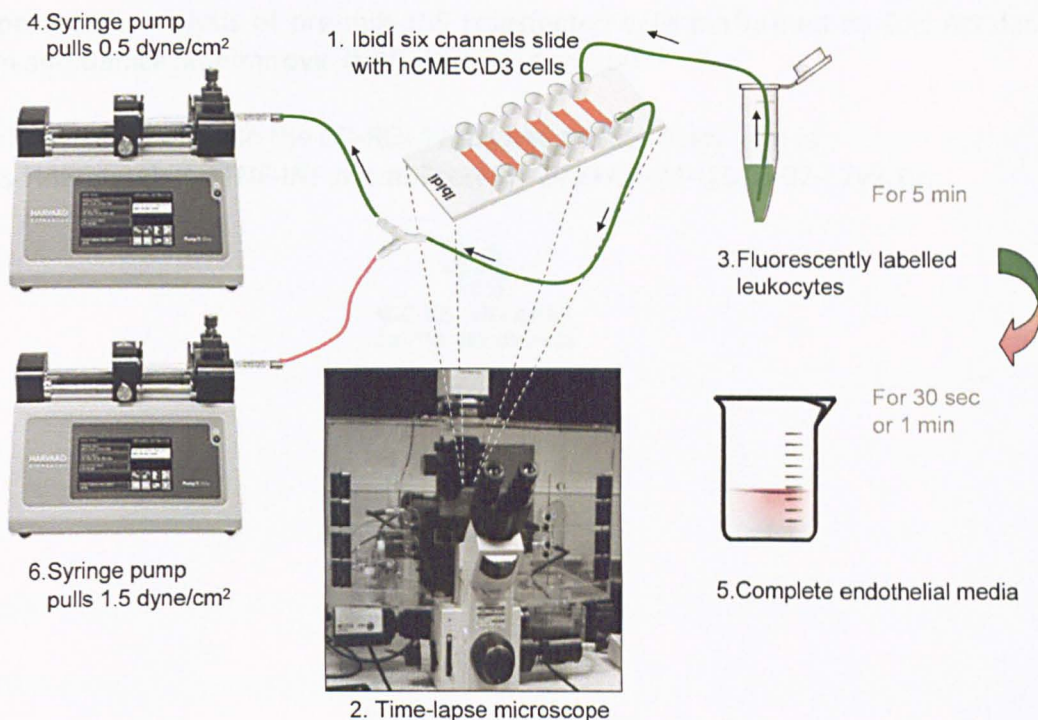
**Fig. 4 Appendix 1: Cellix flow-based adhesion assay set-up.** hCMEC/D3 cells were seeded in the Vena EC™ biochip (1) and treated with TNFα + IFNγ proinflammatory cytokines . The Vena EC™ substrate is sealed by Vena EC ™ biochip (2) on top, with 2 parallel microcapillaries, via a customized frame that was positioned on the platform of the time-lapse microscope (3) and connected to the MirusTM Nanopump (5). Fluorescently labelled leukocytes (4) were pulled at 0.5 dyne/cm$^2$ for 5 min towards the waste (6). Then after 5 min complete endothelial media was pulled at 1.5 dyne/cm$^2$.

**Video 2 Appendix 1:** Representative video of T cell Jurkat adhesion to hCMEC/D3 cells performed with the system described in Fig. 4 Appendix 1.

**Appendix 1**



Fig. 5 Appendix 1: Ibidí flow-based adhesion assay set-up. hCMEC/D3 cells were seeded in Ibidí chambers (1) and treated with TNFα + IFNγ proinflammatory cytokines. The Ibidí chamber was positioned on the stage of a time-lapse microscope (2) and connected to the syringe pumps (4 and 6). Fluorescently labelled leukocytes (3) were pulled at at 0.5 dyne/cm$^2$ for 5 min towards the syringe (4). Then after 5 min complete endothelial media was pulled at 1.5 dyn/cm$^2$ (6).

Video 3 Appendix 1: Representative video of T cell Jurkat adhesion hCMEC/D3 cells performed with the system described in Fig. 5 Appendix 1.

# Appendix 2

Appendix 2 consists of a table showing the results using mass spectrometry (MS)-based proteomic analysis of pre-miR-155 transfected cells performed by DRs Arsalan Haqqani and Danica Stanimirovic (NRC, Ottawa, Canada).

The table is in a Excel file in the CD-ROM attached to the thesis named NRC-IBS-HBECdatabase-TNF-INF-MembProteins-2009-07-24--2010-02-17v2.xls.

NRC-IBS-HBECdatab
ase-TNF-INF-MembPr

# Appendix 3

## 1. Human brain tissues and mouse spinal cord tissues

Snap-frozen brain tissue blocks were collected at post-mortem time ≤ 22 h by the UK Multiple Sclerosis Tissue Bank at the Division of Neuroscience and Mental Health, Imperial College London (Hammersmith Hospital Campus, London, UK) and stored at -80 °C. The snap frozen brain tissue blocks were from patients that had a history of MS and each block was characterised for pathogenic markers of disease. Details are listed in Table Appendix 3. Tissue regions were characterised by the UK MS tissue bank as grey matter lesion (GM), white matter lesion (WML), normal appearing white matter (NAWM), chronic active lesion (CAL), chronic lesion (CL) and active lesion (AL) using Oil-Red-O and anti-MOG antibody. Further histological characterisation of each specimen was performed using haematoxylin/eosin, Luxor fast blue (LFB) and immunostaining for CD68 and MHC II.

| Sample, MS patient case | Age (years) /gender | Post mortem (hours) | Type of MS | Duration disease (years) | Lesion activity | AL block | NAWM block | Activity of disease at death | Cause of death |
|---|---|---|---|---|---|---|---|---|---|
| MS154 | 34/F | 12 | SPMS | NIA | AL/CAL/CL | P5C7 | P5D4 | Progression | Pneumonia |
| MS168 | 88/F | 22 | PPMS | 30 | AL/CAL | A1E2 | P3D3 | Progression | Broncopneumonia |
| MS050 | 72/F | 8 | RRMS-SPMS | 41 | AL/CAL/CL | P1E2 | P5E3 | Progression | Bronchopneumonia |

**Table 1 Appendix 3: Demographic and clinical characteristics and details of multiple sclerosis patients and their snap-frozen brain tissue block.** NIA= no information available, chronic active lesion (CAL), chronic lesion (CL) and active lesion (AL).

Spinal cords from animals with EAE were a kind gift from Drs David Baker and Gregory J. Michael (Center for Neuroscience and Trauma, Blizard Institute Barts and The London School of Medicine and Dentistry, London, Queen Mary University of London, UK.). EAE was induced in Biozzi ABH mice with 1 mg freeze-dried mouse spinal cord homogenate in Freund's adjuvant supplemented with 60 mg Mycobacterium tuberculosis H37Ra and Mycobacterium butyricum as previously described (Al-Izki et al., 2012). Animals were monitored daily to assess the development of relapsing–remitting paralysis and scored as follows: 0=normal; 1=limp tail; 2=impaired righting reflex; 3=hind-limb paresis and 4=complete hind-limb paralysis (Al-Izki et al., 2012).

Each frozen brain tissue was left to reach -20°C and then carefully positioned and attached on the sample stub with Tissue-Tek O.C.T. (Qiagen, Crawley, West Sussex, UK) and cut using a Leica CM-3050-S Cryostat (Leica, Milton Keynes, UK) on superfrost Plus microscope slides (Thermo Scientific, Langenselbold, Germany) and stored at -80 °C. The snap-frozen human brain tissue analyses were carried out on 12-µm thick sections.

## 2. *In Situ* Hybridization (ISH)

**Table 2 Appendix 3: List of chemicals and solutions used for *in situ* hybridization.**

| Chemical or solution | Supplier | Catalogue # |
|---|---|---|
| Anti-Digoxigenin-AP, Fab fragments from sheep | Roche, Mannheim, Germany | 11093274910 |
| Blocking Reagent for nucleic acid hybridization and detection | Roche, Mannheim, Germany | 11096176001 |
| DAPI-Fluoromount-G™ 4',6-diamidino-2-phenylindole | Southernbiotech, Birmingham, USA | 0100-20 |
| Ethanol Ethyl alcohol | Sigma-Aldrich, Dorset, UK | E7023 |
| Hydrochloric acid HCL | Sigma-Aldrich, Dorset, UK | H1758 |
| ImmEdgeTM PEN | VECTOR Laboratories, Peterborough, UK | H-4000 |
| Levamisole (S)-6-Phenyl-2,3,5,6-tetrahydroimidazo[2,1b][1,3]thiazole | VECTOR Laboratories, Peterborough, UK | SP-5000 |
| Magnesium chloride ($MgCl_2$) | Fischer scientific, Loughboroig, UK | M/0600/53 |
| NTB/BCIP 8.75 mg/ml nitro blue tetrazolium chloride and 9.4 mg/ml 5-bromo-4-chloro-3-indolyl-phosphate, toluidine-salt in 67% (v/v) DMSO | Roche Diagnostics, Mannheim, Germany | 11681451001 |
| *p*-formaldehyde | Sigma-Aldrich, Dorset, UK | P6148 |
| Potassium chloride (KCl) | Sigma-Aldrich, Dorset, UK | 4504 |
| Proteinase K | Promega, Madison, USA | V3021 |
| Saline-Sodium Citrate buffer, made with ultrapure water SSC Buffer 20× | Sigma-Aldrich, Dorset, UK | S6639 |
| Sodium Cloride (NaCl) | | |
| Tris Trizma® base 2-Amino-2-(hydroxymethyl)-1,3-propanediol | Sigma-Aldrich, Dorset, UK | T6066 |
| Trizma® hydrocloride (TRIS HCl) | Sigma-Aldrich, Dorset, UK | T5941 |
| TWEEN-20 Polyoxyethylenesorbitan monolaurate | Sigma-Aldrich, Dorset, UK | P7949 |

**Table 3 Appendix 3: Solutions used for *in situ* hybridization.**

| Solution | Composition |
|---|---|
| Buffer 1 | Tris HCl pH 7.5 100 mM, NaCl 150 mM in $H_2O$ |
| Buffer 2 | Buffer 1 with 0.5 % Roche Blocking solution in $H_2O$ |
| Buffer 3 | Tris HCl pH 9.5 100 mM, NaCl 100 mM, $MgCl_2$ 50 mM in $H_2O$ |
| NBT/BCIP | 1% NBT/BCIP, 0.5% levamisole chromogen solution, 0.1% Tween 20 in Buffer 3 |
| Proteinase K | 2µg /ml of proteinase K in 10% Tris HCl 100 mM pH 7.5, 10% ETDA 0.5M in $H_2O$ |
| Hybridization solution | 50% formamide, 5X SSC, 40 µg/ml salmon sperm DNA, 0.1% Tween 20 in $H_2O$ |
| 20X SSC | 3 M NaCl, 0.3 M Tri-sodium citrate pH 7.0 in $H_2O$ |
| KTBS Tween | 50mM Tris HCl pH 7.4, 150 mM NaCl,10 mM KCl, 0.5% Tween20 |

The ISH analysis was carried out on 12-μm thick snap-frozen human brain tissue sections cut using the Leica CM-3050-S Cryostat (Leica, Milton Keynes, UK) and stored at -80 °C. Sections were thawed at RT for 5 min, and the tissue sections circumscribed with ImmEdge™ PEN (Vector Laboratories, Peterborough, UK) and fixed with 4% *p*-formaldehyde for 5 min at RT, then they were treated with 2 μg/mL Proteinase K (Promega, Southampton, UK) for 10 min at 37°C and washed two times with PBS for 5 min. The sections were dehydrated with a graded ethanol series of 1 min each (70, 95 and 100% ethanol) and left to dry at RT for 15 min. Then, the hybridization step with double digoxigenin (DIG) - labelled Locked Acid Nucleic (LNA) specific probe (Exiqon, Vedbaek, Denmark), the Mercury LNA microRNA detection probe sequence 5`-3` for miR-126 /5DigN/GCATTATTACTCACGGTACGA/3DIG_N/, was performed at hybridization temperature of 54 °C for 1.5 h in a SI-600R Incubated Shaker (Medline scientific, Oxon, UK) with gentle shaking, followed by stringent washes (once in 5x SSC 40 ml in a glass jar at 55 °C for 5 min, twice in 1x SSC 40 ml at 55 °C for 5 min, three times 0.2x SSC 40 ml at 55 °C for 5 min and finally in PBS at RT for 5 min).

After blocking with 0.5% Roche blocking solution (Roche Diagnostics, Germany) in Buffer 1, sections were incubated in 1/800 polyclonal sheep anti-digoxigenin-AP antibodies (anti-DIG AP) Fab fragments from sheep coupled to alkaline phosphatase (Roche Diagnostics, Germany) to detect the DIG labelled probe (miR-126) for 2 h at RT. After three washes with Buffer 1 for 5 min, sections were stained with NTB/BCIP for 2 h at 37 °C, changed with fresh one overnight at 37 °C. Samples were washed with KTBS Tween and mounted on slides using fluoromount-G (Southern Biotech, Cambridge, UK). For image acquisition, a Nikon Microphot-FX microscope with x40 objective and Image Pro Plus software (Media Cybernetics Bethesda, USA) were used.

## 3. MiR-126 expression on human MS and EAE spinal cord tissues

To set up *in situ* hybridisation for miRs, we performed an initial study for miR-126 expression on MS (Fig. 1 Appendix 3 ) and EAE (Fig. 2 Appendix 3) tissues, where we were able to detect miR-126.
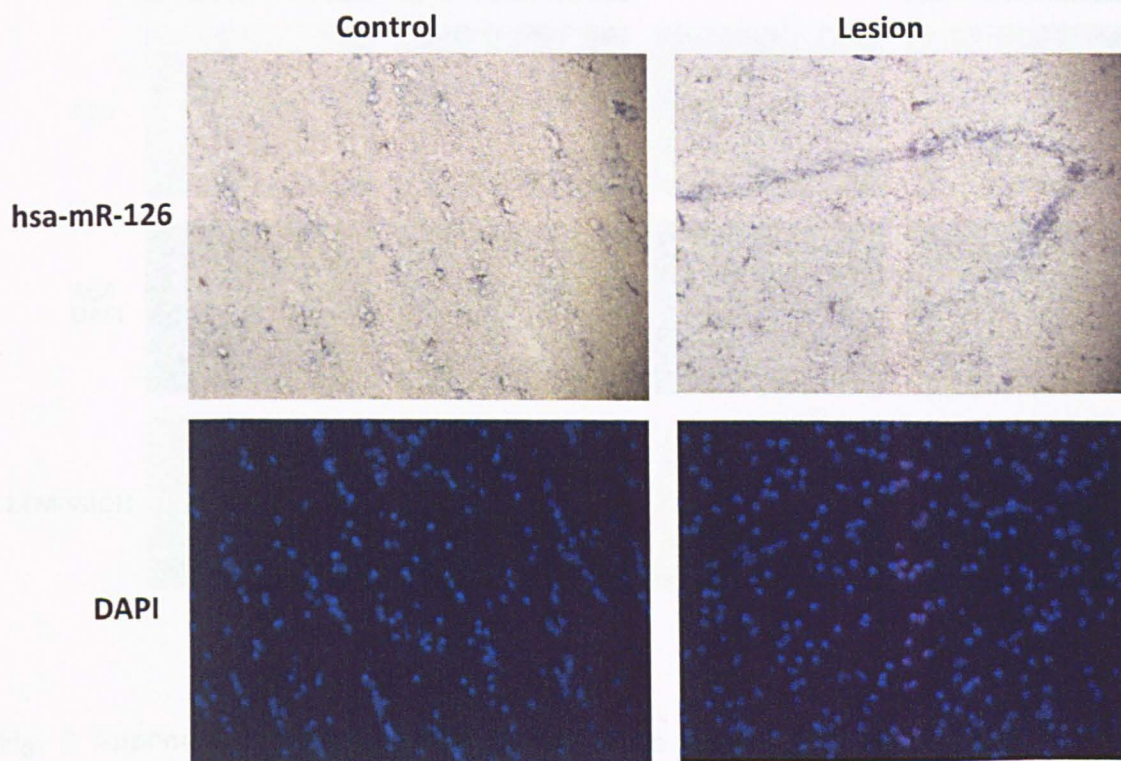


**Fig. 1 Appendix 3: Hsa-miR-126 expression in MS brain sections.** Twelve micron snap frozen brain sections of MS patients were hybridized with hsa-miR-126 probe. X40 images are shown for hsa-miR-126 expression and DAPI nuclei staning in **left panels.** Control (brain snap frozen tissue from patient with no history of MS) and **right panels.** MS lesion. Experiment performed with Dr. Dongsheng Wu, The Open University, UK.
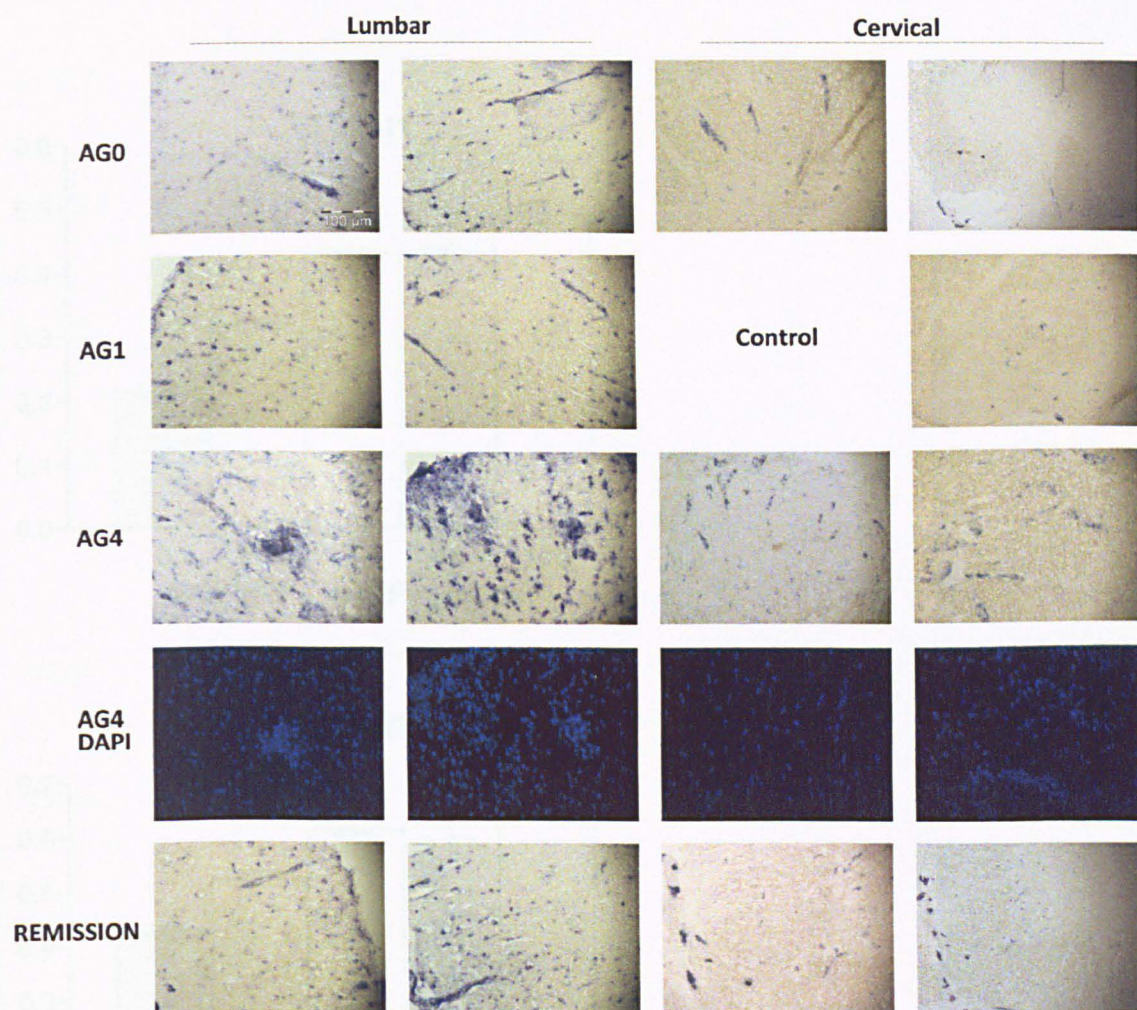
**Fig. 2 Appendix 3: mmu-miR-126 expression in lumbar EAE spinal cord.** Twelve micron frozen EAE cervical and lumbar spinal cord sections at different stages of disease (AG0, AG1, AG4) and in remission sections were hybridized with hsa-miR-126 probe (the sequence of mmu-miR-126 is identical to has-miR-126). Representative X40 images of hsa-miR-126 expression are shown for AG0, AG1, AG4 and remission phases and dapi nuclei staining (AG4 DAPI). Bar represents 100μM. Experiment performed with Dr. Dongsheng Wu, The Open University, UK.
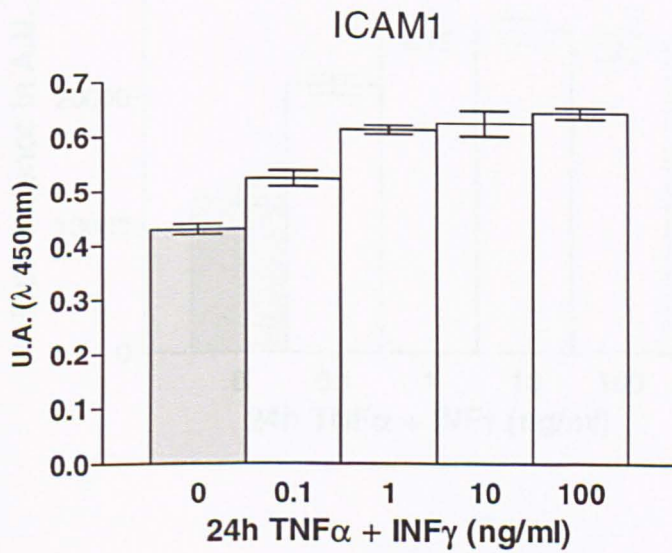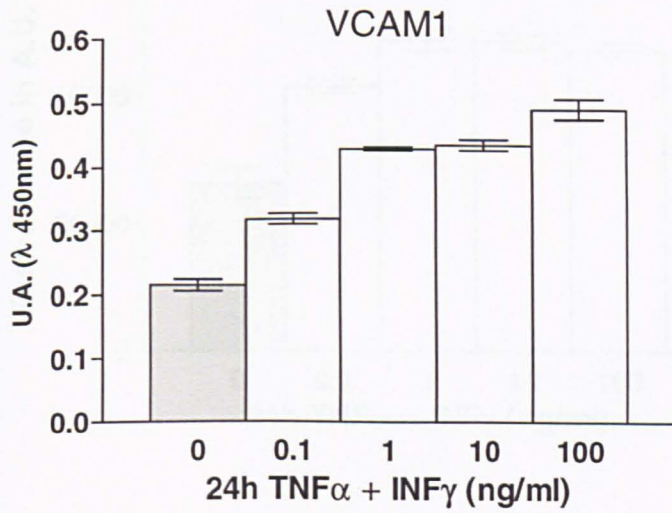
**Fig. 1 Appendix 4: VCAM1 and ICAM1 expression on hCMEC/D3 cells.**
Raw data of a representative experiment expressed in arbitrary units.
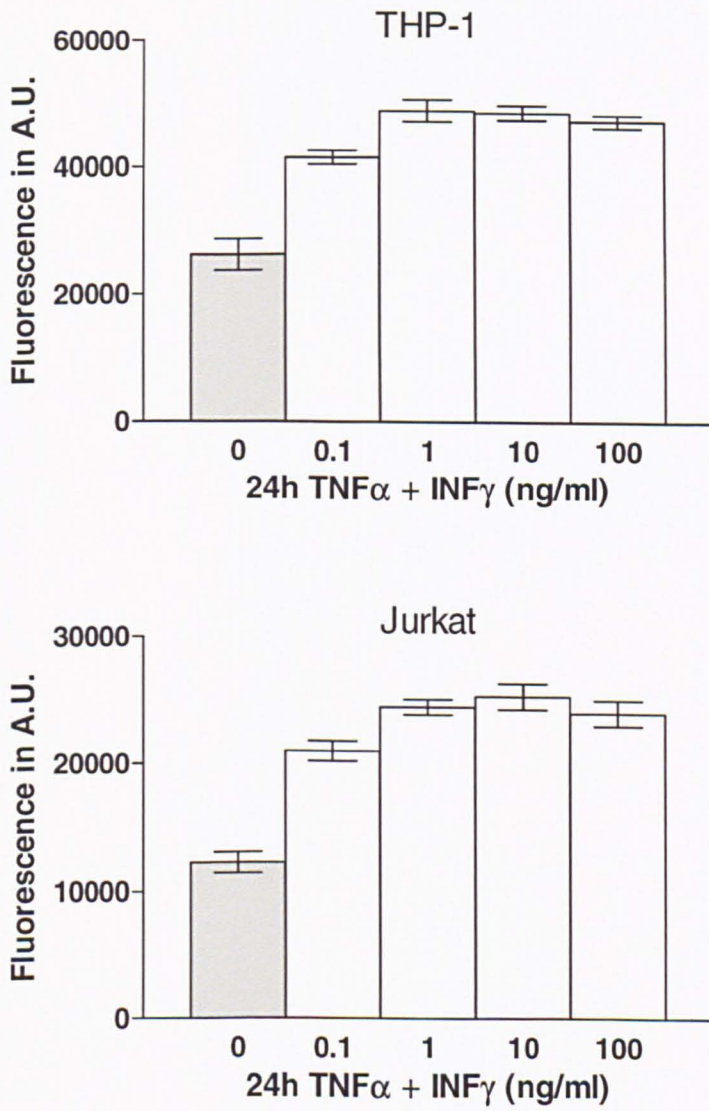
**Fig. 2 Appendix 4: THP-1 and Jurkat adhesion to hCMEC/D3 cells.** Raw data of a representative experiment expressed in arbitrary units.